CHEMICAL CHANGES OCCURING IN NUTS AND OILSEED VARIETIES DURING ROASTING

KAVURMA SIRASINDA KURUYEMİŞ VE YAĞLI TOHUM ÇEŞİTLERİNDE GERÇEKLEŞEN KİMYASAL DEĞİŞİMLER

DİLARA ŞEN

PROF. DR. VURAL GÖKMEN

Supervisor

Submitted to Graduate of Science and Engineering of Hacettepe University

as a Partial Fulfillment to the Requirements

for the Award of the Degree of Doctor of Philosophy

in Food Engineering.

2022

ABSTRACT

CHEMICAL CHANGES OCCURRING IN NUTS AND OILSEED VARIETIES DURING ROASTING

Dilara ŞEN

Doctor of Philosophy, Department of Food Engineering

Supervisor: Prof. Dr. Vural GÖKMEN

August 2022, 144 pages

The consumption of nuts and seeds is considered a part of a healthy diet. They can be consumed raw or as snacks after being roasted generally at 130-200 °C. Roasting provides desirable aroma, color, and also texture, thereby improving overall acceptability. Apart from the physical changes, chemical reactions such as Maillard reaction, sugar degradation, lipid oxidation, protein denaturation, and vitamin degradation also take place during roasting and are affected by the temperature and time of the roasting process. The thermal process can also cause potentially adverse health effects by promoting the formation of potentially toxic or carcinogenic components and causing a loss of nutritional value. The route of these chemical reactions is extremely dependent on the reactants as much as reaction conditions such as pH, temperature, and moisture content. The restricted amount of reducing sugar, low water activity, and neutral pH value of nuts and seeds lead Maillard reaction to follow a different pathway. Therefore the Maillard reaction-related studies carried out in aqueous food matrices and model studies are incoherent to describe the reaction in foods that have limited water content. Since the mobility of the reactants is necessary for these reactions to occur, the reactants gain reactivity with melting in the processes where water activity is limited,

i

such as baking or roasting. In order to better understand these complex reaction systems that take place during roasting, it is necessary to monitor the change in the concentration of the reactants and formed products kinetically. The aim of this thesis is to reveal a kinetic model for Maillard reaction-caramelization and also for acrylamide formation in nuts and seeds as low moisture food systems during roasting by using a multiresponse kinetic modeling approach. To achieve this aim, sunflower seed (*Helianthus annuus L.*), pumpkin seed (*Cucurbita moschata L.*), flaxseed (*Linum usitatissimum L.*), peanut (*Arachis hypogaea L.*), and almond (*Prunus dulcis*) were studied due to their similar compositions to represent of low-moisture foods by considering these kinds of foods as sugar-limited lipid-rich reaction pools and with the available amount of amino acids and sucrose.

In the first part, the proximate composition of nuts and seeds which is the reactants of the Maillard reaction were evaluated. Sucrose was predominant in selected nuts and seeds, while glucose and fructose were rapidly degraded upon roasting. While the highest sucrose concentration was found in peanuts, the least sucrose was found in pumpkin seeds. The highest amount of protein-bound lysine was found in peanut and pumpkin seeds whereas it was the lowest in almonds. Arginine, aspartic acid, and glutamic acid were found to be the most predominant amino acids in all samples.

In the second part of this thesis, changes in the concentration of reactants and products of Maillard reaction and caramelization were evaluated during the roasting of samples at different temperatures for different times. Sucrose decreased gradually during roasting depending on the roasting temperature and time. Almost all free amino acids participated in the reactions and, the highest decrease in the total amino acid content (sum of free amino acids and protein-bound lysine) was found in flaxseeds (72%) and sunflower seeds (71%) followed by peanut (44%), almond (35%) and pumpkin seed (28%) with roasting, respectively. Changes in 5-hydroxymethylfurfural concentration in seeds and nuts showed an overall increasing trend in all samples in relation to the decrease in sugar content. The highest 5-hydroxymethylfurfural formation was observed in sunflower seed after 30 minutes of roasting at 180 °C whereas the least 5-hydroxymethylfurfural content was found in pumpkin seed due to the least amount of sucrose among other samples. The highest furosine content was found in pumpkin seed whereas no detectable amount of furosine was found in raw almond samples. The N-ε-carboxymethyl lysine concentration reached its highest value generally at 180 °C within

30 or 40 min in all samples with the highest concentration in sunflower seeds. The maximum N-ε-carboxyethyl lysine content was found in pumpkin seed roasted at 180 °C for 40 min. Among the raw samples, the highest total α-dicarbonyl compounds concentration was detected in sunflower and pumpkin seed probably due to formation prior to transportation or during sun-drying. α-Dicarbonyl compounds in pumpkin seed, peanut, and almond showed a similar increasing trend during roasting while in flaxseed and sunflower seed they showed a decreasing trend depending on the roasting conditions. 3-deoxyglucosone and methylglyoxal were the most predominant α-dicarbonyl compounds. The levels of acrylamide rapidly increased to a certain extent and started to decrease afterward due to the prolonged roasting times. The highest acrylamide content among all the samples was found in almonds after roasting at 200 °C for 15 min due to the higher amount of free asparagine compared to the other samples.

In the last part, a kinetic model was proposed by using a multiresponse kinetic modeling approach for Maillard reaction and caramelization during the roasting of samples at 160 and 180 °C. Firstly, the Principal Component Analysis (PCA) was run to determine the differences between raw food matrices and the distribution of reactants among the samples. The pumpkin seed obviously separated from the others due to its high-water activity and also lower amounts of sucrose and free amino acids which are the two of the main reactants of the Maillard reaction. Almond, flaxseed, and sunflower seed were clustered together in the same region of the plot indicating similarities in their chemical composition. Peanut was located at the bottom part of the diagram due to its slightly high levels of sucrose and low levels of ash and protein whereas pumpkin seed appeared in a different part of the PCA plot. These results were the basis for the multiresponse modeling of Maillard reaction in low moisture, low reducing sugar-lipid rich systems. Accordingly, it is envisaged that all samples can be explained with a single model, whereas probably different reaction pathways will be dominant in pumpkin seed samples. Accordingly, 3-deoxyglucosone formation via sugar degradation; 5-hydroxymethylfurfural formation from 3-deoxyglucosone, and only in pumpkin seeds the conversion of N-ε-fructoselysine to glyoxal and Heyns product to 1-deoxyglucosone were found to be quantitatively important. N-ε-carboxymethyl lysine and N-ε-carboxyethyl lysine mainly originated through oxidation of N-ε-fructoselysine and the reaction of methylglyoxal with lysine residue, respectively.

Additionally, another kinetic model was proposed for the acrylamide formation during the roasting of these kinds of low-moisture foods at 160, 180, and 200 °C for 5 to 60 minutes. According to the proposed model, sucrose degraded to glucose and fructofuranosyl cation; 5-hydroxymethylfurfural was mainly formed through the 3-deoxyglucosone pathway in all samples at 160 and 180 °C and the reaction of asparagine with 5-hydroxymethylfurfural was found as the predominant pathway for acrylamide formation.

These models might enable us to understand the whole reaction mechanism and develop mitigation strategies for controlling the formation of thermal contaminants such as acrylamide during thermal processing of roasted nuts and seeds as sucrose-rich and low moisture foods by developing optimal thermal processing conditions. This approach also allows us to classify nuts and seeds according to their compositional characteristics, which is more critical for chemical reactions, instead of their botanical nomenclature.

ÖZET

KAVURMA SIRASINDA KURUYEMİŞ VE YAĞLI TOHUM ÇEŞİTLERİNDE GERÇEKLEŞEN KİMYASAL DEĞİŞİMLER

Dilara ŞEN

Doktora, Gıda Mühendisliği Bölümü

Tez Danışmanı: Prof. Dr. Vural GÖKMEN

Ağustos 2022, 144 sayfa

Kuruyemiş ve tohum tüketimi sağlıklı bir diyetin parçası olarak kabul edilmektedir. Bu gıdalar, genellikle 130-200 °C arası bir sıcaklıkta kavrulduktan sonra veya çiğ atıştırmalık olarak tüketilebilmektedir. Kavurma işlemi, arzu edilen aroma, renk ve aynı zamanda tekstür sağlamakta, böylece genel kabul edilebilirliği artırmaktadır. Fiziksel değişikliklerin yanı sıra Maillard reaksiyonu, şeker degradasyonu, lipid oksidasyonu, protein denatürasyonu ve vitaminlerin degradasyonu gibi kimyasal reaksiyonlar da kavurma sırasında meydana gelmekte ve bu reaksiyonlar kavurma işleminin sıcaklık ve süresinden etkilenmektedir. Termal proses ayrıca potansiyel toksik veya kanserojen bileşenlerin oluşumunu teşvik ederek ve besin değeri kaybına neden olarak olumsuz sağlık etkilerine de neden olabilmektedir. Bu kimyasal reaksiyonların izlediği yol, pH, sıcaklık ve nem içeriği gibi reaksiyon koşullarının yanı sıra ortamdaki reaktantlara da son derece bağlıdır. Kuruyemişlerin ve tohumların nötr pH değerine sahip olması, içerdikleri sınırlı miktarda indirgen şeker ve düşük su aktivitesi değerleri, Maillard reaksiyonunun sulu ortamlara kıyasla daha farklı bir yol izlemesine neden olmaktadır. Bu nedenle, sulu gıda matrislerinde gerçekleştirilen Maillard reaksiyonu ile ilgili

çalışmalar ve model çalışmaları, sınırlı su içeriğine sahip gıdalardaki reaksiyonu açıklamak için uygun olmamaktadır. Bu reaksiyonların gerçekleşmesi için reaktantların mobilitesi gerekli olduğundan, pişirme veya kavurma gibi su aktivitesinin sınırlı olduğu proseslerde reaktantlar ancak erime ile reaktivite kazanmaktadır. Kavurma sırasında meydana gelen bu karmaşık reaksiyon sistemlerini daha iyi anlayabilmek için, reaksiyona giren maddelerin ve oluşan ürünlerin derişimlerindeki değişimi kinetik olarak izlemek gerekmektedir. Bu tezin amacı ise, düşük nemli gıda sistemleri olarak ele alınan kuruyemiş ve tohumların kavrulması sırasında gerçekleşen Maillard reaksiyon-karamelizasyon ile akrilamid oluşumu için çok değişkenli kinetik modelleme yaklaşımını kullanarak kinetik bir model ortaya koymaktır. Bu amaçla, yeterli miktarda amino asit ve sukroz içeren; sınırlı şeker içeriğine sahip ancak lipid açısından zengin reaksiyon havuzları olduklarını da göz önünde bulundurarak, düşük nem değerine sahip gıdaları temsil etmesi açısından ayçiçeği çekirdeği (*Helianthus annuus* L.), kabak çekirdeği (*Cucurbita moschata* L.), keten tohumu (*Linum usitatissimum* L.), yer fıstığı (*Arachis hypogaea* L.), badem (*Prunus dulcis*) ile çalışılmıştır.

Birinci bölümde, Maillard reaksiyonunun reaktantları olan kabuklu yemiş ve tohumların yaklaşık bileşimleri değerlendirilmiştir. Çalışılan örneklerde, sukroz baskın şekerken glukoz ve fruktoz kavurma ile hızla parçalanmıştır. En yüksek sukroz konsantrasyonu yer fıstığında bulunurken, en az sukroz konsantrasyonu ise kabak çekirdeğinde bulunmuştur. Proteine bağlı lizin miktarı en yüksek yer fıstığı ve kabak çekirdeğinde en az ise bademde tespit edilmiştir. Arjinin, aspartik asit ve glutamik asit tüm örneklerde en baskın amino asitler olarak ölçülmüştür.

Tezin ikinci bölümünde, örneklerin farklı sıcaklıklarda ve farklı sürelerde kavrulması sırasında gerçekleşen Maillard reaksiyonu-karamelizasyon ürünlerinin ve reaktantlarının konsantrasyonundaki değişimler incelenmiştir. Sukroz, sıcaklığa ve süreye bağlı olarak kavurma sırasında kademeli olarak azalma göstermiştir. Reaksiyonlara hemen hemen tüm serbest amino asitler katılmış ve toplam amino asit içeriğinde (serbest amino asitler ve proteine bağlı lizin toplamı) en yüksek düşüş keten tohumu (%72) ve ayçiçeği çekirdeğinde (%71), ve ardından sırasıyla yer fıstığında (%44), bademde (%35) ve kabak çekirdeğinde (%28) bulunmuştur. Tohum ve kuruyemişlerdeki 5-hidroksimetilfurfural konsantrasyonundaki değişiklikler, şeker içeriğindeki azalmaya bağlı olarak tüm örneklerde genel bir artış eğilimi göstermiştir. En yüksek 5-hidroksimetilfurfural oluşumu 180 °C'de 30 dakikalık kavurma sonrasında

ayçiçeği çekirdeğinde gözlenirken, diğer örneklerle karşılaştırıldığında en az miktarda sukroz içermesi nedeniyle en az 5-hidroksimetilfurfural içeriği kabak çekirdeğinde bulunmuştur. En yüksek furozin içeriği ise kabak çekirdeğinde bulunurken, çiğ badem örneklerinde saptanabilir miktarda furozin bulunamamıştır. N-ε-karboksimetillizin konsantrasyonu tüm örneklerde genellikle 180 °C'de 30 veya 40 dakika içinde en yüksek değerine ulaşmış ve en yüksek konsantrasyon ayçiçeği çekirdeğinde olduğu tespit edilmiştir. En yüksek N-ε-karboksietillizin içeriği ise, 180 °C'de 40 dakika kavrulan kabak çekirdeğinde bulunmuştur. Çiğ örnekler arasında en yüksek toplam α-dikarbonil bileşik konsantrasyonu, nakliye öncesindeki veya güneşte kurutma sırasındaki oluşuma bağlı olarak ayçiçeği ve kabak çekirdeğinde tespit edilmiştir. Kabak çekirdeği, yer fıstığı ve bademdeki α-dikarbonil bileşikleri kavurma sırasında benzer bir artış eğilimi gösterirken keten tohumu ve ayçiçeği çekirdeğinde kavurma koşullarına bağlı olarak azalan bir eğilim göstermiştir. 3-deoksiglukozon ve metilglioksal, en baskın α-dikarbonil bileşikleri olarak bulunmuştur. Akrilamid miktarı, artan kavurma süreleriyle birlikte belirli bir seviyeye kadar hızla yükselmiş ve daha sonra azalmaya başlamıştır. Tüm örnekler arasında en yüksek akrilamid içeriği, diğer örneklere göre daha yüksek serbest asparajin miktarı içermesi nedeniyle bademlerde, 200 °C'de 15 dakikalık kavurma sonrasında bulunmuştur.

Son bölümde, örneklerin 160 ve 180 °C'de kavrulması sırasında gerçekleşen Maillard reaksiyonu ve karamelizasyon mekanizması için çok değişkenli kinetik modelleme yaklaşımı kullanılarak kinetik bir model önerilmiştir. İlk olarak, çiğ gıda matrisleri arasındaki farkları ve reaktantların örnekler arasındaki dağılımını belirlemek için Temel Bileşen Analizi (PCA) yapılmıştır. Kabak çekirdeği, yüksek su aktivitesine sahip olması ve ayrıca Maillard reaksiyonunun ana reaktantlarından ikisi olan sukroz ve serbest amino asitleri daha düşük miktarlarda içermesi nedeniyle diğerlerinden açıkça ayrılmıştır. Badem, keten tohumu ve ayçiçeği çekirdeği, kimyasal bileşimlerindeki benzerlikler nedeniyle grafiğin aynı bölgesinde birlikte kümelenmişlerdir. Yer fıstığı, yüksek orandaki sukroz içeriği ve düşük kül ve protein seviyeleri nedeniyle diyagramın alt kısmında yer alırken, kabak çekirdeği PCA grafiğinin farklı bir bölümünde konumlanmıştır. Bu sonuçlar, düşük neme ve düşük indirgen şeker miktarına sahip - lipid bakımından zengin sistemlerde Maillard reaksiyonunun çok değişkenli kinetik modellemesi için bir temel oluşturmuştur. Buna göre, tüm örneklerin tek bir modelle açıklanabileceği, kabak çekirdeği örneklerinde ise muhtemelen farklı reaksiyon

yollarının hakim olacağı öngörülmüştür. Önerilen modele göre, şeker degradasyonu ile 3-deoksiglukozon oluşumu; 3-deoksiglukozondan 5-hidroksimetilfurfural oluşumu ve sadece kabak çekirdeğinde N-ε-fruktozillizin'in glioksale ve Heyns ürününün 1-deoksiglukozona dönüşümü nicel olarak önemli bulunmuştur. N-ε-karboksimetillizin ve N-ε-karboksietillizin ise esas olarak sırasıyla N-ε-fruktozillizin oksidasyonu ve metilglioksalin lizin rezidüsü ile reaksiyonunu sonucu oluşmaktadır.

Bu çalışmada ayrıca, bu tür düşük nemli gıdaların 160, 180 ve 200 °C'de 5 ila 60 dakika arasında değişen bir süre ile kavrulması sırasında gerçekleşen akrilamid oluşumu için de bir kinetik model önerilmiştir. Önerilen modele göre, sukrozun, glikoz ve fruktofuranozil katyonuna parçalandığı; 5-hidroksimetilfurfuralin, 160 ve 180 °C'de tüm örneklerde 3-deoksiglukozon yolu ile oluştuğu ve asparajinin 5-hidroksimetilfurfural ile reaksiyonunun, akrilamid oluşumu için en baskın yol olduğu belirlenmiştir.

Önerilen bu modeller, tüm reaksiyon mekanizmasını anlamamızı ve optimal ısıl işlem koşulları geliştirerek sukroz bakımından zengin ve düşük nemli gıdaları temsilen kavrulmuş kuruyemiş ve tohumların ısıl işlemi sırasında akrilamid gibi termal kontaminantların oluşumunu kontrol etmek için azaltma stratejileri geliştirmemizi sağlayabilecektir. Bu yaklaşım aynı zamanda kuruyemişleri ve tohumları botanik terminolojileri yerine kimyasal reaksiyonlar için daha kritik olan bileşim özelliklerine göre sınıflandırmamızı sağlamaktadır.

Anahtar Kelimeler: Çok değişkenli kinetik modelleme, kavurma, ileri glikasyon son ürünleri, kuruyemiş ve tohumlar, Maillard reaksiyonu

ACKNOWLEDGEMENTS

CONTENTS

LIST OF FIGURES

LIST OF TABLES

SYMBOLS AND ABBREVIATIONS

Symbols

k   Reaction rate constant

Abbreviations

AA   Amino acids

ACR   Acrylamide

AGEs   Advanced glycation end products

ALEs   Advanced lipoxidation end products

AOAC   Association of Official Analytical Chemists

AP   Amadori product

Arg   Arginine

Asn   Asparagine

bLYS   Protein bound lysine

CEL N-ε-Carboxyethyllysine

CML N-ε-Carboxymethyllysine

DETAPAC   Diethylenetriaminepentaacetic acid

DMG   Dimethylglyoxal

DOLD   3-deoxyglucosone-methyl-dimer

1-DG   1-Deoxyglucosone

3-DG   3-Deoxyglucosone

3,4-DG   3,4-Dideoxyglucosone

DNA   Deoxyribonucleic acid

EFSA   European Food Safety Authority

FFC   Fructofuranosyl cation

FL   Fructosyllysine

GLC	Glucose
GO	Glyoxal
GOLD	Glyoxal-methyl-dimer
His	Histidine
HLB	Hydrophilic-lipophilic-balanced
HMF	5-Hydroxymethylfurfural
HMW	High molecular weight
HP	Heyns product
HPD	Highest posterior density
HPLC	High performance liquid chromatography
IARC	International Agency for Research on Cancer
LC/MS	High performance liquid chromatography mass spectrometry
MCX	Mixed mode cation exchange reversed phase
MGO	Methylglyoxal
MOLD	Methylglyoxal-methyl-dimer
MRM	Multiple reaction monitoring
MRPs	Maillard reaction products
OPD	*o*-Phenylenediamine
P	Product
PUFA	Polyunsaturated fatty acid
RID	Refractive index dedector
SUC	Sucrose
USDA	The United States Department and Agriculture

1. INTRODUCTION

In recent years, with the growing interest in healthy food consumption, an increase in demand for nuts and seeds has been observed. Because these foods contain healthy constituents, they offer an important alternative to consumers. These foods can be consumed raw or after being roasted. They are also used as an ingredient in bakery products such as bread, cake, and cookies. Within the scope of the thesis, peanut, almond, sunflower seed, pumpkin seed, and flaxseed were studied to represent the nuts and seeds.

The chemical composition, nutritional and sensory properties of food can change during the roasting process. The compounds that involve in the development of desired color, taste, and flavor and also the compounds that show antioxidant activity are formed through Maillard reaction, sugar degradation, and lipid oxidation. As a result of the roasting process, undesirable products can also be produced. It was reported that carcinogenic, mutagenic, and cytotoxic compounds such as 5-hydroxymethylfurfural (HMF), acrylamide (ACR), and advanced glycation end products (AGEs) or toxigenic compounds such as furan are formed. Furthermore, these reactions reduce the nutritional value of the food by causing the loss of amino acids.

There is limited information in the literature about the complex mechanism of Maillard reaction and sugar decomposition reactions in foods that are rich in protein and have a limited amount of reducing sugar and water. The Maillard reaction-related studies carried out so far in aqueous food matrices and model studies are incoherent to describe the reaction in foods that have limited water content. In addition, the sugar found in nuts and seeds is mainly in the form of sucrose and due to the low amount of reducing sugar, the Maillard reaction in these foods follows a different pathway than foods with high reducing sugar content and water activity.

This thesis aims to propose a kinetic model for Maillard reaction during the roasting process of low moisture foods according to their compositional characteristics, which were more critical for chemical reactions, instead of their botanical nomenclature. Within this context, the change in the concentration of sugars and amino acids as reactants, thermal contaminants such as HMF and AGEs, and also α-dicarbonyl compounds formed as a result of the Maillard reaction were monitored induced by the roasting process applied at different temperatures and times. The reaction mechanism

1

and interrelation between reactants and products were tried to be enlightened by using the multiresponse kinetic modeling approach.

In the first part of the thesis, the general composition and profile analysis of the ingredients have been performed in nuts and seed samples. By this way, concentrations of reactants and differences in compositional and physicochemical characteristics between samples were determined.

In the second part, in order to be able to explain formation and elimination reactions, the changes in the concentration of Maillard reaction and sugar degradation reactants and products were monitored in roasted samples.

In the last part, a kinetic model was proposed for the Maillard reaction by using a multiresponse kinetic modeling approach. Thus, the complex reaction mechanism was tried to be enlightened in low moisture food systems. In addition, a simplified kinetic model was proposed for the formation of ACR during roasting in low-moisture systems.

2. GENERAL INFORMATION

2.1. Nuts & Seeds

The consumption of nuts and seeds as snacks has increased together with increased demand for healthy food in recent decades. These snacks can be consumed raw or after being roasted. They also find an area of use in bakery products such as bread, cake, and cookie. In recent years nuts and seeds are considered a member of dietary guidelines because of their health-protective effects (Kalogeropoulos et al., 2013).

Sunflower (*Helianthus annuus* L.), seeds are used directly for human consumption as a snack or source of vegetable oil but also it can be incorporated into food formulations. Turkey's production of sunflower is approximately 1950000 tons per year. Sunflower seed is rich in oil, so sunflower seed oil has a great economic value by being one of the major vegetable oil sources for Turkey. The sunflower seed oil has a high amount of unsaturated fatty acids. Linoleic acid is the main fatty acid comprising 22% of total fatty acids and is followed by oleic acid (18%) (Chung et al., 2013). The content of unsaturated fatty acids, protein, fibers, minerals, and vitamins makes sunflower seeds nutritious. The protein content of sunflower seed is approximately 20%. Sulphuric amino acids are particularly abundant and also glutamic acid, aspartic acid, and arginine are present at significant levels. Sunflower seed contains a considerable amount of vitamin E (37.8 mg/100 g). The tocopherol content of sunflower seed is ranged from 314.5 to 1024.5 mg/kg seed (Guo et al., 2017). The most abundant tocopherol is α-tocopherol, with levels of 88.4% to 96.3% of the total tocopherols (Velasco et al., 2003). Vitamin E and other tocopherol content make sunflower seed a valuable source for protection against cardiovascular disease and cancer by their antioxidant properties. Sunflower seeds have also high amounts of vitamin A, B, C, and selenium, magnesium, calcium, phosphorus, iron, potassium, and zinc (Guo et al., 2017).

Pumpkin seed (*Cucurbita moschata* L.) can be consumed as a roasted and salted snack. Pumpkin seeds are preferred in the human diet recently for their anticholesteremic, antioxidant, anticancer, and anti-inflammatory effects (Wang et al., 2017). Seeds have a significant amount of protein, polyunsaturated fatty acids (PUFA), minerals (magnesium, phosphorous, copper and potassium, iron, zinc, manganese), carotenoids, β-carotene, and γ-tocopherol (Patel and Rauf, 2017). Seeds are rich in oil with a rate of 49% of seed; linoleic acid is the most predominant fatty acid (55% of total fatty acid)

followed by oleic acid. Protein and carbohydrate content comprises 30% and 10% of the seed, (USDA, 2018). Pumpkin seeds contain all essential amino acids with a high amount of glutamic acid, aspartic acid, and arginine (Glew et al., 2006, Chung et al., 2013). β-sitosterol is the most predominant phytosterol, with 24.9 mg/100 g seed. The total phenolic content of pumpkin seed oil ranges from 25 to 51/mg gallic acid equivalent/kg of oil and consists of vanillin, tyrosol, luteolin, sinapic acid and vanillic acid (Patel, 2013).

Flaxseed is also known as linseed (*Linum usitatissimum* L.) is produced mainly in Kazakhstan with 933000 tones in 2018 followed by Canada and Russia. Flaxseed has considerable attention because of its beneficial health effects due to its high content of unsaturated fatty acids, dietary fiber components, and phytochemicals such as lignans. The oil fraction constitutes 41% of flaxseed as the most predominant fraction followed by dietary fiber (28%), protein (20%), moisture (7.7%), and ash (3.4%). α-Linolenic acid comprises 58.3% of total fatty acids and makes flaxseed a remarkable source of ω-3 fatty acids. The prevalent amino acids in flaxseed are arginine, aspartic acid, and glutamic acid, and reported protein content varies from 10 to 31%. The soluble and insoluble fiber content of flaxseed is 10% and 30%, respectively. This soluble fiber is composed of L-rhamnose (25.3%), L-galactose (11.7%), L-fructose (8.4%), and D-xylose (29.1%), L-arabinose (20%) and D-xylose/D-galactose (76%). Cellulose (7-11%), lignin (2-7%), and acid detergent fiber (10-14%) fractions constitute insoluble fiber content (Shim et al., 2014). γ-Tocopherol is particularly abundant and δ-tocopherol is ranked second. Flaxseed also contains bioactive compounds such as lignans, *p*-coumaric acid, and ferulic acid. Lignans are known as effective to reduce cardiovascular diseases and inhibit the development of diabetes. The secoisolariciresinol content -major lignan in flaxseed- ranges from 3400 to 7400 mg/kg and makes flaxseed one of the richest sources of lignans in the human diet (Hyvärinen et al., 2006, Tuncel et al., 2017, Bekhit et al., 2018). Flaxseed can be used for fortification of food products due to its ω-3 and ω-6 essential fatty acid, dietary fiber, lignan, vitamin, mineral, and phytosterol content. Thermal process such as roasting is generally applied to flaxseed prior to addition into food products or consumption directly without any food product. Thermal pre-treatment makes flaxseed more chewable and crackable and in this way increases digestibility and bioavailability. Furthermore, the toxicity of cyanogenic glycosides, found in raw flaxseed, is reduced by thermal or solvent treatment. Cyanogenic glucosides may

degrade to a highly toxic compound, hydrogen cyanide (HCN) due to β-glucosidase enzyme activity, a naturally existing enzyme in the flaxseed cell wall. If flaxseed is consumed directly, β-glucosidase enzyme can be active until it reaches the acidic media of the stomach. In the intestine, the enzyme can reactivate due to alkaline conditions which causes poisoning by HCN formation from cyanogens. Thermal treatment reduces total cyanogens or inactivates the β-glucosidase enzyme and so prevents the release of HCN (Tuncel et al., 2017, Bekhit et al., 2018, Feng et al., 2003).

Peanut (*Arachis hypogaea L.*) is an oilseed crop grown in many regions of the world mostly in India (FAO, 2018). Peanut belongs to the legume family but its oil content makes peanut one of the important oilseeds, furthermore, peanut has a great area of use in food products because of its nutritional potential and also organoleptic properties (Arya et al., 2016). Raw or thermally processed peanuts are consumed all around the world. Roasting treatment is used to achieve a desired flavor and color development by affecting physical and sensorial properties. Peanuts are not only consumed directly or roasted as a snack but are also used for the production of peanut butter, peanut oil, peanut paste, peanut flour, peanut beverage or can be incorporated into confections, snack products, soups, and desserts (Arya et al., 2016, Shi et al., 2018). Peanut has great nutritional potential due to its composition. The reason of this is the presence of these components in their most available and beneficial forms such as plant origin protein, unsaturated fatty acid, complex carbohydrates as dietary fiber. The lipid, protein and carbohydrate content of peanut are 50%, 25%, and 16%, respectively. These values are precisely dependent on the cultivar and environment. Oleic acid is the most prevalent fatty acid followed by linoleic acid and palmitic acid (Rodrigues et al., 2011). The major carbohydrates are sucrose and starch whereas the minor are reducing sugars. Peanut contains all of the 20 amino acids with different proportions and arginine is the most abundant amino acid. The members of the legume family such as peanut or soybean are demonstrated to have protein quality equal to meat or egg proteins. Due to its plant-based origin, peanut proteins are readily available and exist together with bioactive compounds when compared with animal protein sources so these give the peanut high nutritional and commercial value (Arya et al., 2016, Rodrigues et al., 2011). Furthermore, peanut contains significant amount of niacin, vitamin E, Coenzyme Q10, resveratrol, phenolic acids, flavonoids and phytosterols what makes peanut a good source of functional compounds. Vitamin E in oil, caffeic acid, chlorogenic acid, ferulic

acid, coumaric acid, stilbene and flavonoids (resveratrol) content gives antioxidant acitivity to peanut. All of these bioactive components make peanut protective against coronary heart diseases (CHD), Alzheimer's disease, cognitive decline, and type II diabetes (Arya et al., 2016, Win et al., 2011).

Almond (*Prunus dulcis*) is one of the most important tree nuts consumed all around the world. Besides its beneficial health effects, almond is consumed raw or roasted or used as an ingredient in food products owing to its unique flavor and taste. Almonds can be incorporated into bakery products, sweets, chocolate, biscuits, desserts, drinks, salads, sauces, and ice creams (Kong and Singh, 2009). Almond is widely accepted as a healthy food that reduces cardiovascular and obesity-related diseases and has anticancer activity due to their fatty acid profile and phenolic content (Kong and Singh, 2009, Lin et al., 2016). The oil content of almond is approximately 50% and unsaturated fatty acids particularly oleic and linoleic acid are the most prevalent constituents (Kong and Singh, 2009). This profile affects the cholesterol level of blood; reduces low density lipoprotein (LDL) and increases high density lipoprotein levels (Lin et al., 2016). These beneficial fatty acids are protected against oxidation by phenolic compounds in almonds that have an antioxidant activity such as proanthocyanidins, anthocyanin, flavan-3-ols, flavonols, and flavanones, isoflavones, lignans, and phenolic acids. Additionally, the other constituents that show antioxidant activity such as α-tocopherol and phytosterols, prevent the oxidation of fatty acids (Bolling et al., 2010). According to the U.S. Department of Agriculture, the protein, carbohydrate, and ash content of almond is 21%, 21,5%, and 3%, respectively. Almond is rich in manganese, copper, potassium, phosphorus, magnesium, and calcium. In addition to its mineral profile, almond is an excellent source of niacin, riboflavin, and vitamin E. Sucrose is the predominant carbohydrate whereas the amount of reducing sugars such as glucose, fructose are more less compared with sucrose (USDA, 2018).

2.2. Roasting

Roasting is an important process for nuts and seeds that provides desirable flavor, aroma, color, and also texture such as crispness thereby improving overall acceptability (Bagheri et al., 2016). Roasting is generally performed at 130-200 °C (Cämmerer and Kroh, 2009, Damame et al., 1990, Lin et al., 2016, Win et al., 2011). These harsh temperatures cause a decrease in the moisture content and so provide prolonged storage. During roasting, the intensity of the yellow-brown pigments formed during roasting, namely changes in the color, is a quick and simple indicator to obtain the best flavor and sensory properties (Shi et al., 2017, Shi et al., 2018). In addition to this, the water activity and moisture content also affect chemical reactions occurring during the roasting process and thereby organoleptic properties.

Roasted nuts and seeds are popular snacks consumed all around the world and they also can be incorporated into favored food products. One of the important goals of the roasting process is the alteration of aroma compounds. Raw products generally contain lower amounts of volatile compounds compared with roasted products. In roasted almonds, the most predominant volatiles are benzyl alcohol and Strecker aldehydes such as benzaldehyde and methional, and also pyrazine, pyrrole, and furan type compounds form due to the sugar degradation and Maillard reaction (Agila and Barringer, 2012, Valdés et al., 2015, Xiao et al., 2014). Pyrazine compounds such as 2,3,5-trimethylypyrazine, 2,5-dimethylpyrazine, 2,3-dimethylpyrazine, and methylpyrazine were detected in roasted peanuts in variable amounts according to genotypes and also pyrazines are attributed to nutty/roasted flavor (Baker et al., 2006, Liu et al., 2011, Lykomitros et al., 2016).

Textural modifications observed in roasted foods are related to microstructural changes caused by the roasting process. Organelle and cytoplasmic network disruption (Idrus and Yang, 2012), thermal modifications in protein bodies and cell-to-cell junctions (Young and Schadel, 1990, Young and Schadel, 1993), swollen epidermal cells on the inner surface, and broken cell walls of parenchyma tissue (Eitenmiller et al., 2011) are certain alterations found in roasted peanuts.

Apart from the physical changes, some chemical reactions occur with desirable consequences as well as undesirable ones. Maillard reaction, sugar degradation, lipid oxidation, protein denaturation, vitamin degradation are the major reactions that take

place in the roasting process. Inactivation of enzymes such as lipase, lipoxygenase is another subsequence as might be expected due to protein denaturation. Roasting also causes the inhibition of microorganisms because of high temperatures (Durmaz and Gökmen, 2010).

Maillard reaction is induced by the interaction between the amino compound and the carbonyl group of reducing sugars. As a consequence, the Maillard reaction cause decrease in total amino acid content, in particular, essential amino acids such as lysine due to its reactivity (Martins et al., 2000). Along with these nutritional losses, undesirable compounds may also be generated through a variety of pathways as a result of the Maillard reaction. The reaction between free asparagine and carbonyl compounds such as reducing sugars, hydroxycarbonyls, dicarbonyls, and lipid oxidation products at temperatures above 120 °C leads to the formation of ACR (Stadler et al., 2004, Zamora and Hidalgo, 2008, Zyzak et al., 2003, Motram et al., 2002, Yaylayan et al., 2003). This compound is classified as a 2A human carcinogen and also has neurotoxic properties (IARC, 1994). Another toxic compound formed by the Maillard reaction is furan, referred to as a possible human carcinogen (Group 2B) (IARC, 1995). Yaylayan (2006) stated that thermal degradation of carbohydrates is a primer source for furan generation, followed by thermal oxidation of ascorbic acid, PUFAs, and carotenoids. The other neo-formed contaminant, HMF, is an important intermediate product generated in Maillard reaction even at low temperatures. HMF is formed mainly through Maillard reaction or sugar decomposition (Kroh, 1994). The conversion of HMF to sulfoxymethylfurfural which is reported to be a genotoxic and nephrotoxic compound makes HMF responsible for negative health effects. It has been demonstrated that high concentrations of HMF are cytotoxic and cause damage to the eyes, skin, respiratory tract, and mucous membrane (Capuano and Fogliano, 2011, Perez Locas and Yaylayan, 2008). α-Dicarbonyl compounds formed as an intermediate product via sugar degradation and lipid oxidation can react with amino acids and catalyze the formation of advanced glycation end products (AGEs) (Göncüoğlu Taş and Gökmen, 2017, Kocadağlı and Gökmen, 2016, Wellner et al., 2011). It has been reported that AGEs are associated with diabetes and also other diseases such as rheumatoid arthritis, Alzheimer's disease, and end-stage renal disease (Singh et al., 2001).

Besides all these undesirable consequences, new compounds are formed having antioxidant activity named melanoidins. It should not be ignored that the Maillard

reaction also causes degradation of naturally existing antioxidants. Therefore, the antioxidant capacity of roasted foods depends on the balance between newly formed antioxidants and remaining natural antioxidants. The melanoidins formed through the Maillard reaction may eliminate the loss of naturally found antioxidants by improving oxidative stability and delaying rancidity (Cämmerer and Kroh, 2009).

2.3. Maillard Reaction

Maillard reaction, also known as nonenzymatic browning, was first discovered by Louis-Camille Maillard in 1912 (Maillard, 1912) via synthesizing glycine peptides in a heated glycerol system by using aldose sugar in amino acid reaction and thereby forming brown colored products (Namiki, 1988). Maillard reaction provides desired brown color and contributes to the improvement of aroma, flavor, and taste as well. In spite of that, Maillard reaction is also responsible for loss of nutritional value of proteins and formation of mutagenic and toxigenic compounds such as furan, ACR and HMF (Capuano and Fogliano, 2011, Cho and Lee, 2014, Rufián-Henares and Pastoriza, 2016). Besides these negative effects, as a result of the Maillard reaction, compounds that have antioxidant activity are formed (Manzocco et al., 2000).

Factors that influence the Maillard reaction are summarized by Namiki (1988). According to Figure 2. 1, pH, moisture content, temperature, sulfite, oxygen, light, heavy metal ions, and certainly reactants can affect the Maillard reaction and cause changes in product distribution. Therefore, the characteristic consequences of browning reaction are extremely dependent on the reactants as much as reaction conditions. The reactant pool is composed of protein, peptide, amino acid, amine, ammonia, and carbonyl compounds, reducing sugar (from oxidation of fatty acids, ascorbic acid, and polyphenols) (Namiki, 1988).
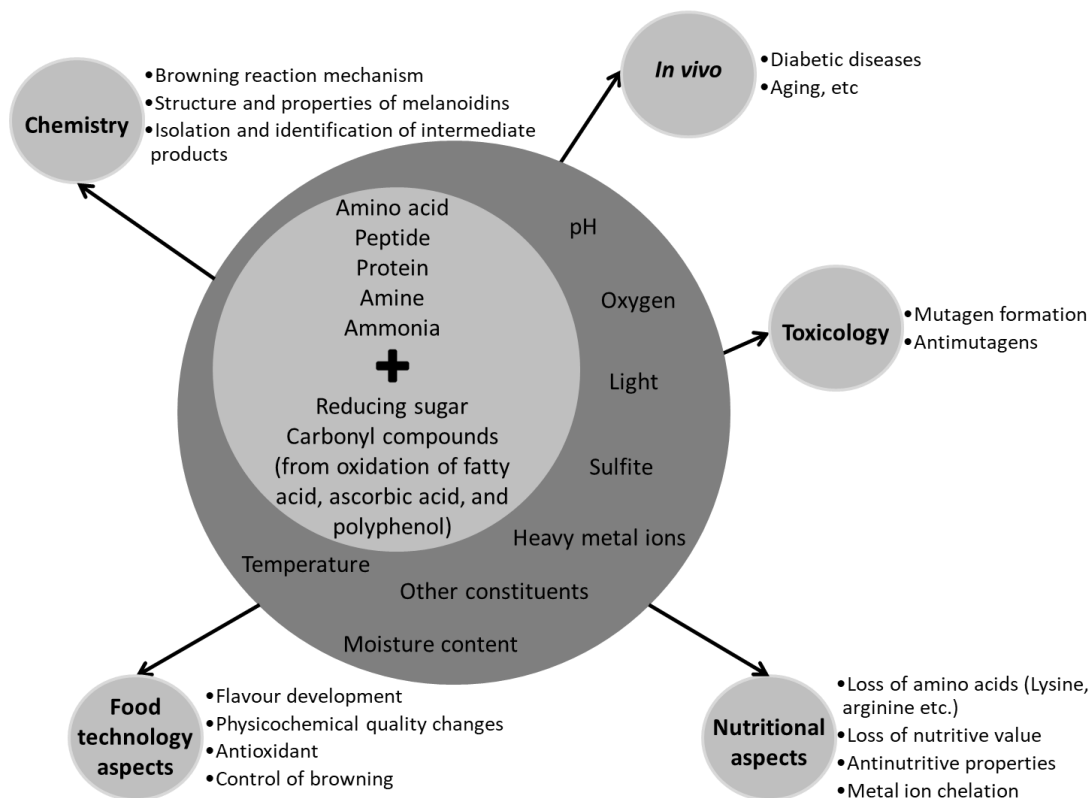
Figure 2. 1 Reactants and factors influencing Maillard reaction and consequences of Maillard reaction, adopted from Namiki (1988)

The monomers – monosaccharides, amino acids, fatty acids, and alcohols- of main components –carbohydrates, lipids and proteins- of food have four different functional groups which are -OH, -COOH, -NH$_2$, and –CHO. The first stage of nonenzymatic browning reaction starts between –CHO and NH$_2$ groups and glycosyl-amino product is formed reversibly. Besides, its products rearrange to form Amadori compound and yield ketosyl-amino products which are subjected to irreversible reactions such as rearrangement, dehydration, and scission. As a result, decomposed and polymerized products are generated including melanoidins and flavor compounds (Namiki, 1988).

As mentioned above the reactants and precursors affect the Maillard reaction and as a consequence, the reaction proceeds with different pathways due to the chemical forms and reactivity of reactants. For instance, aldoses and pentoses lead to more browning rate than ketoses and hexoses, respectively. Also, acidic amino acids are less reactive than basic amino acids (Namiki, 1988). The water content of food is another factor that affects the rate of Maillard reaction. Mobility and reactant solubility and thus rate of chemical reaction increases as water activity increases. The rate of the Maillard reaction

also increases with an increase in water activity and reaches up to a maximum in the range of water activity of 0.65 to 0.75 (Wong et al., 2015). At lower water activity levels, there are not enough dissolved reactants and diffusion becomes limited. However, at high water content, the concentration of reactants is diluted and becomes too low for a high reaction rate even if adequate reactants are dissolved and diffusion occurs easily. In both cases, the Maillard reaction is restricted due to these mentioned effects (Baltes, 1982). Although the Maillard reaction chemistry is focused on mainly aqueous medium, this reaction can also proceed in limited moisture and low water activity environment (Wong et al., 2015). According to the study carried out by Wong et al. (2015), moisture content can affect the reactivity of sugars. They found that while glucose is more reactive at 0% moisture, fructose becomes more reactive at 5-10% moisture. They also showed that at 0% moisture, the browning rate followed pseudo-first-order kinetics in the presence of glycerol, whereas in the absence of glycerol zero-order reaction kinetics was observed.

Maillard reaction is a consecutive and complex reaction system. The scheme generated by Hodge is generally accepted to explain diverse pathways of reaction comprehensively (Hodge, 1953). According to Hodge, the Maillard reaction can be divided into three stages: early, advanced and final stages (Figure 2.2).
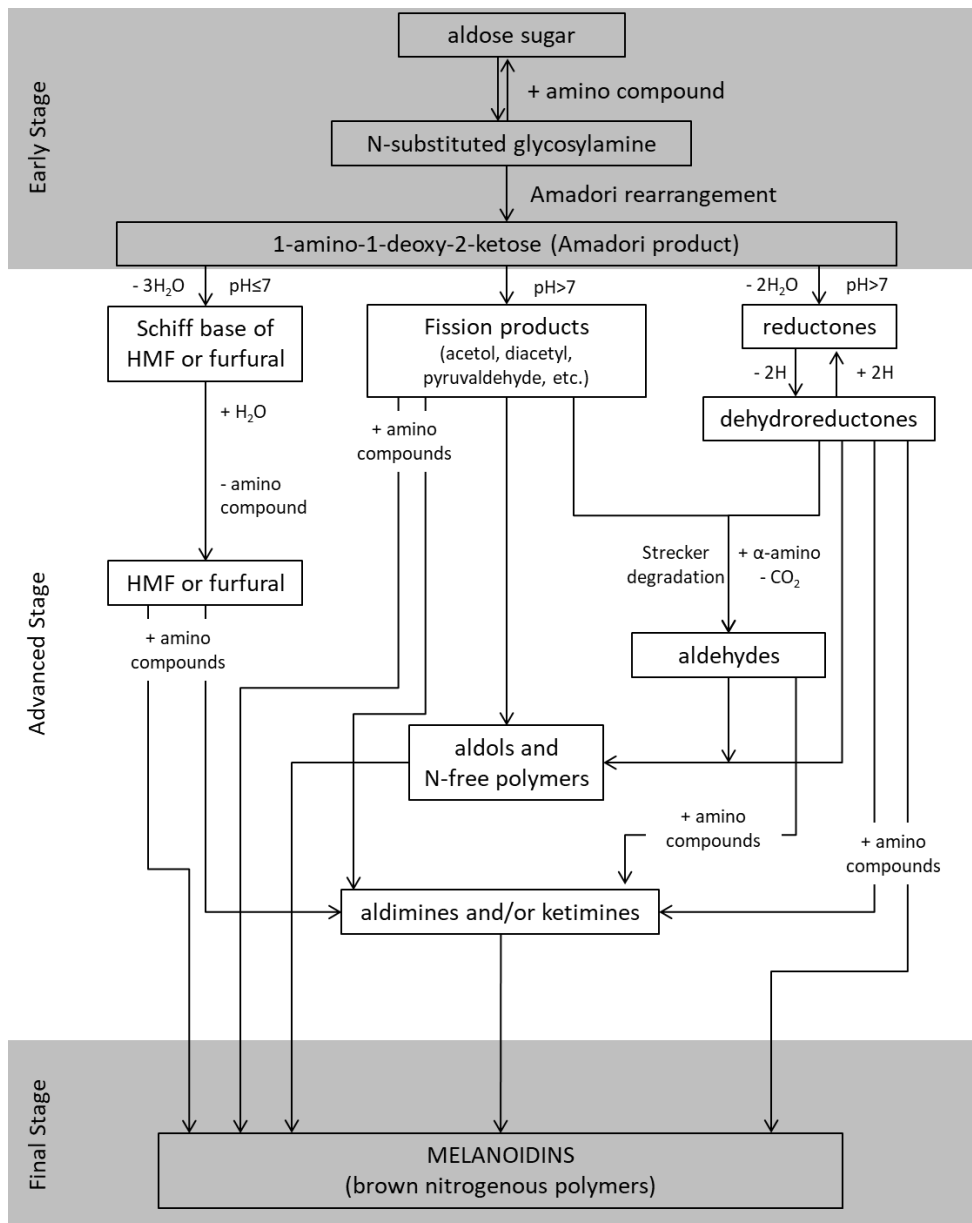
Figure 2. 2 The scheme of Maillard Reaction, adapted from Hodge (1953)

The early stage of the Maillard reaction begins with the condensation of the reducing sugar with a compound with a free amino group, followed by the formation of N-substituted glycosylamine. Until this point reaction occurs reversibly. This unstable compound, N-substituted glycosylamine, rearranges to form Amadori product (1-amino-1-deoxyketose) (Amadori, 1929) subsequently when the aldose sugars are present, and Heyns product (2-amino-2-deoxyaldose) (Heyns and Meinecke, 1953) from ketose sugars through enolization reaction (Figure 2. 3). Amadori compound is claimed to be the first stable compound of the Maillard reaction (Namiki, 1988). Amadori products further can degrade or react with other components in food and in this way have an important role in

the development of characteristic baked and roasted food aroma as well as desired brown color (Yaylayan and Huyghues-Despointes, 1994).
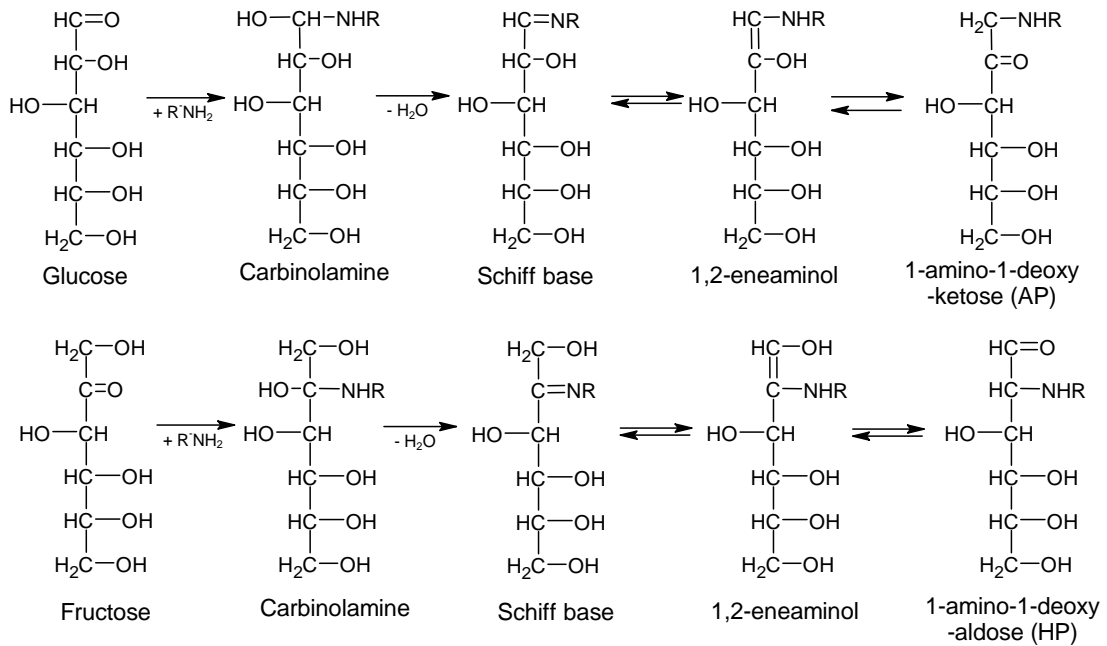
Figure 2. 3 Formation of Amadori and Heyns product

Amadori products can be degraded to furoyl derivatives during acid hydrolysis of food samples. Thus, quantification of protein-bound Amadori products that formed in the early stages of the Maillard reaction, becomes possible (Erbersdobler and Somoza, 2007, Henle et al., 1995). ε-N-(2-furoylmethyl)-L-lysine, known as furosine, is a derivative of N-ε-fructosyllysine (Amadori compound of lysine) and is regarded as a suitable and important indicator for thermal process and inappropriate storage conditions (Rada-Mendoza et al., 2002). Moreover, measuring the furosine content allows the determination of loss in lysine content. Furosine is generally used as a parameter for nutritional evaluation of heat-treated food products such as fruit-based infant foods, jams (Rada-Mendoza et al., 2002), cookies (Gökmen et al., 2008), milk-based sports supplements (Rufián-Henares et al., 2007). Its exposure can induce of DNA damage even at 50 mg/L concentration (Saeed et al., 2017). Additionally, furosine content is an index of dietary intake of AGEs and protein damage from heat treatment (Gökmen et al., 2008). Since furosine is a marker of lysine reaction products that are not nutritionally available, such as the Amadori product, the bioavailability of lysine can also be measured via furosine content (Erbersdobler and Somoza, 2007).

In the advanced stage of the Maillard reaction, Amadori product (AP) and Heyns product (HP) may undergo degradation reactions, and as a result, depending on pH, several α-dicarbonyl compounds are formed. Methylglyoxal (MGO), glyoxal (GO), dimethylglyoxal (DMG), glucosone (G), 3-deoxyglucosone (3-DG), and 1-deoxyglucosone (1-DG) are some of these dicarbonyls.

The major pathways for α-dicarbonyl formation are retro-aldol reactions and α- and β-cleavages (Gobert and Glomb, 2009). Amadori products can take part in enolization and degradation reactions much easier than the sugars that are unreacted. Amadori products undergo enolization reactions between C atoms 1- and 2- as so C atoms 2- and 3-. In basic conditions, the 2,3-enolization reaction is dominated and as a result, reductones and fission products like DMG and acetol are produced. Hereunder, the elimination of the C-4 hydroxyl group promotes the formation of 1-amino-1,4-dideoxy-2,3-hexodiulose whereas the elimination of C-1 amino group and subsequent retro-Michael reaction promotes 1-deoxy-2,3-hexodiulose, namely 1-DG formation. Water elimination from 1-DG leads to the formation of DMG and this alteration makes 1-DG is important for flavor development (Hirsch et al., 1995). The decomposition of 1-DG also leads to the formation of pyruvaldehyde, hydroxydiacetyl, and acetylfuran (Baltes, 1982). On the other hand, in an acidic medium, a 1,2-enolization reaction occurs and eneaminols are formed. Then hydrolytic scission of amine residue, β-elimination, of C-3 hydroxyl group leads to the formation of 3-deoxy-2-hexosuloses, namely 3-DG. As dehydration reactions and displacement of double bond, further reactions lead to formation of 5-hydroxymethyl furfural (HMF) in the presence of hexose sugars and furfural from pentose sugars (Baltes, 1982, Yaylayan and Huyghues-Despointes, 1994).

H$_2$C—NH—R   HC—NH—R   HC=NH$^+$R   HC=O

C=O   C—OH   C—OH   C=O

HO—CH   HO—CH   CH   CH$_2$

HC—OH   HC—OH   HC—OH   HC—OH

HC—OH   HC—OH   HC—OH   HC—OH

H$_2$C—OH   H$_2$C—OH   H$_2$C—OH   H$_2$C—OH

$-H_2O$ $+H_2O$ / $-RNH_2$

1-amino-1-deoxy-ketose   1,2-eneaminol   iminium ion   3-deoxyglucosone

H$_2$C—NH—R   H$_2$C—NH—R   CH$_2$ CH$_3$

C=O   C—OH   C—OH   C=O

HO—CH   HO—C   C=O   C=O

HC—OH   HC—OH   HC—OH   HC—OH

HC—OH   HC—OH   HC—OH   HC—OH

H$_2$C—OH   H$_2$C—OH   H$_2$C—OH   H$_2$C—OH

$-RNH_2$

1-amino-1-deoxy-ketose   2,3-enediol   enol form   1-deoxyglucosone
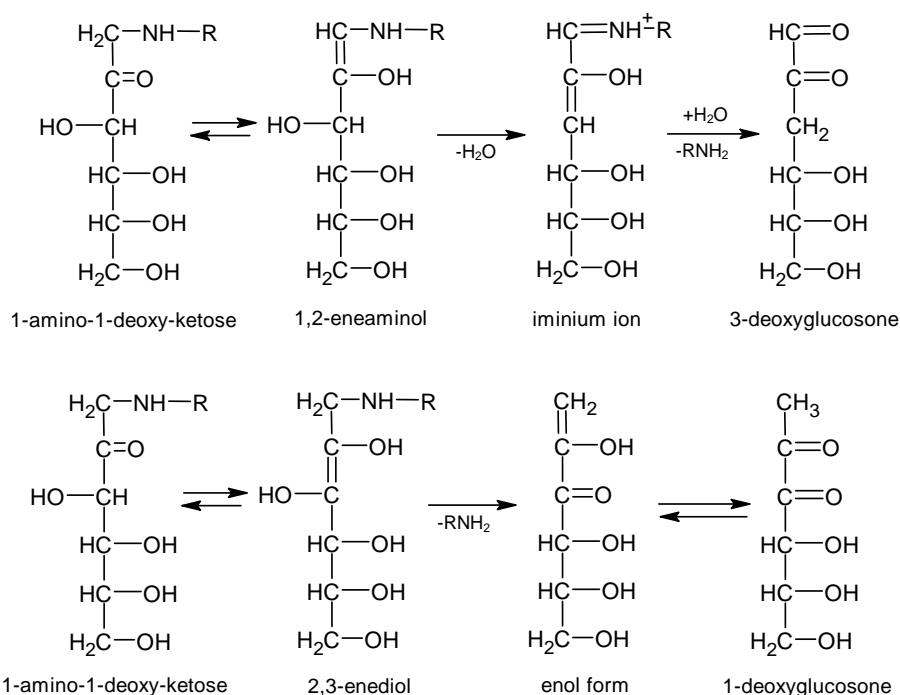
Figure 2. 4 Formation of 1-DG and 3-DG from Amadori product (Belitz et al., 2009)

Another α-dicarbonyl compound, MGO is proposed to be formed through the cleavage of bonds between C3- and C4- atoms in 1-DG and also from 3-DG via retro-aldol reactions (Weenen, 1998, Yaylayan and Keyhani, 2000, Gobert and Glomb, 2009). According to Hollnagel and Kroh (1998), GO, MGO and DMG are formed through retro-aldolization and isomerization reactions of sugar or cleavage of 1-deoxyhexosulose. Also, Thornalley et al. (1999) suggested the formation of MGO via the scission of glyceraldehyde. GO is expressed to originate directly from aldose sugars or imines via retro-aldol reactions and oxidation (Yaylayan and Keyhani, 2000, Thornalley et al., 1999). Hofmann et al. (1999) and Gobert and Glomb (2009) suggested that GO can also be formed by cleavage of the C2-C3 bond in glucosone.

It is not the only way for the formation of α-dicarbonyl compounds through the degradation of Amadori products, they can also be formed by reducing carbohydrates without the participation of amine groups, known as 'caramelization' (Figure 2. 5). Besides, α-dicarbonyl compounds may also originated from the Schiff base under the oxidative conditions, through the Namiki pathway (Hayashi and Namki, 1980). Lipid peroxidation and carbohydrate oxidation are other reactions for the formation of several dicarbonyls (Henle, 2005, Zamora and Hidalgo, 2005, Fujioka and Shibamoto, 2004). For instance, it is reported that lipid oxidation is a great source of GO and MGO

(Zamora and Hidalgo, 2005, Fu et al., 1996). In the case of low water content and acidic conditions, these reactive intermediates (α-dicarbonyl compounds) are formed mainly from Amadori compounds in model systems. However, reactive intermediates generated from sugar react with amino acids and form products in case of high water content and basic conditions (Yaylayan and Huyghues-Despointes, 1994).
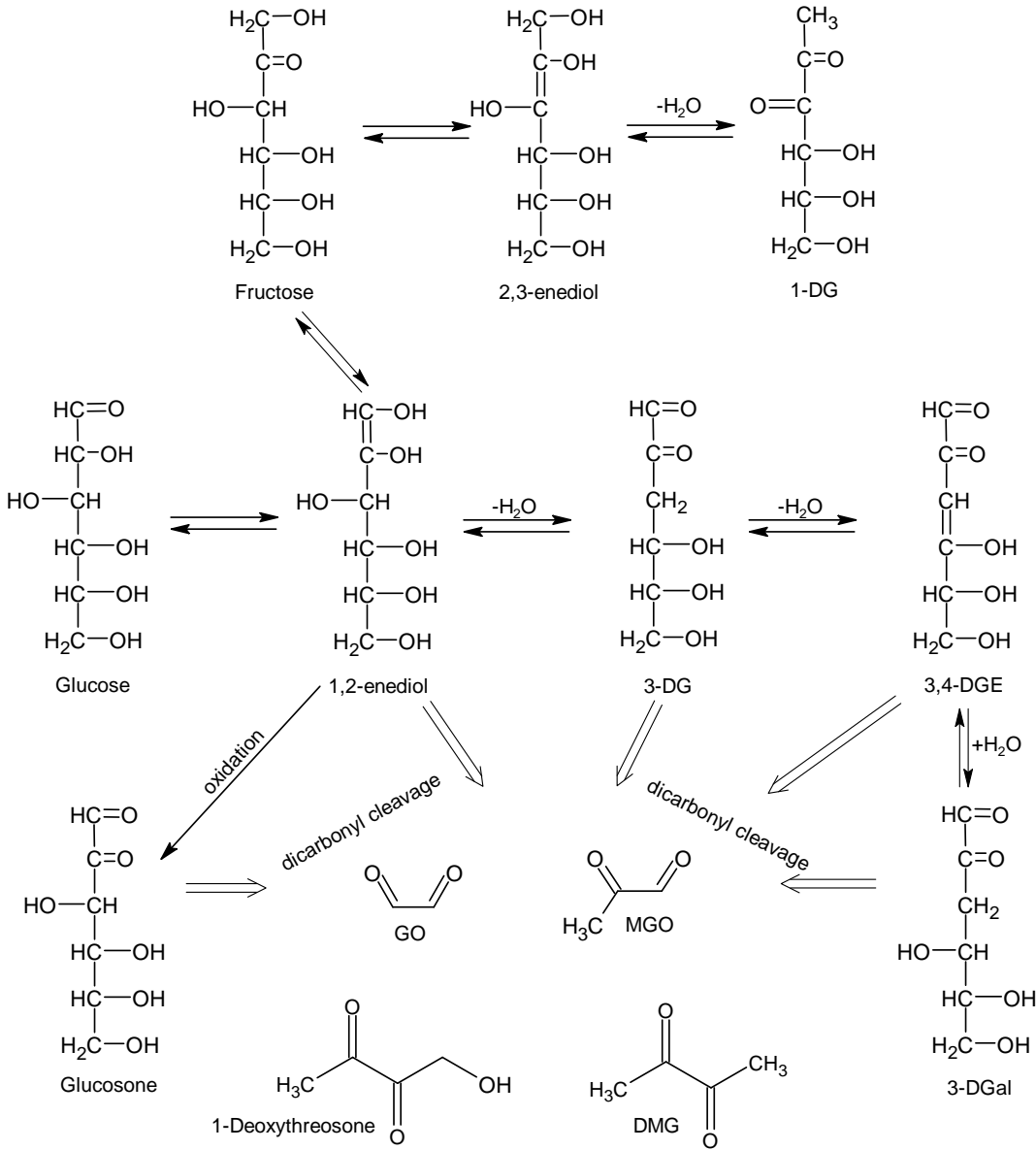
Figure 2. 5 Formation of α-dicarbonyls via degradation of monosaccharides in caramelization and Maillard reaction

α-Dicarbonyl compounds have been detected in many foods in various amounts. Rodrigues et al. (1999) identified DMG and MGO in vinegar, wine, and butter samples in the form of quinoxalines by using ortho-phenylenediamine (OPD). Weigel et al. (2004) reported the presence of GO, MGO, and 3-DG with a higher amount of 3-DG. High levels of 3-DG were found in fruit juices, balsamic vinegar, and cookies as mentioned in the study by Degen et al. (2012). Also, GO and MGO were found in commercial cookies (Arribas-Lorenzo and Morales, 2010). According to Kocadağlı and Gökmen (2014), the dominant α-dicarbonyl is 3-DG in baby foods such as canned fruit, cereal-based infant formula, and vegetable puree, whereas glucosone, 1-DG, GO, MGO and DMG are lower in comparison with 3-DG. In a study carried out by Gensberger et al. (2012) 3-DG, 3-deoxygalactosone, glucosone, 3,4-dideoxyglucosone-3-ene, 1-DG, and MGO were detected in high fructose corn syrup. Daglia et al. (2007) reported that dark roasted coffee contains GO, MGO and DMG in low amounts while light and medium roasted coffees have high amounts of GO and MGO.

During the Maillard reaction antioxidant, antimicrobial, antiallergenic compounds, and also desirable compounds for the development of aroma, color, and flavor are formed. However, thermal treatment and some preservation processes induce the formation of harmful compounds, expressed as neo-formed contaminants or thermal process contaminants. These compounds cause metabolic disorders due to their carcinogenic, mutagenic, and cytotoxic effects (Capuano and Fogliano, 2011). Heterocyclic amines, nitrosamines, polycyclic aromatic hydrocarbons, acrylamide, furan, furfurals, and chloropropanols are some of these contaminants (Skog et al., 1998, Tareke et al., 2002, Maga and Katz, 1979, Gökmen, 2015, Capuano and Fogliano, 2011). Among these thermal process contaminants HMF, ACR, and furan gain considerable attention due to their high toxicological potential.

HMF is generated during the Maillard reaction as an intermediate (Ames, 1992) and from acid-catalyzed dehydration of hexose sugars, namely caramelization (Kroh, 1994). Figure 2. 6shows the formation pathways of HMF from reducing sugars. During caramelization, reducing sugars take place in 1,2-enolization, dehydration, and cyclization reactions. The type of sugar affects the way of reaction. For instance, fructose is more reactive than glucose. Temperature is another factor that affects caramelization likewise caramelization occurs at higher temperatures than the Maillard reaction. As well as in caramelization, the temperature is also an important factor for the

formation of HMF via Maillard reaction (Morales, 2008). High-temperature thermal treatment accelerates the formation of HMF but also inappropriate storage conditions of carbohydrate-rich foods cause HMF formation (Capuano and Fogliano, 2011). HMF, can be used as a quality indicator, as fresh and untreated foods do not contain HMF. Nevertheless, it should not be ignored that in the case of harsh and prolonged thermal process conditions, HMF content may cause misleading results since it undergoes decarboxylation, oxidation, dehydration, and polycondensation reactions (Morales, 2008). In this situation, the measured HMF amount is the difference between formed and degraded HMF. Also, HMF loss can be occurred due to its volatility in baking or roasting processes (Agila and Barringer, 2012). The presence of HMF was detected in a wide variety of foods. Therefore, HMF was used as a quality marker in foods such as honey (Zappalà et al., 2005), beer and fruit juices (Yuan and Chen, 1998, Kim and Richardson, 1992), bakery products (Ramírez-Jiménez et al., 2000), breakfast cereals (Rufian-Henares et al., 2019), and milk or cereal-based baby foods (Gökmen and Şenyuva, 2006). It is already known that HMF is irritating to the eyes, skin, upper respiratory tract, and mucous membrane and also has cytotoxic effects at high concentrations (Capuano and Fogliano, 2011). HMF consists of the carbonyl group, furan ring, and allylic hydroxyl group that gives reaction with amines to form Schiff base and Michael addition. This feature affects the biological reactivity and circumstances of HMF in the body (Morales, 2008). Although the effects of HMF on health are still contradictory, the main probem about HMF is its conversion to 5-sulfoxymethylfurfural. Sulfation of allylic hydroxyl group of HMF leads to the formation of 5-sulfoxymethylfurfural that shows genotoxic and mutagenic effects (Morales, 2008). Although the safe consumption amount of HMF is not clear, it is estimated that people ingest up to 150 mg of HMF per day through various foods (Shapla et al., 2018).
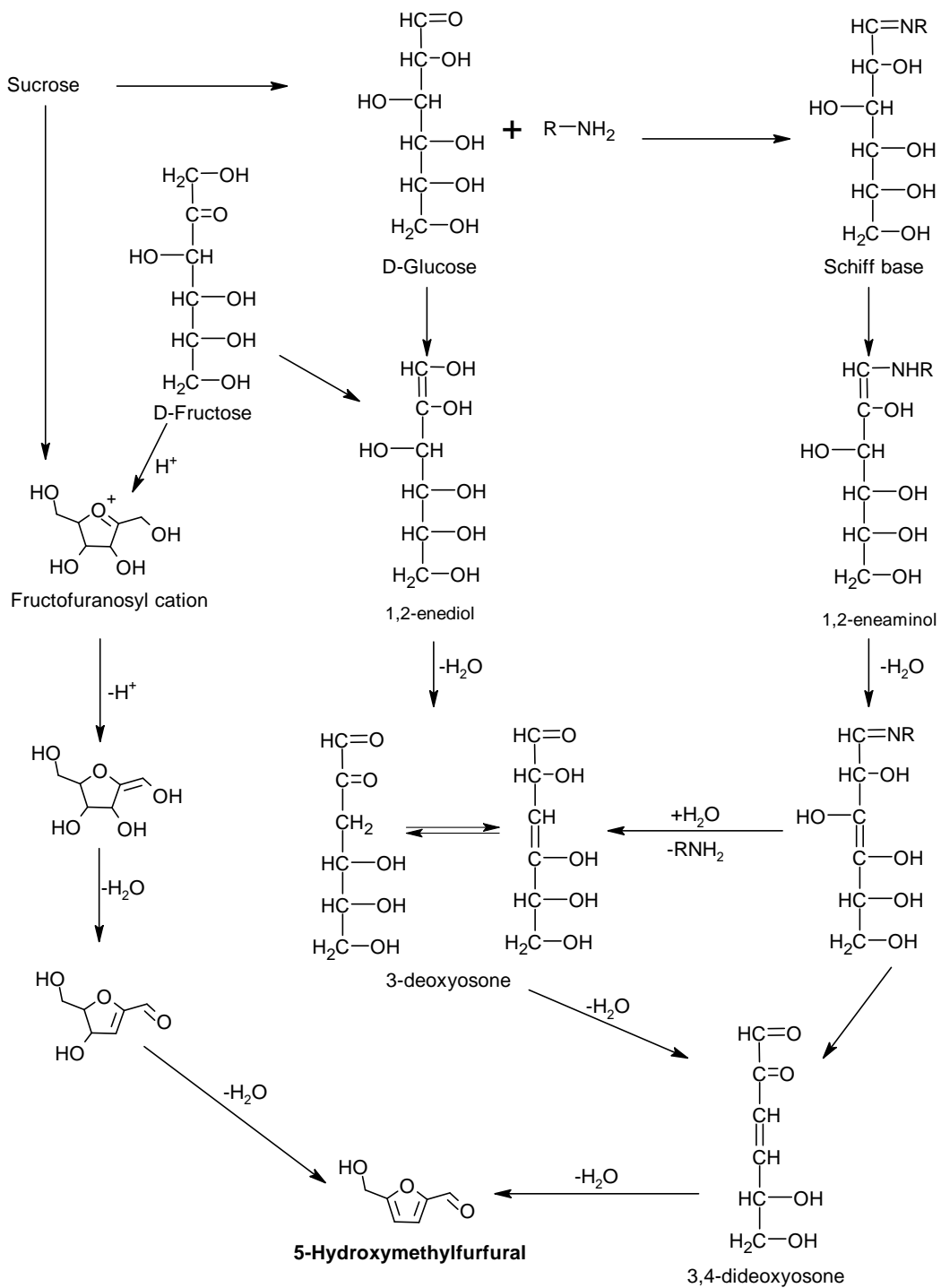
Figure 2. 6 Formation pathways of HMF (Capuano and Fogliano, 2011)

ACR (2-propenamide) is accepted as a heat-induced toxicant, following the determination of ACR in heat-processed foods such as potato chips and crisps, bread, and coffee by the Swedish National Food Administration in 2002. This report induced further research about ACR formation in foods. Classification of ACR as a possible carcinogen (Group 2A) is the reason why asparagine has gained great concern

worldwide (IARC, 1994). In addition to this exposure to high levels of ACR via inhalation or dermal absorption cause neurotoxic effects such as ataxia and skeletal muscle weakness (WHO, 2005). Also, the main metabolite of ACR, glycidamide, is assumed to be responsible for the genotoxicity of ACR (Mills et al., 2008). The average dietary intake of acrylamide in adults is 0.5 µg/kg body weight per day (Mucci and Wilson, 2008).

It was found that reducing sugars and asparagine are precursors of ACR formation (Zyzak et al., 2003, Motram et al., 2002, Stadler et al., 2002). ACR can be formed through deamination and decarboxylation of asparagine without the presence of carbonyl compounds (Yaylayan et al., 2003). However, in the presence of carbonyl groups, the formation rate of acrylamide is much higher. Therefore, as expected, higher levels of ACR are formed in foods rich in reducing sugar and free asparagine (Yaylayan et al., 2003, Capuano and Fogliano, 2011). ACR can be formed during frying, roasting, grilling, and baking processes (Mills et al., 2008). Considering all of these, the high amounts of ACR in fried potato products (Luning and Sanny, 2016), bread, bakery products (Mesias and Morales, 2016), coffee (Anese, 2016), soybean, roasted nuts, and dried fruits (Žilić, 2016) is not improbable.

The different food products exhibit varying amounts of ACR content. It is because of the difference in the composition of food material especially precursors and process conditions such as temperature, water content, and pH (Capuano and Fogliano, 2011, Mills et al., 2008). For instance, different sugar types show different reactivity. Fructose is more reactive than glucose, and glucose is more reactive than sucrose. This difference can be explained by the high mobility and lower melting point of fructose in comparison with the glucose which makes the interaction of precursors more easily (Stadler and Studer, 2016).

ACR formation can occur through various pathways. The major route is thermal degradation of asparagine in the presence of reducing sugars via the Maillard reaction (Figure 2. 7). ACR can also be formed from asparagine alone with a lower rate. Carbonyl compound reacts with asparagine to form a Schiff base (Figure 2. 8). Amadori rearrangement is not necessary for this route for ACR formation. In other words, the Schiff base of asparagine (N-glycosylamine of asparagine) is the major precursor of ACR when compared with its Amadori product (Stadler et al., 2002, Yaylayan, 2009). As shown in Figure 2. 7, decarboxylation of Schiff base yields the formation of

20

azomethine ylide which further degrades with hydrolysis to give imine 1 and imine 2. Through hydrolysis of imine 2, 3-aminopropionamide (3-APA) is generated. Finally, deamination of 3-APA directly leads to ACR formation. In another pathway, ACR may be formed directly through the 1,2-elimination of the ammonia group from imine 2. In some cases, imine 2 converts to decarboxylated Amadori product, and via β-elimination ACR can be formed in lower amounts (Gökmen, 2015, Mills et al., 2008).
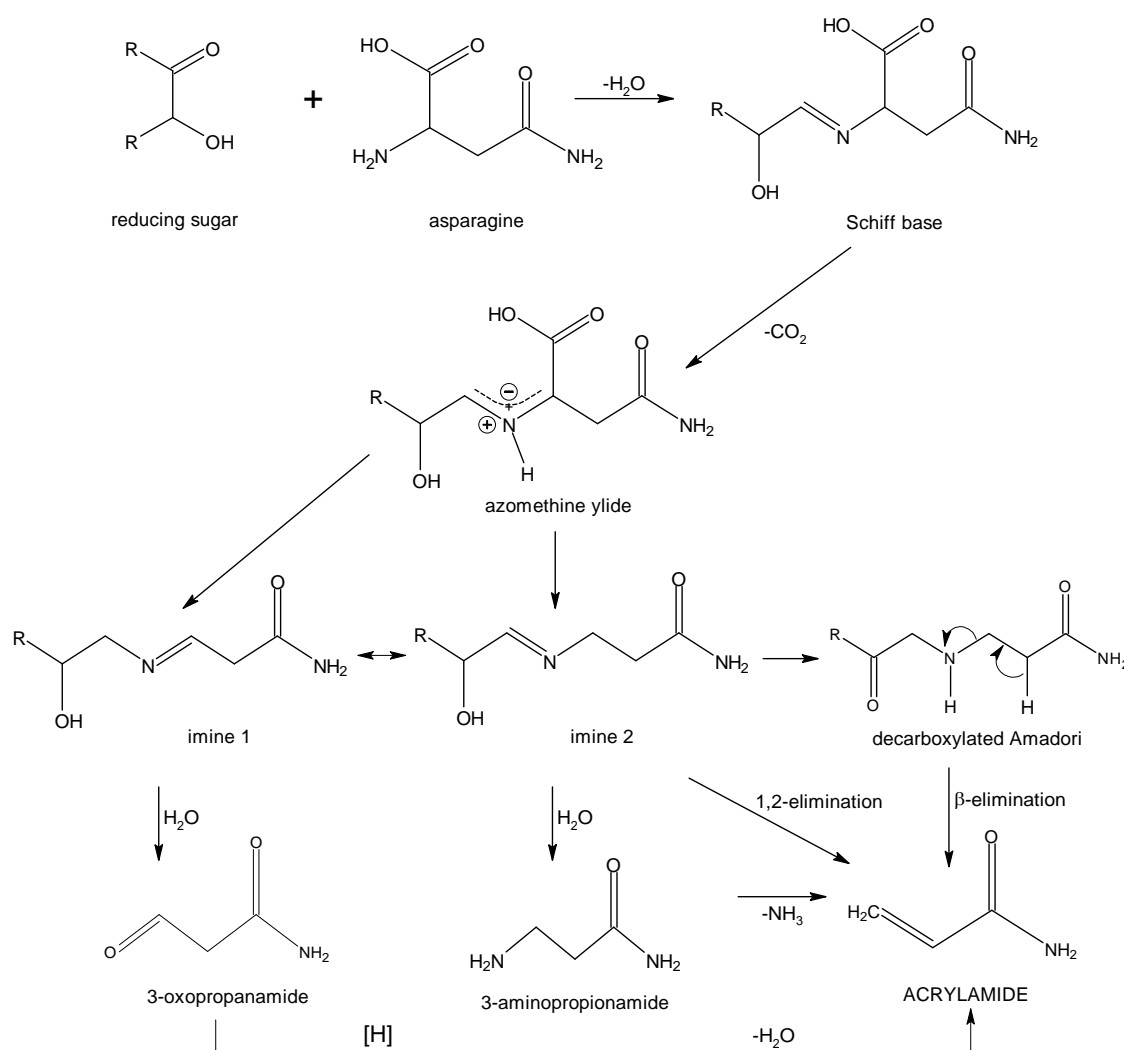
Figure 2. 7 Formation of ACR through reducing sugar-asparagine (Stadler and Studer, 2016)

21
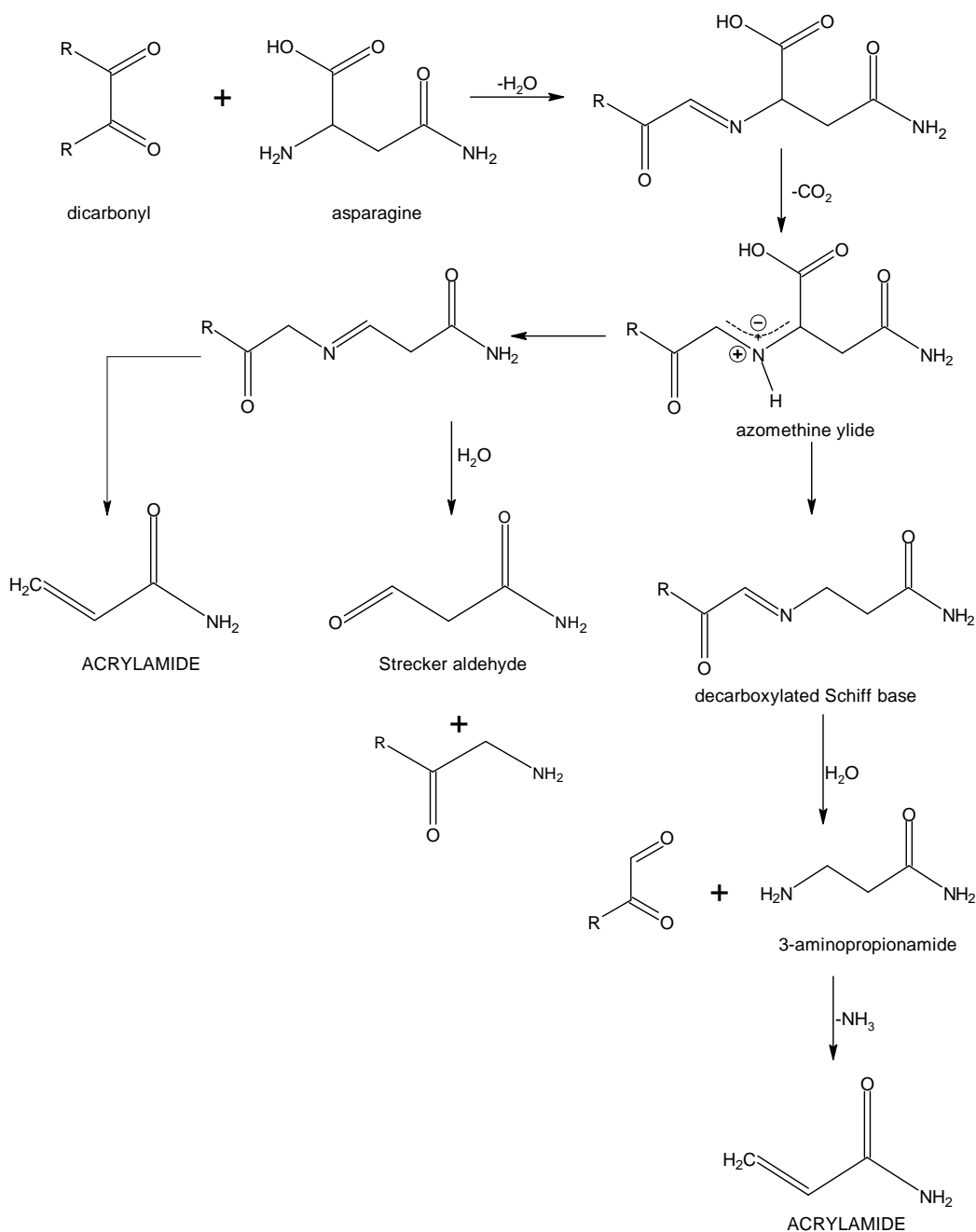
Figure 2. 8 Formation of ACR through dicarbonyl-asparagine (Stadler and Studer, 2016)

Another important source for ACR formation is acrolein. Acrolein can be generated as a result of degradation reactions of carbohydrates, amino acids, and proteins, oxidative degradation reactions of lipids, and through the Maillard reaction. When asparagine is present, acrolein gives a reaction with asparagine to form ACR and so this reaction

makes lipid systems an indirect source for ACR (Gökmen, 2015). The oxidation product of acrolein, acrylic acid, reacts with ammonia and leads to the formation of ACR (Yasuhara et al., 2003).

Strecker degradation also takes part in the advanced stage of the Maillard reaction which is a minor pathway resulting in the formation of Strecker aldehydes. These aldehydes are key intermediate for the generation of organic flavor compounds and, of course, affect the aromas of food. Amadori rearrangement products are important for Strecker degradation as being a source for α-dicarbonyl compounds during the Maillard reaction. α-Amino acids react with α-dicarbonyl compounds and α-dicarbonyl compounds behave as an oxidizing agent that causes oxidative decarboxylation and deamination of amino acids which yields in the formation of Strecker aldehydes. Meanwhile, α-dicarbonyl compounds undergo reductive amination and are converted into 2-amino-ketone as a consequence (Cremer et al., 2000, Yaylayan, 2003).

In the final stage of the Maillard reaction, reactive products formed at previous stages of the Maillard reaction and colored intermediates undergo to condense and polymerize leading to the formation of brown nitrogenous compounds named melanoidins. Melanoidins provide a characteristic brown color to foods such as coffee, cocoa, bread, malt, and honey. Therefore, the relationship between color information and Maillard reaction can be tested by color analysis. Although it is foreseen that the structure of melanoidins is affected by precursors, polymerization degree, and preparation conditions of model solutions, the structure of melanoidins is still unknown because of their complex nature (Namiki, 1988). Cyclizations, retroaldolizations, dehydrations, isomerizations, rearrangements, and condensations of low molecular weight MRPs result in the formation of melanoidins (Wang et al., 2011). Three different suggestions for the structure of melanoidin are summarized by Cämmerer et al. (2002): (1) furan and/or pyrrole polymers are formed during the advanced stages of the Maillard reaction and linked by polycondensation reactions; (2) low molecular weight colored substances cross-link with proteins through lysine or arginine α-amino groups to produce high molecular weight colored melanoidins; and (3) the skeleton of the melanoidin consists mainly of sugar degradation products formed in the early stages of a Maillard reaction, polymerized by aldol-type condensation and possibly linked by amino compounds. Melanoidins include low molecular weight (LMW) and high molecular weight (HMW) fractions and in real foods high molecular weight melanoidins are present

predominantly (Wang et al., 2011). Wang et al. (2011) supposed that LMW chromophoric melanoidins formed in the earlier stages of the Maillard reaction, polymerize or cross-link with other Maillard reaction products to produce HMW melanoidins during the later stages of the Maillard reaction. Melanoidins have functional properties such as an antioxidant and antimicrobial activity that make them a popular research area in recent years. Melanoidin fractions in foods such as coffee, bread crust, beer, biscuit, roasted cocoa, vinegar, and honey exhibit antioxidant activity *in vitro* and in *vivo via* the metal chelating property (Wang et al., 2011, Kim and Lee, 2009).

In the final stage of the Maillard reaction, α-dicarbonyls originate from the Amadori product or directly from reducing sugars, and may react with side chains of peptides or proteins in a nonenzymatic way. The term 'glycation' is used for these nonenzymatic glycosylation reactions. The products that form via these protein modifications are referred to as advanced glycation end products (AGEs). If carbonyl compounds originate from lipid peroxidation, then the term is referred to as advanced lipoxidation end products (ALEs). AGEs can be formed exogenously (in food) and endogenously (in humans), especially with greater amounts in older adults. Although AGEs are a part of normal metabolism, in the case of high levels in tissues, pathogenic effects can be observed such as alteration in structure and function of body proteins via cross-linking with them and cause inflammation through binding with receptors present on the cell surface (Uribarri et al., 2010). On the other hand, AGEs are also naturally present in uncooked animal origin foods and new AGE formation is triggered by thermal treatments such as grilling, frying, and roasting. The AGEs which accumulated in the body due to consumption of daily diets are named dietary AGEs. These dietary AGEs contribute to the AGE pool of the body (Uribarri et al., 2010, Wei et al., 2018). AGEs have been associated with diabetes, cardiovascular diseases such as atherosclerosis, neurodegenerative diseases, such as Alzheimer's disease, Parkinson's disease, vascular dementia, sarcopenia, rheumatoid arthritis, and end-stage renal disease (Luevano-Contreras and Chapman-Novakofski, 2010, Wei et al., 2018). In AGE formation, the side chains of peptide-bound lysine and arginine are the main participants. The carbonyl group of reducing sugar or its oxidation products (GO, MGO and 3-DG) reacts with an guanidino group of arginine or ε-amino group of lysine to form AGEs such as *N-ε-*carboxymethyl lysine, pyrraline, pronyllysine, pentosidine, imidazolones.

N-ε-carboxymethyl lysine (CML) is the first identified amino acid derivative and was initially found in human lens proteins and collagens (Ahmed et al., 1986). CML is generally formed through oxidative cleavage of Amadori products and also from the reaction between the lysine side chain and carbonyl compound originating from lipid peroxidation. There are several pathways for the formation of CML: (1)Amadori products such as fructoselysine, lactulosyllysine, or tagatoselysine can oxidize to form CML, (2) α-dicarbonyl compounds derived from the oxidation of glucose, glyoxal, gives reaction with a lysine residue in proteins and form CML, (3) Glyoxal originated from Namiki pathway (based on the reaction between sugars and amino compound to form a Schiff base) is also precursor for CML formation, (4) glyoxal derived from peroxidation of polyunsaturated fatty acids take place in CML formation pathway, (5) 2,4-dioxo compound formed from dehydration of Amadori product can be converted to CML; this pathway does not need an oxidizing agent, (6) The reaction between ascorbic acid and lysine leads to the formation of CML (Nguyen et al., 2013). CML was detected in various foods such as meat and fish, dairy products, rice, potatoes, pasta, soups and sauces, bread and biscuits, coffee, and fruit and vegetables (Hull et al., 2012).

2.4. Caramelization

Caramelization is another type of non-enzymatic browning reaction observed during the thermal process of food products including isomerization and sugar degradation reactions. Sugar degradation reactions are induced by isomerization reactions. In alkaline and neutral aqueous medium, monosaccharides undergo reversible ionization, mutarotation, and enolization reactions leading to the formation of isomers of monosaccharides (Brands and van Boekel, 2001). The conversion of monosaccharides into their epimers by enolization reactions is called "Lobry de Bruyn-Alberda van Ekenstein transformation" (Speck, 1958) and is followed by irreversible degradation of monosaccharides into carboxylic acids. D-fructose and D-mannose, epimers of D-glucose, can be formed from D-glucose through the formation of 1,2-enediol by the 1,2-enolization reaction. As it is reversible, this reaction results in an equilibrium of D-fructose, D-mannose, and D-glucose (Velisek, 2014).
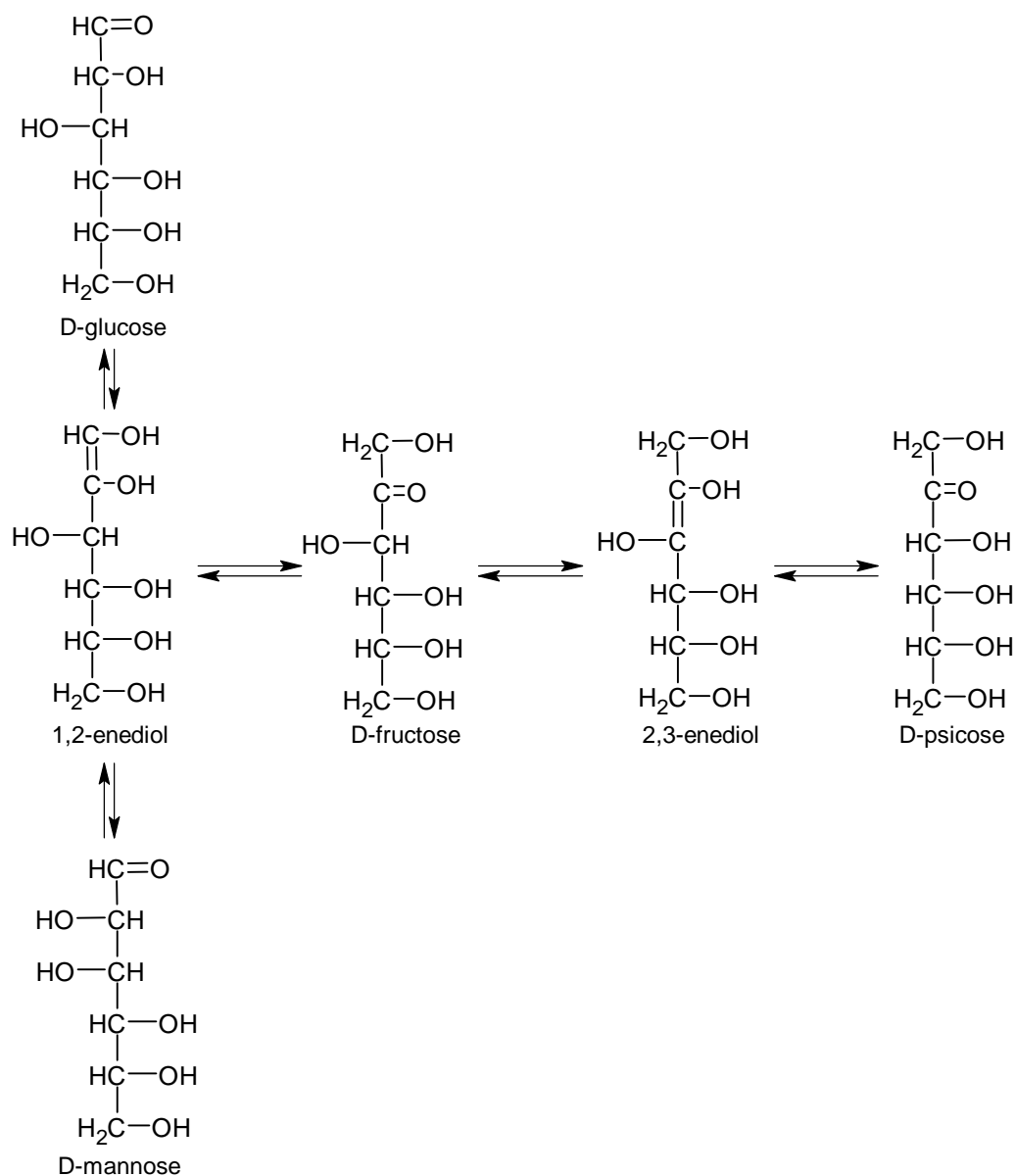
Figure 2. 9 Schematic diagram of Lobry de Bruyn-Alberda van Ekenstein transformation (Velisek, 2014)

This enolization reaction triggers serial degradation reactions: dehydration or β-elimination, dicarboxylic cleaving, retro-aldol reaction, aldol condensation, and finally, a radical reaction (Kroh, 1994). The most important degradation products of thermal caramelization are osuloses, namely α-dicarbonyls which are responsible for the formation of caramel color as well as caramel flavor. Elimination of one water molecule from D-glucose or D-fructose yields 3-DG. 3,4-dideoxyglucosone, which is a cytotoxic intermediate in the degradation of glucose to 5-HMF, is produced after ring-opening, enolization, and one more water elimination (Belitz et al., 2009, Linden et al., 2002). Finally after elimination of one more water molecule from 3,4-dideoxyglucosone, HMF

is obtained. In a study by Perez Locas and Yaylayan (2008), it was also reported that following the degradation of sucrose into fructofuranosyl cation and glucose, HMF can be generated from this cation subsequently in dry systems. According to their study, the HMF formation rate from sucrose and fructose through fructofuranosyl cation is much higher than from glucose through 3-DG pathway. It is also possible that through 2,3-enolization and β-elimination, 4-deoxy-hexo-2,3-diulose and 1-deoxy-hexo-2,3-diulose (1-DG) can be formed from fructose (Velisek, 2014).

Shorter chain α-dicarbonyl sugar fragments like GO, MGO, and DMG can be formed via Maillard reaction as well as directly from carbohydrates. The reactions such as isomerization, retro-aldolization of a sugar molecule, or cleavage of the corresponding α-dicarbonyl compounds are responsible for the formation of these shorter chain sugar fragments (Hollnagel and Kroh, 1998). According to Hollnagel and Kroh (1998), glucose produces more dicarbonyls than fructose and monosaccharides produce more than disaccharides. They explain this situation with the tendency of fructose to form cyclic products instead of fragmentation products.

Glyoxal is reported to be formed directly from aldose sugars or imines through retro-aldolization prior to oxidation (Weenen, 1998, Thornalley et al., 1999).

MGO can be formed via cleavage of 1-DG from C3-C4 bonds (Hollnagel and Kroh, 1998). However, it is also proposed that methylglyoxal is formed from the fragmentation of 3-DG through retro-aldol condensation (Thornalley et al., 1999).

DMG is claimed to be produced as a result of the isomerization of 1-DG by Weenen (1998). They also indicated that the reaction of 3-DG with alanine or cyclohexyl amine yields DMG. This formation is confirmed by Hollnagel and Kroh (1998) as they found the amount of DMG formed from glucose is much higher in the presence of glycine.

These sugar isomerization and degradation reactions arise simultaneously with the Maillard reaction and products generated from these reactions take place in the Maillard reaction.

3. CHEMICAL COMPOSITION OF NUT AND SEED SAMPLES

3.1. Introduction

Nuts and seeds are consumed as healthy snacks or used as an ingredient, especially in bakery products. Their positive contribution to human health and nutritional value make them in demand in the last decades. These foods can be ingested raw or after being roasted. Thermal processes such as roasting can be applied to nuts and seeds to improve desirable color, flavor, and taste. They are also subjected to heat treatment as an ingredient of many food products. During these thermal treatments, alterations in the chemical composition of naturally existing compounds can occur and new products can be formed via chemical reactions. Maillard reaction and sugar degradation are some of the important chemical reactions observed in the roasting process. It is an essential first step to determine the initial composition of foods in order to have comprehensive knowledge about these chemical reactions that may undergo during heat treatment. Therefore, in this chapter, proximate compositions of selected nuts and seeds and precursors of the Maillard reaction have been identified in detail.

3.2. Materials and Methods

3.2.1. Chemicals and Consumables

High purity (>99%) D-sucrose, D-glucose and D-fructose were obtained from Sigma-Aldrich (Diesenhofen, Germany). All amino acids (>98%) were purchased from Merck Co. (Darmstadt, Germany). Hexane (≥95%), hydrochloric acid (37%), methanol (≥99.9%), acetonitrile (≥99.9%), sulfuric acid (95-97%), potassium hexacyanoferrate, zinc sulfate, disodium hydrogen phosphate anhydrous, sodium dihydrogen phosphate dihydrate, sodium hydroxide, boric acid were purchased from Merck (Darmstadt, Germany). The Carrez I and Carrez II solutions were prepared by dissolving 15 g of potassium hexacyanoferrate and 30 g of zinc sulfate in 100 ml of water, respectively. Syringe filters (nylon, 0.45 μm) and Oasis HLB cartridges (30 mg, 1 mL) were supplied by Waters (Millford, MA). Deionized water (0.055 μS/cm) was used throughout the experiments.

3.2.2. Analysis of Proximate Composition

The moisture, oil, protein, and ash content of samples was determined by the method mentioned in the Association of Official Analytical Chemists (AOAC) (AOAC, 1990). Approximately 5 g of sample was placed in an aluminum dish and kept at 105 °C in an oven to a constant weight to determine moisture content (AOAC 925.10). The oil content of samples was calculated by using the Soxhlet extraction method for 6-8 hours with hexane (AOAC 948.22). The Kjeldahl method was used to determine the protein content by multiplying the total nitrogen content by 5.30 (AOAC 984.13). Weighed defatted samples were placed into a dried and pre-weighed crucible and burned with a gradual temperature increase (250-650 °C) for determining the ash content (AOAC 923.03). Ground samples (1 g) were mixed with 20 mL of distilled water and shaken vigorously for 10 min. After centrifugation at 8000g for 3 min, the pH of the supernatants was measured using a pH meter (MeterLab PHM210, France). The water activities of the samples were measured at 25 °C with Novasina LabTouch water activity meter (Novasina AG, Switzerland). All measurements were performed in duplicate.

3.2.3. Extraction of Samples

Triple-stage extraction was performed for one gram of ground sample with 20 mL water (10, 5, 5 mL). Weighed samples and water were vortexed for 5 min and centrifuged at $8000 \times g$ for 5 min in every step of the extraction process. Before centrifuging, tubes were stored at -18 °C for 5 min to obtain a clear extract. Supernatants were collected in another tube and centrifuged at $8000 \times g$ for 5 min.

3.2.4. Analysis of Sugars

Analysis of sugar was performed as described by Kocadağlı and Gökmen (2016) with Agilent 1200 HPLC system. 0.01N H_2SO_4 was used as a mobile phase with a 1 mL/min flow rate.

3.2.5. Analysis of Free Amino Acids and Protein-Bound Lysine

The free and protein-bound lysine content of samples was determined according to the procedure previously described by (Hamzalıoğlu and Gökmen, 2020). Sequant-ZIC-HILIC (250 mm × 4.6 mm i.d., 5 μm) column with a gradient mixture of (A) 0.1% of formic acid in water and (B) 0.1% of formic acid in acetonitrile was used for chromatographic separation.

3.2.6. Statistical Analysis

Experimental data were given as mean ± standard deviation. All the measurements were carried out in triplicates. The significance of differences was statistically analyzed by using one-way ANOVA Duncan's test ($p < 0.05$) by using SPSS Version 16.0.

3.3. Results and Discussion

3.3.1. Proximate Composition

Proximate compositions, pH, and water activities of raw samples were given in Table 3. 1. Oil constituted the largest part of the samples, ranging from 42 to 49% and there was no significant difference between the oil content of samples ($p > 0.05$). The moisture content and water activity were found to be limited in all samples with the highest amount in pumpkin seed samples (6.7%, 0.62).

Table 3. 1 Proximate composition, pH, and water activities of raw samples

	Sunflower Seed	Pumpkin Seed	Flaxseed	Peanut	Almond
Moisture (g/100g)	5.26±0.2[a]	6.7±0.07[b]	3.86±0.15[c]	4.62±0[d]	4.01±0.02[c]
Oil (g/100g)	42.24±14.07[a]	49.08±1.33[a]	42.94±3.04[a]	43.77±0.19[a]	48.02±0,24[a]
Protein (g/100g)	20.11±4.3[b]	17.36±1.56[a,b]	12.76±1.62[a]	12.61±0.42[a]	20.48±2.17[b]
Carbohydrate (g/100g)	28.32±18.07[a]	22.61±2.82[a]	36.65±4.85[a]	36.39±0.62[a]	24.31±2.43[a]
Ash (g/100g)	4.08±0.16[a]	4.24±0.01[a]	3.79±0.08[b]	2.6±0.02[c]	3.18±0[d]
Water activity (25 °C)	0.48±0.02[b,c]	0.62±0[d]	0.43±0.02[a]	0.46±0.01[a,b]	0.5±0.01[c]
pH	7.1±0.03[c]	7.14±0.02[c]	6.62±0.03[a]	7.01±0.04[b]	6.62±0.01[a]

Different superscript letters indicate statistical significance for each comparison ($p < 0.05$)

Chung et al. (2013) determined the proximate composition of nuts and seeds sold in Korea. They reported the main constituent of almond (43.2%), peanut (49.7%), sunflower seed (45.2%), and pumpkin seed (43.9%) as oil and followed by protein. Venkatachalam and Sathe (2006) were reported the lipid content of almonds as 43.36%, the protein content as 19.48%, and the ash content as 2.48%. In another study, lipid and ash content of raw brown flaxseeds was found as 45.2% and 3.5%, respectively (Mueller et al., 2010). In a study investigating the proximate compositions of different Turkish origin seeds, the lipid content of flaxseed was found to be 33.6%, protein content 17.9%, and ash content 3.9% (Bozan and Temelli, 2008).

3.3.2. Sugar Composition and Amino Acid Profile

Sucrose was the predominant sugar in all samples. Sucrose concentration of raw sunflower seed, pumpkin seed, flaxseed, peanut, and almond was 3.2±0.0 g/100 g, 1.3±0.0 g/100 g, 2.3±0.0 g/100 g, 4.0±0.2 g/100 g, and 3.4±0.1 g/100 g, respectively.

Amino acid profiles were given in Table 3. 2. Arginine, aspartic acid, and glutamic acid were found to be the most predominant amino acids in all samples. In addition, it was noteworthy that Asx was significantly higher in almond samples. These amino acids constituted almost 50% of total free amino acids.

Table 3. 2 The concentration of free amino acids and protein-bound lysine in samples (mg/kg sample)

	Pumpkinseed	Sunflower	Flaxseed	Peanut	Almond
Ala	74.7±21.5[a]	243.9±44.7[d]	164.6±0.5[b,c]	128.1±0.6[b]	184.8±21.5[c]
Arg	580.4±167.4[b]	340.4±109.1[a]	272.3±8.6[a]	316.5±10.6[a]	317.4±34.7[a]
Asn	58.4±14.7[a]	264.6±52.6[b]	317.7±7.4[b]	273.7±7.1[b]	1190.8±151[c]
Asp	134.8±34.2[a]	368.5±74.9[c]	288.3±6.4[b]	184.6±4.2[a]	490.3±42.8[d]
Gaba	94.2±24[c]	29.9±6.8[a,b]	9.2±0.5[a]	49.3±1.1[b]	84.8±11[c]
Gln	33.9±10.3[a]	279.3±64.6[c]	126.5±2.5[b]	1±0.2[a]	136.8±17.4[b]
Glu	347.1±97.5[a]	660.5±149.4[b]	592.8±14.8[b]	844.5±25.4[c]	513.4±52[b]
Gly	132.1±37.7[b]	177.3±23.5[c]	86.8±4.6[a]	0±0	0±0
His	66.9±16.4[b,c]	80.8±21.4[b,c]	64.8±1.4[b]	37.3±0.8[a]	90.2±12[c]
Leu	40.7±13.4[a]	166.3±30.9[c]	104.8±2.1[b]	38.4±0.3[a]	112.6±15.1[b]
Ile	38±11.6[a]	163.6±33.3[c]	94.4±1[b]	35.5±1.3[a]	148.2±17.7[c]
Lys	49.7±13.5[a,b]	182.1±48.1[d]	96.1±1.9[c]	35.7±0.7[a]	84.8±11.6[b,c]
Met	17.7±5.8[a]	101.8±19.3[c]	57.3±0.5[b]	11.4±0.2[a]	46.9±6.9[b]
Phe	78.8±20.7[a]	116.5±22.3[b]	139.4±1.1[b]	236.1±2.2[c]	121.6±14.8[b]
Pro	13.5±3.2[a]	78.3±11.8[b]	68.7±2.1[b]	52.6±1.7[b]	195±22.2[c]
Ser	67.8±17.7[a]	143.2±25.7[c]	96.6±1.6[b]	47.4±1[a]	116.4±12.8[b]
Thr	43.1±13[a]	127.2±29.1[c]	103.4±2.2[c]	22.1±0.7[a]	75.8±9.5[b]
Trp	75.4±20.7[a]	202.9±55.8[c]	127.3±2[b]	43.1±1.9[a]	51.2±6.5[a]
Tyr	123.1±39[b]	140.3±38.1[b]	130±3.3[b]	31.2±0.9[a]	100.2±19.1[b]
Val	61.4±18.9[a]	184.1±37.8[c]	123.6±2[b]	65.2±0.1[a]	156.3±17[b,c]
bLys	11771±1313.6[c]	9480.6±724[b]	8242.5±161.8[b]	11719.4±834.9[c]	6933.7±189.1[a]

Superscript letters in each raw indicate statistically significant difference (p<0.05) according to Duncan's test.
Data are expressed as mean±standard deviation.

4. CHANGES IN THE CHEMICAL COMPOSITION OF NUTS & SEEDS AND FORMATION OF MAILLARD REACTION AND SUGAR DEGRADATION PRODUCTS INDUCED BY ROASTING

4.1. Introduction

Roasting is a general process that is applied to seeds and nuts for different purposes. Roasting increases palatability, and crispness, and enhances flavor and sensory properties. In other words, overall acceptability is improved by roasting. During the roasting process, Maillard reaction, sugar degradation, and lipid oxidation are encountered reactions. As a consequence of these reactions, the chemical composition of related food can be changed. Briefly, new products can be formed whereas initial composition changes.

Maillard reaction occurs between carbonyl and amino compounds. Seeds and nuts are good sources of these reactants due to their amino acid and sugar content. Roasting parameters also promote the progress of the Maillard reaction. Lysine loss, formation of mutagenic and carcinogenic compounds, development of flavor, and brown color are characteristic results of the Maillard reaction. According to Hodge (1953), in the first stage, reducing sugars condense with amino compounds followed by Amadori rearrangement. In the advanced stage, Amadori compounds degrade and α-dicarbonyl compounds are formed and these compounds subsequently react with reactive side chains of protein-bound amino acids leading to the formation of advanced glycation end products (AGEs). In the final stage, brown nitrogenous compounds called melanoidins are generated via the condensation of amino compounds and sugar fragments.

In this part of the thesis, the change in the concentration of Maillard reaction precursors and reactants was tracked during the roasting process. Newly formed reaction products during the Maillard reaction and their concentrations have also been identified. Monitoring these changes will help us to understand the reaction mechanism of the whole network in the following part.

4.2. Materials and Methods

4.2.1. Chemicals and Consumables

High purity (>99%) D-sucrose, D-glucose, and D-fructose were obtained from Sigma-Aldrich (Diesenhofen, Germany). All amino acids (>98%) were purchased from Merck Co. (Darmstadt, Germany). 3-Deoxyglucosone (75%), quinoxaline (99%), 2-methylquinoxaline (97%), methylglyoxal (40%), 2,3-dimethylquinoxaline (97%), o-phenylenediamine (98%), diethylenetriaminepentaacetic acid (DETAPAC) (98%), acrylamide and sodium borohydride powder (≥98%) were purchased from Sigma-Aldrich (Steinheim, Germany), whereas furosine standard was purchased from Neosystem Laboratoire (Strasbourg, France). 5- hydroxymethylfurfural (98%) was purchased from Acros (Geel, Belgium). Formic acid (98%), methanol (≥99.9%), and acetonitrile (≥99.9%) were obtained from JT Baker (Deventer, Holland). Potassium hexacyanoferrate, zinc sulfate, disodium hydrogen phosphate anhydrous, sodium dihydrogen phosphate dihydrate, sodium hydroxide, boric acid, hydrochloric acid (37%), and sulfuric acid (95-97%) were purchased from Merck (Darmstadt, Germany). The Carrez I and Carrez II solutions were prepared by dissolving 15 g of potassium hexacyanoferrate and 30 g of zinc sulfate in 100 ml of water, respectively. Syringe filters (nylon, 0.45 μm), Oasis HLB (30 mg, 1 mL), and Oasis MCX (30 mg, 1 mL) cartridges were supplied by Waters (Millford, MA). Deionized water (0.055 μS/cm) was used throughout the experiments.

4.2.2. Roasting of Samples

Raw sunflower seed, pumpkin seed, peanut, almond, and flaxseed samples were purchased from a local market (Ankara, Turkey). 30 grams of sample was placed on an aluminum plate and roasted in an oven (Memmert UN 55, Germany) at 160, 180, and 200 °C for different times ranging between 3 and 60 min. Roasting norms were selected to include both industrial and extreme conditions. After being left to ambient temperature, the samples were thoroughly ground and kept frozen at -18 °C prior to analysis. All samples were roasted in triplicate.

4.2.3. Extraction of Roasted Samples

The extraction step was performed as mentioned in Chapter 3. One gram of ground sample was extracted with 20 mL of water (10, 5, 5 mL). In each extraction step, the mixture was vortexed and centrifuged at $8000 \times g$ for 5 min. Before centrifuging, tubes were stored -18°C for 5 min to obtain a clear extract. The extracts were used for sugar, HMF, acrylamide, free amino acid, and α-dicarbonyl compounds analysis.

4.2.4. Analysis of Sugar

Analysis of sugar was performed for roasted samples as previously described by Kocadağlı and Gökmen (2016) with Agilent 1200 HPLC system.

4.2.5. Analysis of 5-Hydroxymethyl-2-furfural

The extracts precipitated by Carrez solutions were filtered through a 0.45 μm nylon filter and were collected in an autosampler vial. Analysis was carried out according to Kocadağlı et al. (2012).

4.2.6. Analysis of Acrylamide

Acrylamide content was determined with Agilent Ultivo Triple Quadrupole MS coupled to Agilent 1260 HPLC system as described by Hamzalıoğlu and Gökmen (2020) Atlantis T3 column (4.6 × 150 mm, 3 μm) was used for chromatographic separation.

4.2.7. Analysis of α-Dicarbonyl Compounds

Previously prepared co-extracts were precipitated with acetonitrile (1:1). α-Dicarbonyl compounds were derivatized by the procedure described by Kocadağlı and Gökmen (2014) and quantitated by Agilent Ultivo Triple Quadrupole MS coupled to Agilent 1260 HPLC in positive mode as described by Hamzalıoğlu and Gökmen (2020) and with Zorbax Eclipse XDB-C18 column (4.6 × 150 mm, 5 μm) was used for chromatographic separation.

4.2.8. Analysis of Free Amino Acids and Protein-Bound Lysine, Arginine and Histidine

The free and bound amino acid content of samples was determined according to the procedure previously described by Göncüoğlu Taş and Gökmen (2017).

4.2.9. Analysis of Furosine

The furosine content of samples was determined with respect to a previously described by Akıllıoğlu and Gökmen (2014).

4.2.10. Analysis of N-ε-Carboxymethyllysine and N-ε-Carboxyethyllysine

The extraction procedure was carried out according to the previously described method by Charissou et al. (2007). The analysis was carried out by Agilent Ultivo Triple Quadrupole MS coupled to Agilent 1260 HPLC system with positive ionization mode with the following source parameter settings: capillary voltage of 2.0 kV; nozzle voltage of 500 V; gas and sheath gas temperature at 300 °C; gas (nitrogen) flow of 6 L/min. Sheath gas flow was set to 11 L/min and nebulizer pressure was 60 psi. Separation was performed by the SeQuant ZIC-HILIC column at 60 °C. The gradient mixture of 0.1% formic acid in water (A) and 0.1% formic acid in acetonitrile (B) was used as a mobile phase at a flow rate of 1 mL/min. MS system was operated in positive ionization mode. For quantification of CML and CEL content of samples, a matrix-matched calibration method was used and raw samples were used as blank.

4.2.11. Analysis of Color

The color of roasted and raw samples was measured and color values of grounded samples were given as L^* (lightness), a^* (redness), and b^* (yellowness) by the computer vision-based image analysis method described by Ataç Mogol and Gökmen (2014). Digital images of roasted samples were captured by using an illumination system with daylight fluorescent lamps and stored in JPEG format without compression. The CIE L*a*b* values from a region of interest of samples were measured using MATLAB®.

4.2.12. Statistical Analysis

Experimental data were given as mean ± standard deviation. All the measurements were carried out in triplicates. The significance of differences was statistically analyzed by using one-way ANOVA Duncan's test ($p<0.05$) by using SPSS Version 16.0.

4.3. Results and Discussion

4.3.1. Degradation of Maillard Reaction Precursors

Sugars and amino acids are the main precursors for Maillard reaction and sugar degradation. Therefore the change in the amount of these reactants after roasting is very important to elucidate the reaction mechanism.

Sucrose was the predominant sugar in selected nuts and seeds, while glucose and fructose were rapidly degraded as a result of the roasting process. Change in the concentration of sucrose content was shown in Figure 4. 1. Sucrose decreased gradually during roasting depending on the roasting temperature and time. The maximum loss of sucrose was observed in samples roasted at 200 °C for 20 min and was 91, 58, 68, 57, and 53% for sunflower seed, pumpkinseed, flaxseed, peanut, and almond, respectively. At the lower roasting temperatures, a mild decrease in the amount of sucrose was found even after 60 minutes of roasting.

Changes in the concentration of protein-bound lysine and free amino acids during the roasting process were shown in Table 4. 1-5. The initial total free amino acid content of sunflower, pumpkinseed, flaxseed, peanut, and almond was 4051.46±899.41 mg/kg, 2131.65±601.10 mg/kg, 3064.66±56.65 mg/kg, 2453.61±53.19 mg/kg, and 4217.65±493.14 mg/kg sample, respectively. With roasting, the highest decrease in total free amino acid content was observed in sunflower seeds (98%) and flaxseeds (98%). This is followed by peanut (94%), almond (93%), and pumpkinseed (92%).
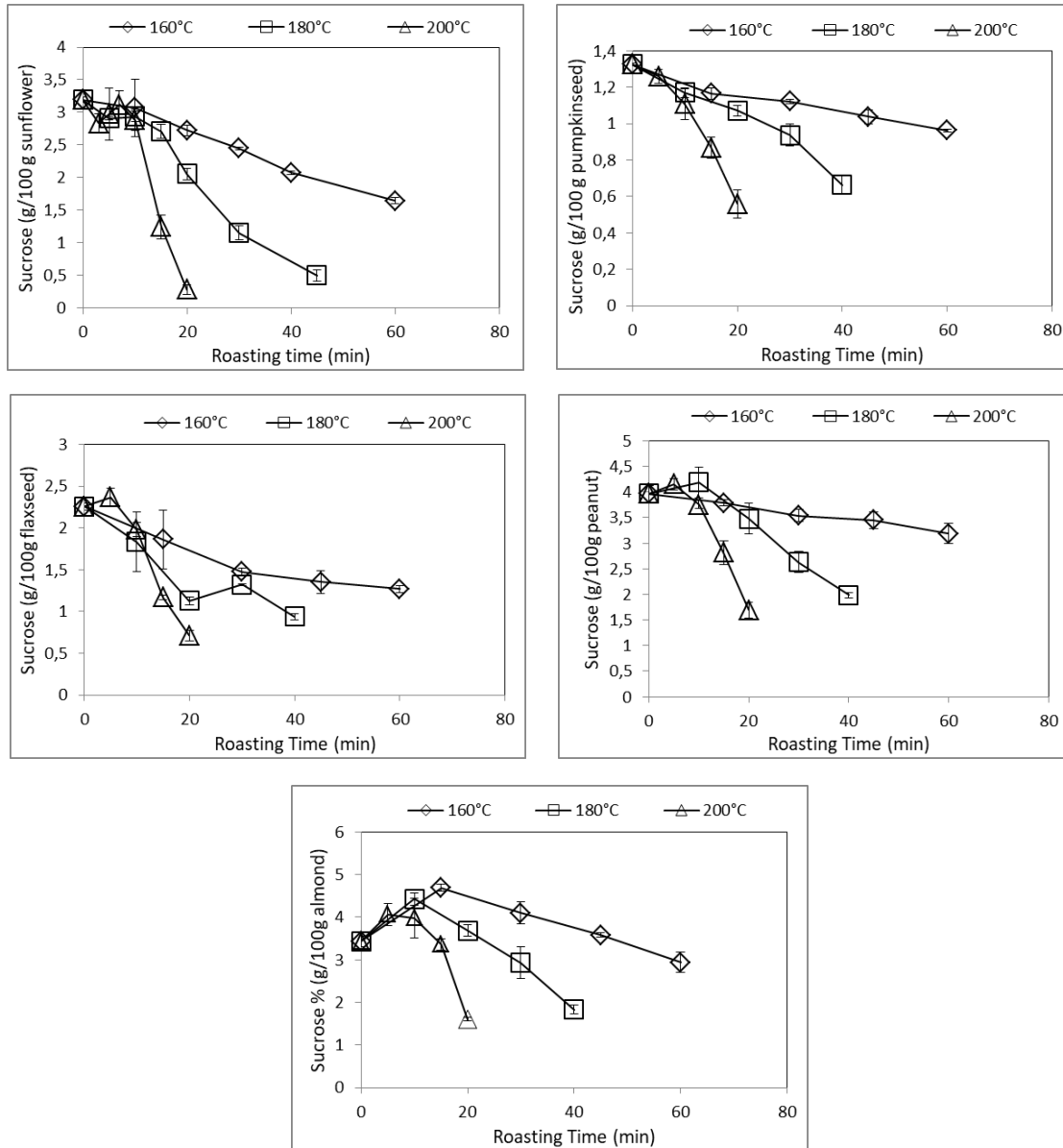
Figure 4. 1 Changes in the concentration of sucrose (g/100g sample)

Table 4. 1 Changes in the concentration of free amino acids and protein-bound lysine in pumpkin seeds by roasting (mg/kg pumpkin seed)

	Non-treated	160 °C				180 °C				200 °C			
		15 min	30 min	45 min	60 min	10 min	20 min	30 min	40 min	5 min	10 min	15 min	20 min
Ala	74.7±21.5[b,c,d]	104.8±9[a]	78.7±2.7[b,c]	52,5±2.8[d,e,f]	57.1±3.9[c,d,e]	76.2±15.2[b,c]	56,6±2,5[d]	30,2±3,6[f,g,h]	18,3±1,3[g,h]	88,6±5,8[a,b]	95,5±13[a,b]	40,2±5,6[e,f,g]	10,9±3,4[h]
Arg	580.4±167.4[b,c]	989±282.3[a]	578.7±46.2[b,c]	412.3±35.2[c,d]	449.5±69.8[c,d]	596.5±173.6[b,c]	381,5±16,9[c,d,e]	242,6±26,6[d,e]	187±11,9[d,e]	680,9±94,8[b,c]	761,7±135,9[a,b]	287,8±63,9[d,e]	79,5±25,7[e]
Asn	58.4±14.7[b]	74.1±5.4[a]	43.8±3.9[c,d]	24.1±0.9[e,f]	22.8±3.1[e,f,g]	54.6±12[b,c]	23,4±1,7[d]	11,9±1[f,g,h]	10±0,9[g,h]	63,3±5,2[a,b]	57±9,9[b,c]	14,5±2,3[f,g,h]	6,1±1,1[h]
Asp	134.8±34.2[c,d,e]	200.5±17.9[a]	141.9±6.5[b,c,d]	97.1±8.3[e,f,g]	101.3±16.2[d,e,f]	149.5±29.9[b,c]	100,9±1,1[d]	56,8±5,7[g,h,i]	40,8±3[h,i]	173,2±9,2[a,b,c]	182±26,7[a,b]	66,5±14,6[f,g,h]	22,3±6,1[i]
Gaba	94.2±24[a,b]	106.8±6.9[a]	52.1±3.5[c]	26.1±1.9[d,e]	21.9±2.1[e]	79.6±17.3[b]	30,2±0,5[e]	12,7±1,2[e]	10,3±0,2[e]	97,1±7,6[a,b]	82,5±11,1[b]	19,6±2,2[e]	7,7±1,1[e]
Gln	33.9±10.3[a]	4.4±0.4[c]	0.6±0.1[c,d]	0.1±0.1[d]	0.1±0[d]	2.9±1.6[c,d]	0±0[c]	0±0[d]	0±0[d]	13,3±0,6[b]	1,6±0,5[c,d]	0±0[d]	0±0[d]
Glu	347.1±97.5[a]	367.4±37[a]	94±7.6[c]	34.3±3.9[c,d]	32.5±5.4[c,d]	270.5±65.3[b]	39,1±1,6[c,d]	16,9±0,5[d]	15,8±0,5[d]	381,8±25,1[a]	239,6±39[b]	21,3±4[d]	9,2±2,5[d]
Gly	132.1±37.7[a]	37.1±4.6[b]	27.8±1.3[b,c,d]	20.3±0.9[b,c,d]	23.8±2.7[b,c,d]	30.3±5[b,c]	23,4±3,8[b,c,d,e,f]	18,5±1,1[c,d]	15,4±1[c,d]	32,9±3,4[b,c]	36,4±5,5[b]	20,1±4,3[b,c,d]	10,6±3,7[d]
His	66.9±16.4[b,c]	89.3±15.6[a]	53.5±5.8[c,d]	30.5±2.7[e,f]	27.4±4.9[e,f,g]	59.6±14.4[b,c,d]	29,3±0,9[d]	12,6±3[f,g,h]	10,1±0,9[g,h]	68,5±6[b,c]	77±9,3[a,b]	17,6±3,3[f,g,h]	5,4±1,5[h]
Ile	38±11.6[a]	37.4±4.1[a]	19.3±1.8[c,d]	10.8±0.8[e,f]	10±1.4[e,f,g]	24±7.3[b,c]	9,7±0,1[d]	2,2±0,8[g,h]	0±0[h]	30,4±2[a,b]	27±4,7[b,c]	4,2±1,6[f,g,h]	0±0[h]
Leu	40.7±13.4[a]	39.3±3.8[a]	20.8±1.8[c,d]	11.3±0.8[e,f]	10.8±1.7[e,f]	25.4±8.1[b,c]	10,6±0,1[d]	2,3±0,9[f,g]	0±0[g]	31,8±2,1[a,b]	28,5±5,2[b,c]	4,3±1,5[f,g]	0±0[g]
Lys	49.7±13.5[a]	47±7.3[b]	27,2±1,8[c,d]	18,1±1[f,g,h]	18,8±2,6[f,g]	31,9±8,7[c,d,e]	17,4±1,7[f]	11,8±1[g,h]	11±0,8[g,h]	39,9±4,2[a,b,c]	36,2±7[b,c,d]	13,1±2,1[g,h]	7±2,1[h]
Met	17.7±5.8[a]	14.4±0.8[b]	6,3±1[d]	1,2±0,4[e]	0,2±0,2[e]	6,6±2,8[d]	0±0[e]	0±0[e]	0±0[e]	11,1±1,1[c]	8,9±1,7[c,d]	0±0[e]	0±0[e]
Phe	78.8±20.7[c,d]	128.2±10.3[a]	79.5±5.6[c,d]	51±3.1[e]	49.8±8.5[e]	89.7±20.4[b,c,d]	49±0,2[e,f]	14.6±2.2[f]	4.8±0.5[f]	96,1±8,5[b,c]	106,2 ±17,2[a,b]	23,1±5,8[f]	0±0[f]
Pro	13.5±3.2[a]	10.6±1.1[b]	7.3±0.5[c,d]	5±0.5[e,f]	5±0.4[e,f]	7.9±1.6[c,d]	5,5±0,1[e]	2,9±0,3[f,g,h]	1,8±0[g,h]	9,1±0,7[b,c]	9,4±1,1[b,c]	3,7±0,4[f,g]	1,3±0,2[h]
Ser	67.8±17.7[a]	63.9±4.8[a,b]	44.3±2.5[c,d,e]	28.2±2[f,g]	31±3.7[e,f,g]	50.3±8.6[b,c,d]	28,4±2,4[e,f]	18.4±1.6[g,h]	15.8±0.7[g,h]	57,1±4,2[a,b,c]	56,3±9,8[a,b,c]	21,6±3,7[g,h]	10,2±5,1[h]
Thr	43.1±13[a]	41.2±3.8[a,b]	23.6 ±1.6[d]	13.6±0.4[e,f]	13.7±1.6[e,f]	29.1±7.5[c,d]	14,9±1,1[e]	6.6±0.7[f,g]	4.4±0.5[f,g]	35,4±1,6[a,b,c]	33,5±5,4[b,c]	8,7±1,1[f,g]	2,6 ±0,6[g]
Trp	75.4±20.7[b,c]	101.5±6.5[a]	60.2±5.8[c,d]	37.9±3.6[e]	38.9±6.8[e]	71.3±15.8[b,c]	37±1,1[d]	12.5±1.6[f]	5.6±0.2[f]	86,4±8,4[a,b]	80,8±12[b]	17,8±4,2[f]	0±0,1[f]
Tyr	123.1±39[b,c]	158.5±13.5[a]	90.5±8.3[c,d]	57.5±5.1[e,f]	56.3±9.4[e,f]	105.5±27.6[b,c,d]	53,5±2,2[d]	18.2±3.1[g]	8.2±0.7[g]	127,4±15,4[b]	116,1±18,3[b,c]	26,9±7,1[f,g]	0,5±0,7[g]
Val	61.4±18.9[a,b]	62.1±6[a]	35.9±3.2[d,e]	22.2±1.7[f,g]	21.6±2.7[f,g]	41.4±11.1[c,d,e]	21,5±0,5[d]	8.1±1.2[g,h]	3.2±0.3[h]	51±3,2[a,b,c]	47,8±7,9[b,c,d]	11,8±2,5[g,h]	0,7±0,6[h]
bLys	11771 ±1313.6[a,b,c]	13033.4 ±323.5[a]	10823±1321.2[b,c,d,e,f]	11202.4 ±191.8[b,c,d,e]	9966.4 ±1276.2[c,d,e,f,g]	12268.1 ±319.5[a,b]	10824.7 ±877.1[b,c,d,e,f]	9142.2 ±898.9[f,g]	9674.6 ±578.5[d,e,f,g]	11522,1 ±706,6[a,b,c,d]	10472,1 ±2036,8[b,c,d,e,f]	9541,7 ±417,6[e,f,g]	8400,7 ±616,5[g]

Superscript letters in each raw indicate statistically significant difference (p<0.05) according to Duncan's test.
Data are expressed as mean±standard deviation.

Table 4. 2 Changes in the concentration of free amino acids and protein-bound lysine in sunflower seeds by roasting (mg/kg sunflower seed)

| | Non-treated | 160 °C | | | | | 180 °C | | | | | | 200 °C | | | | | |
		10 min	20 min	30 min	40 min	60 min	5 min	10 min	15 min	20 min	30 min	45 min	3 min	5 min	7 min	10 min	15 min	20 min
Ala	243,9 ±44,7[h]	114,5 ±15,2[f]	100 ±11,7[e,f]	86,4 ±16[d,e]	55,8 ±3,9[c]	41,5 ±2,9[b,c]	141 ±22,9[g]	92,4 ±4,5[d,e,f]	49,3 ±11,1[b,c]	29,1 ±9,8[a,b]	12,5 ±4,9[a]	13 ±3,2[a]	118,5 ±12,4[f,g]	114 ±24,2[f]	68,1 ±8,4[c,d]	57,1 ±19,4[c]	13,9 ±6,5[a]	10,9 ±0,8[a]
Arg	340,4 ±109,1[a]	147,1 ±21,3[b,c]	118,6 ±5,1[c,d]	104 ±33,3[c,d,e]	64,1 ±11,1[e,f,g]	49,7 ±5,2[f,g,h]	170,1 ±25,6[b]	88,2 ±4,8[d,e,f]	45,3 ±14,9[f,g,h]	27,6 ±9,9[g,h]	14,5 ±4,2[h]	16,8 ±3,7[g,h]	97,8 ±18,4[d,e]	122,4 ±25,4[c,d]	62,8 ±12,7[e,f,g]	63,4 ±28,8[e,f,g]	14,6 ±6,7[h]	12,4 ±1,8[h]
Asn	264,6 ±52,6[a]	195,3 ±16,5[b]	133,5 ±13,8[c]	97,3 ±16,3[c,d]	61,6 ±2,5[d,e]	47,1 ±4,5[e,f,g]	180,4 ±15,1[b]	136,8 ±12[c]	52,3 ±13[e,f]	28,7 ±9,5[e,f,g]	12,6 ±5[f,g]	11,9 ±3,4[f,g]	121,7 ±48,5[c]	195,4 ±39,8[b]	110,3 ±21,2[c]	68,1 ±25,6[d,e]	12,9 ±7,4[f,g]	8,3 ±0,8[g]
Asp	368,5 ±74,9[a]	239,5 ±50,6[c,d]	204,2 ±5,3[d,e]	118,7 ±19,3[f]	53,6 ±4,4[g,h]	41,8 ±4,9[g,h]	307,8 ±55,5[b]	220,7 ±20,1[d,e]	91,7 ±15,8[f,g]	34,5 ±12,1[h]	15,6 ±6,1[h]	17,6 ±3,9[h]	246,6 ±31,6[c,d]	288,1 ±48,9[b,c]	184,1 ±20,3[e]	131,8 ±47,5f	22,2 ±11,3[h]	14,9 ±1,9[h]
Gaba	29,9 ±6,8[a]	14,1 ±1,8[b,c,d]	13,8 ±0,6[b,c,d]	11,6 ±1,7[c,d,e,f]	8 ±0,5[g,h]	6 ±0,4[h,i]	14,8 ±1,7[b,c]	12,3 ±0,4[c,d,e]	8,3 ±2[f,g,h]	5,3 ±1,6[h,i,j]	2,6 ±0,7[j,k]	2,4 ±0,4[j,k]	11,7 ±0,8[c,d,e,f]	15,9 ±2,6b	9,9 ±1[e,f,g]	10,8 ±3[d,e,f,g]	2,9 ±1[i,j,k]	1,8 ±0,1[k]
Gln	279,3 ±64,6[a]	30,3 ±4,3[d]	12,7 ±1,7[d,e]	9,7 ±2,8[d,e]	5,2 ±0,3[d,e]	3,4 ±0,1[d,e]	100,1 ±25[b]	15,2 ±3,2[d,e]	3,8 ±1,4[d,e]	1,7 ±0,8[e]	0,5 ±0,3[e]	0,4 ±0,1[e]	67 ±20,8[c]	55,3 ±17[c]	7,9 ±2,3[d,e]	4,3 ±1,8[d,e]	0,6 ±0,7[e]	0 ±0,1[e]
Glu	660,5 ±149,4[a]	308,7 ±46,8[b,c]	112,2 ±15,1[f,g]	57,3 ±9,8[g,h]	34,9 ±2,3[h]	27,7 ±2,8[h]	365,6 ±52[b]	214,8 ±14,1[d,e]	38,8 ±7[g,h]	19,3 ±7,2[h]	8,9 ±3,5[h]	8,8 ±1,5[h]	278,6 ±69,6[c,d]	370,8 ±72[b]	152,5 ±31,1[e,f]	61,3 ±25,6[g,h]	10,4 ±5,7[h]	5,7 ±0,5[h]
Gly	177,3 ±23,5[a]	50,2 ±4,6[c,d]	49,3 ±2,8[c,d]	47,2 ±5,5[c,d]	36 ±2,7[d,e,f]	29,7 ±1,6[e,f,g,h]	67 ±14,9[b]	42 ±5,1[d,e]	28,6 ±7,4[e,f,g,h,i]	24,6 ±6,7[f,g,h,i]	14,5 ±5,3[i]	18,8 ±4,2[g,h,i]	59,2 ±6,3[b,c]	47,4 ±12,8[c,d]	31,1 ±3,1[e,f,g,h]	32,8 ±5,4[e,f,g]	19,6 ±8,9[g,h,i]	17,2 ±2,4[h,i]
His	80,8 ±21,4[a]	24,4 ±3,1[c,d]	15,9 ±1,1[e]	13,6 ±3,4[e,f]	8,9 ±0,9[e,f,g]	6,6 ±0,3[f,g]	34,7 ±7,1[b]	16,5 ±1,3[d,e]	6,4 ±2,3[f,g]	4 ±1,6[g]	2,1 ±1,3[g]	3 ±0,2[g]	26,8 ±2,5[c]	24,1 ±5,5[c,d]	10,8 ±1,9[e,f,g]	8,5 ±3,2[e,f,g]	2,5 ±1,2[g]	2,5 ±0,5[g]
Ile	163,6 ±33,3[a]	42,2 ±7,1[c]	33,3 ±2,5[c,d,e]	26,9 ±6,3[d,e,f,g]	15,8 ±1,8[f,g,h,i]	11,1 ±1[h,i]	61,2 ±12,8[b]	30,4 ±3,6[c,d,e,f]	11,1 ±3,1[h,i]	4,7 ±2,5[h,i]	0 ±0[i]	0 ±0[i]	41,2 ±13,2[c,d]	42,8 ±9,4[c]	18,6 ±2,8[e,f,g,h]	13,2 ±6,5[g,h,i]	0 ±0[i]	0 ±0[i]
Leu	166,3 ±30,9[a]	42 ±7,2[c]	36 ±2,2[c]	28,3 ±7,4[c,d,e]	15,2 ±1,8[e,f,g]	10,1 ±0,7[f,g]	60,3 ±13,1[b]	30,5 ±3,9[c,d]	10,7 ±2,8[f,g]	4 ±2,5[f,g]	0 ±0[g]	0 ±0[g]	40,7 ±13,5[c]	40,9 ±9,4[c]	17,9 ±2,9[d,e,f]	12,6 ±6,4[f,g]	0 ±0[g]	0 ±0[g]
Lys	182,1 ±48,1[a]	42,2 ±6,1[c]	27,1 ±2,8[c,d]	18,1 ±5,9[d,e,f]	11,2 ±1,3[d,e,f]	8,3 ±0,3[e,f]	61,5 ±10,4[b]	25,5 ±3,2[c,d,e]	7,9 ±2,2[e,f]	5 ±2,3[f]	2,5 ±1[f]	3,7 ±0,5[f]	37,9 ±6,6[c]	38,3 ±8,5[c]	17,2 ±3,6[d,e,f]	12,8 ±5,4[d,e,f]	3,1 ±2[f]	2,3 ±0,3[f]
Met	101,8 ±19,3[a]	32,6 ±4,8[c]	27,8 ±3,1[c,d]	19,7 ±5[d,e,f]	10,8 ±1,1[f,g,h]	6,3 ±0,2[g,h,i]	47,3 ±9,6[b]	23,6 ±1,7[c,d,e]	9,1 ±1,5[g,h,i]	3,7 ±1,5[h,i]	0,3 ±0,3[i]	0 ±0[i]	32,6 ±6,6[c]	32,1 ±6,7[c]	14,7 ±2[e,f,g]	10,2 ±4,9[g,h]	0,1 ±0,2[i]	0 ±0[i]
Phe	116,5 ±22,3[a]	40,8 ±4,4[c,d]	39,3 ±4,3[c,d,e]	29,2 ±5,8[e]	16 ±1,4[f]	9,5 ±0,3[f,g,h]	58,8 ±11,5[b]	31,3 ±3,3[d,e]	12,4 ±2,1[f,g]	4,1 ±2,7[g,h]	0 ±0[h]	0 ±0[h]	43,9 ±6,5[c]	36,7 ±5,8[c,d,e]	18,3 ±2,3[f]	13,1 ±7[f,g]	0 ±0[h]	0 ±0[h]
Pro	78,3 ±11,8[a]	31,6 ±2,4[b,c]	29,3 ±4,3[b,c]	22,5 ±2,6[d,e]	16,4 ±0,5[e,f,g]	12,7 ±0,6[g,h]	34,2 ±4,1[b]	27,5 ±0,7[c,d]	14,9 ±2[f,g,h]	9,5 ±2[h,i]	5,2 ±0,8[i]	4,7 ±0,3[i]	28,5 ±4,2[b,c,d]	32,8 ±5,1[b,c]	22,7 ±2,8[d,e]	20,6 ±6[e,f]	5 ±0,8[i]	4,2 ±0,1[i]

Ser	143,2 ±25,7[a]	30,4 ±7[b,c]	25,7 ±0,7[b,c,d]	22,9 ±4,6[b,c,d,e]	14,8 ±2,3[c,d,e,f]	11,4 ±0,3[d,e,f]	36,1 ±13,7[b]	27,6 ±1,6[b,c,d]	12,6 ±3,2[d,e,f]	7,7 ±3[e,f]	4,7 ±2,1[f]	6,3 ±1,6[f]	23,3 ±23,5[b,c,d,e]	36 ±7,6	19,3 ±3,1[c,d,e,f]	15,1 ±4,3[c,d,e,f]	5 ±2,7[f]	4,1 ±0,8[f]
Thr	127,2 ±29,1[a]	22 ±3,1[c]	16 ±1,4[c,d]	14 ±3,6[c,d,e]	8,4 ±1[d,e,f]	6,2 ±0,6[d,e,f]	38,2 ±9,4[b]	15,5 ±1,3[c,d,e]	6,8 ±2,2[d,e,f]	4,1 ±1,6[e,f]	1,5 ±0,8[f]	1,6 ±0,1[f]	34,4 ±4,2[b]	22,1 ±5,7[c]	10,8 ±1,9[d,e,f]	8,2 ±3,1[d,e,f]	1,8 ±1,1[f]	1 ±0,1[f]
Trp	202,9 ±55,8[a]	154,3 ±21,4[b,c]	143,5 ±9,3[b,c,d]	147,4 ±24,1[b,c,d]	116,7 ±15,9[c,d,e,f]	94,6 ±5,2[e,f]	155,3 ±14,5[b]	118,5 ±15,3[b,c,d,e]	79 ±25,1[f,g]	49,6 ±19,3[g]	10,7 ±6,1[h]	2,3 ±1,4[h]	111,8 ±14,1[d,e,f]	146,2 ±32[b,c,d]	90,9 ±10,8[e,f]	92,4 ±35,8[e,f]	2,8 ±4,3[h]	0 ±0[h]
Tyr	140,3 ±38,1[a]	39 ±5,9[c]	32 ±3,3[c]	24,1 ±7,3[c,d]	13 ±2,1[d,e]	8,8 ±0,8[e]	53,3 ±10,2[b]	24,9 ±2,6[c,d]	8,7 ±2,8[e]	3,6 ±2,2[e]	0 ±0[e]	0 ±0[e]	37,8 ±5[c]	34,1 ±8,5[c]	14,3 ±2,6[d,e]	10,5 ±5,5[d,e]	0 ±0[e]	0 ±0[e]
Val	184,1 ±37,8[a]	51,7 ±6,9[c]	46,1 ±5,1[c]	36 ±8,8[c,d,e]	21,1 ±2,8[e,f,g]	15,3 ±0,9[f,g,h]	69,8 ±13,4[b]	38,6 ±3,6[c,d]	15,8 ±3,8[f,g,h]	8 ±3,4[g,h]	1,5 ±1[h]	0,7 ±0,4[h]	48,7 ±12,9[c]	50,4 ±12,1[c]	25,7 ±3,9[d,e,f]	18,9 ±8,1[f,g]	0,8 ±1,1[h]	0 ±0[h]
bLys	9480,6 ±724[a,b]	8768,4 ±678,4[b,c]	8504,8 ±367[c]	7235,9 ±359,9[d]	6506,7 ±148,2[d]	5744,8 ±208,5[e]	8884 ±675,5[b,c]	9683,5 ±476,4[a]	7229,3 ±611,2[d]	5289 ±380,3[e]	3971,7 ±162[f]	3760,1 ±255,7[f,g]	9554 ±332,7[a,b]	9534,3 ±210,8[a,b]	9117,7 ±220,1[a,b,c]	7035,9 ±652[d]	4007,6 ±209,9[f]	3197,9 ±121,8[g]

Superscript letters in each raw indicate statistically significant difference (p<0.05) according to Duncan's test.
Data are expressed as mean±standard deviation.

Table 4. 3 Changes in the concentration of free amino acids and protein-bound lysine in flaxseed by roasting (mg/kg flaxseed)

	Non-treated	160 °C				180 °C				200 °C			
		15 min	30 min	45 min	60 min	10 min	20 min	30 min	40 min	5 min	10 min	15 min	20 min
Ala	164.6±0.5[a]	60.4±4.4[b]	40.3±1.2[d]	28.3±0.4[e]	24.2±1.2[f]	51.6±1.4[c]	15.7±1.2[g]	9.9±0.4[h]	5.9±0.4[i,j]	50,9±1,9[c]	24,7±1,7[f]	6,4±0,4[i]	3,3±0,5[j]
Arg	272.3±8.6[a]	175.4±67.8[b]	77.9±4.8[c,d]	56.8±8.3[d,e]	49±1.4[d,e]	94.9±0.9[c]	29.2±1.9[e,f]	21.4±1.4[e,f]	13.2±1.2[f]	74,1±7,4[c,d]	30,6±4,1[e,f]	11,1±0,5[f]	9,3±1,4
Asn	317.7±7.4[a]	244.4±24.4[b]	107.2±4.6[e]	62.4±3[f]	52.3±2.1[f,g]	196.9±4.2[d]	25.7±2.2[h]	15.7±1.3[h,i]	10.7±0.2[i]	215,6±4,3[c]	48,1±6,4[g]	8±1[i]	4,6±1,3[i]
Asp	288.3±6.4[a]	255.9±20.1[b]	147.5±4.5[d]	85.2±3.7[e]	66.4±2[f]	234.6±6.5[c]	51.5±1.3[g]	34.9±0.6[h]	28.4±1.1[h,i]	245±6,6[b,c]	94,7±7,2[e]	21±0,9[i,j]	15,2±1,9[j]
Gaba	9.2±0.5[a]	7.2±1.3[b]	4.3±0.1[d]	2.9±0.1[e,f]	2.5±0[f]	5.5±0.1[c]	2.4±0.1[f,g]	1.8±0[g,h]	1.6±0.1[h]	4,9±0,2[c,d]	3,5±0,1[e]	1,6±0,1[h]	1,4±0,1[h]
Gln	126.5±2.5[a]	12.6±3.7[b]	2.2±0.2[d]	1.2±0.1[d]	0.9±0.1[d]	5.7±0.6[c]	0.7±0.3[d]	0.4±0[d]	0.1±0[d]	7,7±1,3[c]	0,8±0,3[d]	0,3±0,1[d]	0,1±0,2[d]
Glu	592.8±14.8[a]	345.3±8.8[c]	103.3±4.3[d]	64.3±0.5[e]	55.7±2.8[e]	329.2±17.7[c]	33.6±1.3[f]	24.2±0.6[f,g]	19.8±1.1[f,g]	475,8±25,5[b]	72,2±11,5[e]	12,7±0,8[g]	8,6±0,8[g]
Gly	86.8±4.6[a]	33.3±1.5[b]	22.3±2.8[d]	15.6±0.8[e]	13.2±0.2[e]	27.7±2.3[c]	9.9 ±0.8[f]	8.3±0.4[f,g]	8±0.8[f,g]	26,4±0,9[c]	13,2±0,2[e]	6,3±0,9[g]	5,7±0,7[g]
His	64.8±1.4[a]	38.2±7.2[b]	19.5±1.3[d]	13.5±0.5[e]	11.9±0.3[e,f]	28.1±0.5[c]	6.5±1[g,h]	5.3±0.1[h]	4.7±0.5[h]	28±0,9[c]	9,7±0,7[f,g]	4±0,9[h]	2,7±0,3[h]
Ile	94.4±1[a]	20.2±2.8[b]	7.7±0.1[d]	4.1±0.4[e]	3.3±0.2[e]	11.1±0.8[c]	0.1±0.2[f]	0±0[f]	0±0[f]	12,4±1,2[c]	1,5±0,7[f]	0±0[f]	0±0[f]
Leu	104.8±2.1[a]	25±3.1[b]	9.2±0.5[d]	4.3±0.3[e]	3.1±0.1[e]	11.4±0.6[c]	0±0[f]	0±0[f]	0±0[f]	12,5±1,3[c]	1,1±0,7[f]	0±0[f]	0±0[f]
Lys	96.1±1.9[a]	28.4±6.7[b]	11.6±0.4[d]	8±1.3[e]	6.6±0.2[e,f]	19±0.4[c]	4.6±0.2[e,f,g]	3.6±0.3[f,g]	3±0.5[f,g]	18,3±1,8[c]	5,6±0,5[e,f,g]	3,4±1,5[f,g]	2,1±0,4[g]
Met	57.3±0.5[a]	9.4±1.5[b]	1.7±0.1[d]	0.1±0.1[e]	0±0[e]	3.6±0.3[c]	0±0[e]	0±0[e]	0±0[e]	4,3±0,5[c]	0±0[e]	0±0[e]	0±0[e]
Phe	139.4±1.1[a]	61±3.3[b]	35.9±0.3[e]	25.4±0.8[f]	21.5±0.4[g]	42.1±0.9[d]	7.5±1[i]	2.4±0.1[j]	0±0.1[j]	45,7±2,7[c]	11,1±1,7[h]	0±0[j]	0±0[j]
Pro	68.7±2.1[a]	55.4±6[b]	37.4±1.7[e]	26.6±1.1[f]	23±0.7[g]	47±1.4[c]	13.5±1.1[h]	8.5±0.3[i]	5.4±0.5[i,j]	43,2±1[d]	20,4±1,5[g]	4,3±0,3[j]	3,2±0,4[j]
Ser	96.6±1.6[a]	26.9±1.8[b]	15.1±1.1[d]	10.6±1[e]	9.2±1[e]	24.1±0.3[c]	6.6±0.1[f]	4.6±0.2[f,g]	4.6±0.9[f,g]	27±1,9[b]	10,8±1,4[e]	3,8±0,6[g]	3,1±0,5[g]
Thr	103.4±2.2[a]	43.8±6.2[b]	22.5±0.1[d]	14.8±1.1[e]	12.5±0.6[e,f]	33.8±0.4[c]	7±0.6[g]	4.5±0.1[g,h]	3±0.5[h]	34,2±1,4[c]	10,9±1,1[f]	2±0,2[h]	1,4±0,2[h]
Trp	127.3±2[a]	116.7±7.2[b]	81.8±0.8[d]	65.4±1.7[d]	59.3±1.9[f]	101.2±5.3[c]	25.4±2.6[h]	13.6±0.3[i]	6.3±1.5[j]	115,9±3,7[b]	36,8±5,1[g]	2,2±0,4[j,k]	0±0[k]
Tyr	130±3.3[a]	48.6±6.7[b]	19.3±0.5[d]	10.9±0.7[e]	8.7±0.4[e,f]	26.8±0.9[c]	2.5±0.5[g,h]	0.4±0.2[h]	0±0[h]	30,4±1,6[c]	5,3±1[f,g]	0±0[h]	0±0[h]
Val	123.6±2[a]	40.4±2.8[b]	22.7±0.2[d]	14.9±0.6[e]	12.7±0.5[f]	28.6±1[c]	5.5±0.5[h]	3±0.2[i]	1.5±0.3[i,j]	29,9±1,4[c]	9±1,3[g]	0,6±0,2[j]	0±0,1[j]
bLys	8242.5 ±161.8[a]	8018.7 ±276.1[a]	5615.1 ±1661.1[a,b,c,d]	6164 ±717[a,b,c]	5087.8 ±408.3[b,c,d,e,f]	6948.6 ±589.2[a,b]	4356.6 ±1029.1[c,d,e,f]	3463.5 ±367.2[d,e,f,g]	3062.6 ±542.9[e,f,g]	6954 ±614,3[a,b]	5474,2 ±21,3[a,b,c,d,e]	2795,6 ±298,3[f,g]	1730,4 ±81,1[g]

Superscript letters in each raw indicate statistically significant difference (p<0.05) according to Duncan's test.

Data are expressed as mean±standard deviation.

Table 4. 4 Changes in the concentration of free amino acids and protein-bound lysine in peanut by roasting (mg/kg peanut)

	Non-treated	160 °C				180 °C				200 °C			
		15 min	30 min	45 min	60 min	10 min	20 min	30 min	40 min	5 min	10 min	15 min	20 min
Ala	128,1±0.6^a	79.1±1.5^d	62±3.3^e	42.5±1.8^f	29.3±0.7^g	93.6±6.7^c	38.7±1.5^f	16.8±2.2^h	12.1±0.4^h	116,9 ±6,5^b	80,3 ±7,9^d	18,2 ±2,7^h	12,8 ±1^h
Arg	316.5±10.6^a	227.4±13.4^c	177±8.4^d	119.1±13.3^f	89.1±9^g	236.7±15.2^c	88±14.5^g	35.6±3.9^h	26.3±2.2^h	278,7 ±23,7^b	154,1 ±16,1^e	29,9 ±5,3^h	21,3 ±2^h
Asn	273.7±7.1^a	181.9±10.4^c	97.1±7.1^d	57.6±1.6^e	48.8±7.4^e	223.2±76.8^b	52.4±10.1^e	27.9±2.1^e	24.6±4.8^e	229,7 ±25^b	119,6 ±13,8^d	25,1 ±3,3^e	19,8 ±1,9^e
Asp	184.6±4.2^a	146.7±6.4^c	111±8.7^e	85.6±3.9^f	59.7±1^g	168.3±13^b	76.4±11.4^f	35.1±1.1^h	29±3.6^{h,i}	179,7 ±0,9^a	129,3 ±6,2^d	37 ±4^h	23,2 ±2,3^i
Gaba	49.3±1.1^a	37.7±1.6^b	23.3±3.3^c	14.8±1.3^d	10.1±0.6^e	39.5±2.9^b	14.2±0.9^d	6.4±0^e	4.6±0.4^f	50,5 ±5,2^a	26,7 ±3,7^c	7,3 ±1^{e,f}	3,5 ±0,1^f
Gln	1±0.2^a	0.5±0.3^b	0±0^d	0±0^d	0±0^d	0.5±0.4^b	0±0^d	0±0^d	0±0^d	0,8 ±0^a	0,3 ±0,5^{b,c}	0 ±0^d	0 ±0^d
Glu	844.5±25.4^a	618.4±30.7^c	253.1±5.7^e	139.9±11.5^f	103±2.3^f	661.4±60.1^b	136.7±3.7^f	56.7±2.2^g	44±1.9^g	836,8 ±37,3^a	328,1 ±37,3^d	60 ±6,3^g	30,5 ±1,3^g
His	37.3±0.8^a	27.6±1.8^d	14±1^f	9.2±1^g	7.7±0.3^g	31.8±1.2^c	7.5±0.7^g	5.2±0.4^h	4.4±0.4^h	35,3 ±1,9^b	15,9 ±0,7^e	4,8 ±0,5^h	4 ±0,4^h
Ile	35.5±1.3^a	26.7±0.5^c	13±1^e	9.1±0.7^f	6.3±0.4^g	28.2±1.8^c	6.8±0.3^{f,g}	2.2±0.2^h	1.6±0.1^h	31,5 ±2,7^b	15,8 ±3,2^d	2,4 ±0,5^h	1,2 ±0,2^h
Leu	38.4±0.3^a	26.7±0.7^c	18.7±2.7^{d,e}	16.7±0.9^{e,f}	13.9±0.6^{f,g}	27.3±2.8^c	13.1±1.2^g	6.6±0.7^h	4.1±0.4^{h,i}	32,4 ±3,4^b	21,6 ±3,1^d	5,8 ±1,3^h	1,7 ±0,2^i
Lys	35.7±0.7^a	25.6±1.3^c	18.3±1.3^d	11.7±0.3^e	9.7±1^{e,f}	27.5±2.2^c	9±1^f	5.6±0.4^g	5.1±0.4^g	33,2 ±0,6^b	19,2 ±3,3^d	5,1 ±0,5^g	4,8 ±0,1^g
Met	11.4±0.2^a	8.6±0.4^b	7.1±0.4^c	6.1±0.3^d	6.1±1.2^d	9.3±0.6^b	5.1±0.4^e	3.2±0.1^f	2.4±0.1^{f,g}	11 ±0,3^a	7,7 ±0,9^c	2,8 ±0,1^f	1,6 ±0^g
Phe	236.1±2.2^b	307.9±29.5^a	204±27^c	159.8±2.9^d	122.3±7.4^e	305.6±31.5^a	145±3.9^{d,e}	54.3±4.1^f	34.3±4.2^{f,g}	326,1 ±42,5^a	198,9 ±1,2^c	51,7 ±7,8^f	11,5 ±0,4^g
Pro	52.6±1.7^b	43.1±2.2^c	26.3±4.1^d	19.3±1.9^e	10.9±1.5^f	43.9±1.9^c	23.1±8.5^{d,e}	5±0.9^{f,g}	2.9±0.5^g	60 ±6^a	28,1 ±0,6^d	6,3 ±1,6^{f,g}	2,6 ±0,2^g
Ser	47.4±1^a	27±1.1^c	19.5±1.2^d	16.8±2.2^d	11.8±1^{e,f}	32.9±3.7^b	12.5±1^e	9.5±0.8^{e,f,g}	7±0.8^g	46,4 ±3,4^a	26,1 ±2,3^c	8,7 ±1,3^{f,g}	7,9 ±3^g
Thr	22.1±0.7^a	14.8±0.9^c	9.6±0.7^e	6.9±0.7^f	4.4±0.5^g	17.8±1.8^b	5.4±0.6^g	2.4±0.4^{h,i}	1.2±0.3^i	20,8 ±1,3^a	11,8 ±1^d	2,8 ±0,9^h	1,3 ±0,8^{h,i}
Trp	43.1±1.9^a	25.9±2.8^c	14.5±0.8^d	9.3±0.6^e	7.9±0.7^e	30.7±2.6^b	7.4±0.6^e	4±0.1^f	3.3±0.1^f	31,6 ±3,3^b	14,8 ±1,3^d	3,7 ±0,3^f	2,9 ±0,1^f
Tyr	31.2±0.9^c	35.6±1.2^b	29.6±3^c	19.3±1.3^d	12.5±0.9^e	37.6±2.6^{a,b}	14.3±1^e	3.5±1^f	1.6±0.1^{f,g}	38,6 ±1,6^a	29,5 ±0,8^c	3,1 ±0,4^f	0,6 ±0,2^g
Val	65.2±0.1^a	42.6±1.3^c	22.8±2.6^e	15.5±0.6^f	10.6±0.3^g	46.5±3.4^c	12.2±0.6^{f,g}	4.5±0.6^h	2.9±0.1^h	57,2 ±6,1^b	28,5 ±4,9^d	4,6 ±0,7^h	2,5 ±0,4^h
bLys	11719.4 ±834.9^a	10997.2 ±672.9^{a,b,c}	9708.2 ±975.7^{b,c,d}	9188.4 ±873.3^{c,d,e}	9286.3 ±481.7^{c,d,e}	11620.1 ±931.3^a	9250.5 ±724^{c,d,e}	8573.4 ±147^{d,e,f}	7758.6 ±165.1^{e,f}	11334,9 ±1127,9^{a,b}	10115,3 ±1867,5^{a,b,c,d}	8765,9 ±1706,8^{d,e}	6903,8 ±500,4^f

Superscript letters in each raw indicate statistically significant difference (p<0.05) according to Duncan's test.

Data are expressed as mean±standard deviation.

43

Table 4. 5 Changes in the concentration of free amino acids and protein-bound lysine in almond by roasting (mg/kg almond)

	Non-treated	160 °C				180 °C				200 °C			
		15 min	30 min	45 min	60 min	10 min	20 min	30 min	40 min	5 min	10 min	15 min	20 min
Ala	184.8±21.5[b,c]	211.5±11.9[a]	141.5±12[d]	69.7±2.7[f]	43.5±8[g]	191±25.7[a,b]	107.4±14.4[e]	25.3±2.3[g]	25.1±2.4[g]	196,1±25,7[a,b]	163,9 ±13[c,d]	41,9±8,2[g]	18,9±0,8[g]
Arg	317.4±34.7[b,c]	487±150.3[a]	248.7±79.4[b,c]	116.9±20.4[d,e]	112.3±97.1[d,e]	348.3±45.7[b]	213.3±18.1[c,d]	49.4±10.3[e]	52.7±16.7[e]	317,6±14,5 [b,c]	307,8±42,8 [b,c]	108,5±23,2 [d,e]	36,9±9,4[e]
Asn	1190.8±151[c]	1827±322.1[a]	660.3±105[d]	231.9±34.9[e,f]	182.1±41.2[e,f]	1514.1±272.2[b]	393.2±38.7[e]	120.2±7.7[f]	141.4±10.9[f]	1436,4±30,2[b]	1043,6±45,6[c]	173,6±36,7[e,f]	93,8 ±14,2[f]
Asp	490.3±42.8[b]	607.9±52.1[a]	421.3±41.7[c]	216.9±5.2[e]	148.9±22.6[f]	564.1±75.7[a]	317.1±35.7[d]	104.5±10.7[f,g]	107.9±5.8[f,g]	563±7[a]	492,4±20,3[b]	156,6±22,5[f]	78,1±8,8[g]
Gaba	84.8±11[a]	14.5±3.1[b]	6±0.7[c,d]	3.9±0.4[c,d]	2.4±0.2[d]	13.4±7.9[b]	5.9±1.2[c,d]	2.3±0.2[d]	1.9±0.1[d]	10,5±1[b,c]	9±1,9[b,c,d]	3,5±0,4 [c,d]	1,8±0[d]
Gln	136.8±17.4[a]	14.5±3[c]	1.1±0.2[d]	0.4±0.2[d]	0±0[d]	14±2.8[c]	0.8±0.5[d]	0±0[d]	0±0[d]	71,5±3,2[b]	2,4±0,8[d]	0,1±0,1[d]	0±0[d]
Glu	513.4±52[c]	627.5±64.4[b]	147.8±6.6[e]	52.7±3[f,g]	38.2±5.9[f,g]	603.3±72[b]	93.5±12.1[e,f]	33.4±1.8[f,g]	29.9±4.4[f,g]	708,3±42,3[a]	385,1±38[d]	46,6±9 [f,g]	23,1±1,5[g]
His	90.2±12[a]	76.5±9.4[b]	38.6±3.9[d]	16.5±0.9[e]	12.7±2.7[e]	76.6±7.8[b]	29.5±5[d]	9.4±1.9[e]	12.2±2.1[e]	76,9±3,6[b]	60,2±3,7[c]	13,1±2,8[e]	8,4±0,8[e]
Ile	148.2±17.7[a]	132.8±6.8[b]	53.7±5.1[d]	12.8±1.3[f]	3.1±1.5[f]	129.6±12.1[b]	28.3±4[e]	0±0[f]	0±0[f]	137,3±5,4[a,b]	96,9±4,5[c]	2,4±1,7[f]	0±0[f]
Leu	112.6±15.1[a]	66.6±1[b]	18.8±2[d]	4.4±0.7[e,f]	1.6±0.6[e,f]	66.3±5.5[b]	9.2±0.6[e]	0±0[f]	0.2±0.4[f]	73,7±3[b]	44±3,6[c]	0,6±0,5[f]	0±0[f]
Lys	84.8±11.6[a]	65.1±1.2[b]	29.8±5.1[e]	15.4±1.2[f]	12.2±2.8[f]	57.4±6.2[c]	22.7±2.1[e]	9.2±1.8[f]	9.3±0.9[f]	62,9±4,3[b,c]	48,1±2,1[d]	12±2[f]	7,3±0,6[f]
Met	46.9±6.9[a]	28.2±3[b,c]	6.4±0.6[e]	0.6±0.3[f]	0±0[f]	26.3±2.8[c]	1.9±0.6[f]	0±0[f]	0±0[f]	32,2±3,6[b]	15,2±2[d]	0±0[f]	0±0[f]
Phe	121.6±14.8[a,b]	110.9±9[b]	42.4±1.4[d]	15.8±2.2[e,f]	6±0.6[f,g]	118.7±11.4[b]	20.7±2.9[e]	2.3±1[g]	1±0.7[g]	130,2±5,8[a]	83,9±7,7[c]	3,8±1,5[g]	0±0[g]
Pro	195±22.2[b]	203±15.5[b]	125.7±7[c]	42±7.7[e]	21.2±3[f,g]	246.3±13.4[a]	99.9±12.3[d]	12.8±1.1[g]	11.1±1[g]	242,4±13[a]	211,2±1,1[b]	31,2±6,8[e,f]	9,8±0,4[g]
Ser	116.4±12.8[a]	99.4±9.8[b,c]	69.7±8.5[d]	37.6±3.4[f]	29.9±4[f,g]	100.2±4.7[b,c]	50.3±9.6[e]	23.3±2.2[g,h]	26.4±6.5[f,g,h]	103,4±7,4[b]	88,9±6,6[c]	26,9±8,3[f,g,h]	16,1±0,2[h]
Thr	75.8±9.5[a]	68.5±2.4[a,b]	30.8±4.5[e]	13.8±0.6[g]	9.7±1.2[g]	59.8±10.1[c]	22.3±4.1[f]	5.8±1[g,h]	5.7±1.9[g,h]	64,5±1,1[b,c]	47,1±2,1[d]	8,8±2,1[g,h]	3,3±0,1[h]
Trp	51.2±6.5[d]	67.3±6.3[c]	29.1±1.8[e]	7.3±0.8[g]	1.9±0.7[g,h]	78.7±3.7[b]	15.5±0.9[f]	0±0[h]	0±0[h]	89,1±8[a]	49,9±5[d]	1,9±0,6[g,h]	0±0[h]
Tyr	100.2±19.1[a]	57.4±6.2[b]	22.7±2.5[d]	9±1.6[e,f]	3.3±0.3[e,f]	48.5±4.1[b]	11.6±2.6[e]	0.5±0.5[e,f]	0.5±0.9[e,f]	54,5±5,6[b]	37,2±0,4[c]	1,8±1 [e,f]	0±0[f]
Val	156.3±17[a]	152.1±9.6[a]	70±6.1[d]	22±1.5[f]	9.7±2.3[f,g]	135.9±13.2[b]	39.9±5.7[e]	4±1.2[g]	3±0.9[g]	146,6±8,4[a,b]	102±4,3[c]	9,6±2,3[f,g]	1,6 ±0[g]
bLys	6933.7 ±189.1[a]	6447.9 ±315.5[b,c]	5280.2 ±84[d]	4098.8 ±357.9[f]	3591 ±98.2[g]	6720.5 ±80.7[a,b]	4589.9 ±227.4[e]	3347.7 ±445.8[g]	2599.9 ±51.8[h]	6926,6 ±256,3[a]	6219,7 ±194[c]	3432,6 ±108,1[g]	2327,7 ±102[h]

Superscript letters in each raw indicate statistically significant difference (p<0.05) according to Duncan's test. Data are expressed as mean±standard deviation.

Protein-bound amino acids are also susceptible to participating in the Maillard reaction due to their reactive side chains (Hemmler et al., 2018). For that reason, changes in the concentration of protein-bound amino acids, which may play a role in the Maillard reaction, were also monitored. It was determined that there was a significant decrease only for protein-bound lysine (bLys), therefore, the change in bLys content was also added to Table 4. 1-5. In addition, the change in protein-bound Arg and His, which have reactive groups for Maillard reaction, was also examined and it was seen that there was no significant difference in their concentration during roasting. The change in these protein-bound amino acids and also bLys to compare was shown in Figure 4. 2-4.

The highest amount of protein-bound lysine was found in peanut (11719.4±835.0 mg/kg sample) and pumpkin seed (11771.0±1313.6 mg/kg sample) whereas it was the lowest in almonds (6933.7±189.1 mg/kg sample). Almost all free amino acids participated in the reactions and, the highest decrease in the total amino acid content (sum of free amino acids and protein-bound lysine) was found in flaxseeds (72%) and sunflower seeds (71%) followed by peanut (44%), almond (35%) and pumpkin seed (28%) with roasting.

A rapid decrease was observed in the amount of sucrose when compared to the degradation rate of amino acids. Amino acids can be regenerated because of the breakdown of the AP/HP which might be the explanation for the slow decrease in the amount of amino acids. Göncüoğlu Taş and Gökmen (2017) were also reported that initial degradation rates of reducing sugars were higher than the degradation rate of amino acids in hazelnuts during roasting.
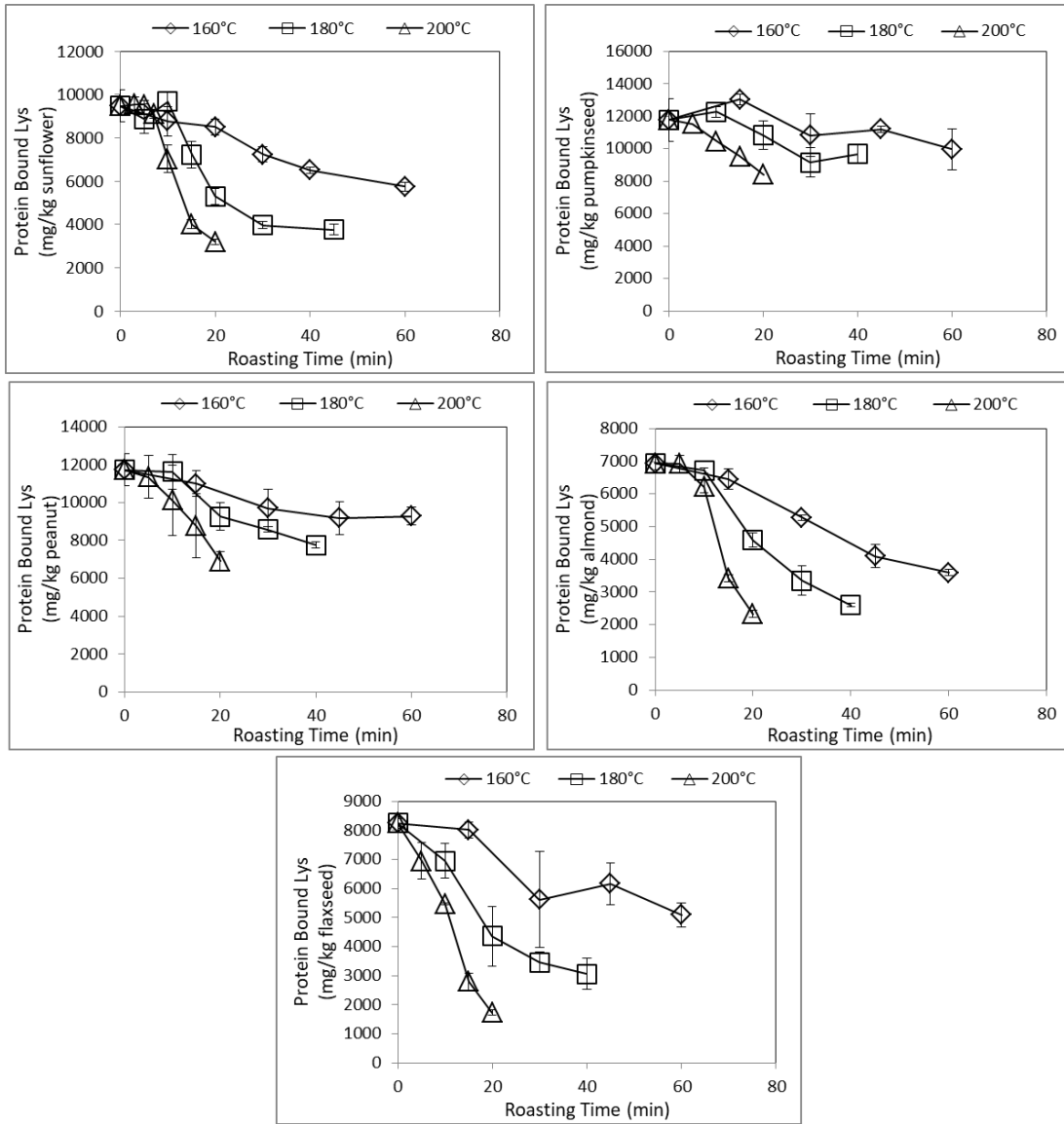
Figure 4. 2 Changes in the concentration of protein-bound lysine content by roasting
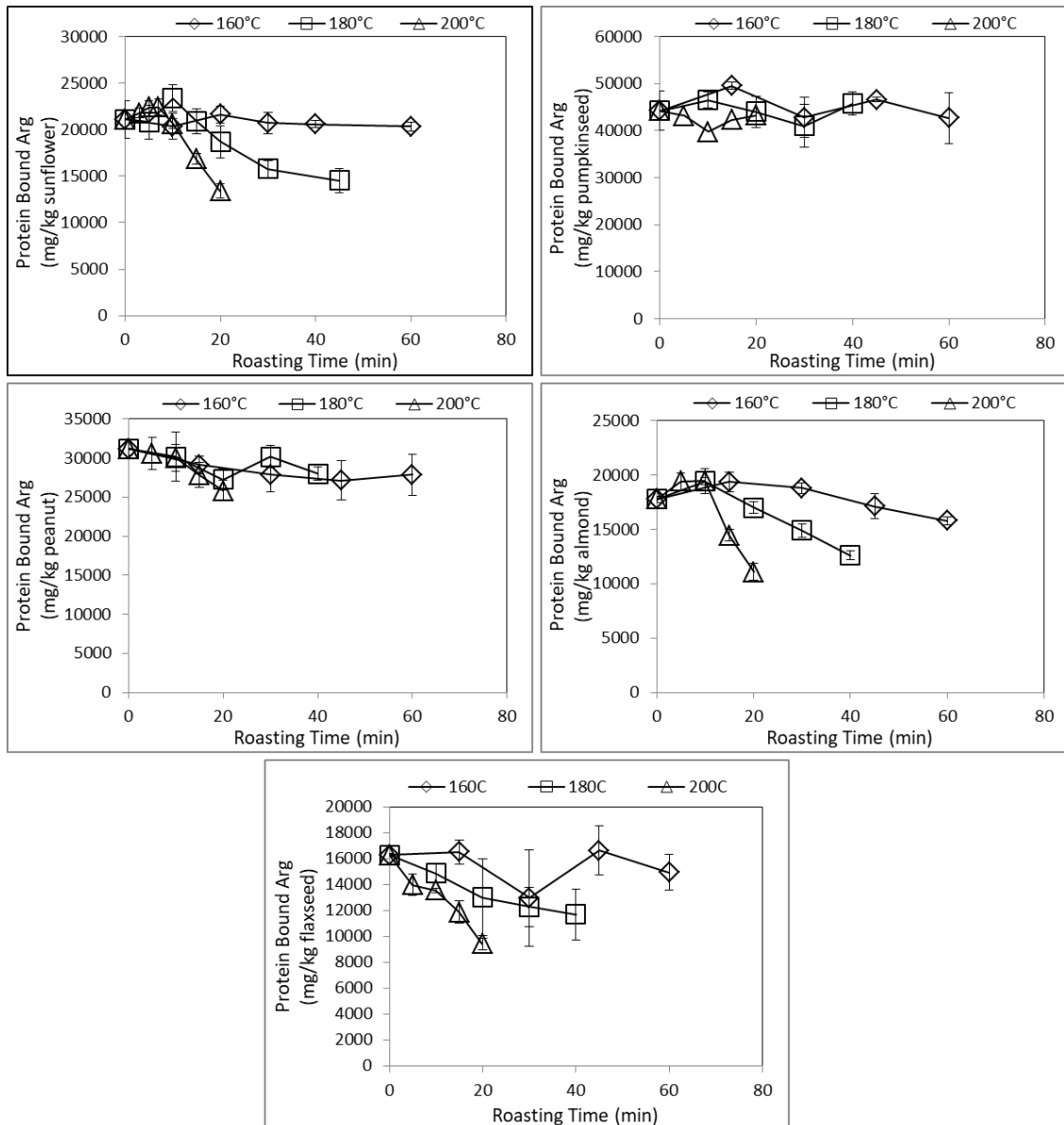
Figure 4. 3 Changes in the concentration of protein-bound arginine content by roasting
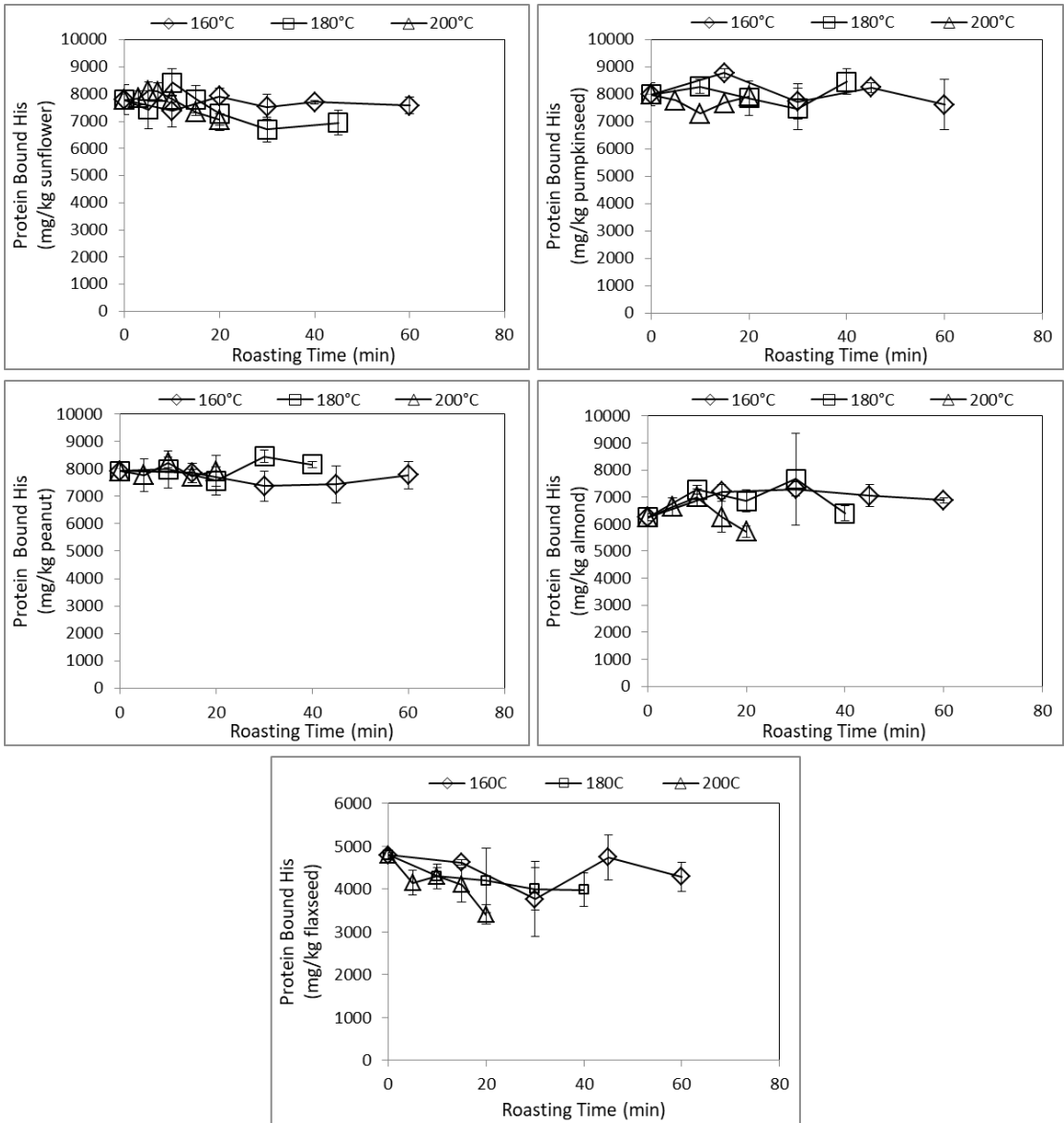
Figure 4. 4 Changes in the concentration of protein-bound histidine content by roasting

4.3.2. Formation of 5-Hydroxymethylfurfural

HMF can be formed as an intermediate in the Maillard reaction or as a result of the caramelization of sugars. As shown in Figure 4. 5 change in HMF concentration in seeds and nuts shows an overall increasing trend in all samples in relation to the decrease in sugar content. The highest HMF formation ($p < 0.05$) was observed in sunflower seed samples (247.0 ± 8.3 mg/kg sunflower) after 30 minutes of roasting at 180 °C. It reached the value of 163 ± 6.3 mg/kg of sunflower seed within 15 minutes at 200 °C; HMF started to degrade with increasing roasting time after this point. In pumpkin seed, only 42.7 ± 0.4 mg/kg HMF was formed due to the least amount of sucrose among other samples. HMF concentration reached the highest value with 40 minutes of roasting at 180 °C in flaxseed (155.4 ± 4.0 mg/kg flaxseed) and peanut (144.4 ± 16.7 mg/kg peanut), whereas in almond samples maximum HMF content (166.2 ± 21.1 mg/kg almond) was observed at 200 °C after 20 minutes. Although there is no information in the literature regarding the amount of HMF in other samples, there are studies on the amount of HMF in almonds. It can be deduced from the figures that the increase in the amount of HMF continued even in high temperatures. Due to the high degradation rate of amino acids compared to sucrose, the amino acids degrade rapidly and there is no amino acid residue present that HMF can react with until the sucrose is completely depleted. Therefore, HMF continues to form from the sucrose still present in the medium. Agila and Barringer (2012) reported that HMF concentration was found to be 905 µg/L in almonds roasted in an oven at 177 °C for 20 min. In addition, the amount of HMF formed by roasting in hazelnut varieties was also examined in different studies. Göncüoğlu Taş and Gökmen (2017) pointed out that the formation of HMF is accelerated by increasing the temperature applied during roasting. In this study, it was reported that the HMF content of hazelnuts reached its maximum value of 278 ± 0.7 mg/kg dw after roasting at 170 °C for 20 minutes. The results obtained in a study carried out by Fallico et al. (2003) also showed that HMF level increased with roasting time. Prolonged roasting times at studied temperatures exceed the estimated dietary intake limit (1.6 mg/day/person) that was determined by EFSA (2005), for 1 portion (~30 g) of the sample, except for pumpkinseed samples.

Although HMF can be formed during storage at low temperatures, its formation rate increases with the increasing temperature in the applied heat treatment. Therefore, HMF

can be used as a marker that shows the heat load during the thermal processes (Capuano and Fogliano, 2011). However, it should be considered that HMF is not stable under the roasting conditions and may degrade depending on the heat treatment conditions, and in this case, HMF amount may be a misleading indicator for the thermal load. It is stated that the reason for this elimination of HMF may be due to the reaction of HMF with free amino acids (Nikolov and Yaylayan, 2011). In a study by Gökmen et al. (2012), it has also been stated that HMF plays a role in the conversion of asparagine to acrylamide during heat treatment.
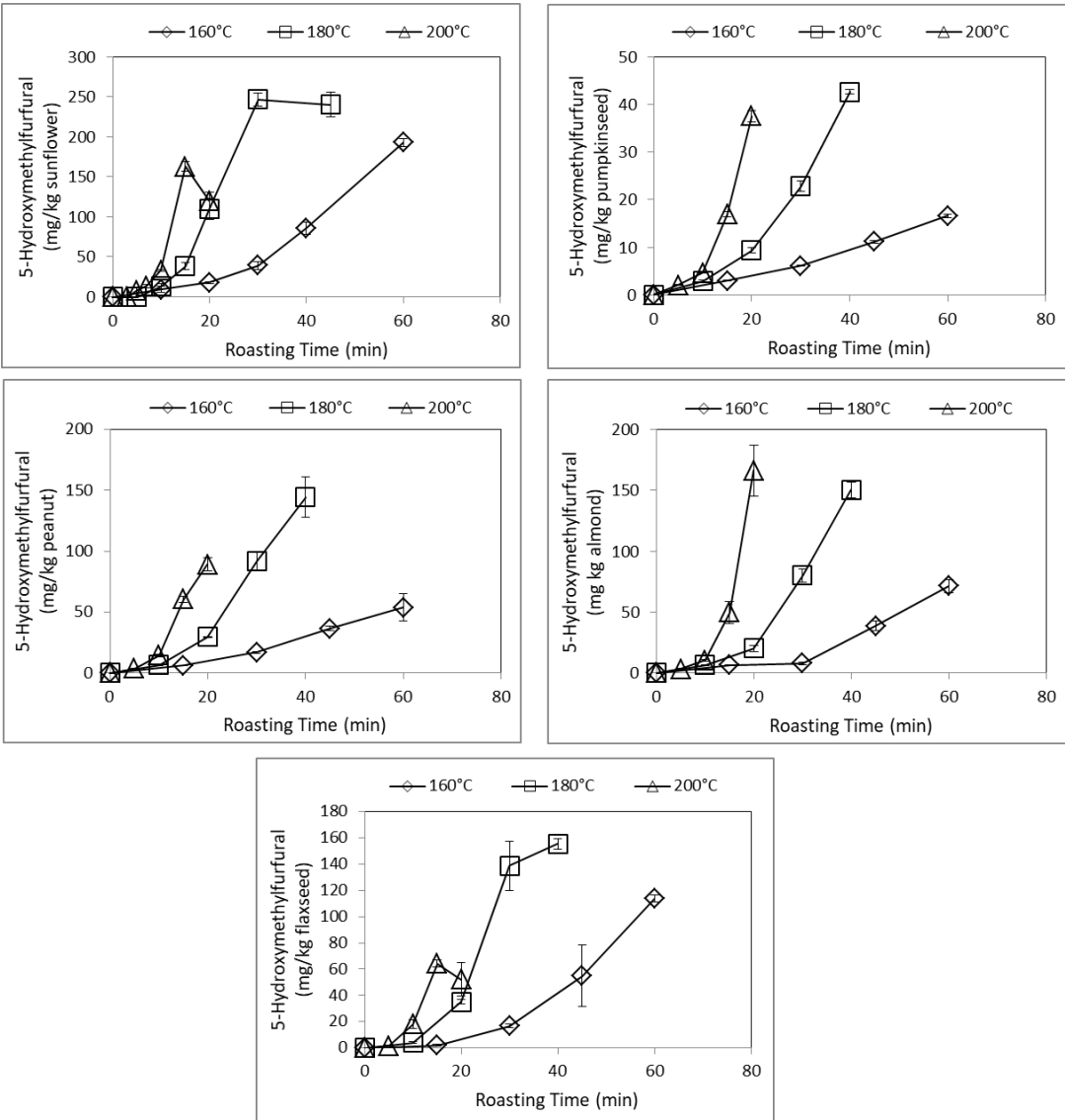
Figure 4. 5 Change in the concentration of 5-Hydroxymethylfurfural by roasting

4.3.3. Formation of Acrylamide

The formation of acrylamide (ACR) triggered by different roasting conditions was also monitored. As seen from Figure 4. 6, the ACR concentration increased to a certain extent with the roasting process, and then, ACR started to degrade with prolonged roasting time. This decrease point in ACR content was observed in the early stages of the roasting process, especially at high temperatures. The amount of detected ACR is the net difference between the amount of generated and eliminated ACR simultaneously during the roasting process. Therefore, it could be stated that the rate of ACR formation is lower than the rate of degradation at the points where the diminish begins.

The highest concentrations of ACR in sunflower seeds were observed after 40 min of roasting at 160 °C (938±97 µg/kg), 20 min at 180 °C (982±197 µg/kg), and 10 min at 200 °C (866±177 µg/kg). At all temperatures, the amount of ACR decreased as the treatment time increased. However, the most intense decrease in the amount of ACR was seen in the roasting process at 200 °C by decreasing to 322±126 µg/kg.

Compared to other samples, the lowest amount of ACR was determined in pumpkin seed samples. ACR level in pumpkinseed samples reached its highest value of 243±7 µg/kg pumpkinseed at 200 °C with 15 minutes of roasting. A decrease in ACR level was observed at 180 °C after 30 minutes and at 200 °C after 15 minutes.

In flaxseed, after reaching a maximum value within 20 min at 180 °C (918±33 µg/kg) and 15 min at 200 °C (1037±29 µg/kg), ACR followed a rapid decrease during prolonged roasting times. Levels of ACR did not significantly change after 45 min at a roasting temperature of 160 °C.

In peanut samples, ACR reached an apparent maximum of 378±65 and 367±26 µg acrylamide/kg peanut after 30 minutes of roasting at 180 °C and 15 minutes at 200 °C, respectively. After this point, ACR content started to decrease slightly.

The highest ACR concentration among the samples was found in almonds reaching up to 3127±131 µg/kg after roasting at 200 °C for 15 min due to the higher amount of free asparagine compared to the other samples. ACR level reached its peak within 20 minutes of heat treatment at 180 °C (2436±16 µg/kg almond) and 45 minutes at 160 °C (1955±220 µg/kg almond) and then drastically decreased with increasing processing time.

Since a decarboxylated Amadori product of asparagine with reducing sugars (*N*-glycosylasparagine) is the direct precursor of ACR (Yaylayan et al., 2003), the change in the amount of free asparagine is also shown in Figure 4. 6. It can be seen from the figure that the formation rate of ACR decreases due to the decrease in the amount of asparagine as the heat treatment proceeds as expected. In addition, these results indicate that asparagine is the limiting reactant in ACR formation.

Schlormann et al. (2015) reported that the ACR content of almonds and pistachios was found to be 1220 and 88 µg/kg after the roasting process at 170.8 °C for 15 min and 185.1 °C for 21 min, respectively. In another study, while ACR could not be detected in raw almond samples, it was determined that the amount of ACR increased with roasting at temperatures ranging from 129-182 °C, and the highest ACR concentration reached 907 µg/kg at 182 °C within 5.7 minutes (Zhang et al., 2011b). In a study by Amrein et al., (2005b), the highest amount of ACR in commercially roasted almonds was determined as 2147 µg/kg. In another study comparing the amounts of ACR formed by roasting in different almond cultivars, the highest ACR content (1681 µg/kg sample) was observed in the cultivar of Carmel, which also has the highest asparagine content (2760 µg/kg), after 12.5 minutes of heat treatment at 162 °C (Amrein et al., 2005a). In a study conducted by Nematollahi et al., (2020), the highest ACR contents were determined as 152.55±13.59 and 171.75±15.31 µg/kg among 6 types of roasted peanut and 3 types of roasted sunflower samples, respectively. The ACR content of roasted sunflower seed was found to be 66 µg/kg in another study (Jagerstad and Skog, 2005). Ölmez et al. (2008) and De Paola et al. (2017) reported the highest ACR content in roasted peanuts as 66 and 42.86 µg/kg, respectively.
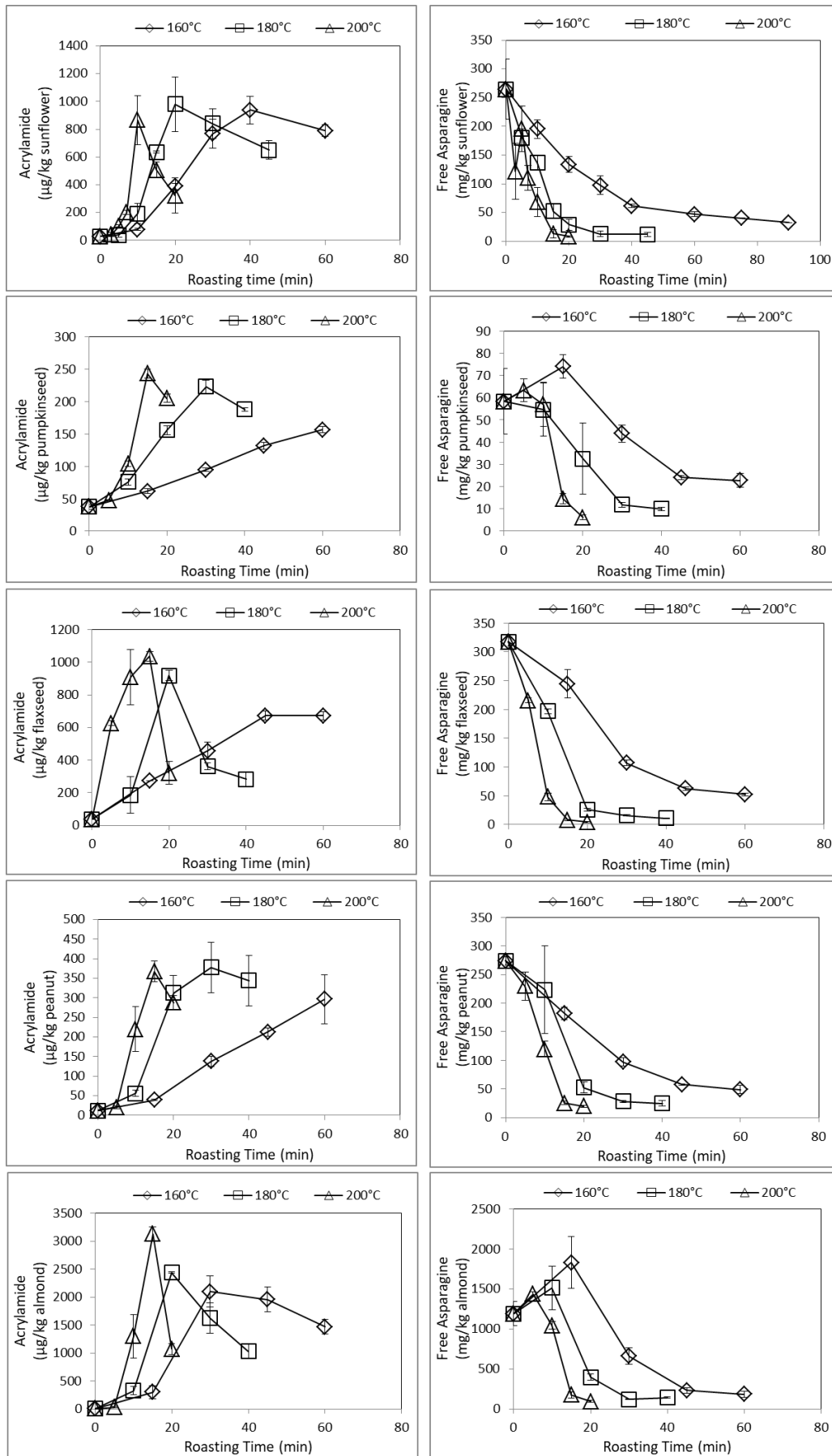
Figure 4. 6 Changes in the concentrations of acrylamide (µg/kg sample) and free asparagine content (mg/kg sample) by roasting

4.3.4. Formation of Furosine

Furosine (N-ε-(furoylmethyl)-L-lysine) content was determined to evaluate the extent of the early stages of the Maillard reaction. The change of furosine concentration in the samples, depending on the roasting parameters, was shown in Figure 4. 7. The furosine content in raw samples was 45.6±0.1, 195.6±49.9, 15.6±1.0, and 47.1±4.0 mg/kg for sunflower, pumpkinseed, flaxseed, and peanut respectively. There is no detectable amount of furosine in raw almond samples. Except for pumpkin seed samples, furosine content increased with the increasing roasting period and started to decrease as the roasting time gets longer. It was found that there was no significant difference (p>0.05) between the maximum amounts of furosine formed at each temperature. In sunflower seed samples, furosine content reached a certain extent, and at roasting times longer than approximately 40 minutes at 160 °C, 20 minutes at 180 °C, and 10 minutes at 200 °C, a decrease was observed in the amount of furosine as it started to degrade. Furosine was thought to be formed in raw pumpkin seed samples under storage conditions before heat treatment, and its amount started to decrease with the thermal treatment. The reason for not observing an increase in the amount of furosine was attributed to the low amount of sucrose in pumpkin seeds. The amount of furosine, which was high at the beginning, decreased due to the degradation of the N-ε-fructosyllysine, to different compounds such as α-dicarbonyls or CML by heat treatment (Ahmed et al., 1986). The results are also in agreement with the findings of Göncüoğlu Taş and Gökmen (2019), who reported that the furosine content of raw hazelnuts was 39.4 ± 2.6 mg/kg in Tombul and 75.7 ± 1.0 mg/kg in the Levant and significantly decreased by roasting. In a study by Rada-Mendoza et al. (2002), they reported that a high concentration of furosine may be associated with storage at at inappriate temperatures. Gökmen et al. (2008) found that the levels of furosine were significantly lower in cookies that contain sucrose than in cookies that contain glucose. The amount of furosine in flaxseed initially increased at 180 °C and 200 °C and reached the highest value of 27.0±0.3 and 29.1±0.8 mg/kg, respectively. Then, started to decrease after 10 minutes of heat treatment with increasing time. At 160 °C, the amount of furosine continued to increase with increasing processing time. In shorter processing times, there was no significant change (p>0.05) in the amount of furosine in peanut samples at 180 °C and 160 °C, whereas a decrease at 180 °C and an increase at 160 °C was observed in the amount of furosine after 30 minutes of heat treatment. The highest amount of furosine (61.7±1.2

54

mg/kg) was measured after 5 minutes of heat treatment at 200 °C. A sharp decrease in furosine concentration was seen after this point.In almonds, the concentration of furosine increased up to 15 minutes at 160 °C and 10 minutes at 180 and 200 °C. At the end of these periods furosine content reached its highest value of 87.7±6.3, 86.6±1.8 and 88.9±9.7 mg/kg, respectively. A decrease in the amount of furosine was observed with heat treatment times longer than this. In the light of the findings, it can be concluded that the Amadori product is seen to undergo more degradation or oxidation with increasing temperature and roasting time.
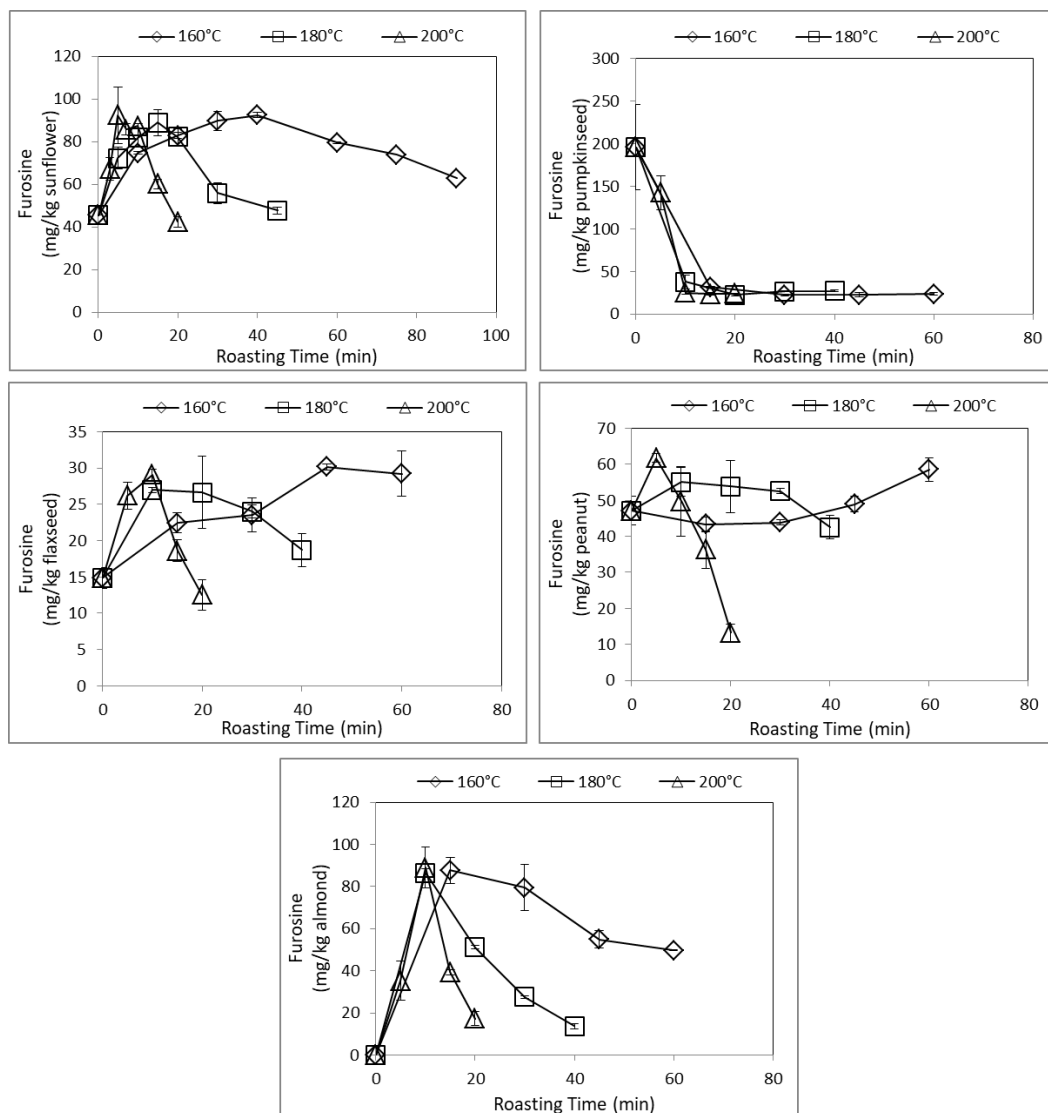
Figure 4. 7 Change in the concentration of furosine content by roasting

4.3.5. Formation of N-ε-Carboxymethyllysine and N-ε-Carboxyethyllysine

The formation of N-ε-Carboxymethyllysine (CML) and N-ε-Carboxyethyllysine (CEL), markers for AGE formation in food, was monitored in roasted samples. Changes in the concentration of CML and CEL were shown in Figure 4.8.

The highest CML concentrations in roasted sunflower seeds were 31.3±2.0 mg/kg sample at 160 °C after 60 min, 43.0±3.1 mg/kg sample at 180 °C after 30 min, and 46.2±0.6 mg/kg sample at 200 °C after 20 min treatment. In pumpkinseed samples, the concentration of CML reached the highest values of 25.2±0.6, 32.5±1.2, and 37.8±4.9 mg/kg sample at 160, 180, and 200 °C, respectively. Maximum CML concentrations detected in flaxseeds were 18.9±1.2, 33.5±1.8, and 42.6±1.8 mg/kg sample at 160, 180, and 200 °C at the end of the longest roasting process. The maximum levels of CML in roasted peanut samples at 160, 180 and 200 °C were as follows: 30.4±6.2 mg/kg sample in 60 min, 37.0±2.7 mg/kg sample in 40 min, and 41.2±1.7 mg/kg sample in 20 min. Different from the others, CML content in almond samples reached the highest level after 45 and 30 minutes at 160 °C (23.1±3.3 mg/kg sample) and 180 °C (28.7±2.9 mg/kg sample), then it started to decrease with the prolonged roasting process. At 200 °C, 26.3±3.8 mg CML/kg sample was detected after 20 min of roasting. Similarly, according to a study conducted on roasted peanuts, the CML content was gradually increased by the roasting process (Wellner et al., 2011). Göncüoğlu Taş and Gökmen (2019) also detected the amount of CML in raw hazelnuts as 6.0 mg/kg sample and the formation of CML was found more than doubled by roasting. In a study by Berk et al. (2019), it was reported that CML concentration reached 25.0±5.0 mg/kg in sesame seeds after roasting at 220 °C.

Similar to CML, the roasting process has enhancing effect also on CEL levels. CEL formation at lower temperatures such as 160 °C was relatively less in all samples. In sunflower seeds, the highest content of CEL was detected after roasting at 200 °C for 15 min (148.28±10.58 mg/kg sample). Among other samples, maximum CEL content was observed in pumpkin seed roasted at 200 °C for 20 min (231.7±23.0 mg/kg). CEL concentration in flaxseed and peanut was found to be reached the highest values of 172.4±3.1 mg/kg and 200.2±4.5 mg/kg after roasting for 15 min at 200 °C. CEL amount in almonds reached its highest level after 30 minutes of roasting at 180 °C and 15 minutes at 200 °C. Likewise, Berk et al. (2019) reported that 83 mg/kg CEL was

detected in sesame seeds roasted at 220 °C. CEL levels were found higher than CML levels although they followed similar trends during roasting. This could be attributed to the higher formation rate of MGO and its faster reaction with lysine compared to glyoxal. They also reported that CML content is lower than CEL content, probably due to high amounts of methylglyoxal formed during the roasting of sesame seeds compared to glyoxal. Similarly, in the study of Zhang et al. (2011a), CEL content was found relatively higher than the CML content in roasted almonds. Berk et al. (2019) also reported that CML content is lower than CEL content, probably due to high amounts of methylglyoxal formed during the roasting of sesame seeds compared to glyoxal.

CML is also formed through the oxidation of Amadori rearrangement products such as N-ε-fructosyllysine. During heat treatment, N-ε-fructosyllysine is rapidly transformed into advanced Maillard reaction products such as CML. Therefore, it is inappropriate to use furosine content as an indicator of heat load (Charissou et al., 2007). As mentioned in the earlier studies (Berk et al., 2019, Göncüoğlu Taş and Gökmen, 2019, Wellner et al., 2011) the higher concentrations of furosine than CML, indicate that of early stages of Maillard reaction are dominant. Likewise, in the studied roasting parameters, although furosine showed a sharp decrease in some samples, its concentration was found to be higher than CML content in all samples. Similar to our findings, in the study conducted on roasted hazelnuts, an increase in CML content by roasting and a higher furosine concentration compared to CML was found by Göncüoğlu Taş and Gökmen (2019). The concentration of CML and CEL decreased with the increase in processing time at 180 and 200 °C. Since another formation route for CML and CEL is the reaction of lysine with glyoxal and methylglyoxal (Zamora and Hidalgo, 2005), the decrease in CEL content might be attributed to their degradation or blockage of methylglyoxal with other compounds (Troise et al., 2015).
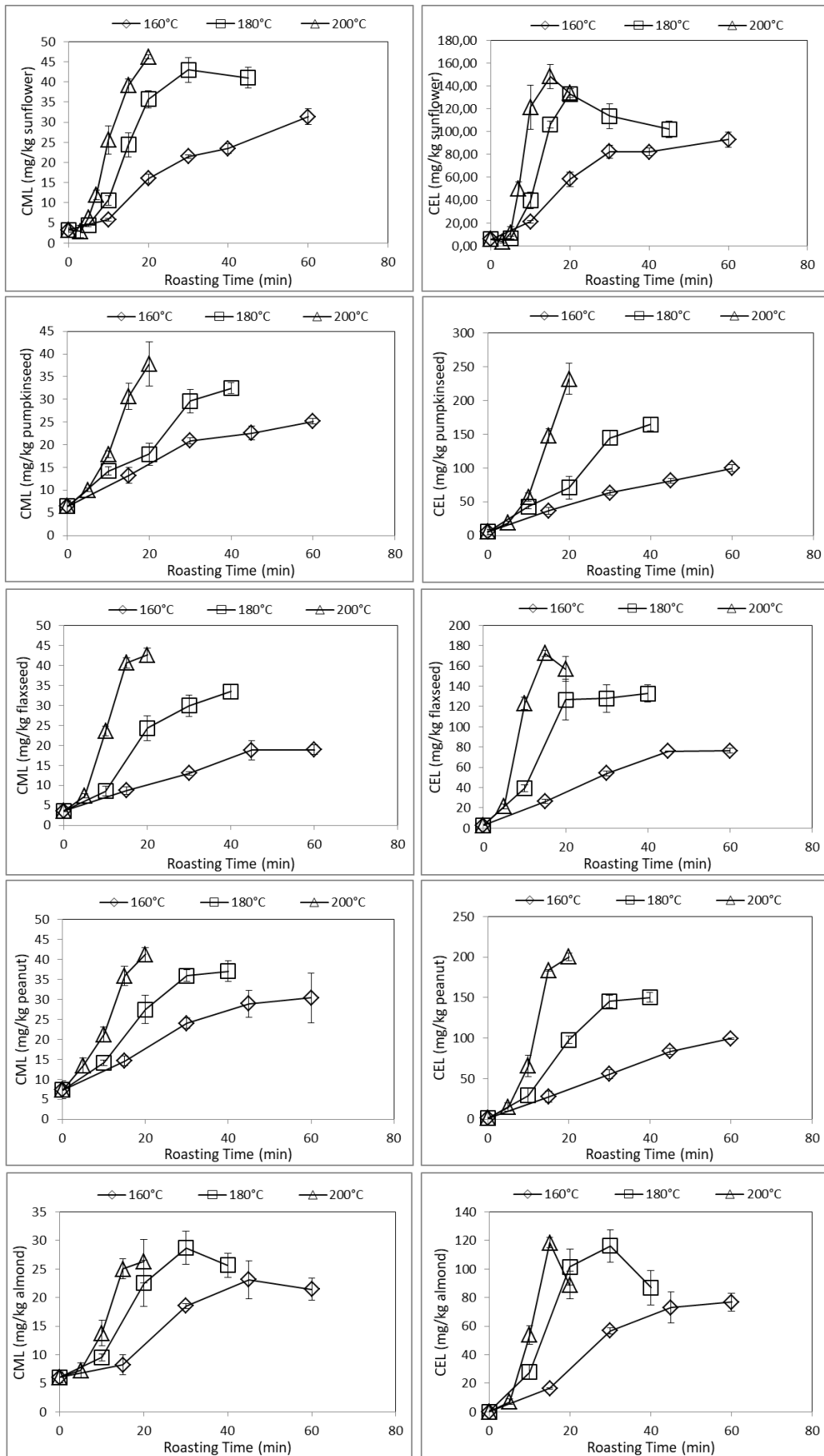
Figure 4. 8 Formation of CML and CEL during roasting process

4.3.6. Formation of α-Dicarbonyls

Figure 4. 9-13 illustrate the formation kinetics of α-dicarbonyl compounds in roasted samples. Among the raw samples, the highest concentration of total α-dicarbonyl compounds was detected in sunflower and pumpkin seed samples probably due to formation prior to transportation or during sun-drying (Göncüoğlu Taş and Gökmen, 2019). Raw flaxseed was found to have the least α-dicarbonyl compound content in comparison to other raw samples.

3-DG reached its highest amount (17.76±0.94 mg/kg) in sunflower seeds after 60 min of roasting at 160 °C. MGO showed similar formation kinetics with 3-DG except in 160 °C. Unlike the 3-DG, no significant difference was observed in the amount of MGO after 30 minutes in the roasting process at 160 °C whereas 3-DG showed a constant increment with extended roasting time at 160 °C. The concentration of 3-DG increased up to 14.17±0.63 mg/kg at 180 °C after 30 min and 12.91±4.46 mg/kg at 200°C after 15 min, respectively. The highest MGO content (12.28±1.95 mg/kg) was detected after roasting at 200 °C for 10 min. The GO content was in the highest concentration which is about 5.52±1.82 mg/kg in raw samples, decreased in the early stages of roasting, then increased but even so could not reach the initial level. The glucosone level was between the limits of 11.97-15.68 mg/kg, and no significant difference was observed (p>0.05).

3-DG, MGO, GO and DMG content of raw pumpkin seeds was 6.45±0.41 mg/kg, 7.05±0.01 mg/kg, 8.48±0.19 mg/kg, and 4.50±0.11 mg/kg respectively. An increase in the temperature and time cause a slight increment in the amount of DMG and GO whereas the concentration of 3-DG and MGO was increased by almost double. A decreasing step was also observed in the formation/elimination kinetics of 3-DG at 180 °C for 10 min of roasting.

Flaxseed was found to be rich in 3-DG, followed by MGO. A trace amount of α-dicarbonyl compounds were detected in raw samples. After reaching the highest value within 20 min at 180 °C (10.62±0.30 mg/kg) and 10 min at 200 °C (8.97±0.65 mg/kg), 3-DG followed a decreasing trend with the prolonged roasting times. The amount of MGO reached similar levels after 20 minutes at 180 °C and 15 minutes at 200 °C whereas it remained at a lower level at 160 °C. The highest DMG concentration was 1.91±0.03 mg/kg at 160 °C. It was found to be 2-2.5 fold higher at 180 and 200 °C

compared to 160 °C. GO content was also increased during roasting and reached 2.13±0.04 mg/kg at 180 °C in 40 min.

An increase in the temperature accelerated the formation of all measured α-dicarbonyl compounds in peanut samples. The maximum 3-DG content was found to be 9.74±1.30 mg/kg after 40 min of roasting at 180 °C. Just like 3-DG, glucosone was also detected in its highest values of 3.20±0.28 mg/kg at 180 °C after 40 min of roasting. MGO increased up to 6.63±0.53 mg/kg by roasting at 160 °C in 60 min, 9.76±0.59 mg/kg at 180 °C in 40 min, and 10.09±0.42 mg/kg at 200 °C in 20 min. Contrary to the higher concentrations of MGO, lower concentrations of GO and DMG were observed. GO showed a similar trend with MGO but increased to lower levels. GO and DMG reached an apparent maximum of 2.67±0.14 mg/kg and 2.41±0.04 mg/kg at 200 °C for 20 min of roasting.

In the roasting of almonds, among the hexodiuloses, 3-DG is the most abundant one. The highest concentration for 3-DG (12.00±1.73 mg/kg) was observed after 20 min of roasting at 200 °C. Glucosone increases after a short lag phase in all temperatures and reached to the maximum value of 2.05±0.04 mg/kg in 40 min at 180°C. The level of MGO and GO increased to a certain degree, but the rate of formation slowed after 30 minutes at 160 °C 20 minutes at 180 °C, and 15 min at 200 °C. Maximum concentrations were attained for MGO, GO, and DMG as 10.38±0.70 mg/kg, 2.36±0.15 mg/kg, and 2.20±0.26 mg/kg, respectively.

As can be seen from the results, α-dicarbonyl compounds in pumpkin seed, peanut, and almond showed a similar increasing trend during roasting while in flaxseed and sunflower they showed a decreasing trend depending on the roasting conditions. In all treated samples, glucosone was found to be the least among all α-dicarbonyl compounds based on the fact that glucosone is susceptible to oxidation and can be easily degraded due to its reductone structure (Gobert and Glomb, 2009). In addition, glucosone could not be detected in any of the roasted sunflower seed, pumpkinseed, and flaxseed samples. A high proportion of MGO and 3-DG was measured in the roasted samples compared to other α-dicarbonyl compounds. 3-DG and MGO were the most predominant, and the amount of 3-DG was above 10 mg/kg in all roasted samples except for peanut samples which were at a slightly lower level.

According to a study investigating dicarbonyl compounds in commonly consumed foods, it was reported that 3-DG was the predominant 1,2-dicarbonyl compound and maximum 3-DG concentrations increase up to 410 mg/L in fruit juices, 2622 mg/L in balsamic vinegar, and 385 mg/kg in cookies. It was also stated in this study that fermented food like yogurt, alcoholic beverages, and soy content varies between 0.02 to 7.6 mg/kg or mg/L, in processed coffee and baked cookies, amounts range from 23 mg/L to 210 mg/kg (Degen et al., 2012). Berk et al. (2019) determined the α–dicarbonyl compound concentrations of sesame seeds during roasting. Consistent with our findings, they indicated that the roasting process triggers the formation of dicarbonyls. They reported that 3-DG and MGO showed a similar formation trend and the highest level for 3-DG and MGO was attained as 3.9 ± 0.6 mg/kg and 5.7 ± 0.9 mg/kg, respectively. From their findings they deduced that dicarbonyl compounds were mainly formed through Maillard reaction and caramelization in roasted sesame seeds rather than lipid oxidation. In another study it was reported that concentrations of 3-DG, MGO, and GO during roasting process were increased and reached up to 3.7, 4.2 and 3.3 mg/kg for Tombul quality hazelnuts and 5.4, 4.8 and 3.3 mg/kg for Levant quality, respectively (Göncüoğlu Taş and Gökmen, 2019). They also observed a slight increase in the content of DMG and 1-DG. It has been suggested that the presence of α-dicarbonyl compounds in raw samples may have formed prior to transportation or during the sun-drying. Göncüoğlu Taş and Gökmen (2016) revealed that the amount of the predominant α-dicarbonyl compound 3-DG and glucosone in raw cocoa samples, which was 17.3 and 3.7 mg/kg dry weight, respectively, decreased by roasting due to degradation to shorter-chain α-dicarbonyl compounds. In a study by Hamzalıoğlu and Gökmen (2020), it was stated that the increase in dicarbonyl content at the beginning of coffee roasting may occur mostly due to sugar fragmentation, but the decrease in the amount of α-dicarbonyl compounds may be associated with their reactions in the final stages of the Maillard reaction. 3-DG and MGO content in thermally processed peanut was found to range from 1.45-2.89 mg 3-DG/kg and 1.90-1.37 mg MGO /kg, whereas it was 2.75-3.80 mg 3-DG/kg and 0.38-1.90 mg MGO /kg for hazelnut (Batool et al., 2020). To the best of our knowledge, there are no studies in the literature focused on the formation of α-dicarbonyl compounds in sunflower seeds, pumpkin seeds, flaxseed, and almond induced by the roasting process.
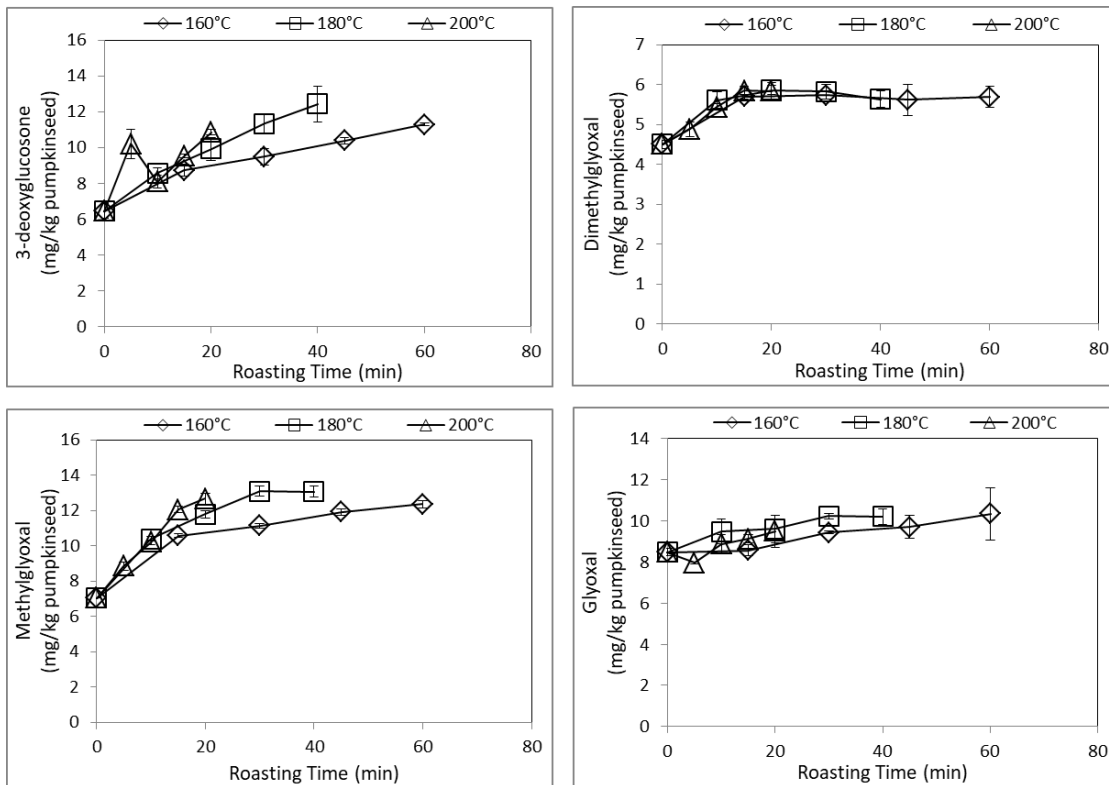
Figure 4. 9 Change in the concentration of α-dicarbonyl compounds during roasting of pumpkin seeds
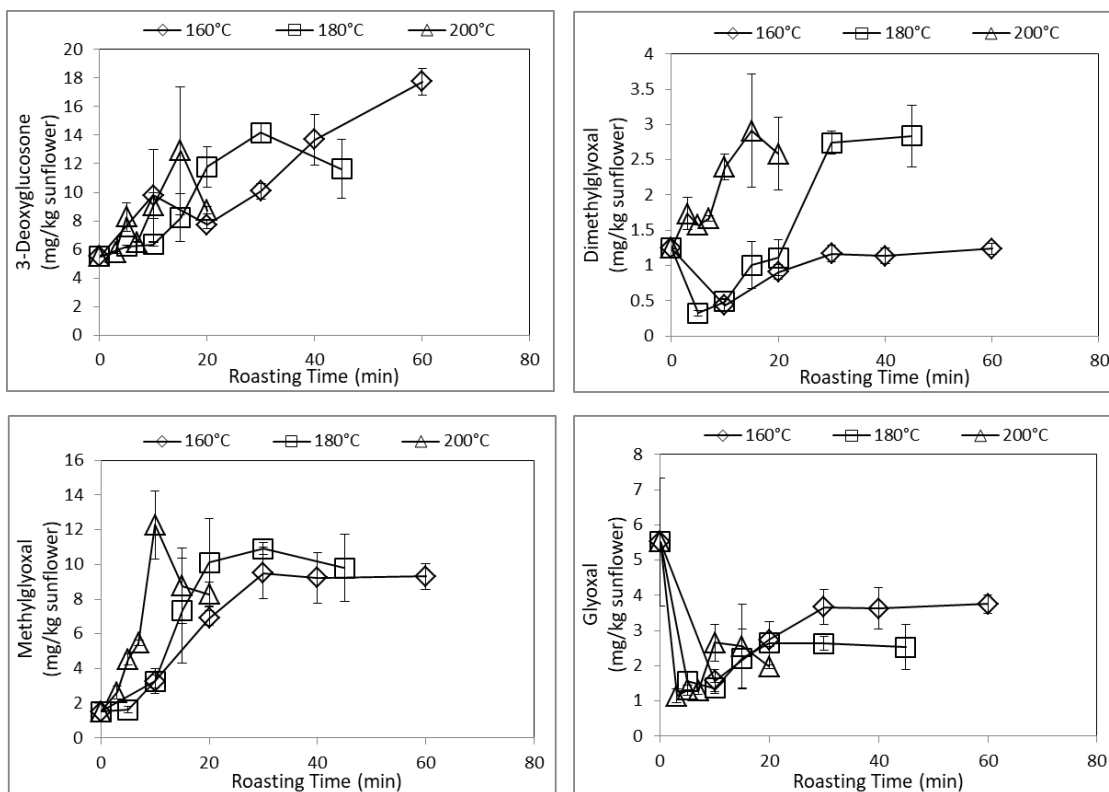
Figure 4. 10 Change in the concentration of α-dicarbonyl compounds during roasting of sunflower seeds
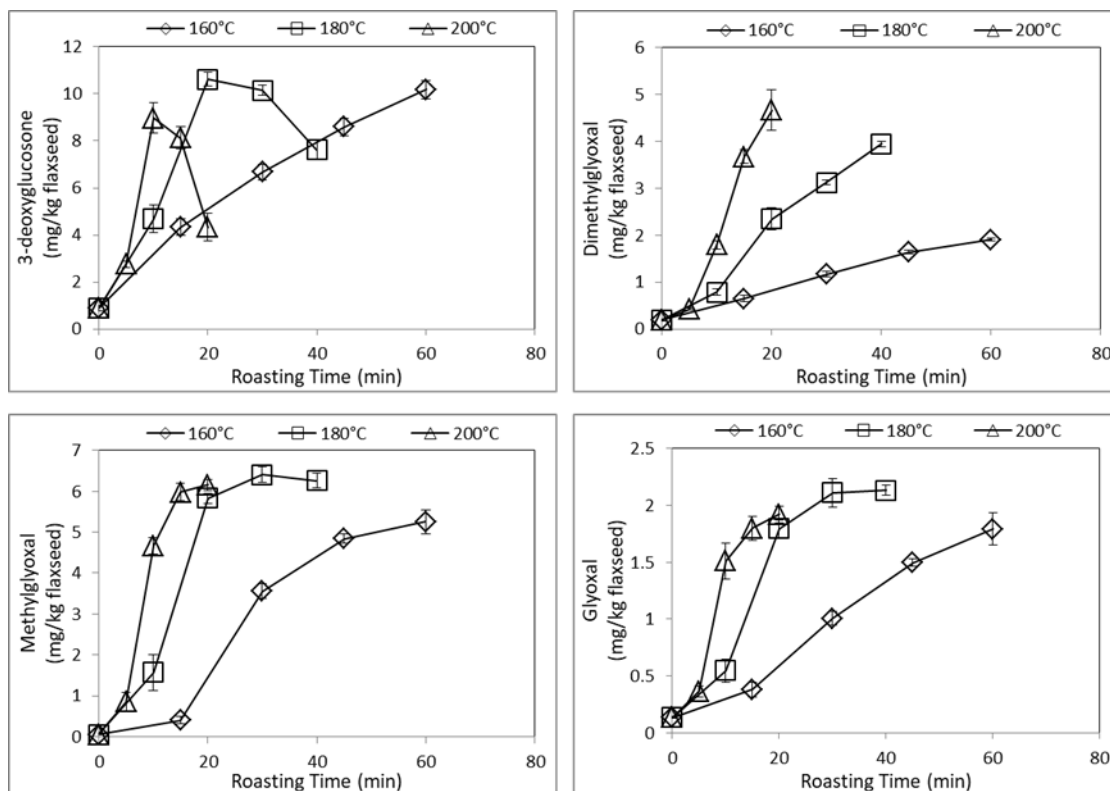
Figure 4. 11 Change in the concentration of α-dicarbonyl compounds during roasting of flaxseeds
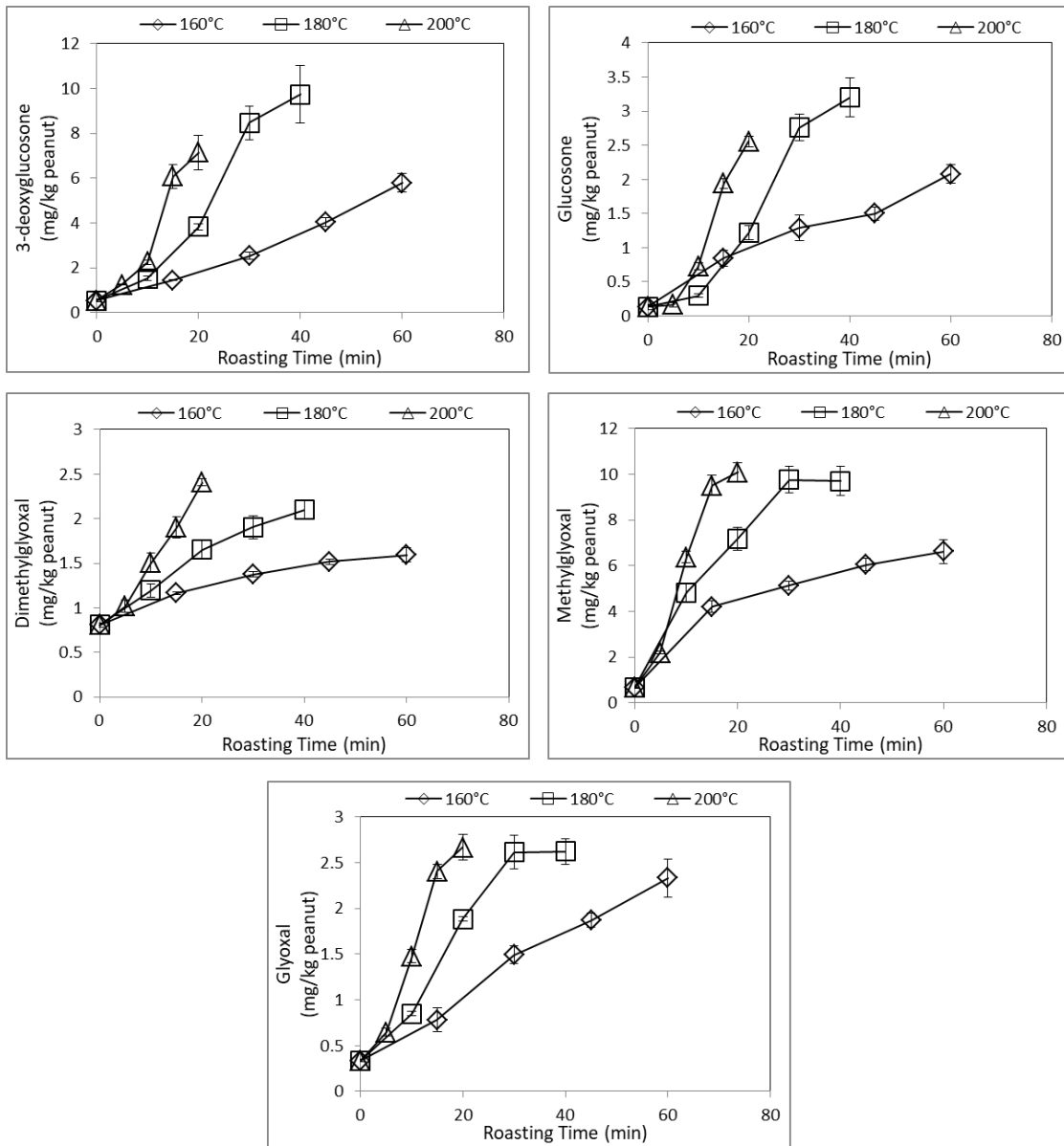
Figure 4. 12 Change in the concentration of α-dicarbonyl compounds during roasting of peanuts
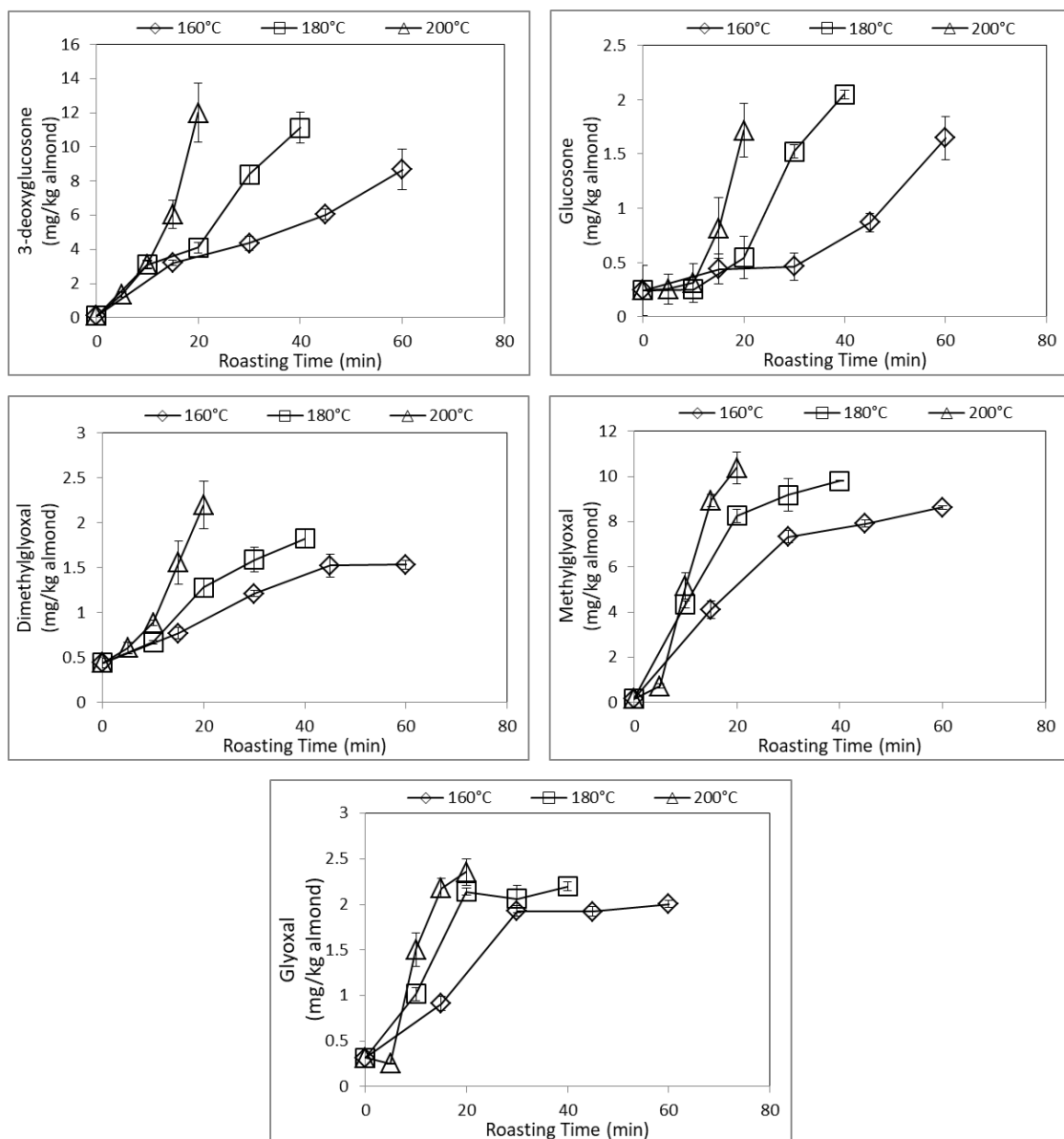
Figure 4. 13 Change in the concentration of α-dicarbonyl compounds during roasting of almonds

4.3.7. Changes in Color During Roasting of Samples

The change of L*a*b* values was listed in Table 4. 6-10. Calculated CIE L* and a* values were correlated with the time of the roasting process. Since CIE L* denotes lightness, it was observed that the L* value decreased as the roasting time increased due to the browning reactions taking place during roasting. In addition, an increase in CIE a* value was observed with increasing roasting time since the positive values of a value are associated with redness. It was also observed that the b* value, which indicates yellowness, was slightly increased with increasing roasting time while it started to decrease in harsh roasting parameters. Similar to our results, Göncüoğlu Taş (2017) determined that the a* value of hazelnuts roasted at 150 and 160 °C increased with increasing roasting time, while the b* value increased until a certain roasting time and then started to decrease. They stated that the L* value decreased with increasing roasting temperature and time. Ataç Mogol (2014) also indicated that L* value was decreased whereas a* and b* values were increased with increasing roasting time for biscuits baked in the conventional process. They also noted that the color change was more correlated with HMF than with acrylamide. The reason for this was explained by the simultaneous Maillard reaction and caramelization during cooking and the formation of HMF by both Maillard reaction and caramelization, while acrylamide was formed only by Maillard reaction. Because of this correlation between the degree of roasting and the color of the product, computer vision-based image analysis can be used as an indicator to predict the intensity of the Maillard reaction.

Table 4. 6 Changes in color values (L*, a*, b*) of sunflowers during roasting
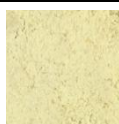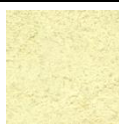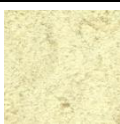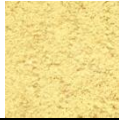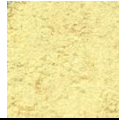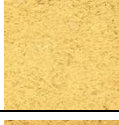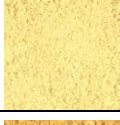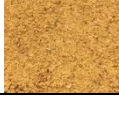
160 °C			180 °C			200 °C		
10'		L* 92.72±3.35 a* -4.45±0.67 b* 29.89±1.85	5'		L* 94.39±0.99 a* -4.46±0.2 b* 26.39±0.64	3'		L* 93.43±1.08 a* -4.05±0.18 b* 24.05±0.74
20'		L* 89.62±0.81 a* -0.46±0.05 b* 44.62±1.07	10'		L* 91.53±0.19 a* -3.52±0.08 b* 36.98±0.66	5'		L* 94.63±0.57 a* -4.62±0.27 b* 29.23±0.95
30'		L* 84.54±0.54 a* 4.98±0.28 b* 48.8±0.45	15'		L* 82.04±0.86 a* 6.14±0.64 b* 49.48±0.5	7'		L* 91.87±1.86 a* -2.89±1.23 b* 41.92±2.98
40'		L* 79.14±1.34 a* 9.85±0.8 b* 50.7±0.11	20'		L* 73.34±3.33 a* 15.5±2.39 b* 51.1±0.79	10'		L* 83.85±3.17 a* 6.45±3.16 b* 51.85±1.95
60'		L* 74.39±1.66 a* 15.22±0.9 b* 50.93±0.96	30'		L* 64.71±1.66 a* 20.67±1.28 b* 46.25±0.62	15'		L* 60.06±4.4 a* 21.19±0.68 b* 43.84±3.48
			45'		L* 45.6±0.92 a* 19.8±0.02 b* 32.21±2.33	20'		L* 41.89±1.25 a* 19.72±0.89 b* 27.76±2.22

Table 4. 7 Changes in color values (L*, a*, b*) of pumpkin seeds during roasting

160 °C			180 °C			200 °C		
15'		L* 76.67±2.02 a* -4.2±0.36 b* 44.02±1.29	10'		L* 76±5.11 a* -3.3±1.51 b* 43.08±0.97	5'		L* 78.81±0.66 a* -5.42±0.39 b* 38.72±1.1
30'		L* 72.18±2.38 a* 1.68±0.34 b* 46.52±1.7	20'		L* 61.67±1.01 a* 6.73±0.5 b* 44.19±0.37	10'		L* 74.07±2.33 a* 0.59±0.99 b* 45.91±0.32
45'		L* 65±4.36 a* 6.44±1.13 b* 46.46±2.96	30'		L* 57.58±0.34 a* 13.92±0.64 b* 45.44±1.39	15'		L* 63.78±3.28 a* 11.44±1.89 b* 49.96±1
60'		L* 61.98±2.91 a* 10.28±1.91 b* 45.61±2.84	40'		L* 49.67±4.89 a* 18.03±0.49 b* 39.05±3.74	20'		L* 54.6±1.77 a* 19.17±0.86 b* 43.96±3.47

Table 4. 8 Changes in color values (L*, a*, b*) of flaxseeds during roasting

160 °C		180 °C		200 °C	
15'	L* 72.52±0.11 a* 3.19±0.24 b* 28.92±0.95	10'	L* 68.47±2.09 a* 3.68±0.24 b* 26.35±1.14	5'	L* 74.63±0.47 a* 2.31±0.16 b* 28.89±0.17
30'	L* 69.42±0.95 a* 3.69±0.36 b* 29.87±0.38	20'	L* 61.59±2.09 a* 7.07±0.7 b* 32.96±0.94	10'	L* 66.77±1.69 a* 5.28±0.31 b* 33.82±1.75
45'	L* 64.83±0.61 a* 5.08±0.44 b* 30.32±1.41	30'	L* 58.1±2.58 a* 10.27±0.26 b* 35.14±1.08	15'	L* 54.5±1.83 a* 11.97±0.5 b* 33.56±0.47
60'	L* 64.3±5.75 a* 6.11±0.64 b* 33.17±4.2	40'	L* 55.17±0.59 a* 12.74±0.84 b* 36.17±0.54	20'	L* 48.04±0.58 a* 13.59±0.79 b* 27.2±1.55

Table 4. 9 Changes in color values (L*, a*, b*) of peanuts during roasting

160 °C		180 °C		200 °C	
15'	L* 81.92±0.35 a* 0.84±0.62 b* 38.39±0.1	10'	L* 82.18±2.04 a* 1.23±0.69 b* 39.08±1.14	5'	L* 85.58±2.11 a* -1.85±0.51 b* 32.12±0.53
30'	L* 76.32±0.86 a* 8.12±0.42 b* 46.12±1.01	20'	L* 70.84±1.48 a* 14.18±0.55 b* 45.27±1.06	10'	L* 75.56±1.23 a* 9.11±1.05 b* 43.98±1.39
45'	L* 72.55±0.15 a* 11.95±0.45 b* 47.15±1.21	30'	L* 62.76±4.8 a* 18.6±0.5 b* 36.84±2.96	15'	L* 65.49±0.46 a* 17.88±0.74 b* 37.21±2.48
60'	L* 72.9±0.47 a* 13.81±0.55 b* 46.86±0.81	40'	L* 62.06±2.06 a* 20.03±0.71 b* 35.68±2.54	20'	L* 53.03±1.79 a* 16.52±0.51 b* 24.12±1

Table 4. 10 Changes in color values (L*, a*, b*) of almonds during roasting

160 °C		180 °C		200 °C	
15'	L* 79.5±0.49 a* 4.19±0.85 b* 31.93±1.07	10'	L* 82.01±1.84 a* 3.36±1.43 b* 33.94±4.01	5'	L* 85.69±0.33 a* -0.87±0.12 b* 23.16±1.12
30'	L* 70.35±2.26 a* 14.23±0.68 b* 49.74±3.64	20'	L* 68.85±1.99 a* 16.07±1.83 b* 48.5±0.89	10'	L* 77.25±2.73 a* 6.76±1.3 b* 41.37±1.72
45'	L* 63.56±2.14 a* 18.32±0.26 b* 42.84±2.3	30'	L* 56.03±4.1 a* 21.36±0.39 b* 39.09±3.97	15'	L* 65.02±2.02 a* 19.31±1.39 b* 47.98±1.07
60'	L* 59.85±2.75 a* 20.64±0.97 b* 39.8±1.64	40'	L* 47.54±0.75 a* 21.15±0.53 b* 33.11±1.89	20'	L* 44.98±3.21 a* 20.02±1.09 b* 30.16±1.99

5. MULTIRESPONSE KINETIC MODELING

5.1. Introduction

The quality of food can be influenced by many factors and quality indicators depending on the type of reaction. To be able to possess food quality, each production step is monitored and controlled in terms of chemical, microbiological and physical changes. If the temperature dependence and rate of reaction are known, then these changes can be predicted and controlled. Kinetic modeling of reactions helps to express quality parameters quantitatively. By applying multiresponse kinetic modeling, the chemistry of reaction and its effects on food properties and also quality indicators associated with related chemical reactions can be determined. van Boekel (2009) gave a detailed explanation of the necessity and superior features of multiresponse kinetic modeling against uniresponse models. In a first-order reaction that which compound A degrades to compound B with a rate constant k, we can only measure compound A with an uniresponse model. If this model is valid, the loss of A should be equal to the concentration of B formed from A. However, if we can also measure the concentration of compound B as in multiresponse kinetic modeling, we can confirm the degradation of compound A to compound B completely or not. In case the first-order uniresponse model does not fit with the change in concentration of B, for example, experimental data is lower than the predicted data, the model should be revised by considering compound A may be decomposed through more than one pathway or compound B may undergo further reactions. Therefore, by using multiresponse kinetic modeling where multiple data is taken into consideration, we can eliminate this uncertainty since we consider changes in the concentration of products as well as reactants. In other words, the mechanism of reactions can be understood.

Maillard reaction, oxidation reactions, sugar isomerization reactions, and the other degradation reactions are some of the complex and consecutive reactions observed in food processes (van Boekel, 2009). Maillard reaction is one of the important challenges in food production or storage as it can cause changes in the taste, color, and aroma of food. Moreover, as a result of the Maillard reaction so many reaction products are generated that affect the nutritional value of food. Maillard reaction consists of complex reaction pathways. To understand the whole network, Hodge (1953) suggested a comprehensive reaction scheme which has been used as a reference by food

technologists to explain the reaction mechanism. The reaction steps summarized in this scheme need to be examined quantitatively for being able to control the Maillard reaction. For one chosen reaction such as degradation of reducing sugar, or change in color, simple kinetic models (zero-, first- and second-order) have been studied (Brands and van Boekel, 2003). However, studying one reaction with simple kinetics cannot give an idea about the whole mechanism due to the complexity of the Maillard reaction. The obtained reaction rates through simple kinetics are a mixture of reaction rates of each reaction pathway and with simple kinetics changes in the concentration of compounds in time cannot be determined. In spite of that, multiresponse kinetic modeling provides a possibility to describe and predict the changes in a quantitative way at any time-temperature combination. Moreover, multiresponse kinetic modeling gives us more realistic models and enables us to understand the whole reaction mechanism. Despite one-response kinetics, multiresponse modeling deals with all measured concentration changes of reactants, intermediates, and end products (Brands and van Boekel, 2003, Martins and Van Boekel, 2005a, Nguyen et al., 2016b).

Brands and van Boekel (2002) suggested some important steps to be considered in the application of multiresponse modeling. (1) Identification of all reactants and products and calculation of mass balance, (2) Identification of primary and secondary reaction pathways and also co-products of these pathways, (3) Determination of the effect of process parameters (temperature, pH, etc.) and reactant concentrations (4) Proposal of model mechanism represents whole reaction network, (5) Test of compatibility of the proposed model with experimental data. Martins and Van Boekel (2005a) define kinetic modeling as an iterative process: "proposing a model, confronting it with experiments, criticizing the model, adjusting the model, and confronting the adapted model with experiments again". The reaction network is translated into a mathematical model to be able to fit experimental data to the proposed model. Hence, differential equations are done for each reaction step and these equations are solved by numerical integration as it is difficult to solve analytically (Brands and van Boekel, 2002).

Since the identification of important intermediates and end products, multiresponse kinetic modeling of the Maillard reaction has been studied in so many model systems. Heated glucose/glycine systems were investigated by Martins and Van Boekel (2005a) with a multiresponse modeling approach. D-fructose, N-(1-deoxy-D-fructos-1-yl)-glycine (DFG), 1-deoxy-2,3-hexodiulose, and 3-deoxy-2-hexosulose, formic and acetic

acid, methylglyoxal, and 5-hydroxymethylfurfural were defined as reactants, intermediates, and end products for their proposed model. According to their study, organic acids were determined as a stable end product and 3-DG was found to be responsible for color formation. They also suggested that acetic acid can be considered as an indicator for the progression of the Maillard reaction.

Martins et al. (2003) used Amadori products N-(1-deoxy-D-fructos-1-yl)-glycine (DFG) as an initial reagent and elucidate the major thermal degradation pathways of DFG by multiresponse kinetic modeling with considering the effects of pH and temperature. According to their study, an increment of temperature to 120 °C and decreasing the pH by 1.3 units have an equal effect on the degradation of DFG and the formation of glycine. 1-DG formation was enhanced by the increase in pH. 1-DG was found in lower amounts when compared with 3-DG due to its high reactivity. The type of sugar was changed with pH; at pH 5.5 the predominant parent sugar was mannose whereas it was glucose at pH 6.8. They also reported that reaction products were affected by pH more than temperature. In the second part of their investigation, Martins and Van Boekel (2003) carried out a multiresponse kinetic analysis to enlighten thermal degradation pathways of DFG that were discussed previously (Martins et al., 2003). DFG, 3-deoxyosone, 1-deoxyosone, methylglyoxal, acetic acid, formic acid, glucose, fructose, mannose, and melanoidins were measured as reactants, intermediates, and end products. According to this study, at lower pH (5.5) 1,2-enolization of DFG is predominant whereas at high pH (6.8) 2,3-enolization is more relevant. The major degradation product of DFG, acetic acid, was mainly formed through 1-DG.

Knol et al. (2010) studied the kinetics of acrylamide formation and showed that temperature has more effect on former steps in fructose-asparagine model systems. They also reported that pH and reducing sugar type play an important role in acrylamide formation and high temperature induces the formation of high concentrations of organic acids and high molecular weight melanoidins.

In a study by Nguyen et al. (2016b), the formation of CML, one of the AGEs, in heated caseinate solutions containing glucose and lactose was investigated. By using multiresponse modeling, formation pathways of CML were suggested as (1) isomerization of sugar with the following degradation via Lobry de Bruyn–Alberda van Ekenstein (LA) arrangement, (2) Maillard reaction between glucose/lactose and lysine residues via Amadori rearrangement product. Kinetic modeling also showed that CML

was not formed from the oxidation of sugars and cannot be used as an indicator for the heat load of foods due to its thermal unstability. Liang et al. (2016) focused on the formation and elimination of another AGE, peptide-bound-pyrraline, by using multiresponse kinetic modeling. They reported that in an equimolar model system of reactants and the model system with excess reactants, glucose-fructose isomerization is dominant compared with glucose-mannose epimerization. The caramelization reaction and peptide-bound-pyrraline elimination are neglectable in equimolar and peptide excess systems.

Unraveling the Maillard reaction mechanism in real foods is hard due to their complex structure. Multiresponse kinetic modeling is a powerful tool for understanding this mechanism. Parker et al. (2012) investigated acrylamide formation kinetics in commercial french fries with consideration of the temperature and moisture profiles of potato strips. They explain that commercial french fries production includes washing, cutting, blanching, treatment in a glucose solution, and par-frying steps prior o frying and these processing steps alter the concentrations of precursors, so they should be taken into consideration while modeling the acrylamide formation. According to their study, the pathway that starts from glucose is bimolecular while fructose is unimolecular. Change in amino acid concentration caused by loss of amino acids during the formation of Maillard reaction products from intermediates. Some of the asparagine were consumed for acrylamide formation and the rest of it forms other Maillard reaction products.

Hamzalıoğlu and Gökmen (2020) proposed a kinetic model for acrylamide formation in coffee during roasting at 200, 220, and 240 °C by using a multiresponse kinetic modeling approach. They indicated that sucrose degrades to glucose and fructofuranosyl cation and HMF was the most important intermediate precursor of ACR. In another multiresponse study carried out by Göncüoğlu Taş and Gökmen (2017), the mechanism of Maillard reaction and caramelization was tried to be enlightened in hazelnuts during roasting at different temperatures. The results indicated that FFC had importance in the formation of HMF; MGO and DMG were mainly formed from 1-DG, and GO was formed via glucose degradation.

Maillard reaction was also investigated in roasted sesame seeds in the studies of Berk et al. (2021) and Berk et al. (2020). According to their proposed models, ACR formation mostly occurred from the reaction of asparagine with HMF. α–dicarbonyl compounds

and AGEs were also monitored in their study. They reported that CML was mainly formed through the oxidation of N-ε-fructoselysine whereas CEL is mainly originated from the reaction of protein-bound lysine with MGO.

In this chapter, a kinetic model for the Maillard reaction/caramelization and ACR formation in low water activity, neutral pH, and sucrose-rich but reducing sugar-poor food systems such as nuts and seeds was proposed. The restricted amount of reducing sugar, low water activity, and neutral pH value in nuts and seeds lead Maillard reaction to follow a different pathway. For instance, at low water content, hydrolysis reactions are limited and dehydration reactions become more prominent. The Maillard reaction-related studies carried out so far in aqueous food matrices and model studies are incoherent to describe the reaction in foods that have limited water content. Since the mobility of the reactants is necessary for these reactions to occur, the reactants gain reactivity with melting in the processes where water activity is limited, such as baking or roasting (Kocadağlı and Gökmen, 2016, Robert et al., 2004). However, there is a lack of comprehensive information about the Maillard reaction occurring in these types of foods.

In addition to pH and water activity, because the kinetics of Maillard reaction products were also affected by the diversity and amount of the reactants, a classification including all these factors for nuts and seeds was performed before modeling studies by using Principle Component Analysis (PCA). This approach allowed us to classify nuts and seeds according to their compositional characteristics, which was more critical for chemical reactions, instead of their botanical nomenclature.

PCA is a convenient way to reveal which variables caused the difference between samples and the correlation between these variables. The close positioning of the variables indicates that these variables are positively correlated with each other, that is, while one variable increases or decreases, other variables also change in the same direction. The obtuse angle between the variables indicates that these variables are not related to each other. The right angle between the variables means that if the variables are on opposite sides of the graphic origin, it is concluded that these variables are inversely correlated. In addition, the distance of a variable from the origin depends on the impact of that variable on the model. Accordingly, the farther the position of a variable is from the origin, the more influential that variable is on that model. The fact that the variable is close to the center indicates that the effect of that variable on this

distribution cannot be clearly explained by the selected principal components. In this case, different plots can be created by selecting different principal components. However, it should be kept in mind that in this case, the explanation rate of variance may change.

In this part of the thesis, kinetic models were revealed for the Maillard reaction/caramelization and also ACR formation during roasting of low-moisture foods by considering these kinds of foods as sugar-limited lipid-rich reaction pools and with the available amount of amino acids and sucrose, independently of the product type. Therefore sunflower seed (*Helianthus annuus L.*), pumpkin seed (*Cucurbita moschata L.*), flaxseed (Linum usitatissimum L.), peanut (*Arachis hypogaea L.*), and almond (*Prunus dulcis*) were studied due to their similar compositions with minor differences in order to represent such a reactant pool. The change in the concentration of sugars and amino acids as reactants, thermal contaminants such as HMF and AGEs, and also α-dicarbonyl compounds as intermediates formed as a result of the Maillard reaction were monitored induced by the roasting process applied at different temperatures and times. The reaction mechanism and interrelation between reactants and products were tried to be enlightened by using the multiresponse kinetic modeling approach.

5.2. Materials and Methods

5.2.1. Proximate composition analysis, pH, and water activity of raw samples

Proximate composition analysis and measurement of pH and water activity of samples were performed as described in Chapter 3.

5.2.2. Analysis of reactants and products of Maillard reaction and caramelization products during the roasting process

Analyses of sugars and amino acids were carried out according to the methods previously described in Chapter 3. Analyses of HMF, α-dicarbonyl compounds, furosine, ACR, and AGEs were performed as described in Chapter 4.

5.2.3. Principle Component Analysis

Principal component analysis (PCA) was run by using Microsoft Office Excel® (2010) and XLSTAT® software (version 2021.2.2, Addinsoft, New York). The significance level was fixed at $p < 0.05$.

5.2.4. Kinetic data analysis

Comprehensive models were proposed for the Maillard reaction/caramelization and acrylamide formation that includes reactants and the formation and degradation pathways of the main and intermediate products. In order to introduce the reaction network to a mathematical model, differential equations were set for each reaction step that was characterized by reaction rate constants (k) as parameters (Appendix A). Numerical integration and estimation of parameters were performed by using Athena Visual Studio software (v.14.2) through non-linear regression using the determinant criterion (Van Boekel, 1996). The concentrations of reactants and products were expressed as μmol/kg. The experimental data were compared with predicted data obtained from the mathematical model and the reaction steps were criticized by model discrimination. The kinetic model was evaluated by examining the goodness of fit of models to experimental data and the highest posterior density intervals of estimated parameters.

5.3. Results and Discussion

5.3.1. Proximate composition, pH, and water activity of raw samples

Proximate compositions, pH, and water activities of raw samples were given in Table 3. 1. It is already known that reactant solubility and mobility and thus rate of chemical reaction increases as water activity increases. The rate of the Maillard reaction also increases with an increase of water activity and reaches up to a maximum in the range of water activity of 0.65 to 0.75 (Wong et al., 2015). Pumpkin seeds were expected to be more susceptible to the Maillard reaction than others as they have the water activity value at which the maximum Maillard reaction rate is generally observed. However, it should be noted that water activity is not the only factor affecting Maillard reaction, and

initial reactant concentrations can also affect the rate of Maillard reaction. These characteristic properties that distinguish pumpkin seeds from others will be discussed in the PCA section.

The pH change in the samples with roasting was shown in Table 5. 1. It has been stated that a single kinetic model can be proposed in cases where the pH drop is less than 1 unit during the Maillard reaction (Martins and Van Boekel, 2005b). Since the change in pH of the studied samples complied with these limits, the proposed model was assumed to be valid for the roasting parameters studied. It was seen that the roasting process reduced the pH value compared to the beginning, and there was a slight decrease in the pH value of samples with increasing roasting time and temperature.

Table 5. 1 Changes in pH of samples during roasting

Temperature	Time (min)	Pumpkinseed	Flaxseed	Peanut	Almond	Time (min)	Sunflower
Raw Sample		7.14±0.02[f]	6.62±0.02[e]	7.01±0.03[f]	6.62±0.01[i]		7.1±0.02[j]
160 °C	15	6.84±0.07[d]	6.18±0.09[d]	7.09±0.07[g]	6.52±0.01[h]	10	6.67±0.07[f,g,h]
	30	6.83±0.03[d]	6.19±0.04[d]	7.01±0.03[f]	6.39±0.03[e,f]	20	6.76±0.04[g,h]
	45	6.8±0.11[d]	6.18±0.02[d]	6.94±0.03[d,e]	6.35±0.03[d,e]	30	6.64±0.06[e,f,g]
	60	6.83±0.06[d]	6.13±0.02[c,d]	6.88±0.01[d]	6.27±0.02[b,c]	40	6.54±0.07[d,e]
						60	6.41±0.05[b,c]
180 °C	10	6.75±0.03[b,c,d]	6.21±0.06[d]	7.01±0.03[f]	6.56±0.03[h]	5	6.98±0.08[i]
	20	6.7±0.03[a,b,c]	6.13±0.02[c,d]	6.96±0.01[e,f]	6.45±0.02[g]	10	6.73±0.02[g,h]
	30	6.65±0.08[a,b]	6.04±0.02[b,c]	6.75±0.04[b]	6.32±0.06[c,d]	15	6.64±0.02[e,f,g]
	40	6.63±0.01[a]	5.98±0.01[a,b]	6.61±0.02[a]	6.22±0.05[b]	20	6.55±0.04[d,e,f]
						30	6.44±0.06[b,c,d]
						45	6.25±0.02[a]
200 °C	5	7.02±0.05[e]	6.16±0.18[d]	7.01±0.02[f]	6.68±0.01[j]	3	6.76±0.07[g,h]
	10	6.78±0.06[c,d]	6.15±0.01[d]	6.98±0.05[e,f]	6.51±0.03[h]	5	6.77±0.14[g,h]
	15	6.68±0.03[a,b,c]	5.97±0.02[a,b]	6.82±0.03[c]	6.41±0.03[f,g]	7	6.8±0.14[h]
	20	6.67±0.01[a,b]	5.88±0.04[a]	6.57±0.01[a]	6.15±0.04[a]	10	6.7±0.05[g,h]
						15	6.45±0.07[c,d]
						20	6.32±0.08[a,b]

5.3.2. Principle component analysis

The Principal Component Analysis (PCA) was run to determine the differences between raw food matrices and the distribution of reactants among the samples. In Figure 5. 1a-b, observations and variables plots based on the data matrix of raw materials were reported. The first principal component (F1) contained 46.79% of the variance, and the

second principal component (F2) contained 26.21%. Attributes associated with pH, water activity (a_w), and moisture content appeared in the right hemicycle pointing out these attributes were well separated along the F1. Protein content was the one that most influenced F2. Total free amino acid content and protein-bound lysine (bLys) influenced both F1 and F2. As can be seen in these figures, mainly F1 obviously separated the pumpkinseed from the others due to its high levels of a_w and moisture and also low levels of sucrose and free amino acid content which are the two of the main reactants of the Maillard reaction. Almond, flaxseed, and sunflower seed were clustered together in the same region of the plot that indicating that they are more similar to each other. Peanut was located at the bottom part of the diagram due to its slightly high levels of bLys content and low levels of protein and ash content.

PCA based on reactant and product concentrations was carried out to examine the differences and correlations between roasted samples. The figures display the relationship between variables and how these variables influence the pattern. In this way, it has been tried to determine whether the relationship between the initial chemical composition and product distribution was significant.

The PCA based on the reactant and product concentrations was also carried out to examine the differences and correlations between roasted samples and the relationship between the initial chemical composition and product distribution (Figure 5. 1) In the PCA model of samples roasted at 160 °C and 180 °C, the first two components explained 69.47% and 76.10% of the variance, respectively. Total dicarbonyl content, especially MGO and 3-DG were the main contributors of F1, (around 13-16%) whereas bLys contributed 24% to F2 as a major component of F2. The influence of sucrose on F1 also became important at high roasting temperatures. Sucrose and α-dicarbonyl compounds were highly negatively correlated as they were located in opposite hemicycles. It can also be deduced from the figure that α-dicarbonyl compounds and bLys which were located in the orthogonal direction, were not related to each other. Fructosyllysine was a less important compound at all roasting temperatures as it was positioned closer to the origin of the coordinates. According to the observation plots for all roasting temperatures (Figure 5. 1d,f), pumpkin seed samples were clustered on the top right quadrant of the PCA diagrams, while the other roasted samples were distributed in the diametrically opposed region with respect to the pumpkin seeds. Since the distribution of Maillard reaction reactants in raw pumpkin seeds was different from

the others as shown in Figure 5. 1b, the appearance of roasted pumpkin seeds in a different region of the PCA plot was expectable. The other samples showed very similar distributions in each other. In pumpkin seed samples, bLys was the distinguishing factor at the beginning of roasting processes, while α-dicarbonyl compounds appeared to correlate fairly well with samples roasted for longer periods. In spite of this, the other samples showed the highest levels of sucrose and total free amino acids at the beginning. Then, compounds such as HMF, CML, and CEL become distinctive as the roasting period increases resulting in the clustering of samples in the lower right region that were roasted for a longer time. At higher temperatures, samples with shorter roasting times began to appear on the right side of the F2 axis. When the observation plot was examined together with the variables plot, it was seen that the reason for this is that the amounts of the attributes located in the lower right part of the diagram occurred at higher levels earlier at higher roasting temperatures.

Principal component analysis showed that both the distribution of reactants in the raw samples and the distribution of reactants and products in the roasted samples differed significantly in the pumpkin seed sample due to its composition. These results were the basis for the multiresponse modeling of Maillard reaction in low moisture, low reducing sugar-lipid rich systems. Accordingly, it is envisaged that all samples can be explained with a single model, whereas probably different reaction pathways will be dominant in pumpkin seed samples.
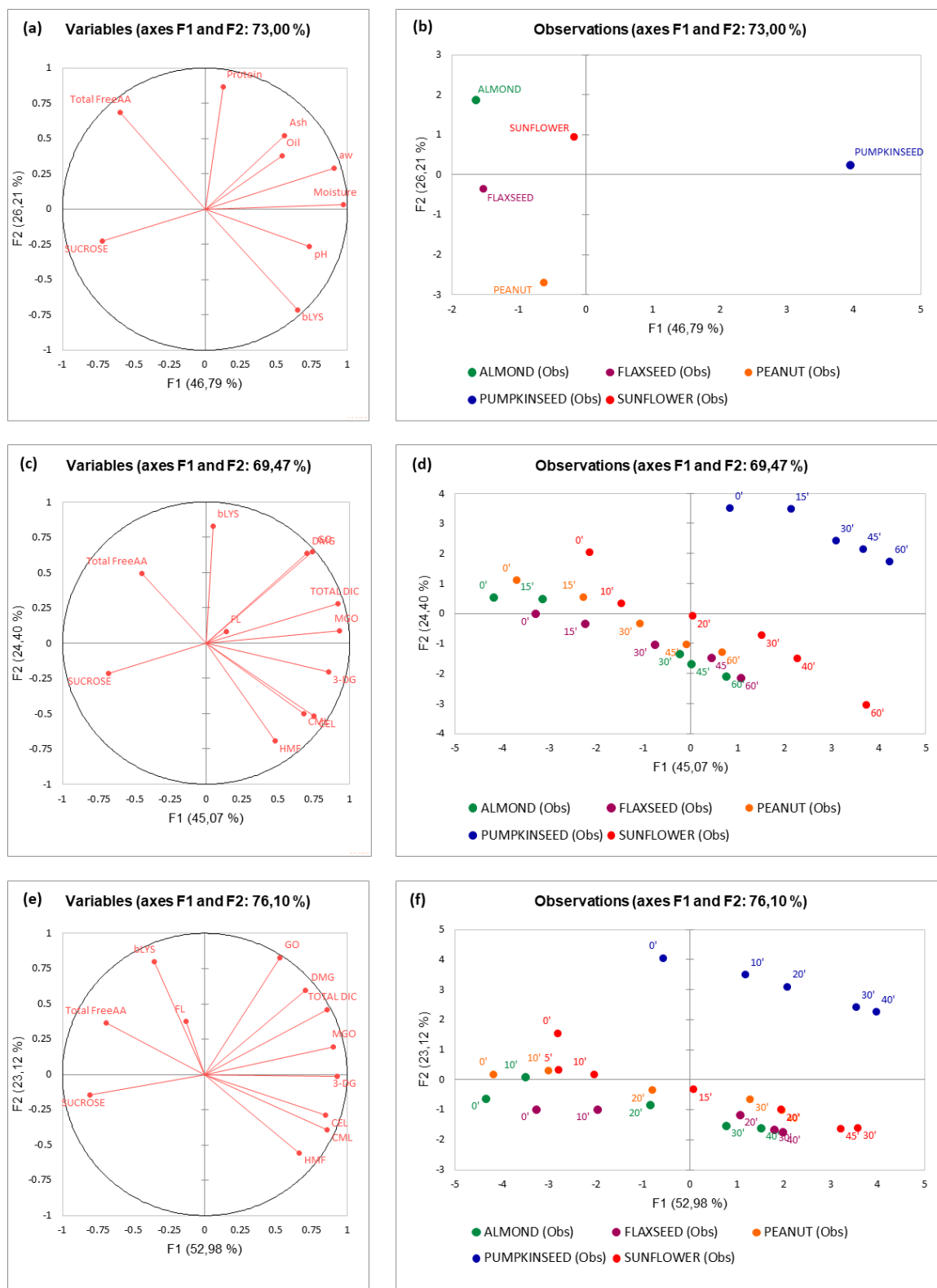
Figure 5. 1 The principal component plot (PCA) for reactants and products of Maillard reaction in samples roasted at different temperatures for different times (a and b: raw samples; c and d: roasted samples at 160 °C; e and f: roasted samples at 180 °C.)

5.3.3. Kinetic Modeling of Maillard Reaction and Caramelization

The reaction mechanism of Maillard reaction and caramelization is uncertain especially in real foods due to its complexity and dependence on reaction conditions. Although the water content should be included in the model as it affects the reaction, the heat and mass transfer coefficient of water were omitted due to the restricted amount of water in nuts and seeds.

First of all, a comprehensive model was built that includes all the formation pathways mentioned in the literature for the Maillard reaction and caramelization (Figure 5. 2).
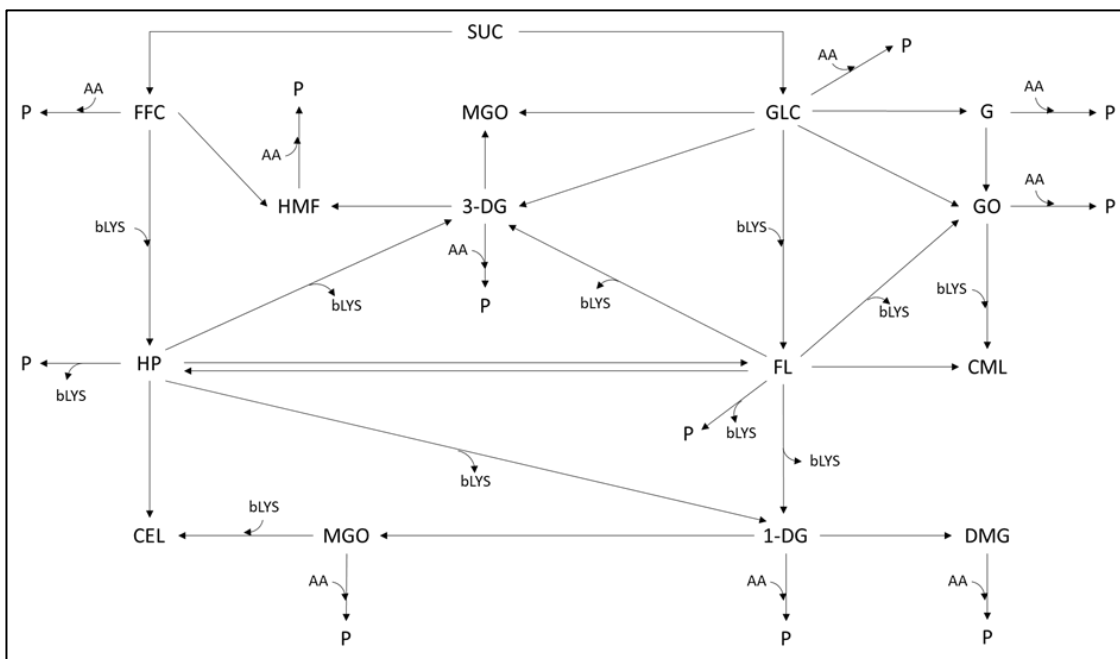
Figure 5. 2 Comprehensive model for Maillard reaction and caramelization during roasting of nuts and seeds. SUC sucrose, GLC glucose, FFC fructofuranosyl cation, bLYS bound lysine, AA total amino acids, FL N-ε-fructoselysine, HP Heyns product, HMF 5-hydroxymethyl furfural, 3-DG 3-deoxyglucosone, 1-DG 1-deoxyglucosone, G glucosone, MGO methylglyoxal, GO glyoxal, CML N-ε-carboxymethyllysine, CEL N-ε-carboxyethyllysine, DMG dimethylglyoxal, P products.

Each step of the comprehensive reaction network given in Figure 5. 2 was represented by an ordinary differential equation, which was characterized by a reaction rate constant (k) as follows:

$$\frac{d[SUC]}{dt} = -k_1[SUC]$$

$$\frac{d[Lys]}{dt} = -(k_8 + k_{28} + k_{31})[HP] + (k_9 + k_{18} + k_{25} + k_{27})[FL] - k_3[FFC][Lys] \\ - k_4[GLC][Lys] - k_{14}[GO][Lys] - k_{16}[MGO][Lys]$$

$$\frac{d[AA]}{dt} = -k_{17}[GLC][AA] - k_{19}[HMF][AA] - k_{20}[FFC][AA] - k_{22}[3-DG][AA] \\ - k_{23}[DMG][AA] - k_{32}[MGO][AA] - k_{33}[1-DG][AA] - k_{34}[G][AA] \\ - k_{35}[GO][AA]$$

$$\frac{d[FL]}{dt} = k_4[GLC][Lys] + k_{29}[HP] - (k_9 + k_{13} + k_{18} + k_{25} + k_{27} + k_{30})[FL]$$

$$\frac{d[HMF]}{dt} = k_2[FFC] + k_{10}[3-DG] - k_{19}[HMF][AA]$$

$$\frac{d[3-DG]}{dt} = k_5[GLC] + k_8[HP] + k_{27}[FL] - (k_{10} + k_{24}[3-DG] - k_{22}[3-DG][AA]$$

$$\frac{d[G]}{dt} = k_7[GLC] - k_{26}[G] - k_{34}[G][AA]$$

$$\frac{d[DMG]}{dt} = k_{12}[1-DG] - k_{23}[DMG][AA]$$

$$\frac{d[MGO]}{dt} = k_{11}[1-DG] + k_{21}[GLC] + k_{24}[3-DG] - k_{16}[MGO][Lys] - k_{32}[MGO][AA]$$

$$\frac{d[GO]}{dt} = k_6[GLC] + k_{25}[FL] + k_{26}[G] - k_{14}[GO][Lys] - k_{35}[GO][AA]$$

$$\frac{d[CML]}{dt} = k_{13}[FL] + k_{14}[GO][Lys]$$

$$\frac{d[CEL]}{dt} = k_{15}[HP] + k_{16}[MGO][Lys]$$

$$\frac{d[FFC]}{dt} = k_1[SUC] - k_2[FFC] - k_3[FFC][Lys] - k_{20}[FFC][AA]$$

$$\frac{d[GLC]}{dt} = k_1[SUC] - k_4[GLC][Lys] - (k_5 + k_6 + k_7 + k_{21})[GLC] - k_{17}[GLC][AA]$$

$$\frac{d[1-DG]}{dt} = k_9[FL] + k_{28}[HP] - (k_{11} + k_{12})[1-DG] - k_{33}[1-DG][AA]$$

$$\frac{d[HP]}{dt} = k_3[FFC][Lys] + k_{30}[FL] - (k_8 + k_{15} + k_{28} + k_{29} + k_{31})[HP]$$

$$\frac{d[P_1]}{dt} = k_{17}[GLC][AA]$$

$$\frac{d[P_2]}{dt} = k_{18}[FL]$$

$$\frac{d[P_3]}{dt} = k_{19}[HMF][AA]$$

$$\frac{d[P_4]}{dt} = k_{20}[FFC][AA]$$

$$\frac{d[P_5]}{dt} = k_{21}[HP]$$

$$\frac{d[P_6]}{dt} = k_{22}[3-DG][AA]$$

$$\frac{d[P_7]}{dt} = k_{23}[DMG][AA]$$

$$\frac{d[P_8]}{dt} = k_{33}[1-DG][AA]$$

$$\frac{d[P_9]}{dt} = k_{32}[MGO][AA]$$

$$\frac{d[P_{10}]}{dt} = k_{34}[G][AA]$$

$$\frac{d[P_{11}]}{dt} = k_{35}[GO][AA]$$

The comprehensive model which was given in Figure 5. 2 involves degradation of sucrose, formation of FL and HP from FFC and GLC, HMF formation from FFC and 3-DG, formation of α-dicarbonyl compounds, CML and CEL formation. The comprehensive kinetic model was solved and predicted data were compared with experimental data at 160 and 180 °C. As can be seen in Figure 5. 3-7, concentrations of FL, HMF, DMG, CML, and CEL could not be estimated well.
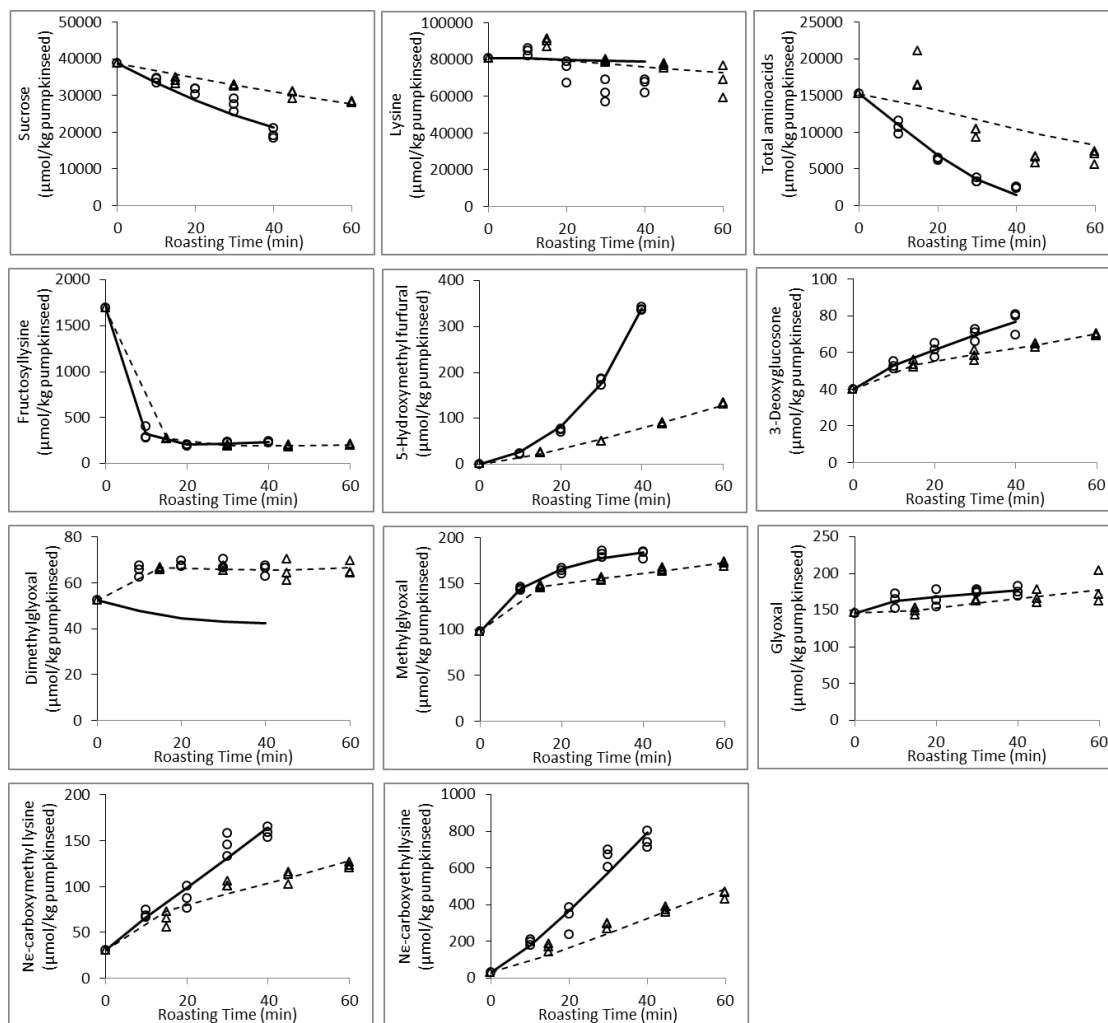
Figure 5. 3 Kinetic model fits (lines) obtained according to comprehensive kinetic model to the obtained experimental data (symbols)of reactants and products during roasting of pumpkinseed at 160°C (Δ;------) and 180°C (○;————)

Figure 5. 4 Kinetic model fits (lines) obtained according to comprehensive kinetic model to the obtained experimental data (symbols)of reactants and products during roasting of sunflower seed at 160°C (Δ;------) and 180°C (○;————)

Figure 5. 5 Kinetic model fits (lines) obtained according to comprehensive kinetic model to the obtained experimental data (symbols)of reactants and products during roasting of flaxseed at 160°C (Δ;------) and 180°C (○;————)

Figure 5. 6 Kinetic model fits (lines) obtained according to comprehensive kinetic model to the obtained experimental data (symbols)of reactants and products during roasting of peanut at 160°C (Δ;------) and 180°C (○;———)

86

Figure 5. 7 Kinetic model fits (lines) obtained according to comprehensive kinetic model to the obtained experimental data (symbols)of reactants and products during roasting of almond at 160°C (Δ;------) and 180°C (○;————)

The comprehensive model was simplified by model discrimination to obtain the proposed reaction mechanism of Maillard reaction and caramelization given in Figure 5. 8. Some reaction steps were removed one by one since it is preferable to omit the steps unless they cause a worse posterior probability. Thus, not only the unknown parameters were reduced but also the estimation parameters that describe best the experimentally observed data were defined precisely. While simplifying the comprehensive model, firstly, the formation and degradation pathways of the compounds whose concentration could not be predicted well were reconsidered.
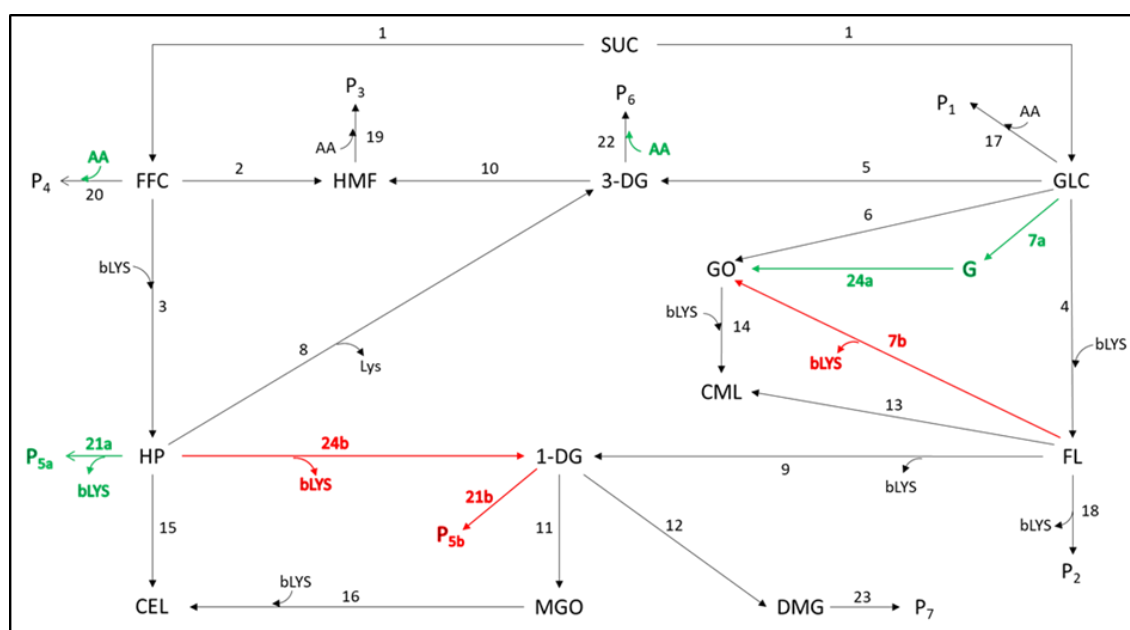
Figure 5. 8 Proposed mechanistic model for Maillard reaction and caramelization during roasting at 160 and 180 °C. Red colored steps designate the differences of pumpkinseed, green colored steps designates the differences of other nuts and seeds. SUC sucrose, GLC glucose, FFC fructofuranosyl cation, bLYS bound lysine, AA total amino acids, FL N-ε-fructoselysine, HP Heyns product, HMF 5-hydroxymethyl furfural, 3-DG 3-deoxyglucosone, 1-DG 1-deoxyglucosone, G glucosone, MGO methylglyoxal, GO glyoxal, CML N-ε-carboxymethyllysine, CEL N-ε-carboxyethyllysine, DMG dimethylglyoxal, P products.

In addition to pH and water activity, because the kinetics of Maillard reaction products were also affected by the diversity and amount of the reactants, a classification including all these factors for nuts and seeds was performed by using PCA before modeling studies. This approach allowed us to classify nuts and seeds according to their compositional characteristics, instead of their botanical nomenclature. Therefore, sunflower, flaxseed, peanut, and almond clustered together by PCA as one group whereas pumpkin seed was classified as a separate group which arose the need for two different proposed mechanistic models for Maillard reaction and caramelization. Each

step of the reaction network given in Figure 5. 8 was represented by an ordinary differential equation, which was characterized by a reaction rate constant.

Differential equations, which are built from the proposed kinetic model of nuts and seeds given in Figure 5. 8 as follows:

$$\frac{d[SUC]}{dt} = -k_1[SUC]$$

$$\frac{d[Lys]}{dt} = -(k_8 + k_{21})[HP] + (k_9 + k_{18})[FL] - k_3[FFC][Lys] - k_4[GLC][Lys] \\ - k_{14}[GO][Lys] - k_{16}[MGO][Lys]$$

$$\frac{d[AA]}{dt} = -k_{17}[GLC][AA] - k_{19}[HMF][AA] - k_{20}[FFC][AA] - k_{22}[3-DG][AA]$$

$$\frac{d[FL]}{dt} = -k_4[GLC][Lys] - (k_9 + k_{13} + k_{18})[FL]$$

$$\frac{d[HMF]}{dt} = k_2[FFC] + k_{10}[3-DG] - k_{19}[HMF][AA]$$

$$\frac{d[3-DG]}{dt} = k_5[GLC] + k_8[HP] - k_{10}[3-DG] - k_{22}[3-DG][AA]$$

$$\frac{d[G]}{dt} = k_7[GLC] - k_{24}[G]$$

$$\frac{d[DMG]}{dt} = k_{12}[1-DG] - k_{23}[DMG]$$

$$\frac{d[MGO]}{dt} = k_{11}[1-DG] - k_{16}[MGO][Lys]$$

$$\frac{d[GO]}{dt} = k_6[GLC] + k_{24}[G] - k_{14}[GO][Lys]$$

$$\frac{d[CML]}{dt} = k_{13}[FL] + k_{14}[GO][Lys]$$

$$\frac{d[CEL]}{dt} = k_{15}[HP] + k_{16}[MGO][Lys]$$

$$\frac{d[FFC]}{dt} = k_1[SUC] - k_2[FFC] - k_3[FFC][Lys] - k_{20}[FFC][AA]$$

$$\frac{d[GLC]}{dt} = k_1[SUC] - k_4[GLC][Lys] - (k_5 + k_6 + k_7)[GLC] - k_{17}[GLC][AA]$$

$$\frac{d[1-DG]}{dt} = k_9[FL] - (k_{11} + k_{12})[1-DG]$$

$$\frac{d[HP]}{dt} = k_3[FFC][Lys] - (k_8 + k_{15} + k_{21})[HP]$$

$$\frac{d[P_1]}{dt} = k_{17}[GLC][AA]$$

$$\frac{d[P_2]}{dt} = k_{18}[FL]$$

$$\frac{d[P_3]}{dt} = k_{19}[HMF][AA]$$

$$\frac{d[P_4]}{dt} = k_{20}[FFC][AA]$$

$$\frac{d[P_5]}{dt} = k_{21}[HP]$$

$$\frac{d[P_6]}{dt} = k_{22}[3 - DG][AA]$$

$$\frac{d[P_7]}{dt} = k_{23}[DMG]$$

Differential equations, which are built from the proposed kinetic model of pumpkin seeds given in Figure 5. 8 as follows:

$$\frac{d[SUC]}{dt} = -k_1[SUC]$$

$$\frac{d[Lys]}{dt} = -(k_8 + k_{24})[HP] + (k_7 + k_9 + k_{18})[FL] - k_3[FFC][Lys] - k_4[GLC][Lys] \\ - k_{14}[GO][Lys] - k_{16}[MGO][Lys]$$

$$\frac{d[AA]}{dt} = -k_{17}[GLC][AA] - k_{19}[HMF][AA]$$

$$\frac{d[FL]}{dt} = -k_4[GLC][Lys] - (k_7 + k_9 + k_{13} + k_{18})[FL]$$

$$\frac{d[HMF]}{dt} = k_2[FFC] + k_{10}[3 - DG] - k_{19}[HMF][AA]$$

$$\frac{d[3 - DG]}{dt} = k_5[GLC] + k_8[HP] - (k_{10} + k_{22})[3 - DG]$$

$$\frac{d[DMG]}{dt} = k_{12}[1 - DG] - k_{23}[DMG]$$

$$\frac{d[MGO]}{dt} = k_{11}[1 - DG] - k_{16}[MGO][Lys]$$

$$\frac{d[GO]}{dt} = k_6[GLC] + k_7[FL] - k_{14}[GO][Lys]$$

$$\frac{d[CML]}{dt} = k_{13}[FL] + k_{14}[GO][Lys]$$

$$\frac{d[CEL]}{dt} = k_{15}[HP] + k_{16}[MGO][Lys]$$

$$\frac{d[FFC]}{dt} = k_1[SUC] - (k_2 + k_{20})[FFC] - k_3[FFC][Lys]$$

$$\frac{d[GLC]}{dt} = k_1[SUC] - k_4[GLC][Lys] - (k_5 + k_6)[GLC] - k_{17}[GLC][AA]$$

$$\frac{d[1-DG]}{dt} = k_9[FL] + k_{24}[HP] - (k_{11} + k_{12} + k_{21})[1-DG]$$

$$\frac{d[HP]}{dt} = k_3[FFC][Lys] - (k_8 + k_{15} + k_{24})[HP]$$

$$\frac{d[P_1]}{dt} = k_{17}[GLC][AA]$$

$$\frac{d[P_2]}{dt} = k_{18}[FL]$$

$$\frac{d[P_3]}{dt} = k_{19}[HMF][AA]$$

$$\frac{d[P_4]}{dt} = k_{20}[FFC]$$

$$\frac{d[P_5]}{dt} = k_{21}[1-DG]$$

$$\frac{d[P_6]}{dt} = k_{22}[3-DG]$$

$$\frac{d[P_7]}{dt} = k_{23}[DMG]$$

According to the proposed model, the degradation products of some α-dicarbonyl compounds were excluded from the model as they increased the number of unknown parameters and caused incompatibility in the model. However, some rate constants could not be estimated within the specified confidence interval. This can be explained by the fact that the relevant rate constants are in the steps which include unquantified compounds, such as reactions involving HP, GLC, or FFC. Therefore, the proposed models involve the following reactions: sucrose degradation, AP/HP formation, HMF formation via FFC and 3-DG pathway, formation of α-dicarbonyl compounds through

sugar or AP/HP degradation, CML and CEL formation from AP/HP or α-dicarbonyl compounds, elimination reactions of HMF and α-dicarbonyl compounds.
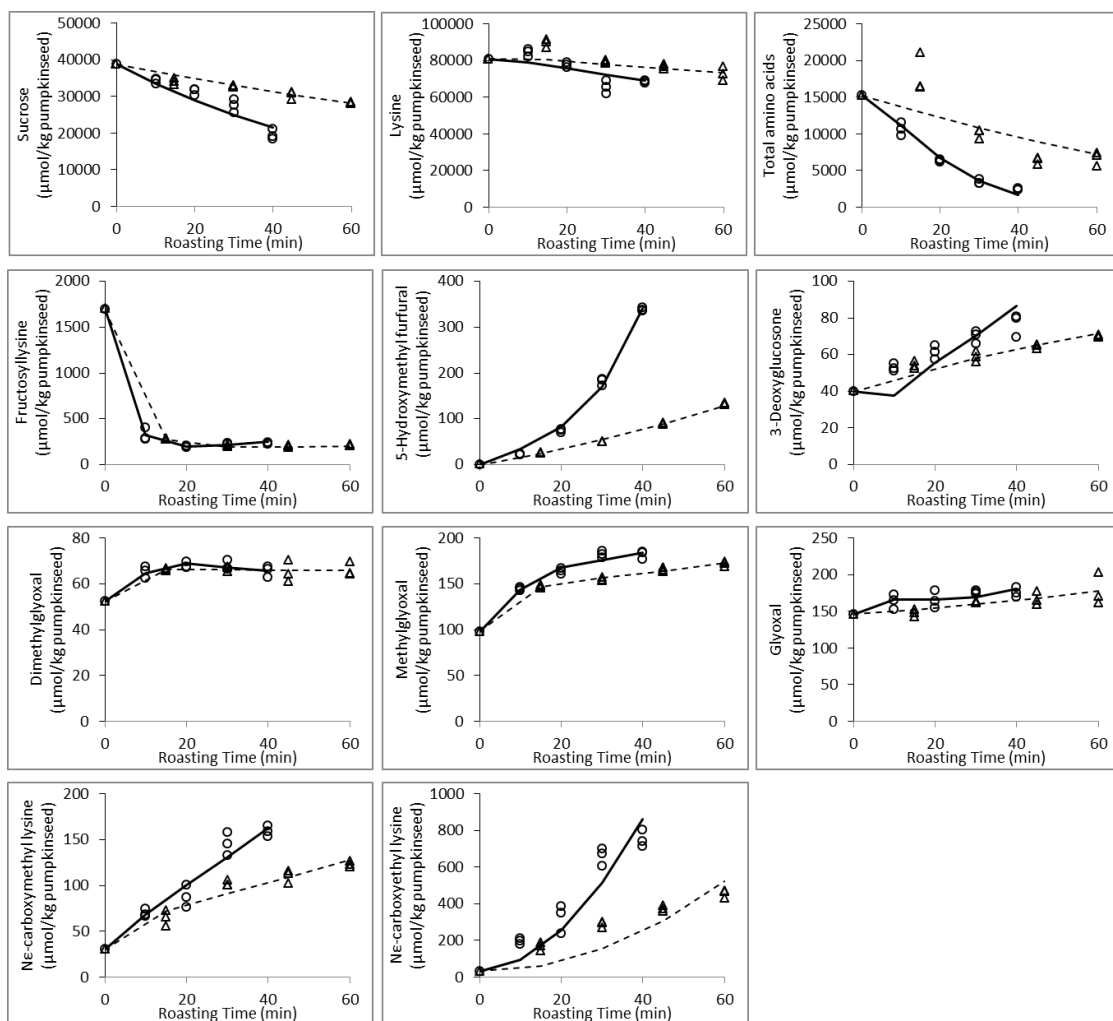
Figure 5. 9 Kinetic model fits (lines) to the obtained experimental data (symbols)of reactants and products during roasting of pumpkinseed at 160°C (Δ;-------) and 180°C (○;————)
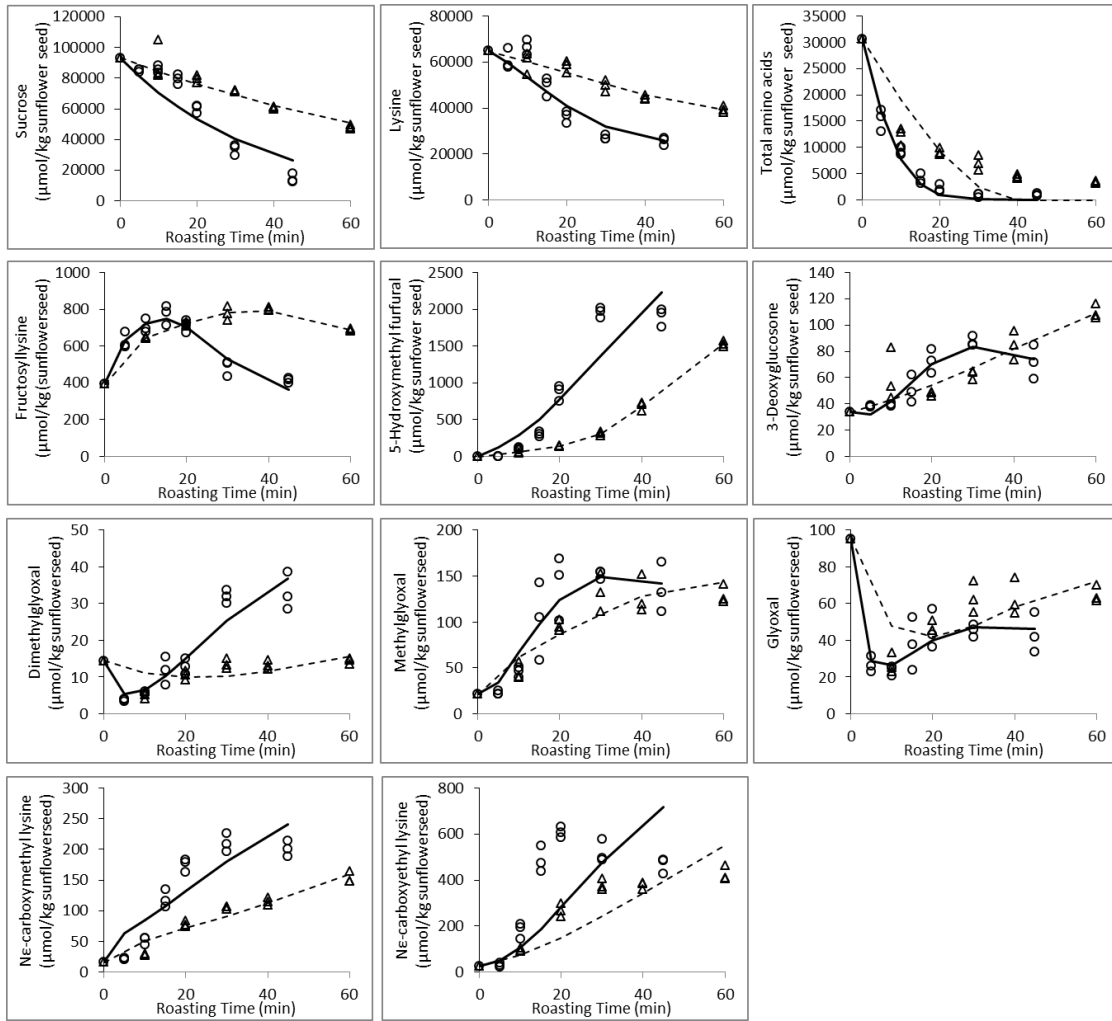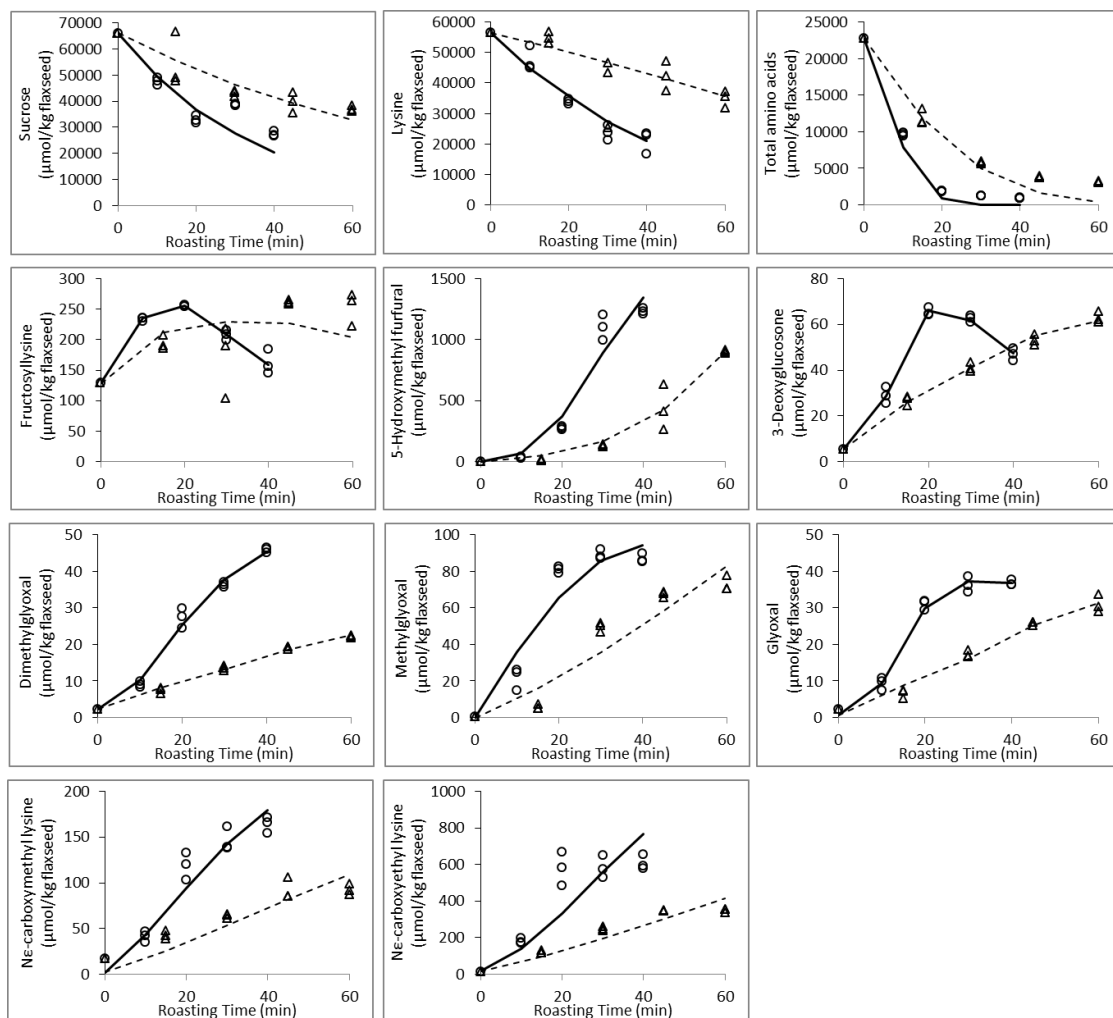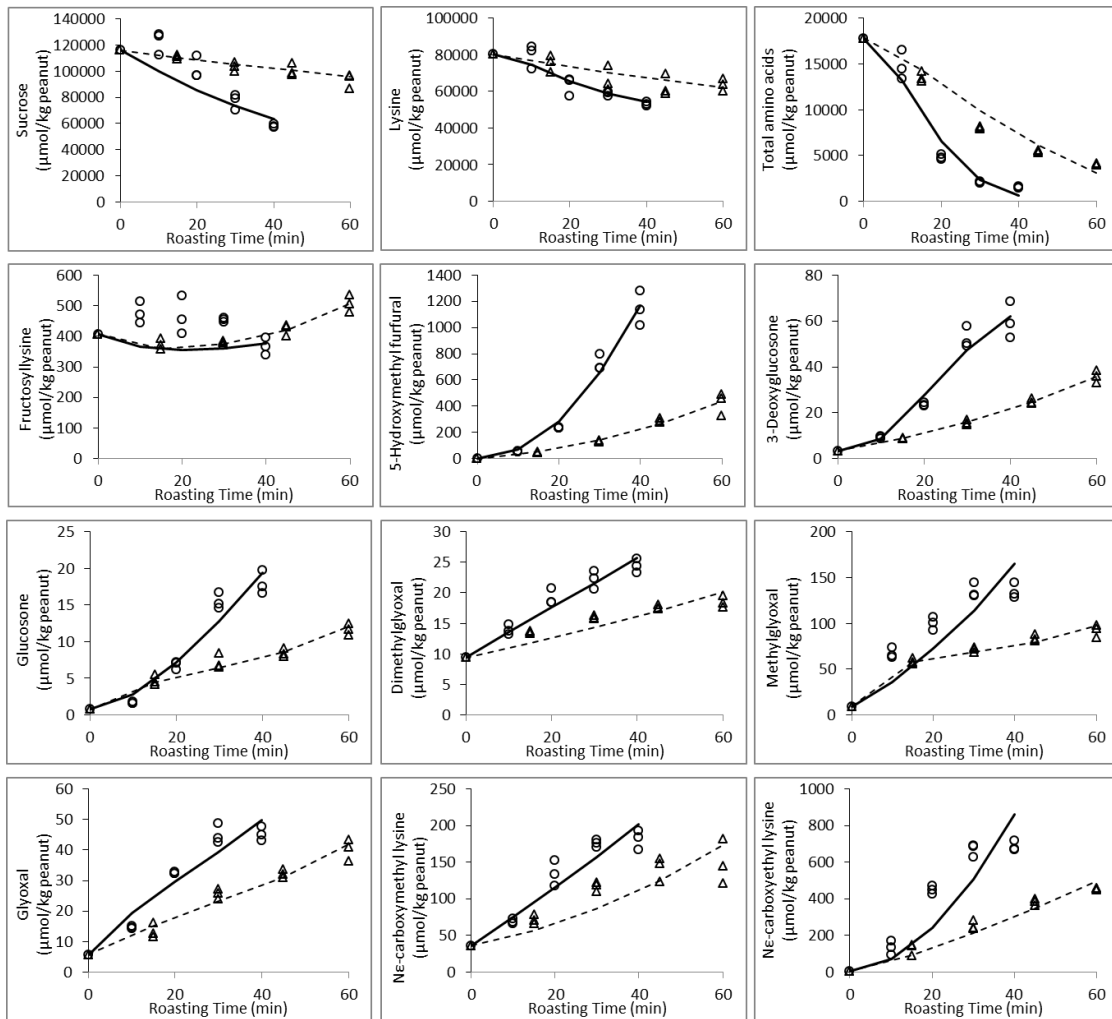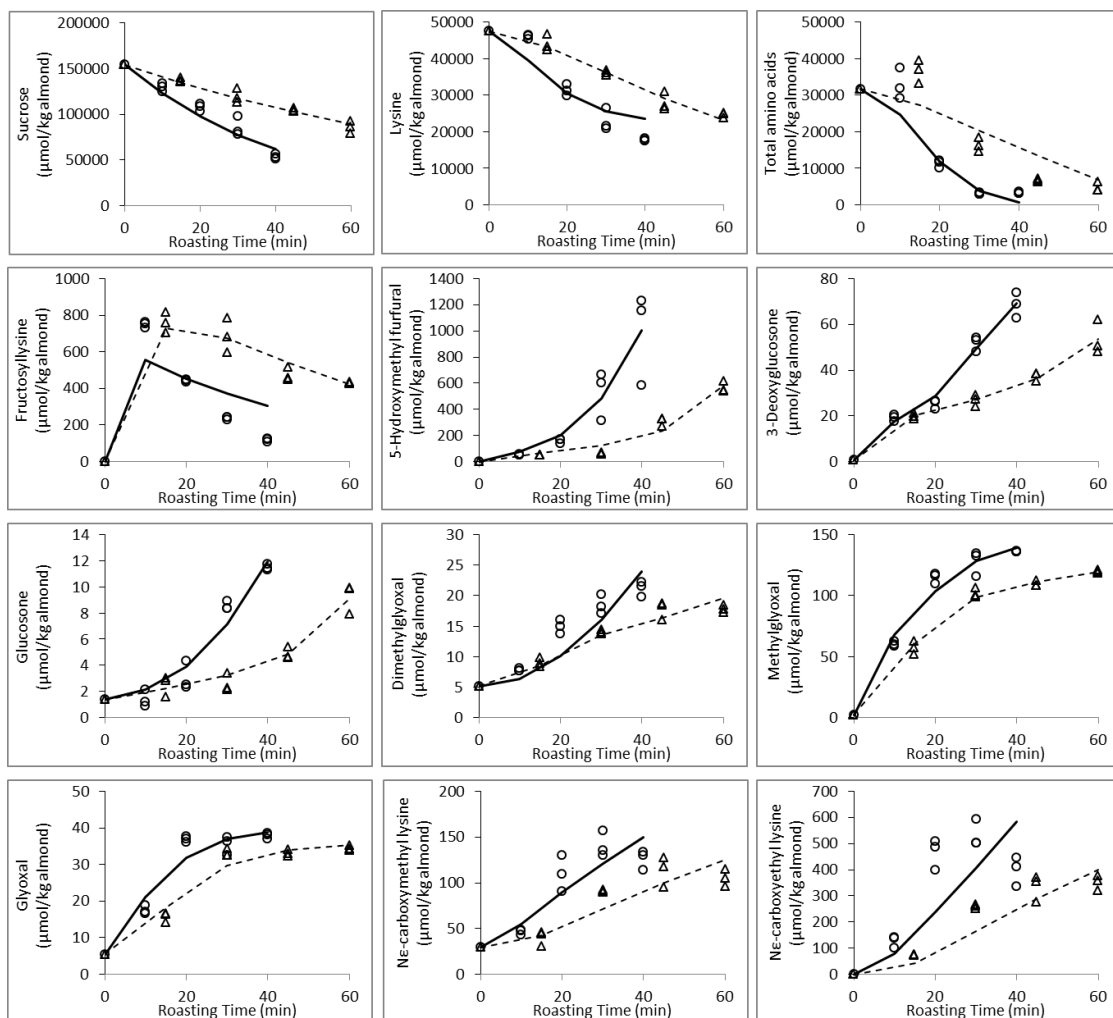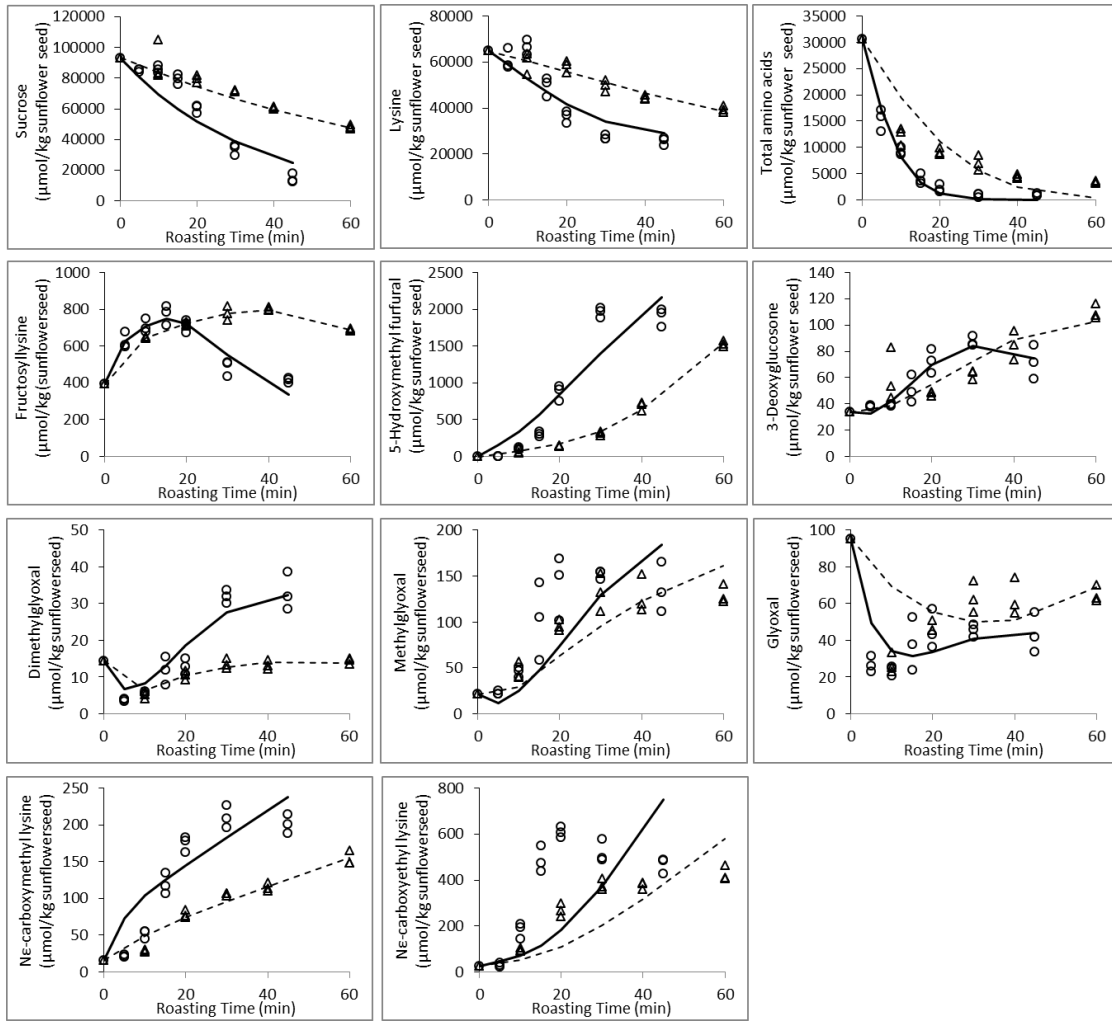
Figure 5. 10 Kinetic model fits (lines) to the obtained experimental data (symbols)of reactants and products during roasting of sunflower seed at 160°C (Δ;-------) and 180°C (○;————)
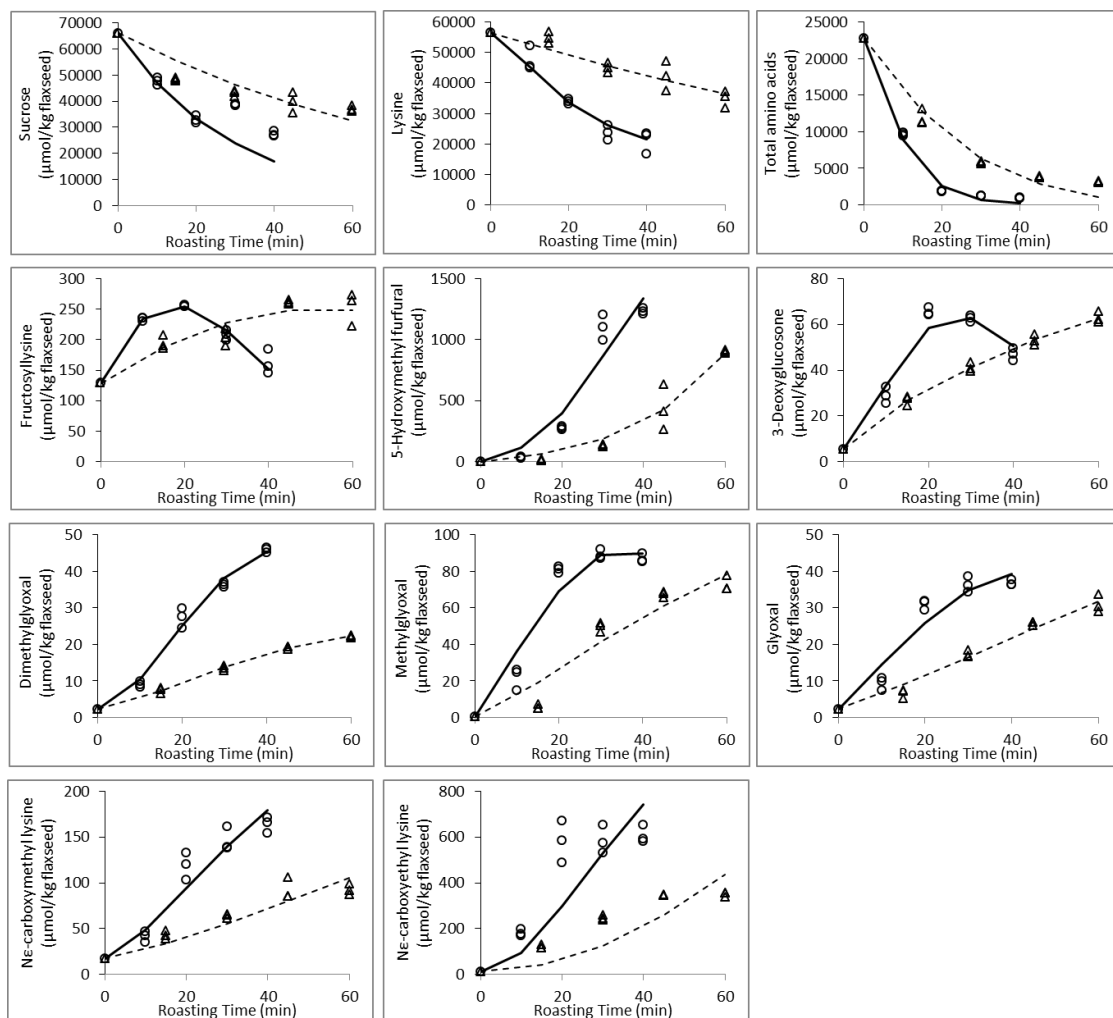
Figure 5. 11 Kinetic model fits (lines) to the obtained experimental data (symbols) of reactants and products during roasting of flaxseed at 160°C (Δ;-------) and 180°C (○;————)
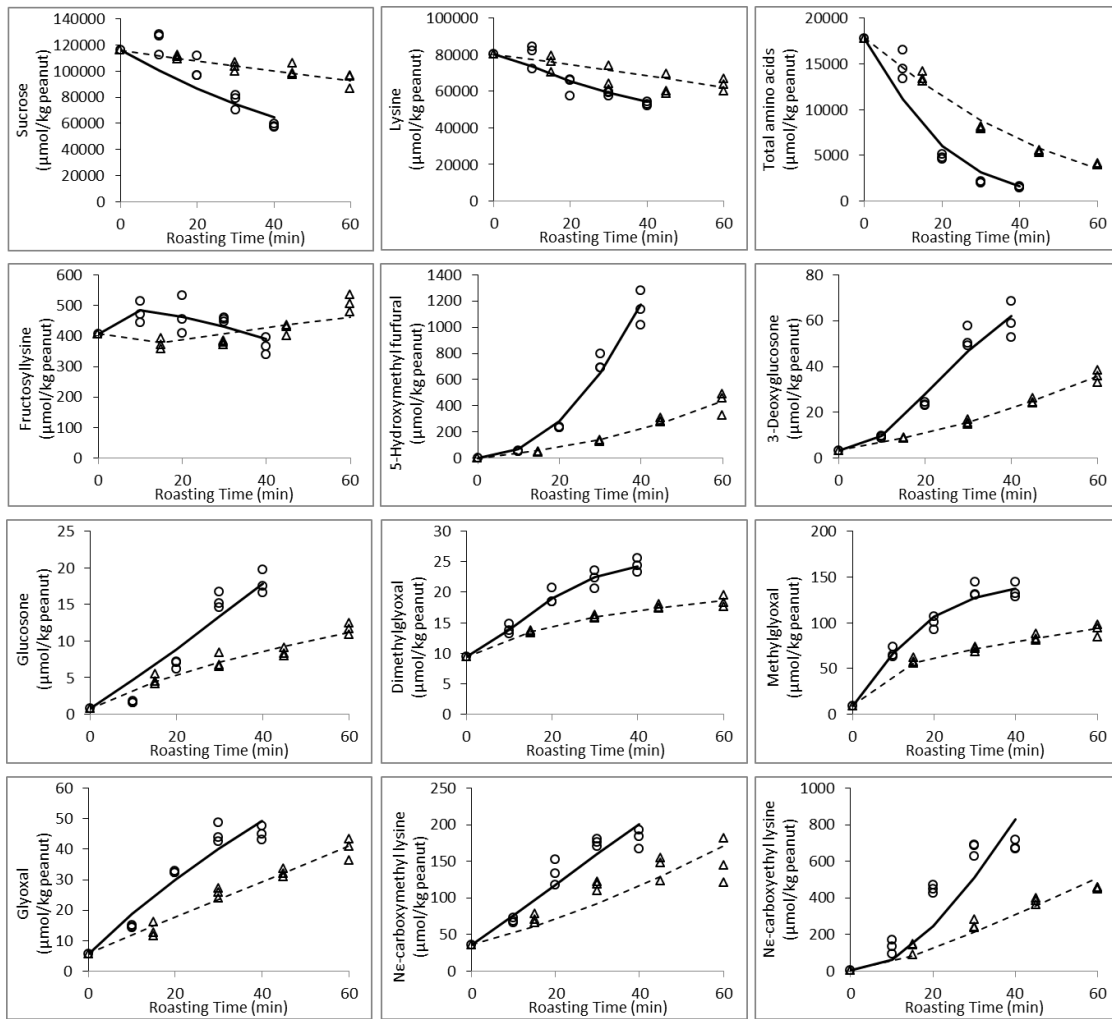
Figure 5. 12 Kinetic model fits (lines) to the obtained experimental data (symbols) of reactants and products during roasting of peanut at 160°C (Δ;-------) and 180°C (○;————)

Figure 5. 13 Kinetic model fits (lines) to the obtained experimental data (symbols)of reactants and products during roasting of almond at 160°C (Δ;-------) and 180°C (○;————)
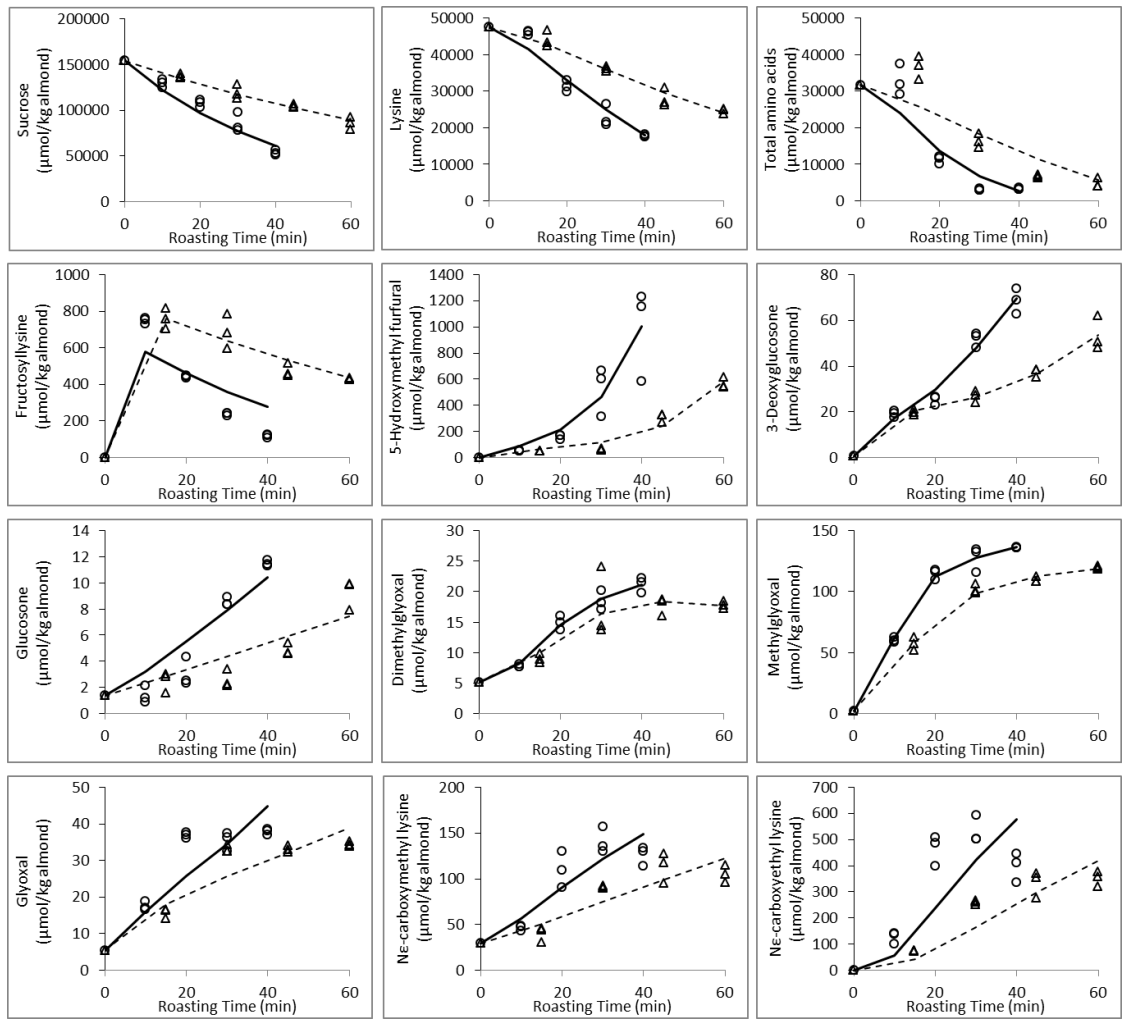
Kinetic model fits to the obtained experimental data of reactants and products during the roasting of samples were given in Figure 5. 9-13. The reaction rate constants (k), given in ±95% HPD, of elementary reaction steps in the proposed model, were presented for each roasting temperature (Table 5. 2). The reaction rate constants of most of the elementary reaction steps were found within a ±95% HPD interval.

Table 5. 2 Estimated reaction rate constants (k, min^{-1}x10^{3}) with 95% highest posterior density (HPD) intervals at different temperatures according to the proposed model for Maillard reaction and caramelization during roasting of samples

Reaction Rate Constant	Elemantary reaction step**	Sunflower seed		Flaxseed		Peanut		Almond		Pumpkınseed	
		160°C	180°C	160°C	180°C	160°C	180°C	160°C	180°C	160°C	180°C
k1	SUC→FFC+GLC	11.24±1.31	29.43±3.3	11.72±1.16	33.37±30.19	3.72±0.5	14.62±3.94	9.09±0.65	23.07±2.96	5.34±0.4	14.78±2.15
k2	FFC→HMF	0±0	89.49±44.3	0±0	0±0	13.2±15.83	0.85±1.25	0±0	2.77±6.3	0±0	0±0
k3	FFC+bLYS→HP	96.83±44.55	61.50±ind***	27.3±12.54	5.51±30.36	22.04±ind***	1.94±2.75	0.78±0.3	1.02±0.29	1.98±12.45	29.3±43.3
k4	GLC+bLYS→FL	5.43±ind***	8.98±8.22	0.40±ind***	2.72±ind***	11.91±3.85	212.65±115.3	50.3±ind***	8.01±9.78	1.87±0.43	0.13±0.15
k5	GLC→3-DG	38.23±80.83	5.10±ind***	34.94±21.88	208.64±107.2	15.09±22.47	0±0	544.68±535.8	2.53±ind***	10.91±1.4	8.12±10.36
k6	GLC→GO	0.17±2.4	2.12±1.36	1.21±0.28	8.51±6.9	4.35±2.1	24.97±ind***	3.13±2.58	0.27±0.52	4.3±2.34	0.49±0.57
k7a	GLC→G	202.14±418.3	298.11±524.9	885.53±341.1	2295.25±557.4	1.64±0.61	5.8±2.95	0.22±0.07	0.03±0.03	-	-
k7b	FL→GO+bLYS	-	-	-	-	-	-	-	-	0±0	5.36±1.83
k8	HP→3-DG+bLYS	0.57±3.76	0±0	2.67±1.8	0±0	0.5±0.36	2.23±1.16	0±0	0.96±1.77	0±0	0±0
k9	FL→1-DG+bLYS	364.36±365.5	96.26±93	18.17±7.83	111.85±22.7	28.22±3.29	27.83±13.51	17.11±2.19	46.49±11.22	180.61±10.78	156.17±31.28
k10	3-DG→HMF	568.79±143.8	109.98±90.19	1024.28±612.3	918.19±431.4	279.32±180	807.82±291.8	2528.66±1625	601.45±822	37.53±1.19	552.83±278.7
k11	1-DG→MGO	5.36±5.63	20.73±26.49	217.84±185.6	232.42±172.4	1266.25±656.4	342±290.5	124.06±26.3	218.46±164	18.02±3.06	14.4±ind***
k12	1-DG→DMG	94±34.71	5.27±4.89	69.49±57.57	18.6±10.93	199.59±ind***	29.65±26.09	11.82±5.48	7.7±5.95	6.36±1.75	5.36±1.11
k13	FL→CML	0.8±1.7	0±0	6.87±0.78	11.94±8.12	3.43±1.53	7.4±2.05	1.07±1.77	4.12±7.52	3.44±1.44	0.98±2.86
k14	GO+bLYS→CML	0.56±0.35	2.7±0.56	0±0	1.96±2.34	0.53±0.35	0.41±0.51	1.05±1.37	1.68±4.69	0.04±0.04	0.23±0.09
k15	HP→CEL	0±0	0±0	0.55±0.22	0±0	0±0	0.96±0.49	0±0	0±0	1.67±2.49	3.03±1.36
k16	MGO+bLYS→CEL	2.16±0.51	5.12±2.22	0.86±0.82	9.87±2.1	1.8±0.15	1.31±0.82	2.56±0.33	5.37±1.18	0.08±0.07	0.13±0.09
k17*	GLC+AA→P$_1$	34.37±32.36	54.6±45.15	52.15±14.04	327.74±504.1	61.84±ind***	463.95±416.1	0±0	0±0	50.8±ind***	9.5±13.06
k18	FL→P$_2$+bLYS	0±0	974.55±1172	0±0	0±0	525.68±83.19	2243.87±314.4	1275.86±324.3	4742.99±924.9	3.3±ind***	37.46±33.29
k19*	HMF+AA→P$_3$	9.85±5.59	0±12.9	26.48±29.5	13.35±27.76	0±0	0±0	29.29±25.55	24.79±62.13	0±0	43.66±28.72
k20*	FFC+AA→P$_4$	317.56±ind***	183.93±133.2	72.74±ind***	2.68±39.94	51.53±40.31	3.44±8.73	0.71±0.99	2.27±1.27	0±0	98.3±ind***
k21a	HP→P$_{5a}$+bLYS	6.75±7.4	16.52±14.19	2.85±5.94	8.3±21.12	0.2±13.55	17.82±24.66	7.46±8.81	0±0	-	-
k21b	1-DG→P$_{5b}$	-	-	-	-	-	-	-	-	475.6±ind***	179.69±78.25
k22*	3-DG+AA→P$_6$	9.89±61.77	3.13±3.7	0±0	85.75±58.98	24.67±45.31	42.3±109.4	369.63±300.9	36.06±44.36	0±0	0±0
k23	DMG→P$_7$	18591.15±19730	229.67±237.2	41.88±18.15	23.34±19.55	90.85±52.51	32.02±25.85	45.79±29.39	16.8±12.37	8.7±5.12	16.28±6.97
k24a	G→GO	0.22±0.4	0.02±0.16	0±0	0±0	40.39±20.9	0±0	0±0	0±0	-	-
k24b	HP→1-DG+bLYS	-	-	-	-	-	-	-	-	1.32±1.92	0±0

*Reaction rate constant unit: kg µmol^{-1}min^{-1}x10^{3}

**SUC sucrose; GLU glucose; FFC fructofuranosyl cation; HMF 5-hydroxymethyl furfural; bLYS protein bound lysine; FL N-ε-fructoselysine; HP Heyns product; 3-DG 3-deoxyglucosone; GO glyoxal; G glucosone; 1-DG 1-deoxyglucosone; MGO methylglyoxal; DMG dimethylglyoxal; CML N-ε-carboxymethyllysine; CEL N-ε-carboxyethyllysine; AA total amino acids; P products

***ind: Indeterminate, which means a large uncertainty in the estimated parameter within 95% confidence interval.

Degradation of sucrose and HMF formation

Sucrose degrades to free glucose and FFC, especially under low moisture conditions (Perez Locas and Yaylayan, 2008). Glucose is also interconverted into fructose through 1,2-enolization. However, these steps were removed from the model in order not to increase the number of unknown molecules since fructose and glucose were unquantified in this system. FFC can be also generated directly from fructose in another way. However, in such a dry condition, fructose formation is very difficult to occur (Perez Locas and Yaylayan, 2008). Göncüoğlu Taş and Gökmen (2017) also excluded the FFC formation step from fructose from the proposed model because the k value of this step was zero and therefore it was kinetically insignificant in the comprehensive model. Therefore, the degradation of sucrose to form glucose and FFC was considered the main mechanism in nuts and seeds during roasting and involved in the proposed model.

Sucrose, glucose, and FFC are the direct precursors of HMF in nuts and seeds during roasting. During heat treatment in dry systems, HMF can be formed directly from FFC or glucose via 3-DG. It was determined that the 3-DG pathway was predominant in HMF formation for all samples according to reaction rate constants (Table 5. 2). The results were in agreement with the findings of Göncüoğlu Taş and Gökmen (2017)who stated that the contribution of FFC to HMF formation is less than 3-DG. However, they also emphasized that FFC was an important source in HMF formation and the model was not suitable when this step was removed due to the fact that FFC is an intermediate that cannot be detected experimentally and the dehydration steps in the formation of HMF from FFC are reduced to one step.

Formation of Amadori/Heyns product

Maillard reaction starts with the condensation of reducing sugar with a compound that has a free amino group and leading to the formation of *N*-substituted glycosylamine. This unstable compound rearranges to form Amadori product (1-amino-1-deoxyketose) (Amadori, 1929) or Heyns product (2-amino-2-deoxyaldose) (Heyns and Meinecke, 1953) according to the present sugar type. Since the predominant amino acid with a reactive side chain was lysine and other glycated amino acids were not determined due to the lack of commercial standards in this study, the formation of AP was based on N-

fructosyllysine and indicated as FL instead of AP in the model. FL (Amadori compound of lysine) was quantified by measuring ε-N-(2-furoylmethyl)-L-lysine, known as furosine generated via degradation of FL to furoyl derivatives with acid hydrolysis.

Compared to protein-bound arginine and histidine, protein-bound lysine was the most reactive amino acid in nuts and seeds. Protein-bound lysine decreased, although protein-bound arginine and histidine did not change significantly ($p > 0.05$) in any nut and seed samples during roasting (Figure 4. 3-4). The reaction of glucose with protein-bound lysine led to the formation of AP, named N-ε-fructosyllysine (FL), in roasted nuts and seeds. HP, formed from the reaction of fructose or FFC with amine, could not be measured as no standard compound was available. However, the HP formation was involved in the model from the FFC only, since sucrose degraded to FFC and glucose especially in dry systems at high temperatures. The formation of AP and HP that actually consist of several steps were shown in one step in order to reduce the number of unknown parameters since the compounds in the intermediate steps could not be detected. The comprehensive model also includes interconversion of HP to FL. Since the increase in the number of unmeasurable reactants and products in the model, such as HP, reduces the possibility of accurate estimates in multiresponse modeling, these steps were excluded from the model.

HP formation from FFC (*k3*) appears to be more important than FL formation from glucose (*k4*) in samples indicating that FFC was more important in the early stages of Maillard reaction except for peanut roasted at 180 °C and almond (Table 5. 2). Although the reaction rates of pumpkin seed roasting at 160 and 180 °C differed in most of the reaction steps compared to other samples, it showed similar behavior in the case of AP/HP formation where *k3>k4* (Table 2). Berk et al. (2021)also reported that the reaction rate constant of HP formation from the reaction of FFC with bound lysine was predominant compared to FL formation during sesame seed roasting at 200 and 220 °C.

Formation of α-dicarbonyl compounds and their reactions with amino acids

α-Dicarbonyl compounds can arise through the degradation of AP or directly from reducing carbohydrates even in the absence of amines (Hollnagel and Kroh, 1998, Martins et al., 2003). Formation routes of measured α-dicarbonyls are as follows: 3-DG is formed through 1,2-enolization from AP or glucose. Dehydration reactions of 2,3-

101

enediols lead to the formation of 1-DG. Glucosone is generated via the oxidation of glucose through the 1,2-enediol pathway. Short-chain α-dicarbonyls such as GO, MGO, and DMG are formed from the fragmentation of long-chain α-dicarbonyls. In proposed models, 3-DG formation through the FL step was excluded (Figure 5. 8) to simplify the kinetic model as it was estimated in lower bound. On the other hand, it was found that the formation pathway of 3-DG through glucose dehydration ($k5$) was predominant in all samples, while in peanut samples, the formation over the Maillard reaction ($k8$) became predominant as the high temperature was influential. The degradation pathway of HP to 1-DG ($k24$) was found to be more important than its degradation to 3-DG ($k8$) in pumpkin seed whereas the formation of 1-DG from the HP step was removed from the proposed model for the other nuts and seeds. Göncüoğlu Taş and Gökmen (2017) stated that the breakdown of the HP in the 3-DG formation during the roasting of hazelnuts is more important compared to the breakdown of the Amadori product. On the contrary, they also found that degradation of the Amadori compound became more important for 1-DG formation. In addition, Berk et al. (2021) reported that the formation of 3-DG through glucose was the important pathway although the degradation of the Amadori product is more effective in the formation of 1-DG in the Maillard reaction during the roasting of sesame seeds. Glucosone formation rate ($k7$) was found to be higher in flaxseed, followed by sunflower, peanut, and almond, respectively. However, its degradation to GO ($k24$) rate was found to be higher in peanuts at 160 °C followed by sunflower seed. MGO is formed through the cleavage of bonds between C 3- and C4- atoms in 1-DG and from 3-DG via retro-aldol reactions (Gobert and Glomb, 2009, Weenen, 1998). According to Hollnagel and Kroh (1998), MGO is also formed through isomerization and retro-aldolization reactions of sugar. However, the data predicted from the comprehensive model (Figure 5. 2) for MGO formation did not fit with the experimental data. Therefore, the compatibility of the model with the experimental data was tested by excluding the formation steps one by one. Finally, the predicted concentration data were well fitted with the experimental data when only the formation of MGO through the 1-DG pathway ($k11$) was included in the proposed model. Göncüoğlu Taş and Gökmen (2017) also found the best model fit when they included only the MGO formation pathway through 1-DG during the roasting of hazelnut. Additionally, Kocadağlı and Gökmen (2016) found the 1-DG pathways as the most dominant route for MGO formation. The higher reaction rate constant ($k11$) of MGO formation compared to other short-chain dicarbonyl compounds

could be explained by the reactivity of 1-DG. Gobert and Glomb (2009) explained the high reactivity of 1-DG with its reductone structure.

In the proposed kinetic model for the samples other than pumpkin seed, the GO formation step from FL was removed to achieve the best model fit. It was found that the formation of GO via the glucose degradation ($k6$) pathway was dominant especially at high temperatures during roasting of nuts and seeds other than pumpkin seed. In the proposed pumpkin seed model, the rate constants indicated that GO mainly forms through the degradation of glucose ($k6$) at 160 °C. However, at 180 °C, GO mainly originated from the Amadori product ($k7$) which showed the temperature dependence of the GO formation during the roasting of pumpkin seeds.

DMG is claimed to be formed because of the isomerization of 1-DG by Weenen (1998). The reaction rate constants of this step ($k12$) were higher in the nut and seed samples compared to pumpkin seed except for sunflower seed at 180 °C. Additionally, the formation rate of MGO over 1-DG ($k11$) is higher than the rate of DMG formation ($k12$) except for sunflower roasted at 160 °C. The rate constant of DMG formation through 1-DG ($k12$) decreased when the roasting temperature increased. The degradation step of DMG to product ($k23$) was involved in the model and similar to the rate constants in the formation of DMG, the degradation reaction rate constant of DMG during roasting of nuts and seeds was again found to be higher than that of pumpkin seed.

In the advanced stage, Strecker aldehydes are formed because of the reaction between α-dicarbonyl compounds and α-amino acids (Yaylayan, 2003). Additionally, α-dicarbonyl compounds undergo condensation and polymerization that leads to the formation of brown nitrogenous compounds named melanoidins. In the comprehensive model (Figure 5. 2), the reaction of all α-dicarbonyl compounds with free amino acids was also included and the neo-formed compounds were shown as products (P_{1-7}). However, when all the product formation steps were included in the model, the predicted data were not fit well with the experimental data. Therefore, the model was also tested by considering the self-reactions of α-dicarbonyl compounds instead of their reactions with amino acids. Finally, the self-reaction of DMG ($k23$) and the reaction of 3-DG with amino acids ($k22$) were found to be important. In the proposed model of pumpkin seed, only the self-reactions of α-dicarbonyl compounds were involved. In pumpkin seed, the degradation reaction of DMG to product was triggered by increased

temperature whereas in other nuts and seeds rate constant of this reaction decreased with increasing roasting temperature.

Formation of CML/CEL

AGEs are formed by the reaction of α-dicarbonyls formed as a result of the Maillard reaction with reactive sides of protein or peptide-bound amino acids. Among these end products, CML and its homologue CEL are two of the most widely studied AGEs. The formation of CML and CEL depends on the reactants in the food matrix and heat treatment parameters. CML and CEL can arise from the oxidation of AP/HP or the reaction of α-dicarbonyls such as GO and MGO with the ε-amino group of lysine. CML can be formed from AP and also GO originated from glucose or the Namiki pathway is a precursor for CML formation (Nguyen et al., 2013). CEL is considered to be formed mainly from MGO according to Surh and Tannenbaum (1994). Treibmann et al. (2017) reported that CEL formation is also in correlation with HP concentrations. Therefore, both formation pathways were included in the model.

CML was found to be mostly formed from FL (*k13*) except for sunflower seeds roasted at 180 °C where formation through the reaction of GO and bound lysine (*k14*) became apparently predominant. This difference can be attributed to the fact that sunflower seeds have a matrix rich in polyunsaturated fatty acids which might be a source of GO due to lipid oxidation (Fujioka and Shibamoto, 2004).

The rate constant of CEL formation through MGO (*k16*) was found relatively low in comparison to the HP pathway (*k15*) in pumpkin seed samples whereas in all other samples MGO pathway was predominant. The difference between the composition of pumpkin seed and other nuts and seeds, which was classified as shown in PCA plots (Figure 5. 1), could be the reason for the difference in dominant CEL formation pathways.

The higher CEL concentration compared to CML in the roasted samples could be explained by the comparison of the reaction rate constants in the proposed models. MGO formation rate was higher than the GO formation rate (*k11>k6, k11>k24*) and the CEL formation rate from MGO was higher than the CML formation rate from GO (*k16>k14*) (except in pumpkin seeds) which indicated that MGO reacted faster with lysine than GO.

104

It was observed that the CEL remained constant or decreased in some samples, especially at the end of the roasting periods at high temperatures. These observations were also supported by the previous studies (Nguyen et al., 2016b, Niquet-Leridon et al., 2015, Troise et al., 2015). However, since CEL is considered a stable end product (Nguyen et al., 2013), further degradation step of CEL was not included in the model mechanisms. The reason for the decrease in the CEL concentration with increased thermal load should be proved chemically to understand further reactions of CEL in the Maillard reaction.

5.3.4. Kinetic Modeling of Acrylamide Formation

The current challenge in this study was to propose a kinetic model for ACR formation in low moisture, sucrose-rich but reducing sugar-poor food systems such as nuts and seeds.

A comprehensive model including all reported pathways in ACR formation occurring in low moisture conditions was built and presented in Figure 5. 14. As the aim of this study was to prove whether the dominant pathways were valid here, instead of finding the best model fit/compatible model, the comprehensive model was simplified by considering the important reaction pathways identified in previous studies.
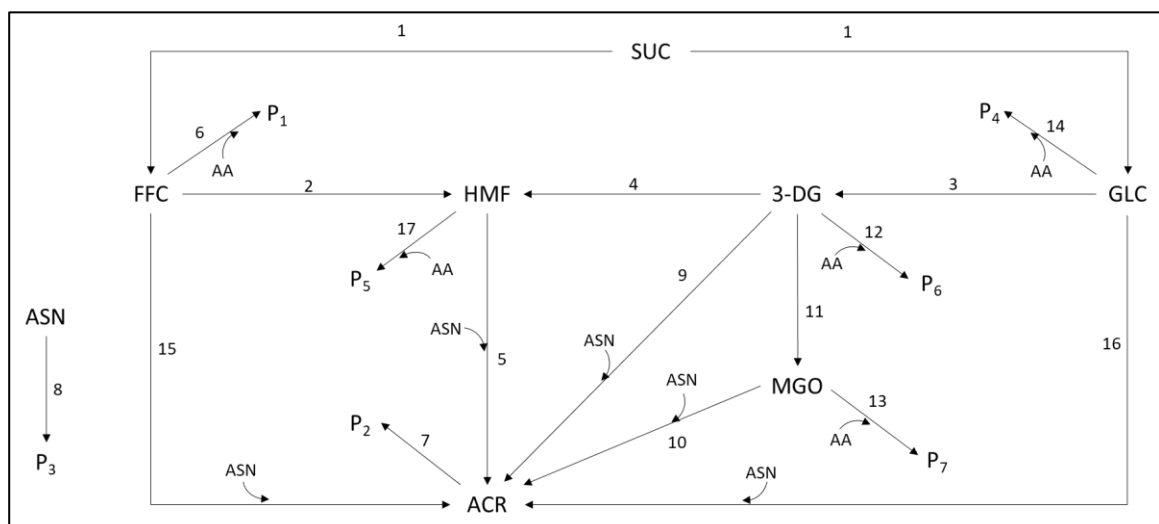
Figure 5. 14 The comprehensive mechanistic model for acrylamide formation in nuts and seeds during roasting. SUC: sucrose; GLC: glucose; FFC: Fructofuranosyl cation; AA: total amino acids; ASN: asparagine; 3-DG: 3-deoxyglucosone; MGO: methylglyoxal; HMF: 5-hydroxymethyl-2-furfural; ACR: acrylamide; P: products.

Each step of the comprehensive reaction network given in Figure 5. 14 was represented by an ordinary differential equation, which was characterized by a reaction rate constant (k) as follows:

$$\frac{d[SUC]}{dt} = -k_1[SUC]$$

$$\frac{d[Asn]}{dt} = -k_5[HMF][Asn] - k_8[Asn] - k_9[3-DG][Asn] - k_{10}[MGO][Asn]$$
$$- k_{15}[FFC][Asn] - k_{16}[GLC][Asn]$$

$$\frac{d[HMF]}{dt} = k_2[FFC] + k_4[3-DG] - k_5[HMF][Asn] - k_{17}[HMF][AA]$$

$$\frac{d[ACR]}{dt} = k_5[HMF][Asn] + k_9[3-DG][Asn] + k_{10}[MGO][Asn] + k_{15}[FFC][Asn]$$
$$+ k_{16}[GLC][Asn] - k_7[ACR]$$

$$\frac{d[AA]}{dt} = -k_6[FFC][AA] - k_{12}[3-DG][AA] - k_{13}[MGO][AA] - k_{14}[GLC][AA]$$
$$- k_{17}[HMF][AA]$$

$$\frac{d[3-DG]}{dt} = k_3[GLC] - k_4[3-DG] - k_9[3-DG][Asn] - k_{11}[3-DG] - k_{12}[3-DG][AA]$$

$$\frac{d[GLC]}{dt} = k_1[SUC] - k_3[GLC] - k_{14}[GLC][AA] - k_{16}[GLC][Asn]$$

$$\frac{d[FFC]}{dt} = k_1[SUC] - k_2[FFC] - k_6[FFC][AA] - k_{15}[FFC][Asn]$$

$$\frac{d[MGO]}{dt} = k_{11}[3-DG] - k_{10}[MGO][Asn] - k_{13}[MGO][AA]$$

$$\frac{d[P_1]}{dt} = k_6[FFC][AA]$$

$$\frac{d[P_2]}{dt} = k_7[ACR]$$

$$\frac{d[P_3]}{dt} = k_8[Asn]$$

$$\frac{d[P_4]}{dt} = k_{14}[GLC][AA]$$

$$\frac{d[P_5]}{dt} = k_{17}[HMF][AA]$$

$$\frac{d[P_6]}{dt} = k_{12}[3 - DG][AA]$$

$$\frac{d[P_7]}{dt} = k_{13}[MGO][AA]$$
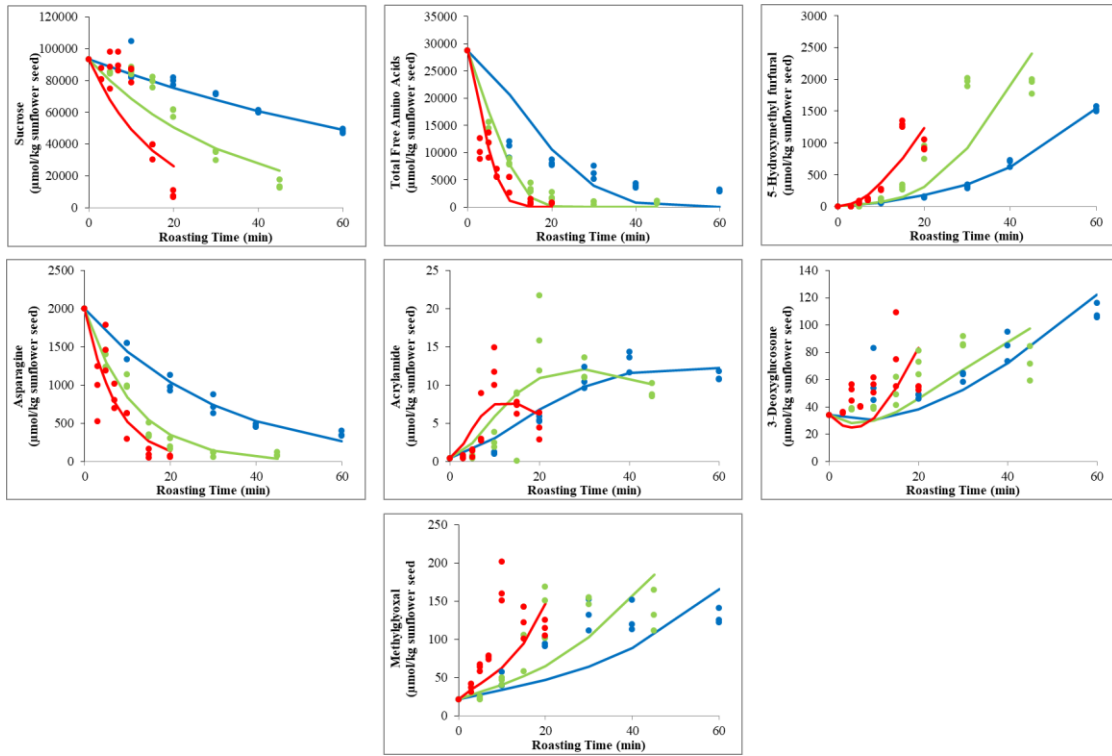
Figure 5. 15 Kinetic model fits (lines) obtained according to comprehensive kinetic model to the obtained experimental data (symbols)of reactants and products during roasting of sunflower. Blue colour for markers and lines designates 160°C, green 180°C and red 200°C.
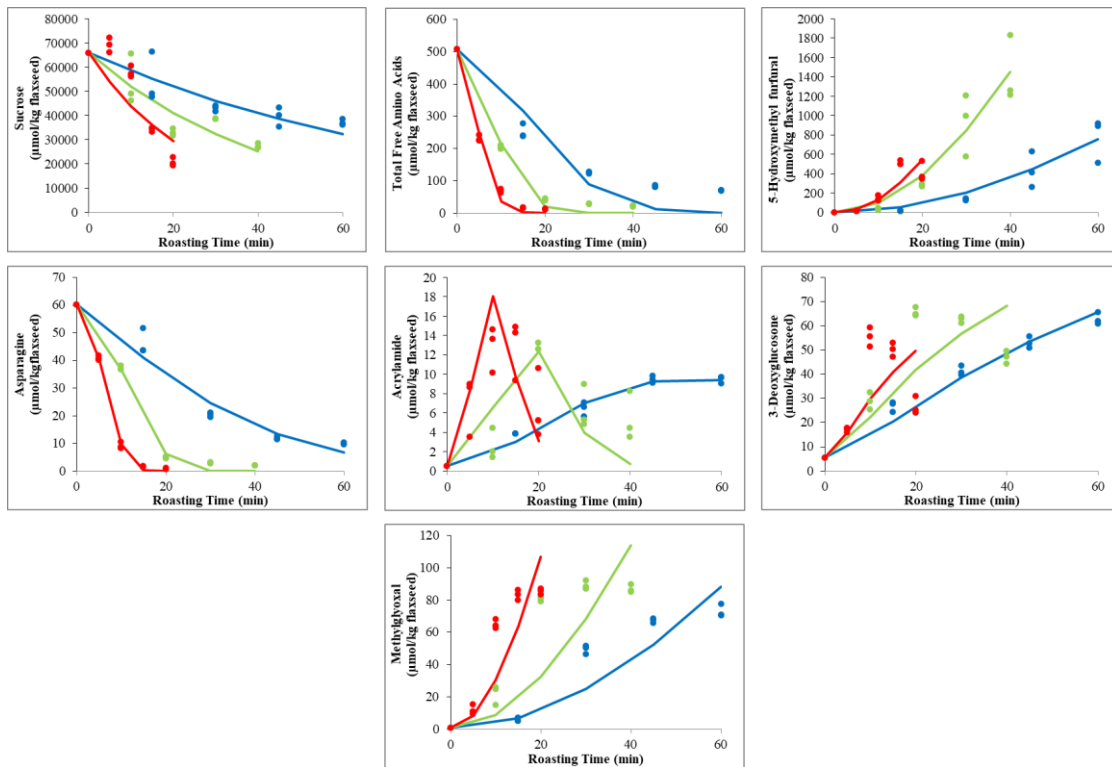
Figure 5. 16 Kinetic model fits (lines) obtained according to comprehensive kinetic model to the obtained experimental data (symbols)of reactants and products during roasting of flaxseed. Blue colour for markers and lines designates 160°C, green 180°C and red 200°C.

108
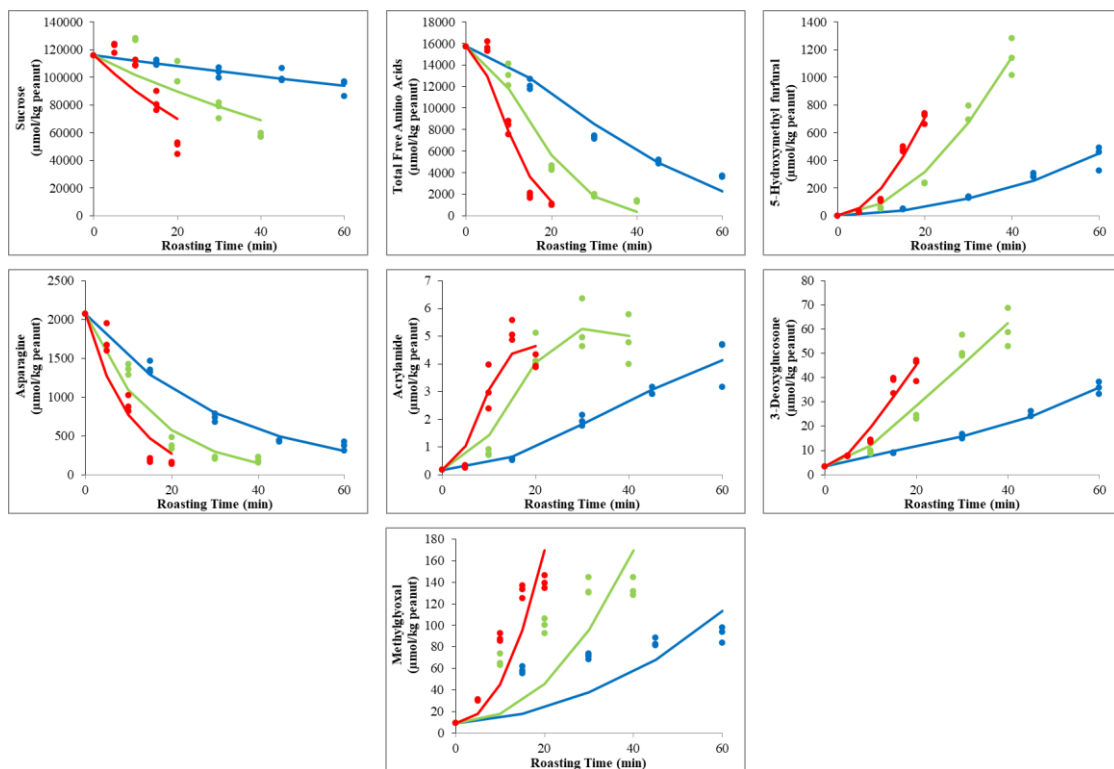
Figure 5. 17 Kinetic model fits (lines) obtained according to comprehensive kinetic model to the obtained experimental data (symbols)of reactants and products during roasting of peanut. Blue colour for markers and lines designates 160°C, green 180°C and red 200°C.
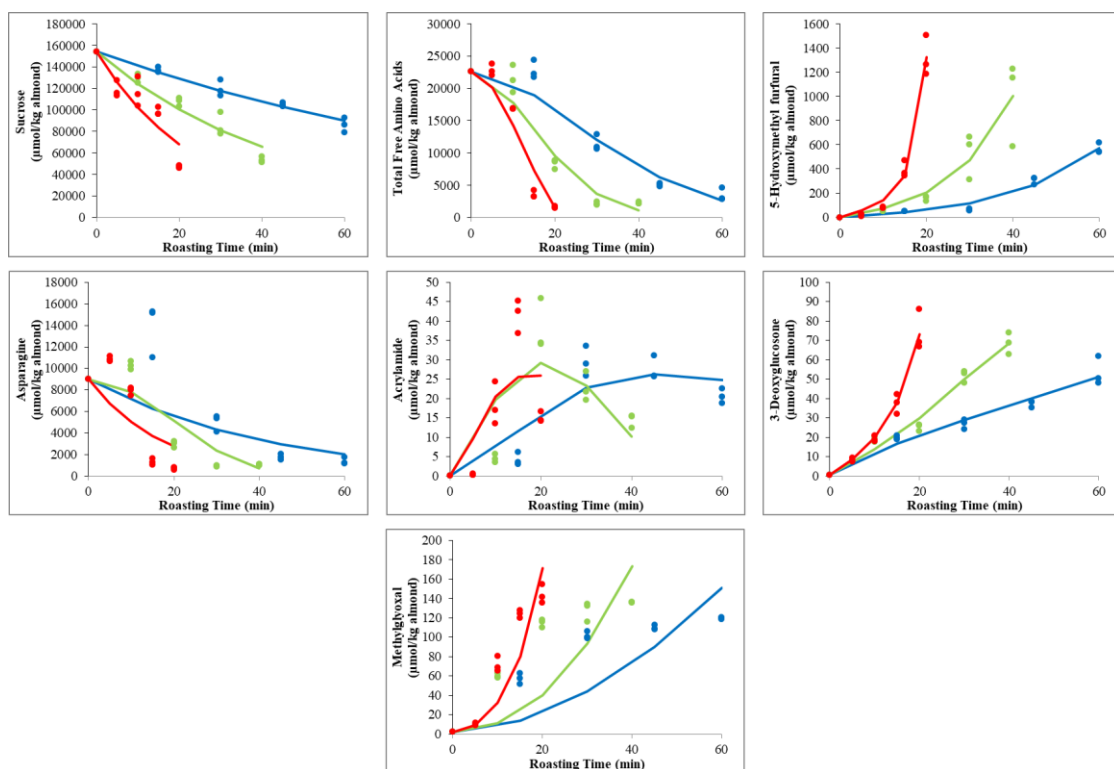
Figure 5. 18 Kinetic model fits (lines) obtained according to comprehensive kinetic model to the obtained experimental data (symbols)of reactants and products during roasting of almond. Blue colour for markers and lines designates 160°C, green 180°C and red 200°C.

As could be clearly seen from Figure 5. 15-18, concentrations of 3-DG, MGO, and ACR only in almond samples could not be estimated well. Further simplifications were done to obtain well-fitted kinetic models and increase the precision of the estimated parameters by excluding kinetically insignificant pathways one by one, which were illustrated in grey. Finally, a simple and adequate kinetic model for ACR formation was proposed by using six responses as shown in Figure 5. 19. The proposed reaction network was mainly composed of degradation of sucrose to glucose and FFC, 3-DG formation, HMF formation through 3-DG or FFC, ACR formation from HMF, and elimination reactions of FFC, ACR, and free asparagine.
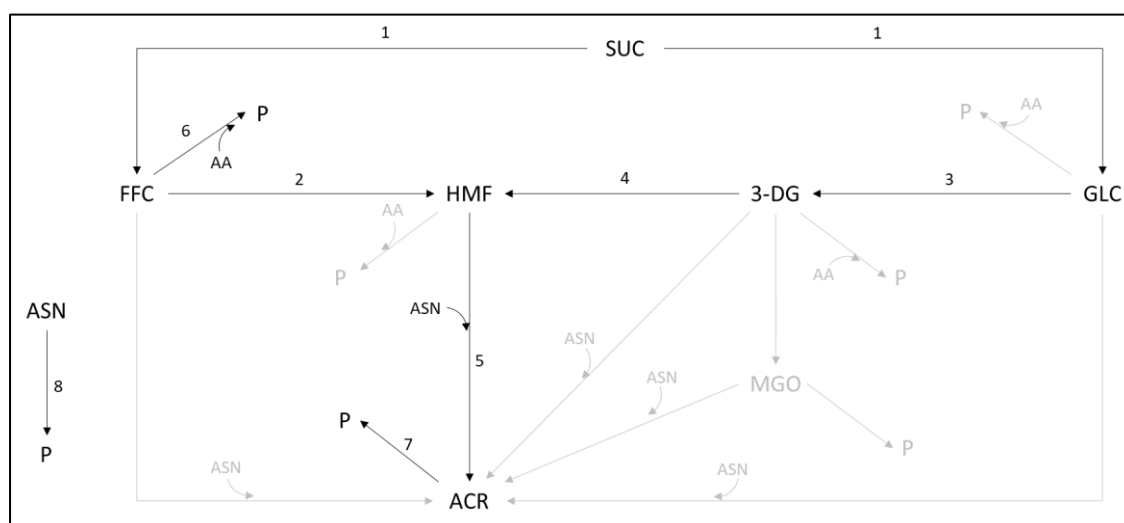
Figure 5. 19 Proposed mechanistic model for acrylamide formation during roasting at 160, 180 and 200 °C.

The reaction network was translated into a mathematical model to fit the experimental data to the proposed model. Each step of the comprehensive reaction network given in Figure 5. 19 was represented by an ordinary differential equation, which was characterized by a reaction rate constant (k) as follows:

$$\frac{d[SUC]}{dt} = -k_1[SUC]$$

$$\frac{d[Asn]}{dt} = -k_5[HMF][Asn] - k_8[Asn]$$

$$\frac{d[HMF]}{dt} = k_2[FFC] + k_4[3-DG] - k_5[HMF][Asn]$$

$$\frac{d[ACR]}{dt} = k_5[HMF][Asn] - k_7[ACR]$$

$$\frac{d[AA]}{dt} = -k_6[FFC][AA]$$

$$\frac{d[3-DG]}{dt} = k_3[GLC] - k_4[3-DG]$$

$$\frac{d[GLC]}{dt} = k_1[SUC] - k_3[GLC]$$

$$\frac{d[FFC]}{dt} = k_1[SUC] - k_2[FFC] - k_6[FFC][AA]$$

$$\frac{d[P_1]}{dt} = k_6[FFC][AA]$$

$$\frac{d[P_2]}{dt} = k_7[ACR]$$

$$\frac{d[P_3]}{dt} = k_8[Asn]$$

Differential equations written for each reaction step were solved by numerical integration. Kinetic model fits to the obtained experimental data of reactants and products during the roasting of samples were given in Figure 5. 20-23. The markers indicate the obtained experimental data at 160 °C, 180 °C, and 200 °C for each roasted sample whereas the lines show the estimated kinetic model fits calculated by the program.

The reaction rate constants (k), given in ±95% HPD, of elementary reaction steps in the proposed model, were presented for each roasting temperature (Table 5. 3). The reaction rate constants of most of the elementary reaction steps were found within a ±95% HPD interval.
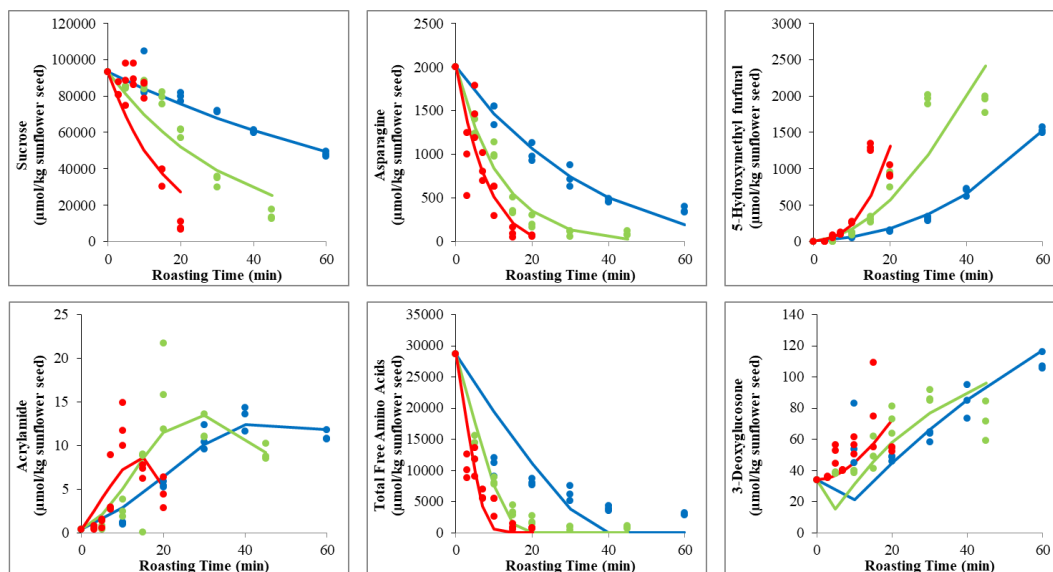
Figure 5. 20 Kinetic model fits (lines) to the obtained experimental data (symbols)of reactants and products during roasting of sunflower seed. Blue colour for markers and lines designates 160°C, green 180°C and red 200°C.
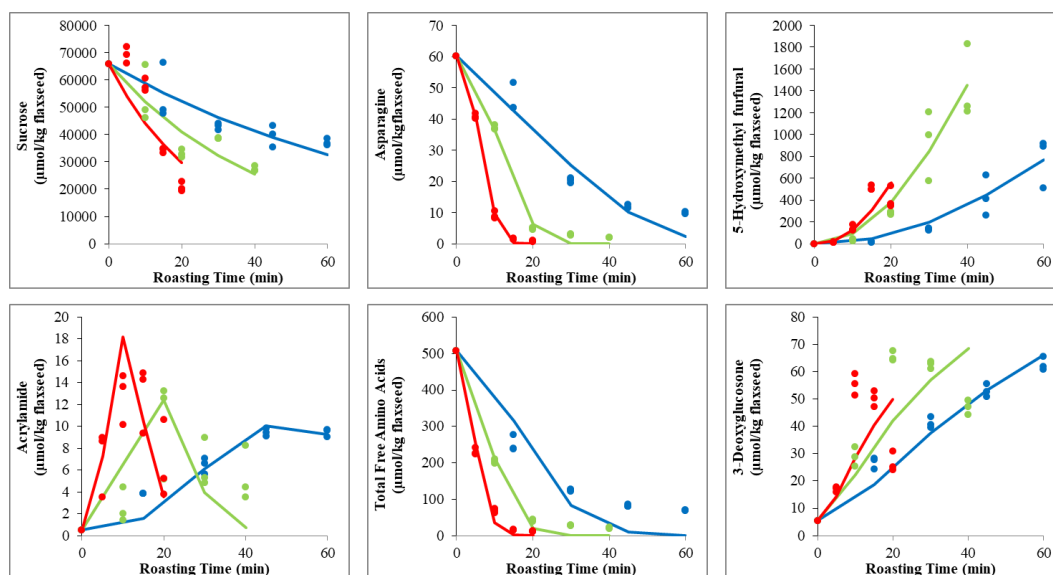
Figure 5. 21 Kinetic model fits (lines) to the obtained experimental data (symbols)of reactants and products during roasting of flaxseed. Blue colour for markers and lines designates 160°C, green 180°C and red 200°C.
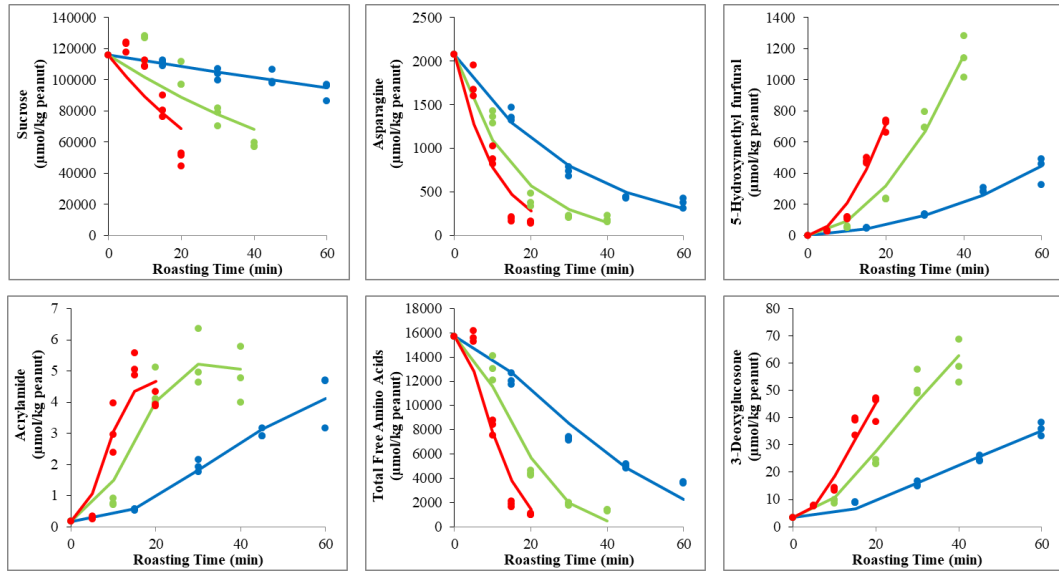
Figure 5. 22 Kinetic model fits (lines) to the obtained experimental data (symbols)of reactants and products during roasting of peanut. Blue colour for markers and lines designates 160°C, green 180°C and red 200°C.
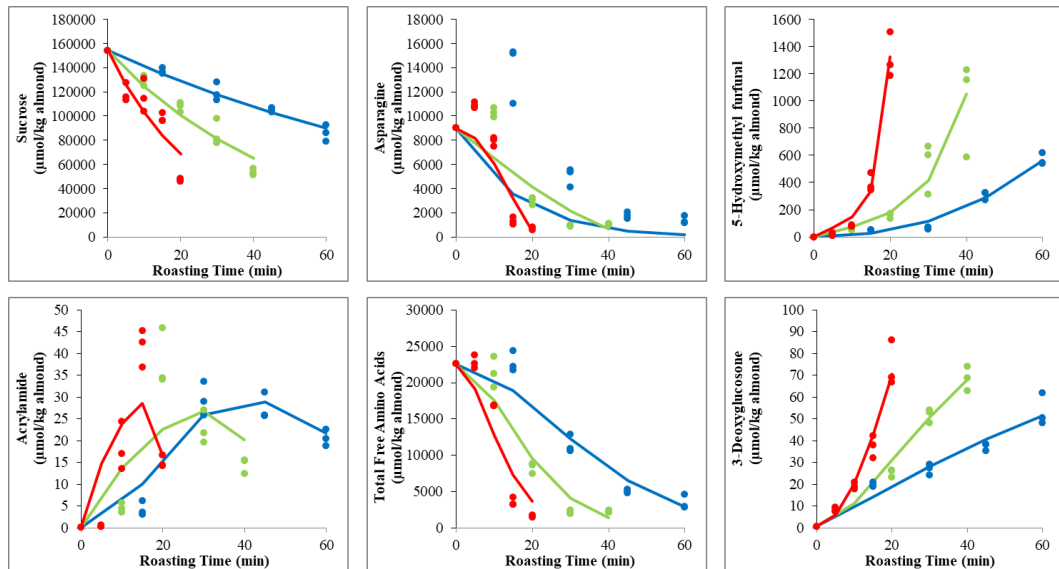
Figure 5. 23 Kinetic model fits (lines) to the obtained experimental data (symbols)of reactants and products during roasting of almond. Blue colour for markers and lines designates 160°C, green 180°C and red 200°C.

Table 5. 3 Estimated reaction rate constants (k, $min^{-1} \times 10^3$) with 95% highest posterior density (HPD) intervals at different temperatures according to the proposed model for acrylamide formation during roasting of samples

Elementary reaction step**		Sunflower Seed			Flaxseed			Peanut			Almond		
		160°C	180°C	200°C	160°C	180°C	200°C	160°C	180°C	200°C	160°C	180°C	200°C
1	SUC → FFC+GLC	10.6±1.38	29.2±6.03	61.9±19.89	11.78±1.8	23.7±4.06	39.9±12.4	3.4±0.47	13.3±3.56	26.2±8.69	9.0±0.64	21.4±2.2	40.4±7.49
2	FFC → HMF	0.7±0.68	0±0	4.7±3.19	0±0	0±0	0±0	1.3±0.66	1.6±0.58	1.9±0.78	0±0	3.0±1.96	14.1±2.82
3	GLC → 3-DG	1.2±0.25	1.4±0.28	0.1±0.02	0.8±0.14	1.7±0.3	1.6±0.48	0.3±0.16	0.2±0.14	0.2±0.17	0.4±0.31	0.1±0.05	0.1±0.01
4	3-DG → HMF	419.4±75.03	939.2±178.7	0±0	370.2±52.55	951.2±189.2	1100.1±342.1	142.6±94.06	118.7±109.2	153.6±184.4	450.2±381.9	108.4±75.6	0±0
5*	HMF + Asn → ACR	16.5±7	8.8±4.48	135.9±180.2	126.3±32.51	677.9±236.2	3514.2±1102	1.6±0.78	5.4±2.99	12.7±11.6	28.1±25.81	138.5±126	572.0±184.4
6*	FFC+AA → P1	1022.1±30710	85.2±129.7	57.9±63.29	5.9±1.94	12.3±2.38	23.6±7.32	8.4±3.57	5.3±2.14	6.6±3.14	1.4±0.33	1.9±0.5	2.6±0.95
7	ACR → P2	424.6±187.3	110.2±71.97	2091.7±2151	44.9±15.15	172.2±60.13	219.0±50.73	41.4±35.1	193.7±144.7	544.4±638.1	132.5±535.4	4605.6±3659	21412.5±5286
8	Asn → P3	30.8±3.29	86.3±9.14	126.2±34.36	20.8±4.86	27.1±10.39	38.5±9.49	31.6±2.01	63.9±9.24	97.1±24.49	65.0±82.67	27.9±21.34	0±0

*Reaction rate constant unit: kg $\mu mol^{-1} min^{-1} \times 10^3$
**SUC sucrose; GLC glucose; FFC fructofuranosyl cation; HMF 5-hydroxymethyl furfural; 3-DG 3-deoxyglucosone; ACR acrylamide; AA total amino acids; P products

Degradation of sucrose

Although sucrose is not a reducing sugar, it indirectly participates in the formation of ACR through forming new carbonyl sources for the Maillard reaction by thermal degradation. In low-moisture systems, sucrose degrades to glucose and FFC through cleavage of the glycosidic bond, and this step was considered the main mechanism for the degradation of sucrose. The formation of FFC from fructose was not included in the comprehensive model since it was reported that this step is difficult to occur (Perez Locas and Yaylayan, 2008). In addition, the interconversion of glucose and fructose through 1,2-enolization is also possible (Martins and Van Boekel, 2005a). However, this step was also excluded from the model in order to decrease the number of parameters and thus increase the precision of the estimation process. The best model fit was obtained and the concentrations of sucrose were well estimated when only degradation of sucrose to glucose and FFC was included in the model. The increase in the roasting temperature caused a substantial increase in the reaction rate constants of sucrose degradation (*k1*) in all roasted samples with relatively higher values in sunflower seeds (Table 5. 3).

Formation of α-dicarbonyl compounds

The α-dicarbonyl compounds that have been reported to be involved in the ACR formation such as 3-DG and MGO were included in the comprehensive model. FFC can react with an amine to form a fructofuranosyl amine, which is rearranged to form a Heyns product. The reaction of glucose with an amine compound followed by rearrangement to a more stable compound Amadori product is also possible. In later stages, the degradation of AP and HP leads to the formation of 3-DG. However, in previous studies, the reaction rate constants of the 3-DG formation step through Amadori or Heyns product were found to be very low or zero which means they were kinetically less important in these circumstances (Berk et al., 2020, Göncüoğlu Taş and Gökmen, 2017, Hamzalıoğlu and Gökmen, 2020). Hence, side reaction steps such as these were not indicated even in the comprehensive model. Apart from these, 3-DG can also be formed through the removal of one molecule of water from glucose in caramelization (Belitz et al., 2009). In this context, the model fits were well estimated in the case of adding only this route (*k3*) for the formation of 3-DG. It was determined that the rate constant of this reaction step (*k3*) was lower in the samples roasted at 200 °C compared to other roasting temperatures. Additionally, it should be considered that

there were deviations in the 3-DG model fits of flaxseed and sunflower seed samples at 180 and 200 °C only in prolonged roasting times.

The predominant short-chain α-dicarbonyl MGO was also included in the comprehensive model as it was stated by Stadler et al. (2004) that MGO may also take part in the formation of ACR. It was reported that one of the possible formation pathways of MGO is from 3-DG via retro-aldolization (Weenen, 1998). However, previous studies reported that more important steps were determined in ACR formation and the MGO pathway was less significant in ACR formation compared to other α-dicarbonyl pathways (Stadler et al., 2004). Besides, MGO formation and elimination steps were included in the comprehensive model, but the model could not fit well with observed data. Therefore, these steps were omitted from the model and a better model fit was obtained.

Formation of HMF

There are generally two formation pathways considered for the formation of HMF: dehydration of FFC (*k2*) and 3-DG (*k4*) (Jadhav et al., 2011). The cyclic form of FFC facilitates its conversion to HMF under dry conditions (Perez Locas and Yaylayan, 2008). HMF is also generated by the removal of 3 molecules of water from glucose through 3-DG (Belitz et al., 2009). These two formation pathways were included in the proposed model.

It was determined that the 3-DG pathway was predominant in HMF formation at 160 and 180 °C. At 200 °C, the FFC pathway (*k2*) became dominant in almonds and sunflower seeds, whereas in others HMF was still formed mainly through 3-DG (*k2*). The reason for the 3-DG pathway to becoming quantitatively less significant in the formation of HMF in almond samples roasted at 200 °C might be attributed to a decrease in the rate of 3-DG formation from GLC. In addition, conversion of FFC to other products (*k6*) was found to be kinetically more important than dehydration of FFC to HMF (*k2*) in all samples except almonds.

However, FFC is known to be an important precursor for HMF, and it should be considered that the lower rate constants of the FFC pathway (*k2*) did not mean that this step is unimportant. FFC plays an important role in explaining the amount of HMF formed. The higher rate constants of the 3-DG pathway (*k4*) might also be associated with the fact that FFC could not be measured experimentally and this multi-step

116

conversion was shown as a single step in the model. These observations were also supported by the findings of (Göncüoğlu Taş and Gökmen, 2017) who reported that the calculated reaction rate constants of HMF formation via FFC were relatively lower than the rate constants of HMF formation via 3-DG. However, they also stated that the model prediction obtained when the FFC pathway was excluded in the same kinetic model was not compatible with the experimental data and therefore the increase in the amount of HMF could not be explained by only the 3-DG pathway. By doing so, they also indicated that the HMF formation step from FFC is crucial, although the rate constant was found to be lower.

Formation of ACR

Asparagine provides the backbone of ACR and the formation of ACR from asparagine can occur by the involvement of various carbonyl compounds. Parker et al. (2012) defined two pathways for the formation of ACR as the specific and generic amino acid pathways. The reaction of asparagine directly with reducing sugar to form ACR was called a specific amino acid route. The generic amino acid route, another possible way for the formation of ACR, is the reaction of asparagine with dicarbonyls/hydroxycarbonyls formed through Amadori products of reducing sugars and α-amino acids. Parker et al. (2012) have also drawn attention to the importance of the contribution of both pathways in ACR formation. According to them, the predominance of the reaction pathways is affected by the composition of the medium and the process parameters. Especially, in the presence of more reactive amino acids than asparagine can be the source of α-amino acids required for the generic amino acid pathway. In addition to these reaction pathways, the formation of ACR as a result of the reaction of FFC with asparagine was also included in the comprehensive model, since it was reported by Perez Locas and Yaylayan (2008) that FFC can react with amines.

Another source of ACR formation was found to be HMF. The role of HMF in the ACR formation mechanism was first described by Gökmen et al. (2012). In this study, it was stated that HMF was more effective than glucose in the formation of ACR from asparagine in low moisture systems. This was explained by the fact that HMF has a lower melting point and is, therefore, more thermodynamically favorable to form amine condensation products. Since HMF is involved in the formation of ACR in this way, FFC also contributes to the formation of ACR in another way by dehydrating to HMF, as well as reacting with asparagine to form ACR as a carbonyl source.

When the involvement of different carbonyl compounds in ACR formation was compared in light of the results obtained in previous studies (Bertuzzi et al., 2020), it was concluded that the most predominant pathway in dry systems was ACR formation in the presence of HMF (Berk et al., 2020, Hamzalıoğlu and Gökmen, 2020, Nguyen et al., 2016a). Indeed, in previous studies and for the comprehensive model mentioned in this study, the reaction rate constants for ACR formation pathways from carbonyl sources other than HMF were calculated as zero or relatively low. In a study by Stadler et al. (2004), the reaction between asparagine and glucose was found kinetically more important than the reaction of asparagine with α-dicarbonyl compounds in ACR formation. Additionally, Nguyen et al. (2016a), in a study investigating the effect of sugar type on ACR formation in biscuits, determined that the effect of glucose was negligible when compared to fructose. Similar results to model systems were also obtained in the food matrix. Hamzalıoğlu and Gökmen (2020) calculated the reaction rate constants of ACR formation from FFC and glucose as zero during the roasting process of coffee. In another study, Berk et al. (2020) found that the reaction of asparagine with HMF was more important than with glucose. To sum up, since the aim was to determine a simple model, only the involvement of HMF (*k5*) was included and the other carbonyl sources were excluded in the proposed model for the conversion of asparagine to ACR. In the proposed kinetic model considered in this way, it was observed that the model was well fitted to the experimental data. It can be concluded that the pathway comprising HMF is kinetically important in the formation of ACR through Maillard reaction during roasting process in dry systems with low reducing sugar content but with a significant amount of sucrose.

When the rate constants of the ACR formation were examined, it was seen that the estimated parameters increased with increasing temperature. However, the highest rate constant was determined in the flaxseed samples as a result of roasting at 200 °C. ACR can also undergo further reactions with amino acids which are called Michael type additions (Friedman and Levin, 2008). However, unimolecular degradation without the involvement of amino acids fitted better to experimental data instead of the bimolecular reaction of ACR for the elimination of degradation into products (*k7*). According to the results, the reaction rate constant of this step increased with temperature in the samples as in the case of formation reaction except for sunflower, while the highest rate constant was observed in almonds. Additionally, except in a flaxseed sample, this elimination

step was found to be more important than the formation rate of ACR (Table 5. 3). (Knol et al., 2005) also proposed a kinetic model that suggests ACR is an intermediate not an end-product of the Maillard reaction and undergoes further degradation reactions.

It has been shown in different studies that asparagine can also degrade to products such as aspartic acid and fumaric acid during roasting (De Vleeschouwer et al., 2009). The decomposition of asparagine to several products was also indicated in the model ($k8$) to obtain the best model fit and k8 increased with increasing temperature in all samples except almond.

6. GENERAL CONCLUSION AND DISCUSSION

Maillard reaction and caramelization are a series of complex reactions that take place during roasting and their outcomes contribute to the formation of desirable characteristics of the food products such as brown color, taste, flavor, and antioxidant properties. On the other hand, these reactions can be responsible for the loss of the nutritional value of proteins. The thermal process can also cause potentially adverse health effects by promoting the formation of potentially toxic or carcinogenic components. The characteristic consequences of these reactions are extremely dependent on the reactants as much as reaction conditions such as pH, temperature, and moisture content.

This study aimed to reveal a kinetic model for the Maillard reaction -caramelization during roasting of low-moisture foods by considering these kinds of foods as sugar-limited lipid-rich reaction pools and with the available amount of amino acids and sucrose, independently of the product type. Therefore, sunflower seed (*Helianthus annuus L.*), pumpkin seed (*Cucurbita moschata L.*), flaxseed (*Linum usitatissimum L.*), peanut (*Arachis hypogaea L.*), and almond (*Prunus dulcis*) were studied due to their similar compositions with minor differences to represent such a reactant pool. The reaction mechanism and interrelation between reactants and products were tried to be enlightened by using the multiresponse kinetic modeling approach.

It was observed that the predominant sugar in the studied samples was sucrose and it gradually decreased with the roasting process. Amino acids also decreased with roasting and the highest decrease was determined in flaxseed and sunflower seed. Depending on the decrease in sugar, an overall increasing trend was observed in the amount of HMF. While the highest amount of furosine was measured in pumpkin seed, no detectable amount of furosine was found in raw almonds. Among the α-dicarbonyl compounds, 3-DG and MGO were determined to be the most dominant α-dicarbonyls. CEL and CML concentrations showed similar trends during roasting. However, CEL concentration was higher than CML because of the higher formation rate of MGO and faster reaction with protein-bound lysine. The highest ACR concentration was measured in almonds due to the high amount of free asparagine. The Maillard reaction also triggered the formation of colored compounds. While the L* value decreased with the roasting process, an

increase was observed in the a* value. While b* value increased in temperate roasting parameters, it started to decrease in harsh conditions.

In this thesis, the roasting process was also carried out with extreme parameters in order to reveal a kinetic model. In the commercial roasting process, such high temperatures are not reached and these products are generally roasted at temperatures between 140-180 °C. Formation of thermal process contaminants are induced even with these commercial roasting parameters. The importance of the effect of these roasted foods on the daily intake of heat induced compounds should be taken into account. Considering the daily consumption amounts of nuts (30 g), the highest HMF intake is from sunflower (7.4 mg/day). It was found that HMF formation remained at much lower levels in pumpkin seeds, while roasting conditions were very important in almonds and peanuts, and the amount of HMF formed by roasting at 160 °C remained within safer limits. In sunflower seeds and flaxseeds, the amount of HMF increased significantly even at 160 °C. Although the safe consumption amount of HMF is not clear, it is estimated that people ingest up to 150 mg of HMF per day through various foods. However, while making these evaluations, it should be taken into account that HMF is not only taken from these foods. Furosine is another compound arised during thermal processing and its exposure can induce of DNA damage. Additionally, furosine content is an index of dietary intake of AGEs and protein damage from heat treatment. Since furosine is a marker of lysine reaction products that are not nutritionally available, such as the Amadori product, the bioavailability of lysine can also be measured via furosine content. While furosine started to degrade at high temperature within long roasting times, the concentration of furosine in sunflower seeds and almonds reaches up to 90 mg/kg sample in short roasting times. Furosine content of pumpkinseed was found as comparably lower than the others due to rapid degradation of furosine triggered by roasting. Therefore, roasting parameters become important in terms of furosine formation. The ACR content of roasted products is also important since it is specified as a probable human carcinogen. As the roasting progressed, the increasing ACR concentration in all samples started to decrease after reaching its maximum value. This is due to the key role of precursors in the formation of ACR, and therefore elimination reactions became dominant in the absence of asparagine. Due to the high asparagine content, the highest ACR content (3127±131 µg/kg) was detected in almonds, while the low asparagine content caused the ACR content to remain at lower levels in pumpkin

seed. Although peanut contains approximately the same amount of asparagine as sunflower, the concentration of ACR in peanut remained at more low levels compared to sunflower. It was found that the ACR content in flaxseed, sunflower, and especially almond, was significantly higher when compared to many ACR-rich foods such as French fries or potato crisps (300-2300 µg/kg). Even if ACR started to degrade in almonds during long roasting times, its levels were found to be still above 1000 µg/kg. AGEs also have potential health risks as they can promote oxidative stress and inflammation and are linked to many multiple chronic diseases. It was determined that the amount of CML and CEL in the roasted samples did not exceed 45mg/kg and 250 mg/kg, respectively. When a general evaluation is made in terms of the formation of thermal process contaminants, roasting at 160 °C until the desired color and texture is obtained provides more acceptable results than the one done at higher temperatures. However, it should be noted that these foods contribute to the daily intake of AGEs, but they are only a small part of the diet and these contaminants can also be obtained from other foods.

Since the presence of water affects the progress of chemical reactions, it is not appropriate to explain the reaction mechanism in dry systems with the mechanisms put forward for aqueous systems. In addition to pH and water activity, because the kinetics of Maillard reaction products were also affected by the diversity and amount of the reactants, a classification including all these factors for nuts and seeds was performed before modeling studies. This approach allowed us to classify nuts and seeds according to their compositional characteristics, which was more critical for chemical reactions, instead of their botanical nomenclature. Therefore, sunflower, flaxseed, peanut, and almond clustered together by PCA as one group whereas pumpkin seed was classified as a separate group which arose the need for two different proposed mechanistic models for Maillard reaction and caramelization.According to the proposed model for Maillard reaction, the results obtained for all samples were as follows: the formation of HMF through 3-DG was found to be quantitatively important; sugar degradation was more predominant than Maillard reaction in the formation of 3-DG; 1-DG showed a tendency to degradation to MGO rather than DMG; FL oxidation was mainly responsible for CML formation whereas CEL was formed dominantly from the reaction of MGO with lysine residue. In pumpkin seed, as distinct from this model, it was determined that the conversion of AP and HP into α-dicarbonyl compounds was also important, and hence

steps of GO formation from FL and 1-DG formation from HP were not excluded in the proposed model. Although two different models were obtained, the similarity between the dominant paths was also remarkable due to similarities in their compositional characteristics.

In this study, a simplified kinetic model was also proposed for the formation of ACR during roasting in low-moisture systems. The rate constants for elementary reaction steps were estimated by multiresponse kinetic modeling of sucrose, total free amino acids, asparagine, HMF, 3-DG, and ACR concentrations in sunflower seed, flaxseed, peanut, and almond roasted at 160, 180, and 200 °C. Although the proposed model does not exactly express the whole Maillard reaction mechanism, it explains the measured responses related to the formation of ACR in nuts and seeds during roasting. The model that best fitted the experimental data was determined by model discrimination.

The proposed model consisted of reaction steps including sucrose degradation, formation of α-dicarbonyl compounds, HMF, and ACR. The conversion of free asparagine, FFC, and ACR to different products was also included in the proposed model whereas the further conversions of glucose, 3-DG, and HMF were excluded. The contribution of HMF was demonstrated to the formation of ACR in the roasting process of low moisture food systems. Due to its low melting temperature, HMF is a thermodynamically more favorable reactant in the formation of ACR during roasting of low moisture food systems. Since we aimed at obtaining a simple and inclusive model in this study, we firstly proposed a reaction scheme by eliminating the pathways that were determined not to be kinetically important for the formation of ACR in our previous studies. The model may help optimize the roasting process for the mitigation of ACR formation in nuts and seeds.

The proposed models gave insight into the whole reaction network and the complex mechanism of Maillard reaction and caramelization reactions in real foods according to their compositional classification. The roasting of nuts and seeds was explained in this manner and the dominant pathways were also revealed. These models might also enable us to develop mitigation strategies for controlling the formation of thermal contaminants such as ACR during the thermal processing of roasted nuts and seeds by developing optimal thermal processing conditions. Further studies could enlighten the details of the proposed mechanism by measuring and incorporating more intermediate and advanced reaction products into the model to improve the accuracy of the proposed model. It

should also be mentioned that consideration of the classification of food products according to their Maillard reaction and caramelization reactants could be a necessary approach before further modeling studies.

7. REFERENCES

AGILA, A. & BARRINGER, S. 2012. Effect of roasting conditions on color and volatile profile including HMF level in sweet almonds (Prunus dulcis). *J Food Sci,* 77**,** C461-8.

AHMED, M. U., THORPE, S. R. & BAYNES, J. W. 1986. Identification of N(ε)-carboxymethyllysine as a degradation product of fructoselysine in glycated protein. *The Journal of Biological Chemistry,* 261**,** 4889-4894.

AKILLIOĞLU, H. G. & GÖKMEN, V. 2014. Effects of hydrophobic and ionic interactions on glycation of casein during Maillard reaction. *J Agric Food Chem,* 62**,** 11289-95.

AMADORI, M. 1929. The condensation product of glucose and p-anisidine. *Atti della Accademia Nazionale dei Lincei,* 9**,** 226-230.

AMES, J. M. 1992. The Maillard Reaction. *In:* HUDSON, B. J. F. (ed.) *Biochemistry of Food Proteins.* Boston, MA: Springer US.

AMREIN, T., LUKAC, H., ANDRES, L., PERREN, R., ESCHER, F. & AMADÒ, R. 2005a. *Acrylamide in Roasted Almonds and Hazelnuts.*

AMREIN, T. M., ANDRES, L., SCHÖNBÄCHLER, B., CONDE-PETIT, B., ESCHER, F. & AMADÒ, R. 2005b. Acrylamide in almond products. *European Food Research and Technology,* 221**,** 14-18.

ANESE, M. 2016. Chapter 9 - Acrylamide in Coffee and Coffee Substitutes. *In:* GÖKMEN, V. (ed.) *Acrylamide in Food.* Academic Press.

AOAC 1990. Official methods of analysis of the association of official analytical chemists.

ARRIBAS-LORENZO, G. & MORALES, F. J. 2010. Analysis, Distribution, and Dietary Exposure of Glyoxal and Methylglyoxal in Cookies and Their Relationship with Other Heat-Induced Contaminants. *Journal of Agricultural and Food Chemistry,* 58**,** 2966-2972.

ARYA, S. S., SALVE, A. R. & CHAUHAN, S. 2016. Peanuts as functional food: a review. *J Food Sci Technol,* 53**,** 31-41.

ATAÇ MOGOL, B. 2014. *Mitigation of Thermal Process Contaminants by Alternative Technologies.* Hacettepe University.

ATAÇ MOGOL, B. & GÖKMEN, V. 2014. Computer vision-based analysis of foods: A non-destructive color measurement tool to monitor quality and safety. *Journal of the science of food and agriculture,* 94.

BAGHERI, H., KASHANINEJAD, M., ZIAIIFAR, A. M. & AALAMI, M. 2016. Novel hybridized infrared-hot air method for roasting of peanut kernels. *Innovative Food Science & Emerging Technologies,* 37**,** 106-114.

BAKER, G. L., CORNELL, J. A., GORBET, D. W., O'KEEFE, S., SIMS, C. A. & TALCOTT, S. 2006. Determination of Pyrazine and Flavor Variations in Peanut Genotypes During Roasting. *Journal of Food Science,* 68**,** 394-400.

BALTES, W. 1982. Chemical changes in food by the maillard reaction. *Food Chemistry* 9**,** 59-73.

BATOOL, Z., XU, D., WU, M., JIAO, W., ROOBAB, U., WENG, L., ZHANG, X., LI, X., LIANG, Y., LI, B. & LI, L. 2020a. Determination of α-dicarbonyl compounds and 5-hydroxymethylfurfural in commercially available preserved dried fruits and edible seeds by optimized UHPLC–HR/MS and GC–TQ/MS. *Journal of Food Processing and Preservation,* 44.

BEKHIT, A. E.-D. A., SHAVANDI, A., JODJAJA, T., BIRCH, J., TEH, S., MOHAMED AHMED, I. A., AL-JUHAIMI, F. Y., SAEEDI, P. & BEKHIT, A. A. 2018. Flaxseed: Composition, detoxification, utilization, and opportunities. *Biocatalysis and Agricultural Biotechnology,* 13**,** 129-152.

BELITZ, H.-D., GROSCH, W. & SCHIEBERLE, P. 2009. *Food Chemistry*, Springer-Verlag Berlin Heidelberg.

BERK, E., AKTAĞ, I. G. & GÖKMEN, V. 2021. Formation of α-dicarbonyl compounds and glycation products in sesame (Sesamum indicum L.) seeds during roasting: a multiresponse kinetic modelling approach. *European Food Research and Technology,* 247**,** 2285-2298.

BERK, E., HAMZALIOĞLU, A. & GÖKMEN, V. 2019. Investigations on the Maillard Reaction in Sesame (Sesamum indicum L.) Seeds Induced by Roasting. *J Agric Food Chem,* 67**,** 4923-4930.

BERK, E., HAMZALIOĞLU, A. & GÖKMEN, V. 2020. Multiresponse kinetic modelling of 5-hydroxymethylfurfural and acrylamide formation in sesame (Sesamum indicum L.) seeds during roasting. *European Food Research and Technology,* 246**,** 2399-2410.

BERTUZZI, T., MARTINELLI, E., MULAZZI, A. & RASTELLI, S. 2020. Acrylamide determination during an industrial roasting process of coffee and the influence of asparagine and low molecular weight sugars. *Food Chem,* 303**,** 125372.

BOLLING, B. W., BLUMBERG, J. B. & CHEN, C. O. 2010. The influence of roasting, pasteurisation, and storage on the polyphenol content and antioxidant capacity of California almond skins. *Food Chem,* 123**,** 1040-1047.

BOZAN, B. & TEMELLI, F. 2008. Chemical composition and oxidative stability of flax, safflower and poppy seed and seed oils. *Bioresour Technol,* 99**,** 6354-9.

BRANDS, C. M. J. & VAN BOEKEL, M. 2002. Kinetic modeling of reactions in heated monosaccharide-casein systems. *Journal of Agricultural and Food Chemistry,* 50**,** 6725-6739.

BRANDS, C. M. J. & VAN BOEKEL, M. A. J. S. 2001. Reactions of Monosaccharides during Heating of Sugar−Casein Systems Building of a Reaction Network Model. *J. Agric. Food Chem.,* 49**,** 4667−4675.

BRANDS, C. M. J. & VAN BOEKEL, M. A. J. S. 2003. Kinetic modelling of reactions in heated disaccharide–casein systems. *Food Chemistry,* 83**,** 13–26.

CÄMMERER, B., JALYSCHKO, W. & KROH, L. W. 2002. Intact Carbohydrate Structures as Part of the Melanoidin Skeleton. *Journal of Agricultural and Food Chemistry,* 50**,** 2083-2087.

CÄMMERER, B. & KROH, L. W. 2009. Shelf life of linseeds and peanuts in relation to roasting. *LWT - Food Science and Technology,* 42**,** 545-549.

CAPUANO, E. & FOGLIANO, V. 2011. Acrylamide and 5-hydroxymethylfurfural (HMF): A review on metabolism, toxicity, occurrence in food and mitigation strategies. *LWT - Food Science and Technology,* 44**,** 793-810.

CHARISSOU, A., AIT-AMEUR, L. & BIRLOUEZ-ARAGON, I. 2007. Evaluation of a gas chromatography/mass spectrometry method for the quantification of carboxymethyllysine in food samples. *J Chromatogr A,* 1140**,** 189-94.

CHO, H. & LEE, K.-G. 2014. Formation and Reduction of Furan in Maillard Reaction Model Systems Consisting of Various Sugars/Amino Acids/Furan Precursors. *Journal of Agricultural and Food Chemistry,* 62**,** 5978-5982.

CHUNG, K. H., SHIN, K. O., HWANG, H. J. & CHOI, K. S. 2013. Chemical composition of nuts and seeds sold in Korea. *Nutr Res Pract,* 7**,** 82-8.

CREMER, D. R., VOLLENBROEKER, M. & EICHNER, K. 2000. Investigation of the formation of Strecker aldehydes from the reaction of Amadori rearrangement products with a-amino acids in low moisture model systems. *European Food Research and Technology,* 211**,** 400–403.

DAGLIA, M., PAPETTI, A., ACETI, C., SORDELLI, B., SPINI, V. & GAZZANI, G. 2007. Isolation and Determination of α-Dicarbonyl Compounds by RP-HPLC-DAD in Green and Roasted Coffee. *Journal of Agricultural and Food Chemistry,* 55**,** 8877-8882.

DAMAME, S. V., CHAVAN, J. K. & KADAM, S. S. 1990. Effects of roasting and storage on proteins and oil in peanut kernels. *Plant Foods Hum Nutr,* 40**,** 143-8.

DE PAOLA, E. L., MONTEVECCHI, G., MASINO, F., GARBINI, D., BARBANERA, M. & ANTONELLI, A. 2017. Determination of acrylamide in dried fruits and edible seeds using QuEChERS extraction and LC separation with MS detection. *Food Chem,* 217**,** 191-195.

DE VLEESCHOUWER, K., PLANCKEN, I. V. D., LOEY, A. V. & HENDRICKX, M. E. 2009. Role of precursors on the kinetics of acrylamide formation and elimination under low moisture conditions using a multiresponse approach – Part I: Effect of the type of sugar. *Food Chemistry,* 114**,** 116-126.

DEGEN, J., HELLWIG, M. & HENLE, T. 2012. 1,2-dicarbonyl compounds in commonly consumed foods. *J Agric Food Chem,* 60**,** 7071-9.

DURMAZ, G. & GÖKMEN, V. 2010. Impacts of roasting oily seeds and nuts on their extracted oils. *Lipid Technology,* 22**,** 179-182.

EFSA 2005. Opinion of the Scientific Panel on Food Additives, Flavourings, Processing Aids and Materials in contact with Food (AFC) on a request from the Commission related to Flavouring Group Evaluation 13: Furfuryl and furan derivatives with and without additional side-chain substituents and heteroatoms from chemical group 14. *The EFSA Journal,* 215**,** 1-73.

EITENMILLER, R., CHOI, S. & CHUN, J. 2011. Effects of Dry Roasting on the Vitamin E Content and Microstructure of Peanut (Arachis hypogaea). *Journal of Agriculture & Life Science,* 45(4)**,** 121-133.

ERBERSDOBLER, H. F. & SOMOZA, V. 2007. Forty years of furosine – Forty years of using Maillard reaction products as indicators of the nutritional quality of foods. 51**,** 423-430.

FALLICO, B., ARENA, E. & ZAPPALÀ, M. 2003. Roasting of hazelnuts. Role of oil in color development and hydroxymethylfurfural formation. *Food Chemistry,* 81**,** 569-573.

FAO 2018. FAOSTAT database collections. In Food and Agriculture Organization of the United Nations: Rome, 2020.

FENG, D., SHEN, Y. & CHAVEZ, E. R. 2003. Effectiveness of different processing methods in reducing hydrogen cyanide content of flaxseed. *Journal of the Science of Food and Agriculture,* 83**,** 836-841.

FRIEDMAN, M. & LEVIN, C. E. 2008. Review of Methods for the Reduction of Dietary Content and Toxicity of Acrylamide. *Journal of Agricultural and Food Chemistry,* 56**,** 6113-6140.

FU, M., REQUENA, J., JENKINS, A., LYONS, T., BAYNES, J. & THORPE, S. 1996. The advanced glycation end product, N-epsilon-(carboxymethyl)lysine, is a product of both lipid peroxidation and glycoxidation reactions. *The Journal of Biological Chemistry,* 271 9982–9986.

FUJIOKA, K. & SHIBAMOTO, T. 2004. Formation of genotoxic dicarbonyl compounds in dietary. *Lipids, ,* 39**,** 481-486.

GENSBERGER, S., MITTELMAIER, S., GLOMB, M. A. & PISCHETSRIEDER, M. 2012. Identification and quantification of six major α-dicarbonyl process

contaminants in high-fructose corn syrup. *Analytical and Bioanalytical Chemistry,* 403**,** 2923-2931.

GLEW, R. H., GLEW, R. S., CHUANG, L. T., HUANG, Y. S., MILLSON, M., CONSTANS, D. & VANDERJAGT, D. J. 2006. Amino acid, mineral and fatty acid content of pumpkin seeds (Cucurbita spp) and Cyperus esculentus nuts in the Republic of Niger. *Plant Foods Hum Nutr,* 61**,** 51-6.

GOBERT, J. & GLOMB, M. A. 2009. Degradation of glucose: reinvestigation of reactive alpha-Dicarbonyl compounds. *J Agric Food Chem,* 57**,** 8591-7.

GÖKMEN, V. 2015. *Acrylamide in Food: Analysis, Content and Potential Health Effects*, Academic Press.

GÖKMEN, V., KOCADAĞLI, T., GÖNCÜOĞLU, N. & MOGOL, B. A. 2012. Model studies on the role of 5-hydroxymethyl-2-furfural in acrylamide formation from asparagine. *Food Chem,* 132**,** 168-74.

GÖKMEN, V. & ŞENYUVA, H. Z. 2006. Improved Method for the Determination of Hydroxymethylfurfural in Baby Foods Using Liquid Chromatography−Mass Spectrometry. *Journal of Agricultural and Food Chemistry,* 54**,** 2845-2849.

GÖKMEN, V., SERPEN, A., AÇAR, Ö. Ç. & MORALES, F. J. 2008. Significance of furosine as heat-induced marker in cookies. *Journal of Cereal Science,* 48**,** 843-847.

GÖNCÜOĞLU TAŞ, N. 2017. *Investigation of Chemical Reactions in Hazelnut Induced by Roasting* Hacettepe University.

GÖNCÜOĞLU TAŞ, N. & GÖKMEN, V. 2016. Effect of alkalization on the Maillard reaction products formed in cocoa during roasting. *Food Research International,* 89**,** 930-936.

GÖNCÜOĞLU TAŞ, N. & GÖKMEN, V. 2017. Maillard reaction and caramelization during hazelnut roasting: A multiresponse kinetic study. *Food Chem,* 221**,** 1911-1922.

GÖNCÜOĞLU TAŞ, N. & GÖKMEN, V. 2019. Effect of Roasting and Storage on the Formation of Maillard Reaction and Sugar Degradation Products in Hazelnuts (Corylus avellana L.). *J Agric Food Chem,* 67**,** 415-424.

GUO, S., GE, Y. & NA JOM, K. 2017. A review of phytochemistry, metabolite changes, and medicinal uses of the common sunflower seed and sprouts (Helianthus annuus L.). *Chem Cent J,* 11**,** 95.

HAMZALıOĞLU, A. & GÖKMEN, V. 2020. 5-Hydroxymethylfurfural accumulation plays a critical role on acrylamide formation in coffee during roasting as confirmed by multiresponse kinetic modelling. *Food Chem,* 318**,** 126467.

HAYASHI, T. & NAMKI, M. 1980. Formation of Two-Carbon Sugar Fragment at an Early Stage of the Browning Reaction of Sugar with Amine. *Agricultural and Biological Chemistry,* 44**,** 2575-2580.

HEMMLER, D., ROULLIER-GALL, C., MARSHALL, J. W., RYCHLIK, M., TAYLOR, A. J. & SCHMITT-KOPPLIN, P. 2018. Insights into the Chemistry of Non-Enzymatic Browning Reactions in Different Ribose-Amino Acid Model Systems. *Scientific Reports,* 8**,** 16879.

HENLE, T. 2005. Protein-bound advanced glycation endproducts (AGEs) as bioactive amino acid derivatives in foods. *Amino Acids,* 29**,** 313-22.

HENLE, T., ZEHETNER, G. & KLOSTERMEYER, H. 1995. Fast and sensitive determination of furosine. *Zeitschrift für Lebensmittel-Untersuchung und Forschung,* 200**,** 235-237.

HEYNS, K. & MEINECKE, K. H. 1953. The formation and preparation of D-glucosamine from fructose and ammonia. *Chemische Berichte,* 86**,** 1453-1562.

HIRSCH, J., MOSSINE, V. V. & FEATHER, M. S. 1995. The detection of some dicarbonyl intermediates arising from the degradation of Amadori compounds (the Maillard reaction). *Carbohydrate Research,* 273**,** 171-177.

HODGE, J. E. 1953. Dehydrated Foods, Chemistry of Browning Reactions in Model Systems. *Journal of Agricultural and Food Chemistry,* 1**,** 928-943.

HOFMANN, T., BORS, W. & STETTMAIER, K. 1999. Studies on Radical Intermediates in the Early Stage of the Nonenzymatic Browning Reaction of Carbohydrates and Amino Acids. *Journal of Agricultural and Food Chemistry,* 47, **,** 379−390.

HOLLNAGEL, A. & KROH, L. W. 1998. Formation of α-dicarbonyl fragments from mono- and disaccharides under caramelization and Maillard reaction conditions. *Zeitschrift für Lebensmitteluntersuchung und -Forschung A,* 207**,** 50-54.

HULL, G. L. J., WOODSIDE, J. V., AMES, J. M. & CUSKELLY, G. J. 2012. Nε-(carboxymethyl)lysine content of foods commonly consumed in a Western style diet. *Food Chemistry,* 131**,** 170-174.

HYVÄRINEN, H. K., PIHLAVA, J.-M., HIIDENHOVI, J. A., HIETANIEMI, V., KORHONEN, H. J. T. & RYHÄNEN, E.-L. 2006. Effect of Processing and Storage on the Stability of Flaxseed Lignan Added to Bakery Products. *Journal of Agricultural and Food Chemistry,* 54**,** 48-53.

IARC 1994. Acrylamide. In IARC Monographs on the Evaluation of the Carcinogenic Risk of Chemicals to Humans. Lyon, France: International Agency for Research on Cancer.

IARC 1995. IARC Monographs, International Agency for Research on Cancer (IARC).

IDRUS, N. F. M. & YANG, T. A. 2012. Comparison between Roasting by Superheated Steam and by Convection on Changes in Color, Texture and Microstructure of Peanut (*Arachis hypogaea*). *Food Science and Technology Research,* 18**,** 515-524.

JADHAV, H., PEDERSEN, C. M., SOLLING, T. & BOLS, M. 2011. 3-Deoxy-glucosone is an intermediate in the formation of furfurals from D-glucose. *ChemSusChem,* 4**,** 1049-51.

JAGERSTAD, M. & SKOG, K. 2005. Genotoxicity of heat-processed foods. *Mutat Res,* 574**,** 156-72.

KALOGEROPOULOS, N., CHIOU, A., IOANNOU, M. S. & KARATHANOS, V. T. 2013. Nutritional evaluation and health promoting activities of nuts and seeds cultivated in Greece. *Int J Food Sci Nutr,* 64**,** 757-67.

KIM, H.-J. & RICHARDSON, M. 1992. Determination of 5-hydroxymethylfurfural by ion-exclusion chromatography with UV detection. *Journal of Chromatography A,* 593**,** 153-156.

KIM, J. S. & LEE, Y. S. 2009. Enolization and racemization reactions of glucose and fructose on heating with amino-acid enantiomers and the formation of melanoidins as a result of the Maillard reaction. *Amino Acids,* 36**,** 465-74.

KNOL, J. J., LINSSEN, J. P. H. & VAN BOEKEL, M. A. J. S. 2010. Unravelling the kinetics of the formation of acrylamide in the Maillard reaction of fructose and asparagine by multiresponse modelling. *Food Chemistry,* 120**,** 1047-1057.

KNOL, J. J., VAN LOON, W. A. M., LINSSEN, J. P. H., RUCK, A.-L., VAN BOEKEL, M. A. J. S. & VORAGEN, A. G. J. 2005. Toward a Kinetic Model for Acrylamide Formation in a Glucose−Asparagine Reaction System. *Journal of Agricultural and Food Chemistry,* 53**,** 6133-6139.

KOCADAĞLI, T. & GÖKMEN, V. 2014. Investigation of alpha-dicarbonyl compounds in baby foods by high-performance liquid chromatography coupled with electrospray ionization mass spectrometry. *J Agric Food Chem,* 62**,** 7714-20.

KOCADAĞLI, T. & GÖKMEN, V. 2016. Multiresponse kinetic modelling of Maillard reaction and caramelisation in a heated glucose/wheat flour system. *Food Chem,* 211**,** 892-902.

KOCADAĞLI, T., GÖNCÜOĞLU, N., HAMZALIOĞLU, A. & GÖKMEN, V. 2012. In depth study of acrylamide formation in coffee during roasting: role of sucrose decomposition and lipid oxidation. *Food & Function,* 3.

KONG, F. & SINGH, R. P. 2009. Digestion of Raw and Roasted Almonds in Simulated Gastric Environment. *Food Biophysics,* 4**,** 365-377.

KROH, L. W. 1994. Caramelisation in food and beverages. *Food Chemistry,* 51**,** 373-379.

LIANG, Z., LI, L., QI, H., ZHANG, Z. X. & LI, B. 2016. Kinetic Study on Peptide-Bound Pyrraline Formation and Elimination in the Maillard Reaction Using Single- and Multiple-Response Models. *J Food Sci,* 81**,** C2405-C2424.

LIN, J. T., LIU, S. C., HU, C. C., SHYU, Y. S., HSU, C. Y. & YANG, D. J. 2016. Effects of roasting temperature and duration on fatty acid composition, phenolic

composition, Maillard reaction degree and antioxidant attribute of almond (Prunus dulcis) kernel. *Food Chem,* 190**,** 520-528.

LINDEN, T., COHEN, A., DEPPISCH, R., KJELLSTRAND, P. & WIESLANDER, A. 2002. 3,4-Dideoxyglucosone-3-ene (3,4-DGE): a cytotoxic glucose degradation product in fluids for peritoneal dialysis. *Kidney Int,* 62**,** 697-703.

LIU, X., JIN, Q., LIU, Y., HUANG, J., WANG, X., MAO, W. & WANG, S. 2011. Changes in volatile compounds of peanut oil during the roasting process for production of aromatic roasted peanut oil. *J Food Sci,* 76**,** C404-12.

LUEVANO-CONTRERAS, C. & CHAPMAN-NOVAKOFSKI, K. 2010. Dietary advanced glycation end products and aging. *Nutrients,* 2**,** 1247-65.

LUNING, P. & SANNY, M. 2016. Chapter 8 - Acrylamide in Fried Potato Products. *In:* GÖKMEN, V. (ed.) *Acrylamide in Food.* Academic Press.

LYKOMITROS, D., FOGLIANO, V. & CAPUANO, E. 2016. Flavor of roasted peanuts (Arachis hypogaea) - Part II: Correlation of volatile compounds to sensory characteristics. *Food Res Int,* 89**,** 870-881.

MAGA, J. A. & KATZ, I. 1979. Furans in foods. *C R C Critical Reviews in Food Science and Nutrition,* 11**,** 355-400.

MAILLARD, L. 1912. Action des acides amines sur les sucres : formation des melanoidines par voie methodique. *Comptes Rendus Chimie,* 154**,** 66-68.

MANZOCCO, L., CALLIGARIS, S., MASTROCOLA, D., NICOLI, M. C. & LERICI, C. R. 2000. Review of non-enzymatic browning and antioxidant capacity in processed foods. *Trends in Food Science & Technology,* 11**,** 340-346.

MARTINS, S. I. F. S., JONGEN, W. M. F. & VAN BOEKEL, M. A. J. S. 2000. A review of Maillard reaction in food and implications to kinetic modelling. *Trends in Food Science & Technology,* 11**,** 364-373.

MARTINS, S. I. F. S., MARCELIS, A. T. M. & VAN BOEKEL, M. A. J. S. 2003. Kinetic modelling of Amadori N-(1-deoxy-d-fructos-1-yl)-glycine degradation pathways. Part I—Reaction mechanism. *Carbohydrate Research,* 338**,** 1651-1663.

MARTINS, S. I. F. S. & VAN BOEKEL, M. A. J. S. 2003. Kinetic modelling of Amadori N-(1-deoxy-d-fructos-1-yl)-glycine degradation pathways. Part II—Kinetic analysis. *Carbohydrate Research,* 338**,** 1665-1678.

MARTINS, S. I. F. S. & VAN BOEKEL, M. A. J. S. 2005a. A kinetic model for the glucose/glycine Maillard reaction pathways. *Food Chemistry,* 90**,** 257-269.

MARTINS, S. I. F. S. & VAN BOEKEL, M. A. J. S. 2005b. Kinetics of the glucose/glycine Maillard reaction pathways: influences of pH and reactant initial concentrations. *Food Chemistry,* 92**,** 437-448.

MESIAS, M. & MORALES, F. J. 2016. Chapter 7 - Acrylamide in Bakery Products. *In:* GÖKMEN, V. (ed.) *Acrylamide in Food.* Academic Press.

MILLS, C., MOTTRAM, D. S. & WEDZICHA, B. L. 2008. Acrylamide. *Process-Induced Food Toxicants*, 21-50.

MORALES, F. J. 2008. Hydroxymethylfurfural (HMF) and Related Compounds. *Process-Induced Food Toxicants*, 135-174.

MOTRAM, D. S., WEDZICHA, B. L. & DODSON, A. T. 2002. Acrylamide is formed in the Maillard reaction. *Nature,* 419**,** 448-449.

MUCCI L.A., WILSON K.M. 2008 Acrylamide intake through diet and human cancer risk. *J Agric Food Chem.* 13;56(15):6013-9.

MUELLER, K., EISNER, P., YOSHIE-STARK, Y., NAKADA, R. & KIRCHHOFF, E. 2010. Functional properties and chemical composition of fractionated brown and yellow linseed meal (Linum usitatissimum L.). *Journal of Food Engineering,* 98**,** 453-460.

NAMIKI, M. 1988. Chemistry of Maillard Reactions: Recent Studies on the Browning Reaction Mechanism and the Development of Antioxidants and Mutagens.

NEMATOLLAHI, A., KAMANKESH, M., HOSSEINI, H., HADIAN, Z., GHASEMI, J. & MOHAMMADI, A. 2020. Investigation and determination of acrylamide in 24 types of roasted nuts and seeds using microextraction method coupled with gas chromatography–mass spectrometry: central composite design. *Journal of Food Measurement and Characterization,* 14**,** 1249-1260.

NGUYEN, H. T., VAN DER FELS-KLERX, H. J., PETERS, R. J. & VAN BOEKEL, M. A. 2016a. Acrylamide and 5-hydroxymethylfurfural formation during baking of biscuits: Part I: Effects of sugar type. *Food Chem,* 192**,** 575-85.

NGUYEN, H. T., VAN DER FELS-KLERX, H. J. & VAN BOEKEL, M. A. 2016b. Kinetics of N(epsilon)-(carboxymethyl)lysine formation in aqueous model systems of sugars and casein. *Food Chem,* 192**,** 125-33.

NGUYEN, H. T., VAN DER FELS-KLERX, H. J. & VAN BOEKEL, M. A. J. S. 2013. Nϵ-(carboxymethyl)lysine: A Review on Analytical Methods, Formation, and Occurrence in Processed Food, and Health Impact. *Food Reviews International,* 30**,** 36-52.

NIKOLOV, P. Y. & YAYLAYAN, V. A. 2011. Reversible and covalent binding of 5-(hydroxymethyl)-2-furaldehyde (HMF) with lysine and selected amino acids. *J Agric Food Chem,* 59**,** 6099-107.

NIQUET-LERIDON, C., JACOLOT, P., NIAMBA, C. N., GROSSIN, N., BOULANGER, E. & TESSIER, F. J. 2015. The rehabilitation of raw and brown butters by the measurement of two of the major Maillard products, N(epsilon)-carboxymethyl-lysine and 5-hydroxymethylfurfural, with validated chromatographic methods. *Food Chem,* 177**,** 361-8.

ÖLMEZ, H., TUNCAY, F., ÖZCAN, N. & DEMIREL, S. 2008. A survey of acrylamide levels in foods from the Turkish market. *Journal of Food Composition and Analysis,* 21**,** 564-568.

PARKER, J. K., BALAGIANNIS, D. P., HIGLEY, J., SMITH, G., WEDZICHA, B. L. & MOTTRAM, D. S. 2012. Kinetic model for the formation of acrylamide during the finish-frying of commercial french fries. *J Agric Food Chem,* 60**,** 9321-31.

PATEL, S. 2013. Pumpkin (Cucurbita sp.) seeds as nutraceutic: a review on status quo and scopes. *Mediterranean Journal of Nutrition and Metabolism,* 6**,** 183-189.

PATEL, S. & RAUF, A. 2017. Edible seeds from Cucurbitaceae family as potential functional foods: Immense promises, few concerns. *Biomed Pharmacother,* 91**,** 330-337.

PEREZ LOCAS, C. & YAYLAYAN, V. A. 2008. Isotope Labeling Studies on the Formation of 5-(Hydroxymethyl)-2-furaldehyde (HMF) from Sucrose by Pyrolysis-GC/MS. *Journal of Agricultural and Food Chemistry,* 56**,** 6717-6723.

RADA-MENDOZA, M., OLANO, A. & VILLAMIEL, M. 2002. Furosine as Indicator of Maillard Reaction in Jams and Fruit-Based Infant Foods. *Journal of Agricultural and Food Chemistry,* 50**,** 4141-4145.

RAMíREZ-JIMÉNEZ, A., GARCíA-VILLANOVA, B. & GUERRA-HERNÁNDEZ, E. 2000. Hydroxymethylfurfural and methylfurfural content of selected bakery products. *Food Research International,* 33**,** 833-838.

ROBERT, F., VUATAZ, G., POLLIEN, P., SAUCY, F., ALONSO, M.-I., BAUWENS, I. & BLANK, I. 2004. Acrylamide Formation from Asparagine under Low-Moisture Maillard Reaction Conditions. 1. Physical and Chemical Aspects in Crystalline Model Systems. *Journal of Agricultural and Food Chemistry,* 52**,** 6837-6842.

RODRIGUES, A. C., STRÖHER, G. L., FREITAS, A. R., VISENTAINER, J. V., OLIVEIRA, C. C. & DE SOUZA, N. E. 2011. The effect of genotype and roasting on the fatty acid composition of peanuts. *Food Research International,* 44**,** 187-192.

RODRIGUES, J. A., BARROS, A. A. & RODRIGUES, P. G. 1999. Differential pulse polarographic determination of alpha-dicarbonyl compounds in foodstuffs after derivatization with o-phenylenediamine. *Journal of Agricultural and Food Chemistry,* 47**,** 3219−3222.

RUFIÁN-HENARES, J. A., DELGADO-ANDRADE, C., JIMÉNEZ-PÉREZ, S. & MORALES, F. J. 2007. Assessing nutritional quality of milk-based sport supplements as determined by furosine. *Food Chemistry,* 101**,** 573-578.

RUFIAN-HENARES, J. A., DELGADO-ANDRADE, C. & MORALES, F. J. 2019. Application of a Fast High-Performance Liquid Chromatography Method for

Simultaneous Determination of Furanic Compounds and Glucosylisomaltol in Breakfast Cereals. *Journal of AOAC INTERNATIONAL,* 89**,** 161-165.

RUFIÁN-HENARES, J. A. & PASTORIZA, S. 2016. Maillard Reaction. *In:* CABALLERO, B., FINGLAS, P. M. & TOLDRÁ, F. (eds.) *Encyclopedia of Food and Health.* Oxford: Academic Press.

SAEED, Y., WANG, J. Q., ZHENG, N. 2017. Furosine Induces DNA Damage and Cell Death in Selected Human Cell Lines: A Strong Toxicant to Kidney Hek-293 Cells. *Food Sci. Biotechnol.*, 26 (4), 1093−1101.

SCHLORMANN, W., BIRRINGER, M., BOHM, V., LOBER, K., JAHREIS, G., LORKOWSKI, S., MULLER, A. K., SCHONE, F. & GLEI, M. 2015. Influence of roasting conditions on health-related compounds in different nuts. *Food Chem,* 180**,** 77-85.

SHAPLA, U.M., SOLAYMAN, M., ALAM, N. KHALIL, M.I., GAN, S.H. 2018. 5-Hydroxymethylfurfural (HMF) levels in honey and other food products: effects on bees and human health. *Chemistry Central Journal,* 12, 35.

SHI, X., DAVIS, J. P., XIA, Z., SANDEEP, K. P., SANDERS, T. H. & DEAN, L. O. 2017. Characterization of peanuts after dry roasting, oil roasting, and blister frying. *Lwt,* 75**,** 520-528.

SHI, X., DEAN, L. O., DAVIS, J. P., SANDEEP, K. P. & SANDERS, T. H. 2018. The effects of different dry roast parameters on peanut quality using an industrial belt-type roaster simulator. *Food Chem,* 240**,** 974-979.

SHIM, Y. Y., GUI, B., ARNISON, P. G., WANG, Y. & REANEY, M. J. T. 2014. Flaxseed (Linum usitatissimum L.) bioactive compounds and peptide nomenclature: A review. *Trends in Food Science & Technology,* 38**,** 5-20.

SINGH, R., BARDEN, A., MORI, T. & BEILIN, L. 2001. Advanced glycation end-products: a review. *Diabetologia,* 44**,** 129-146.

SKOG, K. I., JOHANSSON, M. A. E. & JÄGERSTAD, M. I. 1998. Carcinogenic Heterocyclic Amines in Model Systems and Cooked Foods: A Review on Formation, Occurrence and Intake. *Food and Chemical Toxicology,* 36**,** 879-896.

SPECK, J. C. 1958. The Lobry De Bruyn-Alberda Van Ekenstein Transformation. *In:* WOLFROM, M. L. (ed.) *Advances in Carbohydrate Chemistry.* Academic Press.

STADLER, R. H., BLANK, I., VARGA, N., ROBERT, F., HAU, J., GUY, P., ROBERT, M.-C. & RIEDIKER, S. 2002. Acrylamide from Maillard reaction products. *Nature,* 419**,** 449-450.

STADLER, R. H., ROBERT, F., RIEDIKER, S., VARGA, N., DAVIDEK, T., DEVAUD, S., GOLDMANN, T., HAU, J. & BLANK, I. 2004. In-Depth Mechanistic Study on the Formation of Acrylamide and Other Vinylogous

Compounds by the Maillard Reaction. *Journal of Agricultural and Food Chemistry,* 52**,** 5550-5558.

STADLER, R. H. & STUDER, A. 2016. Chapter 1 - Acrylamide Formation Mechanisms. *In:* GÖKMEN, V. (ed.) *Acrylamide in Food.* Academic Press.

SURH, Y.-J. & TANNENBAUM, S. R. 1994. Activation of the Maillard Reaction Product 5-(Hydroxymethyl)furfural to Strong Mutagens via Allylic Sulfonation and Chlorination. *Chemical Research in Toxicology,* 7**,** 313-318.

TAREKE, E., RYDBERG, P., KARLSSON, P., ERIKSSON, S. & TÖRNQVIST, M. 2002. Analysis of Acrylamide, a Carcinogen Formed in Heated Foodstuffs. *Journal of Agricultural and Food Chemistry,* 50**,** 4998-5006.

THORNALLEY, P. J., LANGBORG, A. & MINHAS, H. S. 1999. Formation of glyoxal, methylglyoxal and 3-deoxyglucosone in the glycation of proteins by glucose. *The Biochemical journal,* 344 Pt 1**,** 109-116.

TREIBMANN, S., HELLWIG, A., HELLWIG, M. & HENLE, T. 2017. Lysine-Derived Protein-Bound Heyns Compounds in Bakery Products. *Journal of Agricultural and Food Chemistry,* 65**,** 10562-10570.

TROISE, A. D., FIORE, A., WILTAFSKY, M. & FOGLIANO, V. 2015. Quantification of Nepsilon-(2-Furoylmethyl)-L-lysine (furosine), Nepsilon-(Carboxymethyl)-L-lysine (CML), Nepsilon-(Carboxyethyl)-L-lysine (CEL) and total lysine through stable isotope dilution assay and tandem mass spectrometry. *Food Chem,* 188**,** 357-64.

TUNCEL, N. B., UYGUR, A. & KARAGÜL YÜCEER, Y. 2017. The Effects of Infrared Roasting on HCN Content, Chemical Composition and Storage Stability of Flaxseed and Flaxseed Oil. *Journal of the American Oil Chemists' Society,* 94**,** 877-884.

URIBARRI, J., WOODRUFF, S., GOODMAN, S., CAI, W., CHEN, X., PYZIK, R., YONG, A., STRIKER, G. E. & VLASSARA, H. 2010. Advanced glycation end products in foods and a practical guide to their reduction in the diet. *J Am Diet Assoc,* 110**,** 911-16 e12.

USDA 2018. USDA National Nutrient Database for Standard Reference, Legacy. Agricultural Research Service, Nutrient Data Laboratory.

VALDÉS, A., BELTRÁN, A., KARABAGIAS, I., BADEKA, A., KONTOMINAS, M. G. & GARRIGÓS, M. C. 2015. Monitoring the oxidative stability and volatiles in blanched, roasted and fried almonds under normal and accelerated storage conditions by DSC, thermogravimetric analysis and ATR-FTIR. *European Journal of Lipid Science and Technology,* 117**,** 1199-1213.

VAN BOEKEL, M. A. J. S. 1996. Statistical Aspects of Kinetic Modeling for Food Science Problems. *Journal of Food Science,* 61**,** 477-486.

VAN BOEKEL, M. A. J. S. 2009. Multiresponse Kinetic Modeling of Chemical Reactions. *Kinetic Modeling of Reactions in Foods.* CRC Press.

VELASCO, L., FERNÁNDEZ-MARTÍNEZ, J. M., GARCÍA-RUÍZ, R. & DOMÍNGUEZ, J. 2003. Genetic and environmental variation for tocopherol content and composition in sunflower commercial hybrids. *The Journal of Agricultural Science,* 139**,** 425-429.

VELISEK, J. 2014. *The Chemistry of Food*, Wiley-Blackwell.

VENKATACHALAM, M. & SATHE, S. K. 2006. Chemical composition of selected edible nut seeds. *J Agric Food Chem,* 54**,** 4705-14.

WANG, H.-Y., QIAN, H. & YAO, W.-R. 2011. Melanoidins produced by the Maillard reaction: Structure and biological activity. *Food Chemistry,* 128**,** 573-584.

WANG, L., LIU, F., WANG, A., YU, Z., XU, Y. & YANG, Y. 2017. Purification, characterization and bioactivity determination of a novel polysaccharide from pumpkin (Cucurbita moschata) seeds. *Food Hydrocolloids,* 66**,** 357-364.

WEENEN, H. 1998. Reactive intermediates and carbohydrate fragmentation in Maillard chemistry. *Food Chemistry,* 62**,** 393-401.

WEI, Q., LIU, T. & SUN, D.-W. 2018. Advanced glycation end-products (AGEs) in foods and their detecting techniques and methods: A review. *Trends in Food Science & Technology,* 82**,** 32-45.

WEIGEL, K. U., OPITZ, T. & HENLE, T. 2004. Studies on the occurrence and formation of 1,2-dicarbonyls in honey. *European Food Research and Technology,* 218**,** 147-151.

WELLNER, A., NUßPICKEL, L. & HENLE, T. 2011. Glycation compounds in peanuts. *European Food Research and Technology,* 234**,** 423-429.

WHO 2005. Summary report of the sixty-fourth meeting of the Joint FAO/WHO expert committee on food additive (JECFA). Rome, Italy: The ILSI Press International Life Sciences Institute.

WIN, M. M., ABDUL-HAMID, A., BAHARIN, B. S., ANWAR, F. & SAARI, N. 2011. Effects of roasting on phenolics composition and antioxidant activity of peanut (Arachis hypogaea L.) kernel flour. *European Food Research and Technology,* 233**,** 599-608.

WONG, C. W., WIJAYANTI, H. B. & BHANDARI, B. R. 2015. Maillard Reaction in Limited Moisture and Low Water Activity Environment. *Water Stress in Biological, Chemical, Pharmaceutical and Food Systems.*

XIAO, L., LEE, J., ZHANG, G., EBELER, S. E., WICKRAMASINGHE, N., SEIBER, J. & MITCHELL, A. E. 2014. HS-SPME GC/MS characterization of volatiles in raw and dry-roasted almonds (Prunus dulcis). *Food Chem,* 151**,** 31-9.

YASUHARA, A., TANAKA, Y., HENGEL, M. & SHIBAMOTO, T. 2003. Gas Chromatographic Investigations of Acrylamide Formation in Browning Model Systems. *Journal of Agricultural Food Chemistry,* 51**,** 3999−4003

YAYLAYAN, V. A. 2003. Recent Advances in the Chemistry of Strecker Degradation and Amadori Rearrangement: Implications to Aroma and Color Formation. *Food Science and Technology Research,* 9 1–6.

YAYLAYAN, V. A. 2006. Precursors, Formation and Determination of Furan in Food. *Journal für Verbraucherschutz und Lebensmittelsicherheit,* 1**,** 5-9.

YAYLAYAN, V. A. 2009. Acrylamide formation and its impact on the mechanism of the early Maillard reaction. *Journal of Food and Nutrition Research,* 48**,** 1–7.

YAYLAYAN, V. A. & HUYGHUES-DESPOINTES, A. 1994. Chemistry of Amadori rearrangement products: analysis, synthesis, kinetics, reactions, and spectroscopic properties. *Crit Rev Food Sci Nutr,* 34**,** 321-69.

YAYLAYAN, V. A. & KEYHANI, A. 2000. Origin of Carbohydrate Degradation Products in L-Alanine/ D-[13C] Glucose Model Systems. *Journal of Agricultural and Food Chemistry,* 48, **,** 2415−2419.

YAYLAYAN, V. A., WNOROWSKI, A. & PEREZ-LOCAS, C. 2003. Why asparagine needs carbohydrates to generate acrylamide. *Journal of Agricultural and Food Chemistry,* 51**,** 1753−1757.

YOUNG, C. & SCHADEL, W. 1990. Transmission and Scanning Electron Microscopy of Peanut (Arachis hypogaea L. CV. Florigiant) Cotyledon After Roasting. *Food Structure,* 9**,** 109-112.

YOUNG, C. & SCHADEL, W. 1993. A comparison of the effects of oven roasting and oil cooking on the microstructure of peanut (Arachis hypogaea L. cv. Florigiant) cotyledon. *Food Structure,* 12**,** 59-66.

YUAN, J.-P. & CHEN, F. 1998. Separation and Identification of Furanic Compounds in Fruit Juices and Drinks by High-Performance Liquid Chromatography Photodiode Array Detection. *Journal of Agricultural and Food Chemistry,* 46**,** 1286-1291.

ZAMORA, R. & HIDALGO, F. J. 2005. Coordinate contribution of lipid oxidation and Maillard reaction to the nonenzymatic food browning. *Crit Rev Food Sci Nutr,* 45**,** 49-59.

ZAMORA, R. & HIDALGO, F. J. 2008. Contribution of Lipid Oxidation Products to Acrylamide Formation in Model Systems. *Journal of Agricultural and Food Chemistry,* 56**,** 6075-6080.

ZAPPALÀ, M., FALLICO, B., ARENA, E. & VERZERA, A. 2005. Methods for the determination of HMF in honey: a comparison. *Food Control,* 16**,** 273-277.

ZHANG, G., HUANG, G., XIAO, L. & MITCHELL, A. E. 2011a. Determination of advanced glycation endproducts by LC-MS/MS in raw and roasted almonds (Prunus dulcis). *J Agric Food Chem,* 59**,** 12037-46.

ZHANG, G., HUANG, G., XIAO, L., SEIBER, J. & MITCHELL, A. E. 2011b. Acrylamide formation in almonds (Prunus dulcis): influences of roasting time and temperature, precursors, varietal selection, and storage. *J Agric Food Chem,* 59**,** 8225-32.

ŽILIĆ, S. 2016. Chapter 10 - Acrylamide in Soybean Products, Roasted Nuts, and Dried Fruits. *In:* GÖKMEN, V. (ed.) *Acrylamide in Food.* Academic Press.

ZYZAK, D. V., SANDERS, R. A., STOJANOVIC, M., TALLMADGE, D. H., EBERHART, B. L., EWALD, D. K., GRUBER, D. C., MORSCH, T. R., STROTHERS, M. A., RIZZI, G. P. & VILLAGRAN, M. D. 2003. Acrylamide Formation Mechanism in Heated Foods. *Journal of Agricultural and Food Chemistry,* 51**,** 4782-4787.

8. ANNEXES

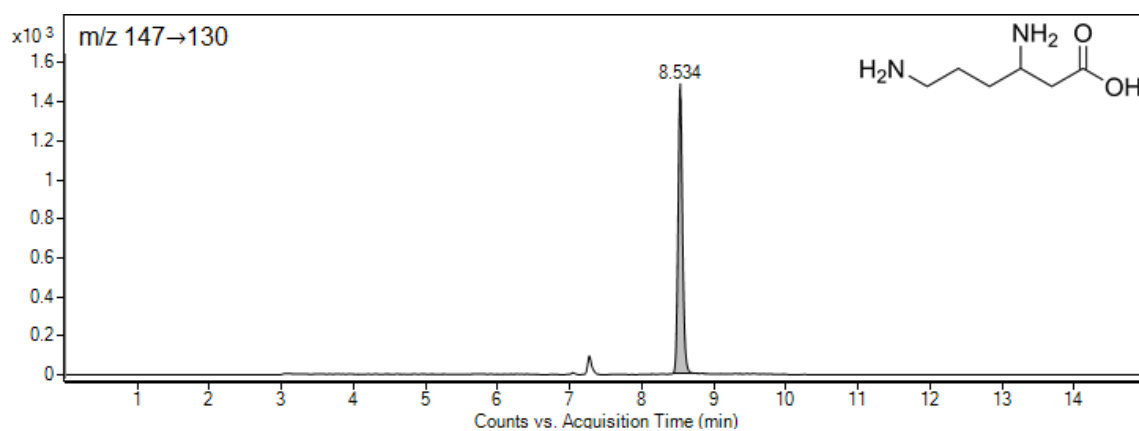## 8.1. ANNEX 1-Chromatograms for Maillard Reaction Products

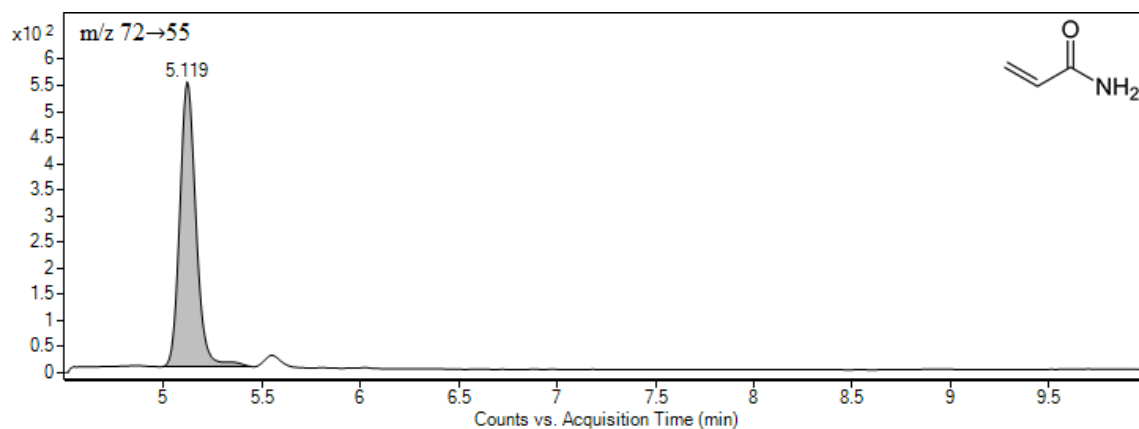**Figure A1.** The extracted ion chromatograms of lysine

Figure A2. The extracted ion chromatograms of acrylamide
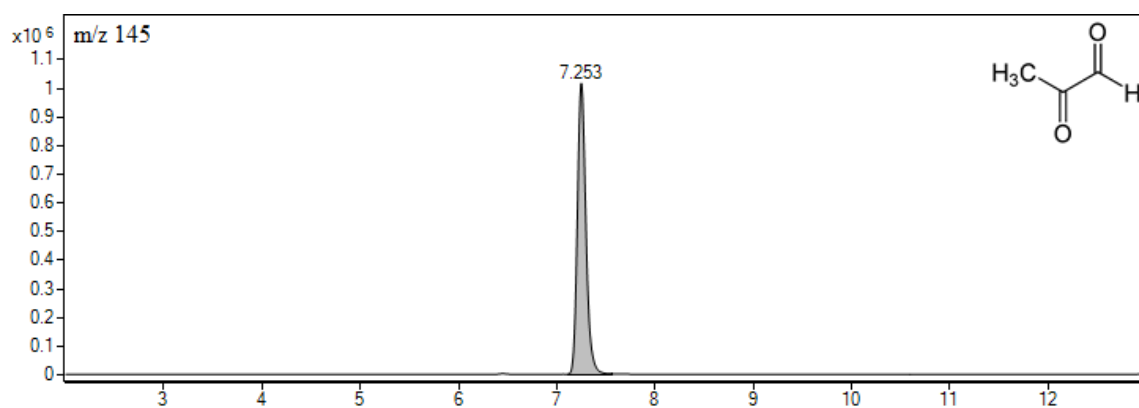

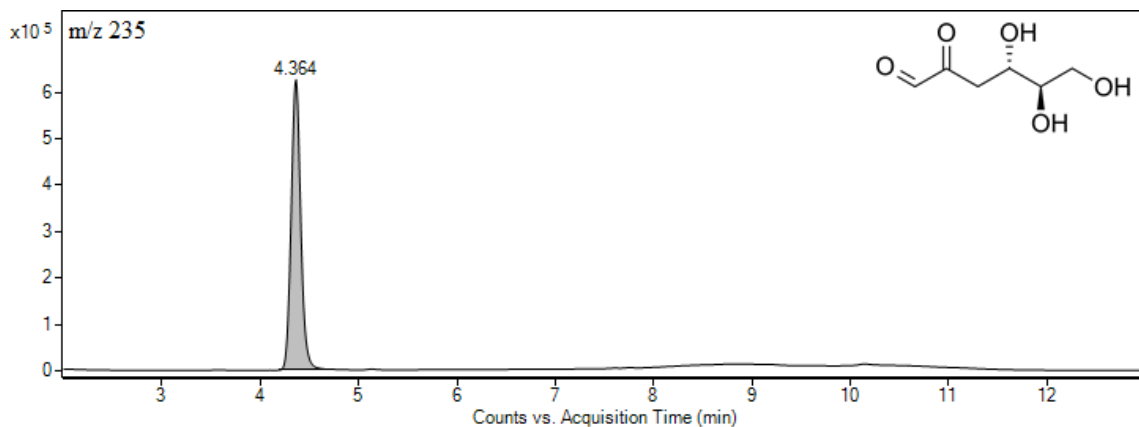**Figure A3.** The extracted ion chromatograms of the quinoxaline derivatives of methylglyoxal

Figure A4. The extracted ion chromatograms of the quinoxaline derivatives of 3-deoxyglucosone
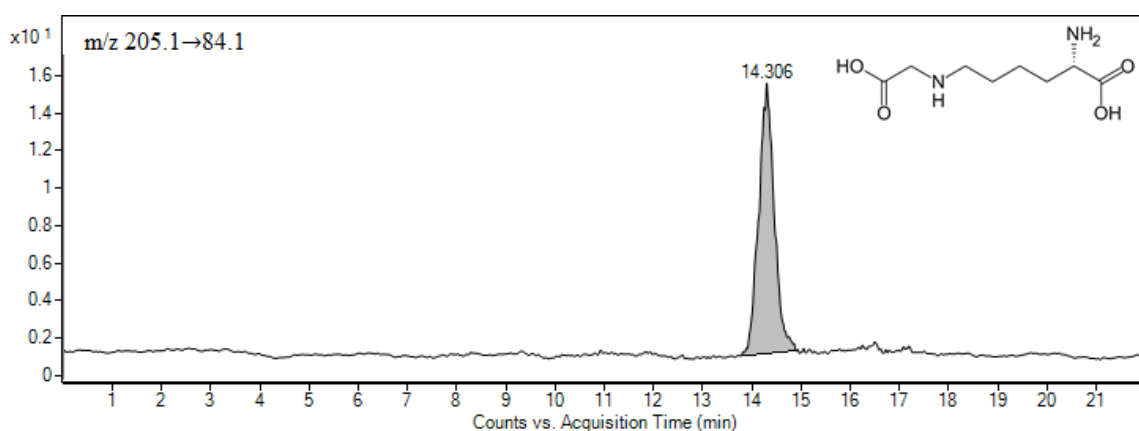

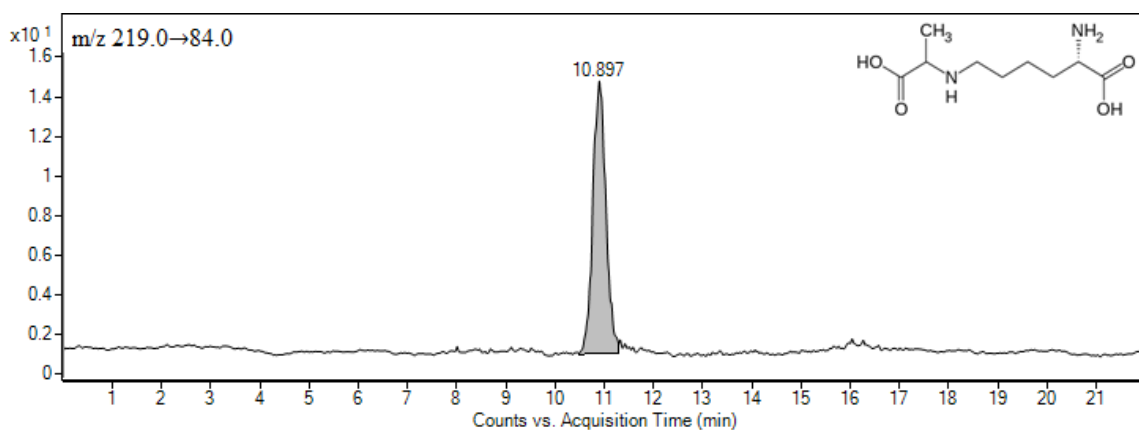**Figure A5.** The extracted ion chromatograms of N-ε-Carboxymethyllysine

Figure A6. The extracted ion chromatograms of N-ε-Carboxyethyllysine

8.2. ANNEX 2- Publications

Şen, D., Gökmen, V., 2022. Kinetic Modeling of Maillard and Caramelization Reactions in Sucrose-Rich and Low Moisture Foods Applied for Roasted Nuts and Seeds, *Food Chemistry*, 395, 133583.